Electronic Supplementary Information (ESI)

Diastereoselective Intramolecular Oxidopyrylium-alkene [5+2]-Cycloaddition of Substrates with a β-chiral Center on Alkene Tethers: Synthesis of 8-Oxabicyclo-[3.2.1]-octenone Heterocycles

Arun K. Ghosh*, and Denver Hopkins

Department of Chemistry; Department of Medicinal Chemistry and Molecular pharmacology, Purdue University, 560 Oval Drive, West Lafayette, Indiana 47907

akghosh@purdue.edu

Table of Contents

General Information All chemicals were purchased from commercial suppliers unless otherwise stated. All reactions were carried out under an argon atmosphere in either flame or oven-dried (120 °C) glassware. Anhydrous organic solvents were obtained as follows. Tetrahydrofuran (THF) was freshly distilled from Na/benzophenone. N,N-diisopropylethylamine (DIPEA), diisopropylamine (DIPA), and pyridine were distilled over calcium hydride. Isobutryaldehyde, ethyl acetate, acetone, benzaldehyde, pivalaldehyde, allyl bromide, and 2-furaldehyde were fractionally distilled. All other reagents were reaction grade. Stainless steel syringes and cannula were used to transfer air- or moisture-sensitive liquids. Thin-layer chromatography (TLC) analysis was conducted using glass backed silica gel plates. (60 Å, 250 μm thick, F-254 indicator) Flash column chromatography was performed using 230−400 mesh and 60 Å pore diameter silica gel. Organic solvents were removed under vacuum using a rotatory evaporator at 30 °C. 1H and 13C NMR spectra was obtained on Bruker AV-III-400-HD, or NEO500 instruments. 13C NMR spectra were obtained at 100 and 126 MHz. Chemical shifts were reported as parts per million (ppm) with respect to the residual solvent peak (CDCl3, 7.26 ppm for 1H and 77 ppm for 13C). NMR data are reported as the value δ (chemical shift),J-value (Hz), integration, and splitting pattern where s = singlet, d =doublet, t = triplet, q = quartet, p = quintet, m = multiplet, dd =doublet of doublets and so on. HPLC chromatography was conducted on an Agilent 1260 Infinity II instrument. Purity and diatereomeric ratio was determined by the area under the curve of chromatographs in 215nm. High-resolution mass spectrometry (HRMS) spectra were recorded under positive electron spray ionization (ESI+) and positive atmospheric pressure chemical ionization (APCI+) conditions using an LTQ Orbitrap Mass Spectrometer at the Purdue University Department of Chemistry Mass Spectrometry Center.

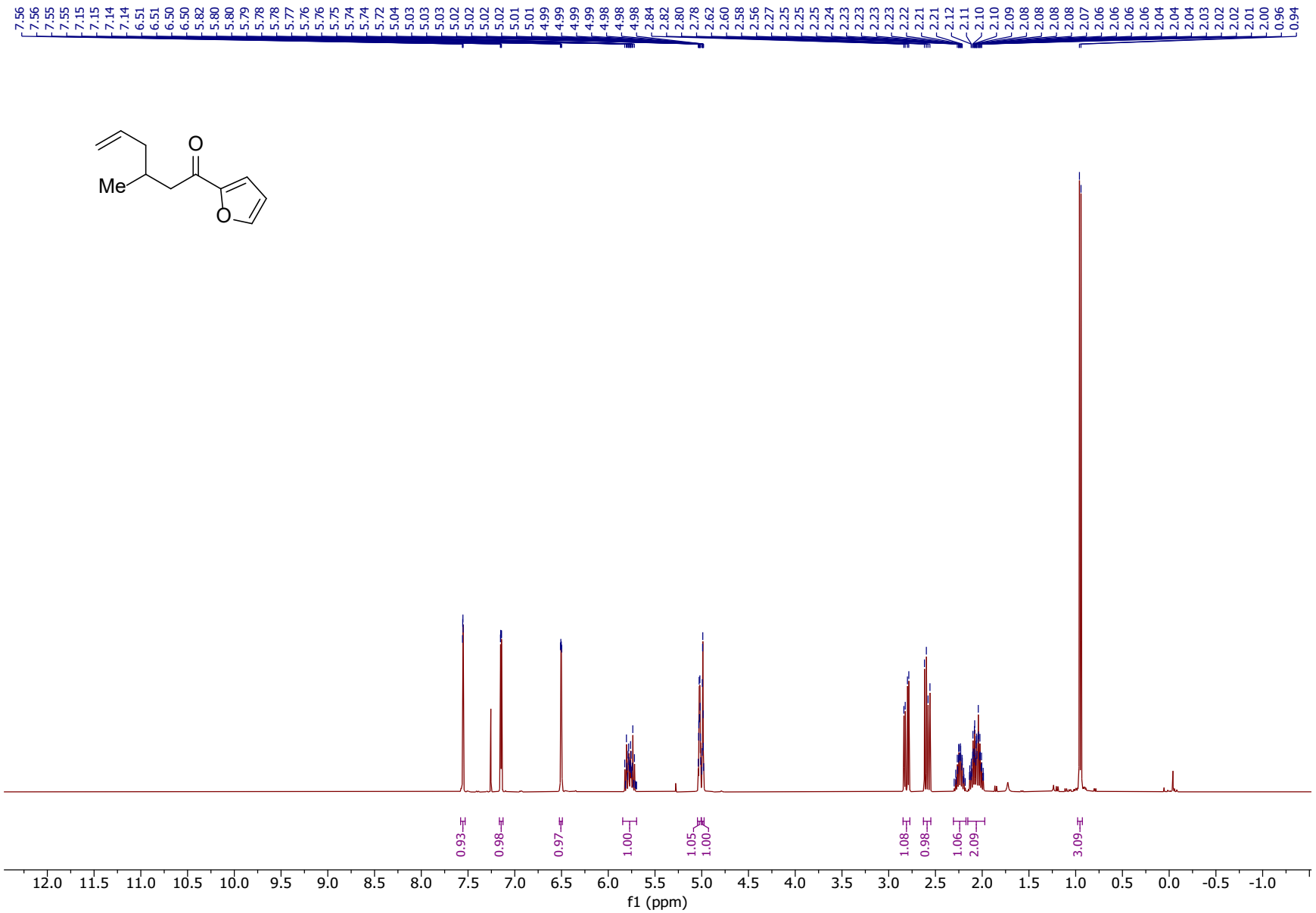

Figure S1: ^{1}H NMR (400 MHz, $CDCl_3$) of β-allyl ketone 13a

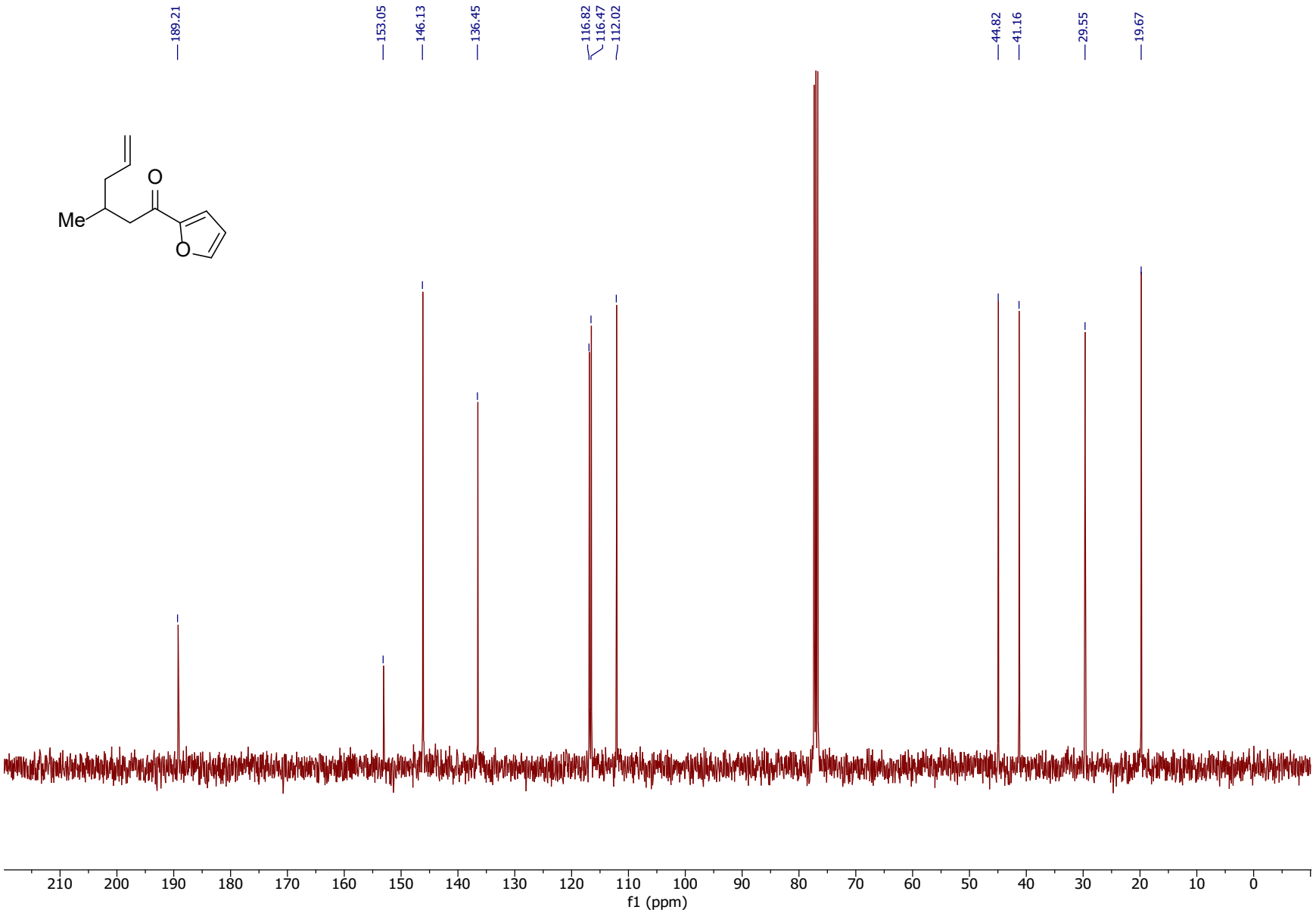

Figure S2: $^{13}C\{^{1}H\}$ (100 MHz, $CDCl_3$) of β-allyl ketone 13a

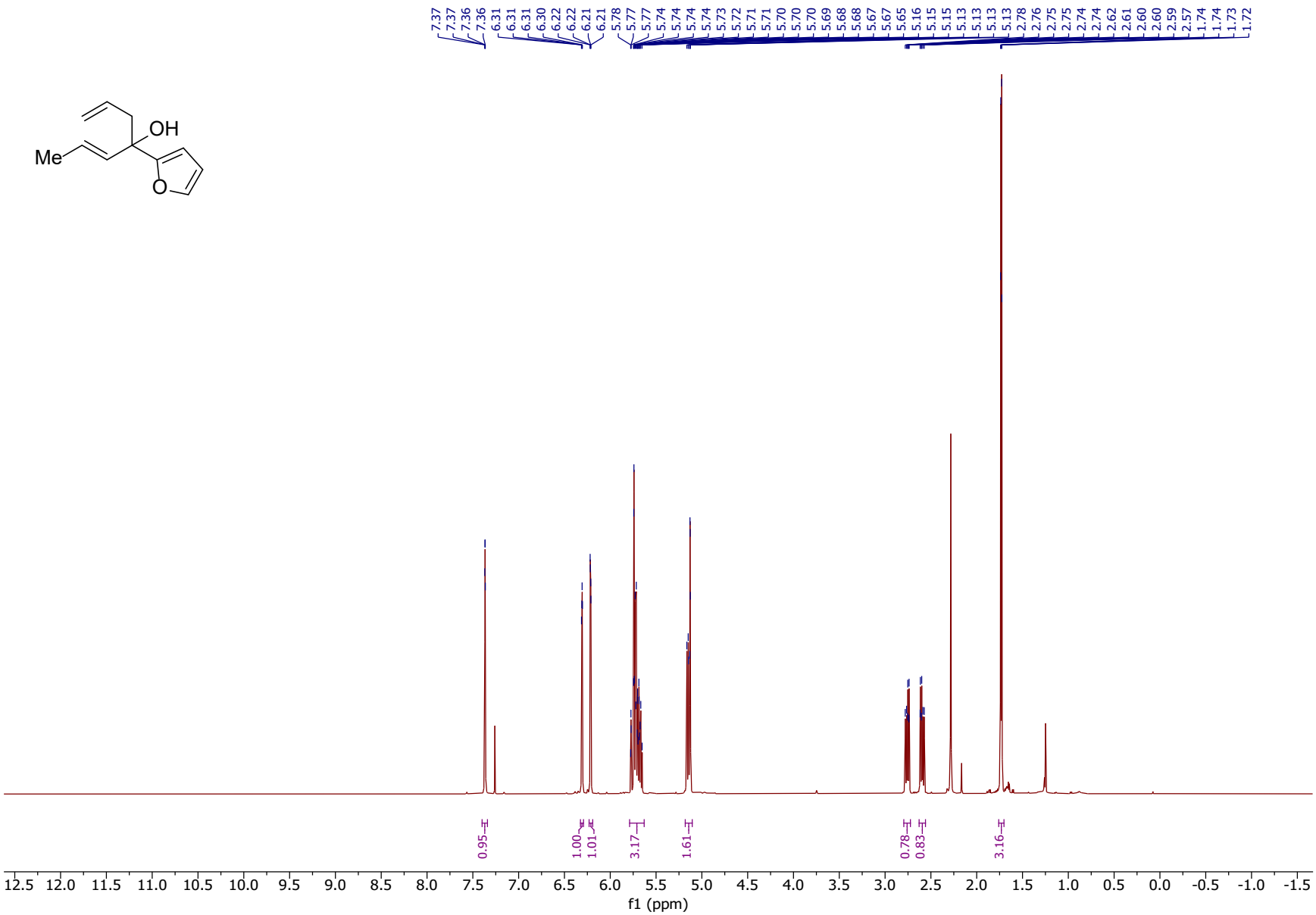

Figure S3: ^{1}H NMR (500 MHz, $CDCl_3$) of diene 15

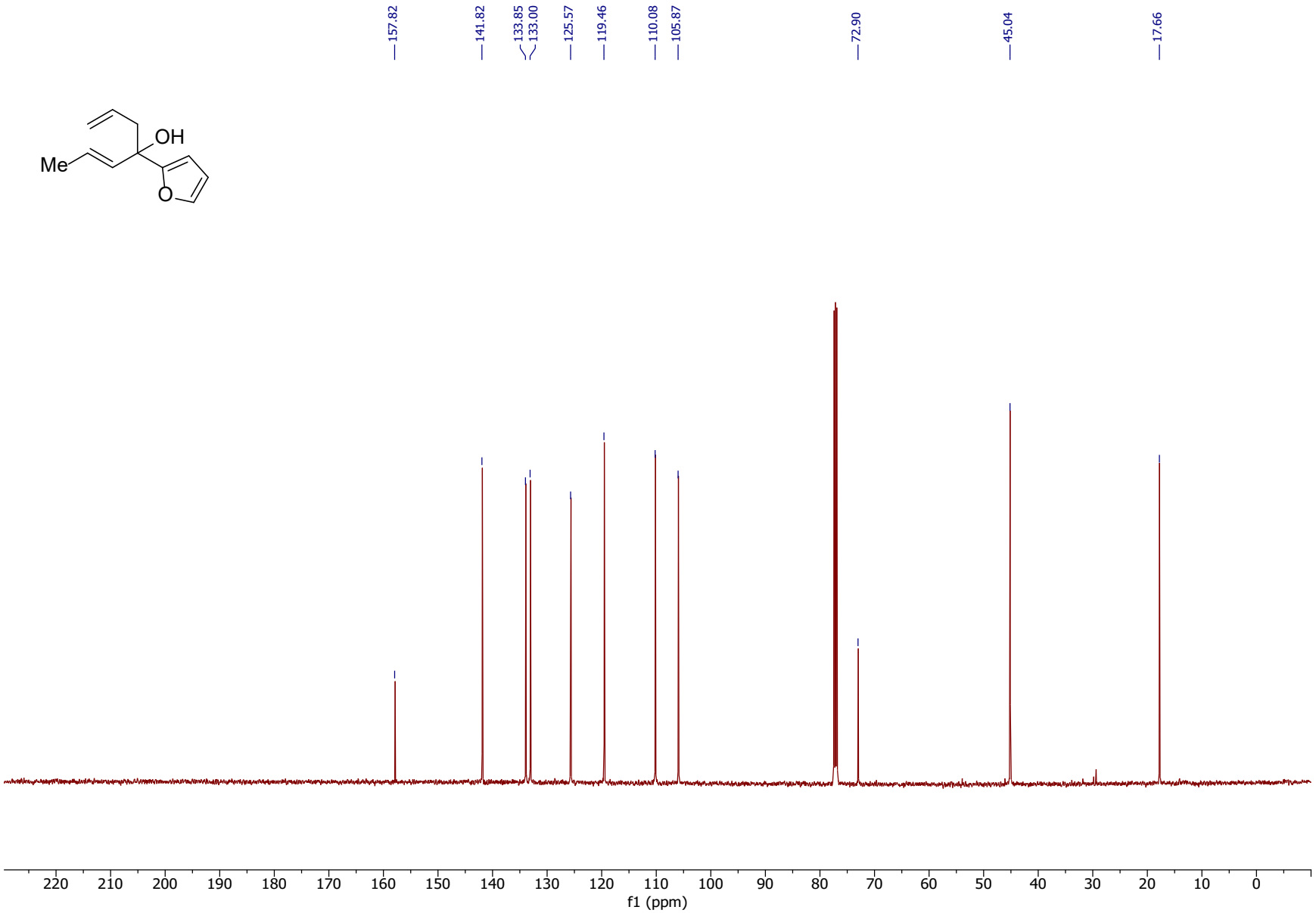

Figure S4: $^{13}C\{^{1}H\}$ (125 MHz, $CDCl_3$) of diene 15

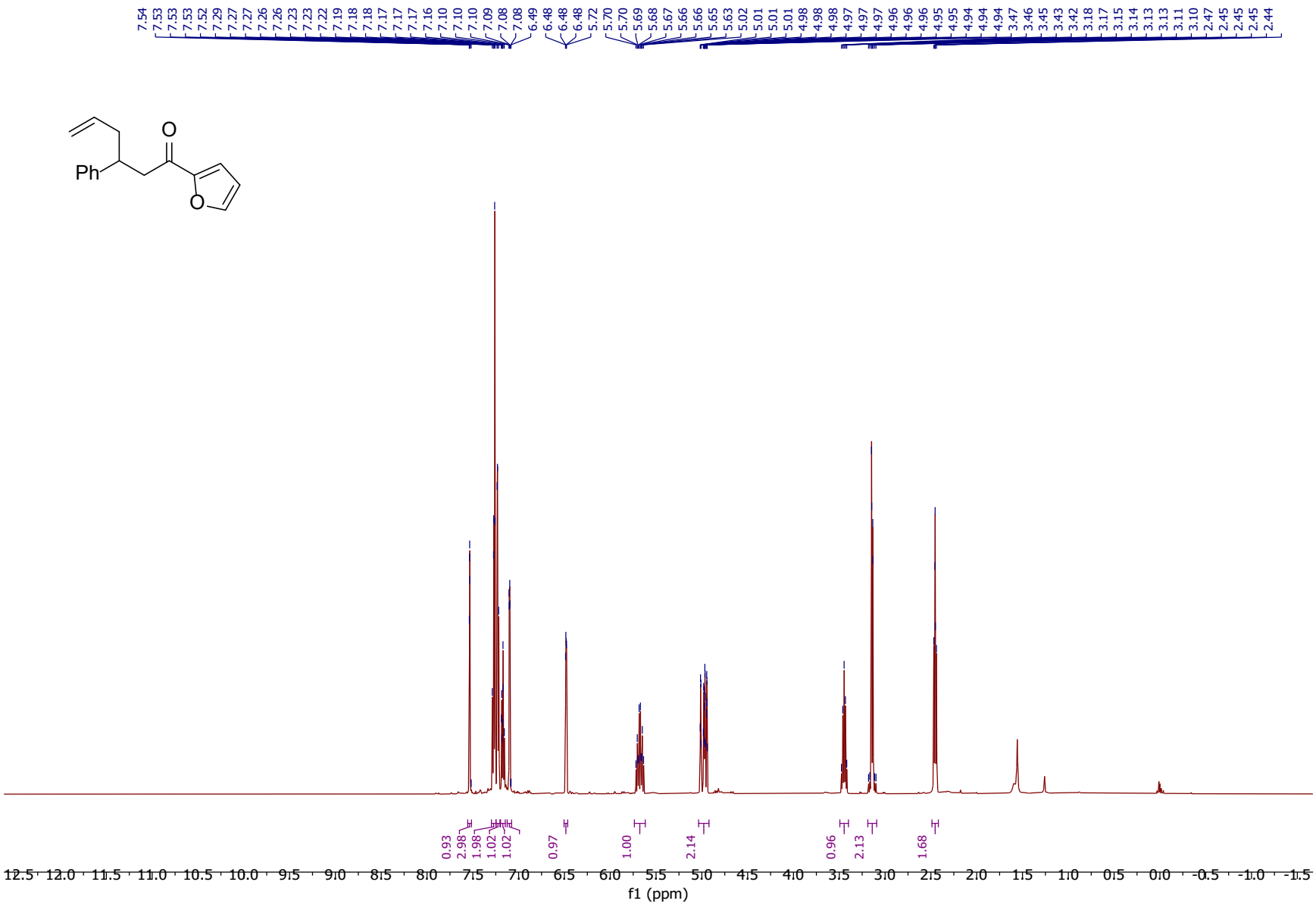

Figure S5: ^{1}H NMR (500 MHz, $CDCl_3$) of β-allyl ketone 13b

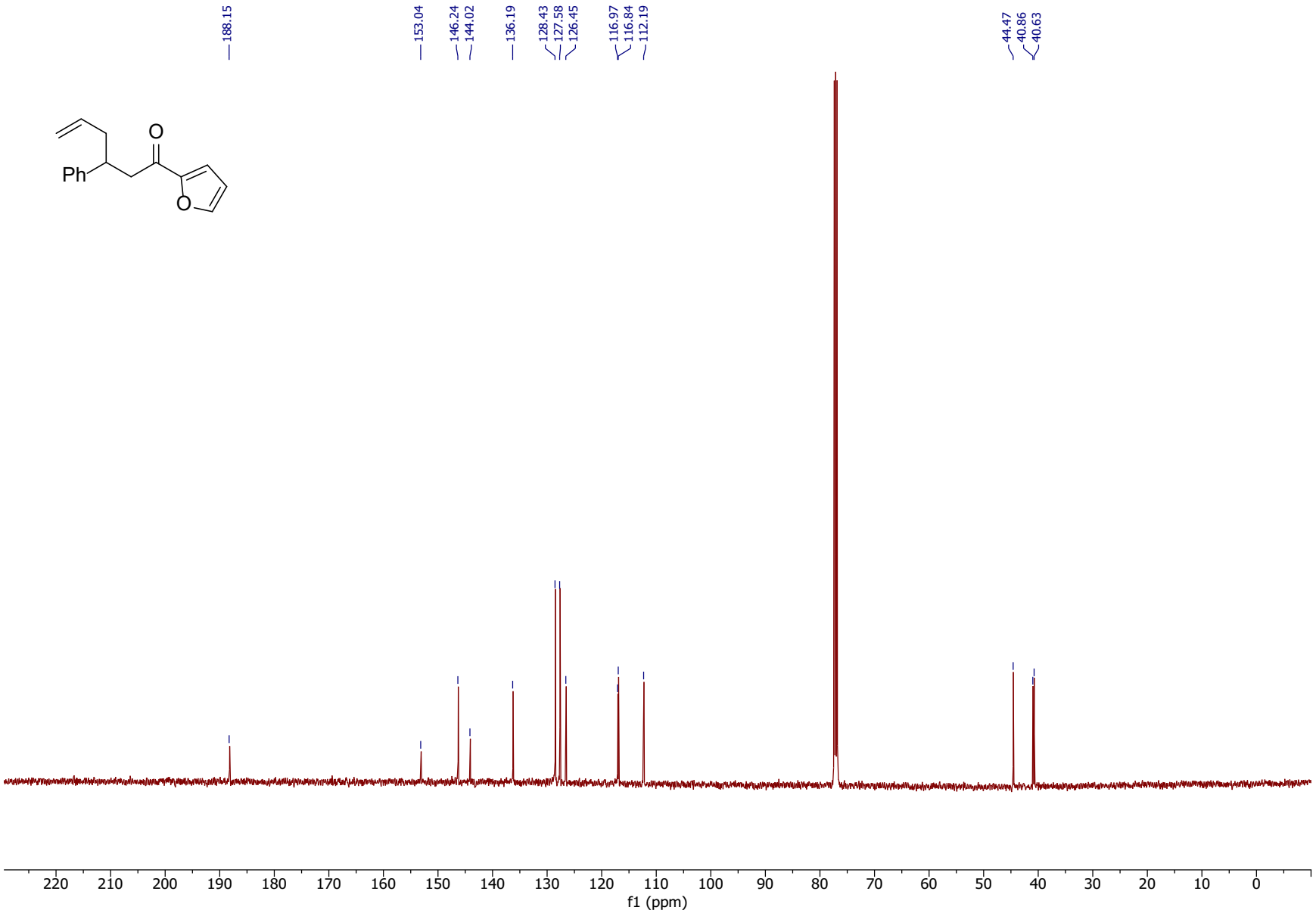

Figure S6: $^{13}C\{^{1}H\}$ (125 MHz, $CDCl_3$) of β-allyl ketone 13b

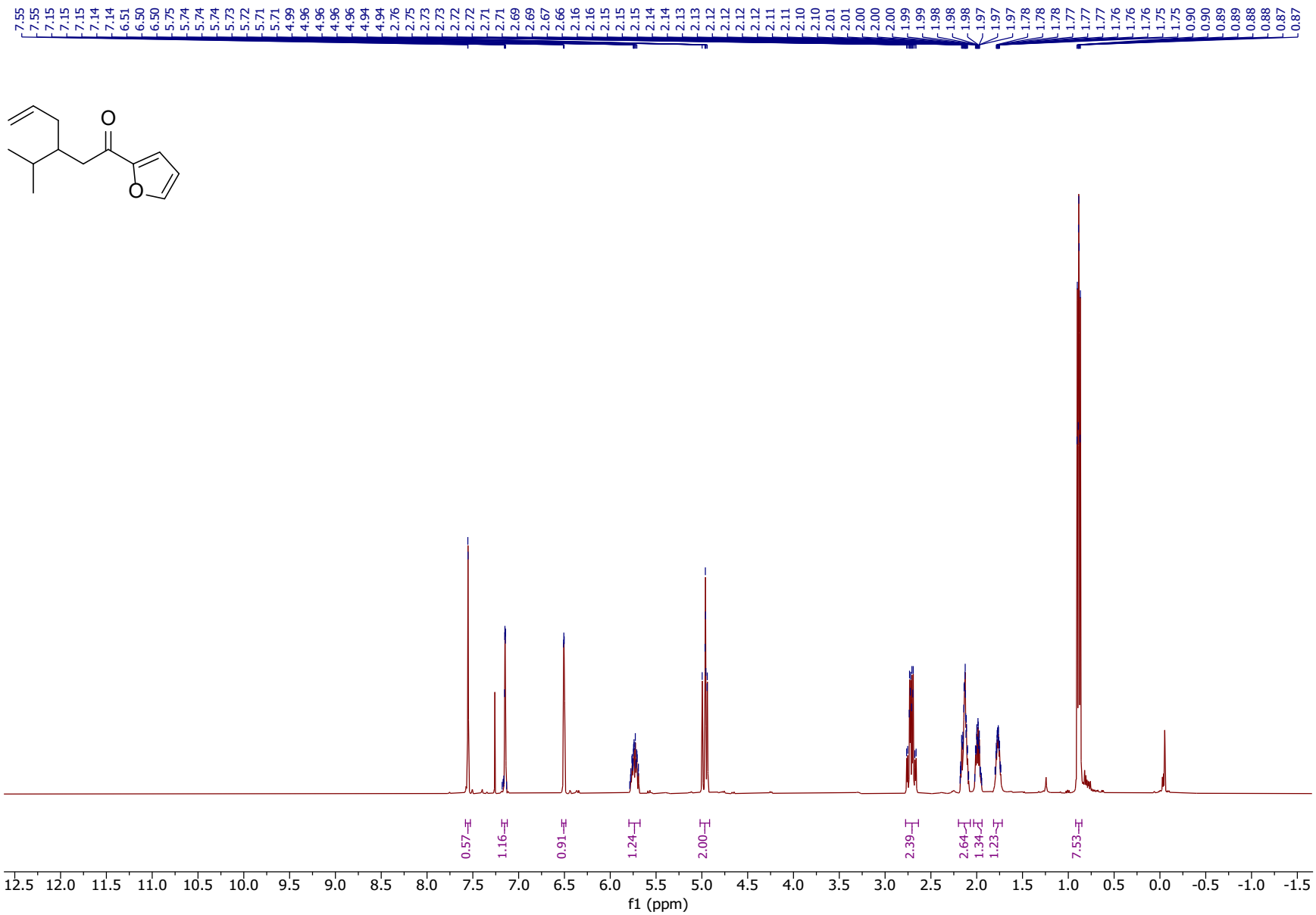

Figure S7: ^{1}H NMR (400 MHz, $CDCl_3$) of β-allyl ketone 13c

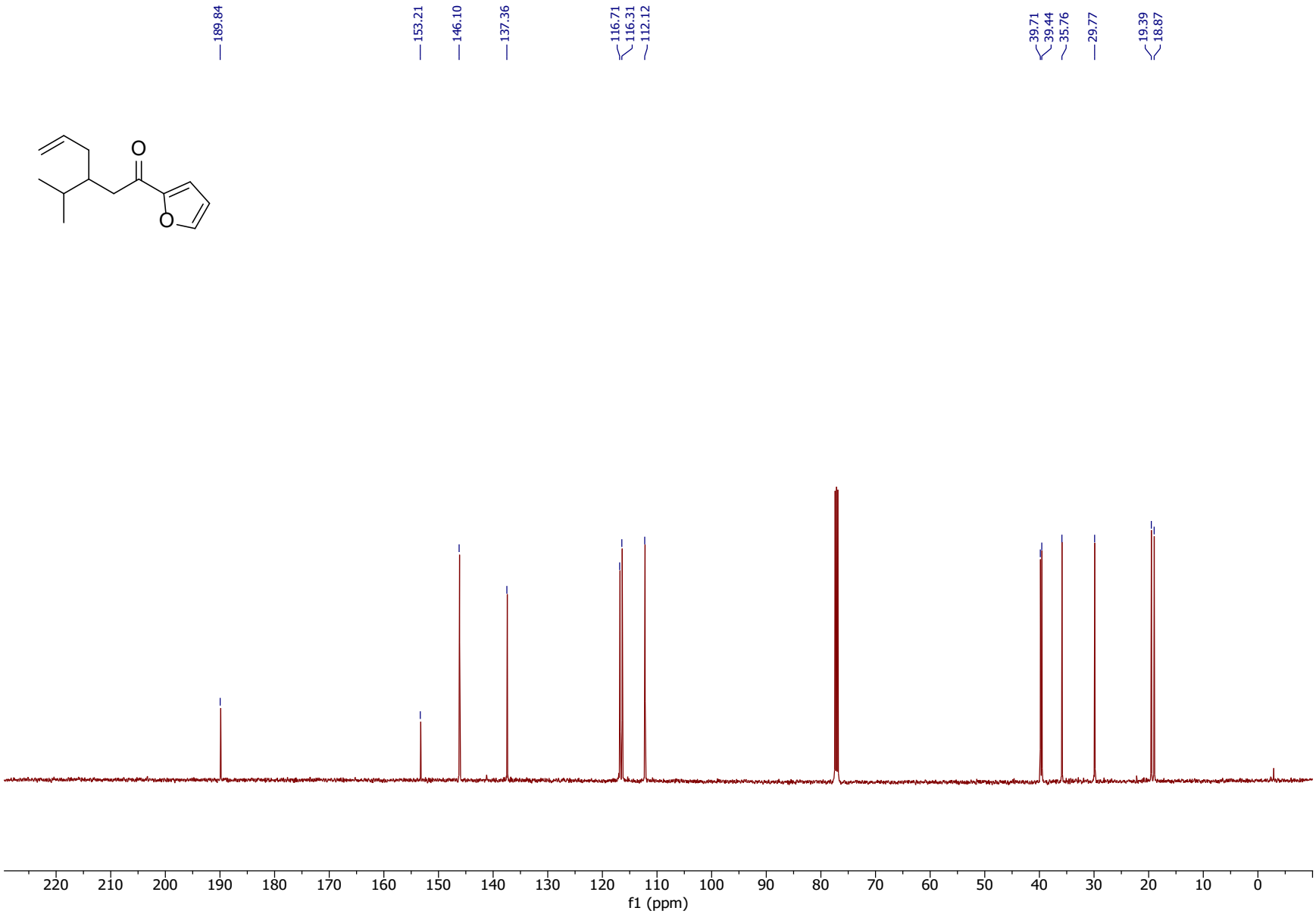

Figure S8: $^{13}C\{^{1}H\}$ (100 MHz, $CDCl_3$) of β-allyl ketone 13c

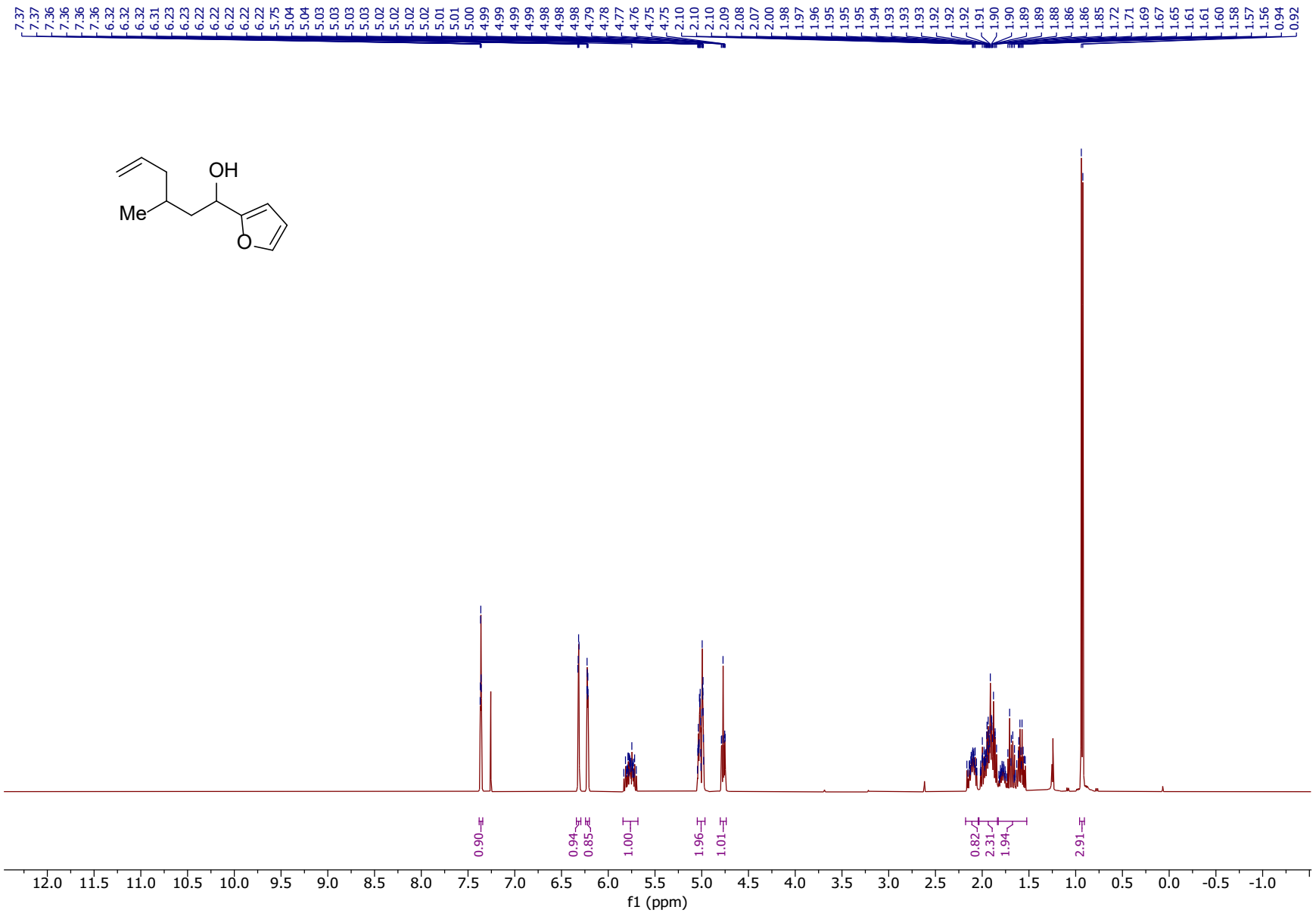

Figure S9: ^{1}H NMR (400 MHz, $CDCl_3$) of furanol 15a

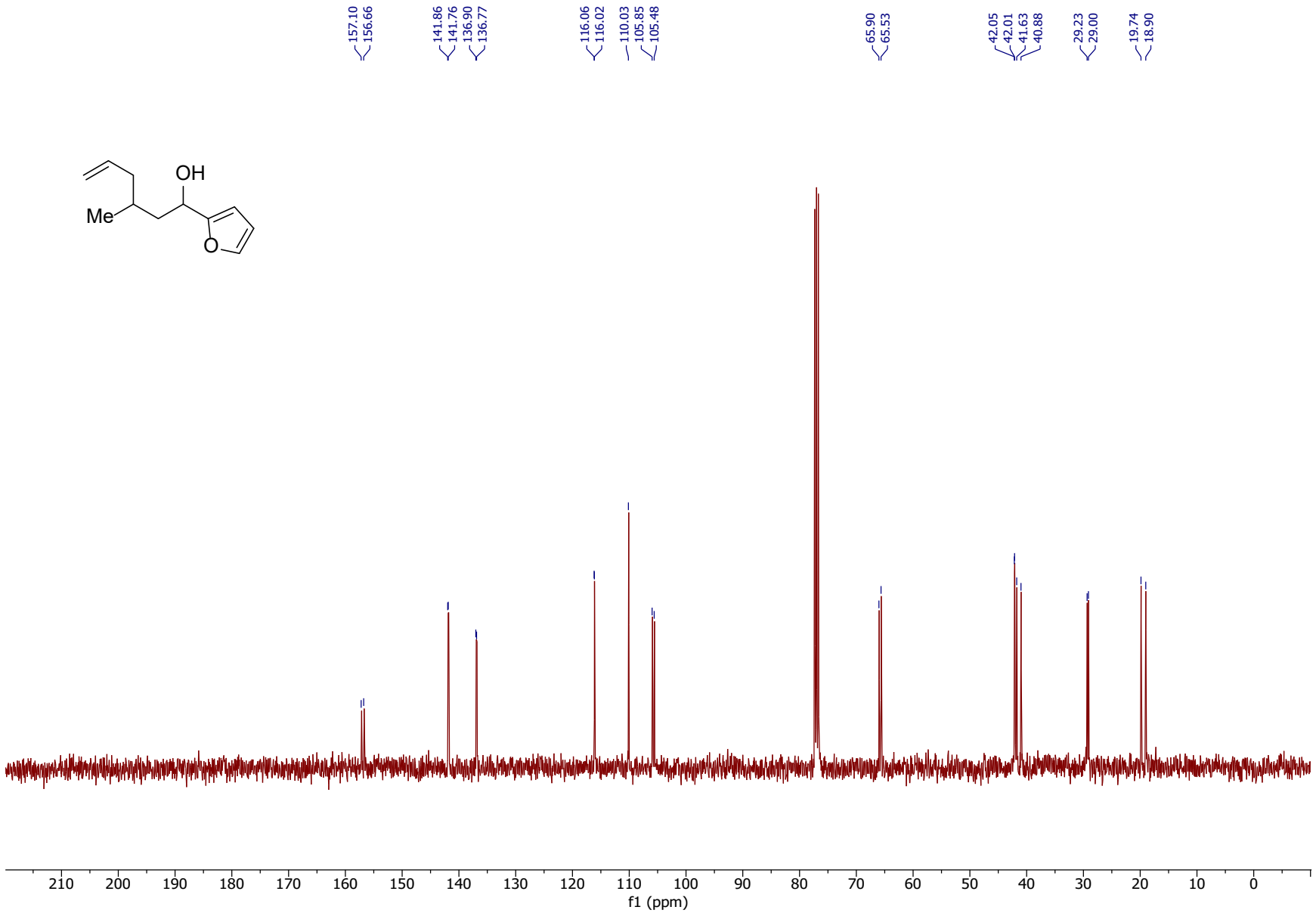

Figure S10: $^{13}C\{^{1}H\}$ (100 MHz, $CDCl_3$) of furanol 15a

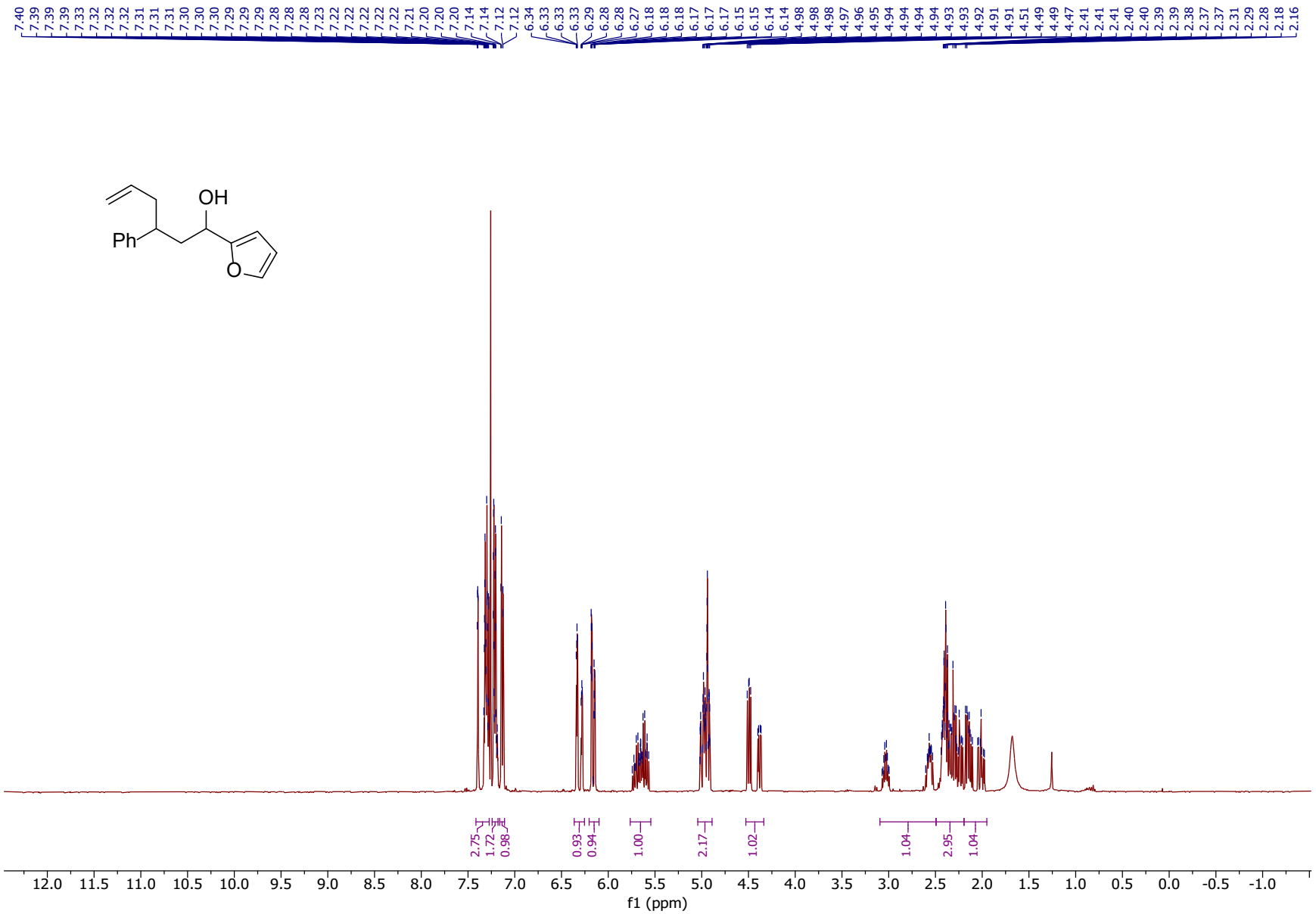

Figure S11: ^{1}H NMR (400 MHz, $CDCl_3$) of furanol 15b

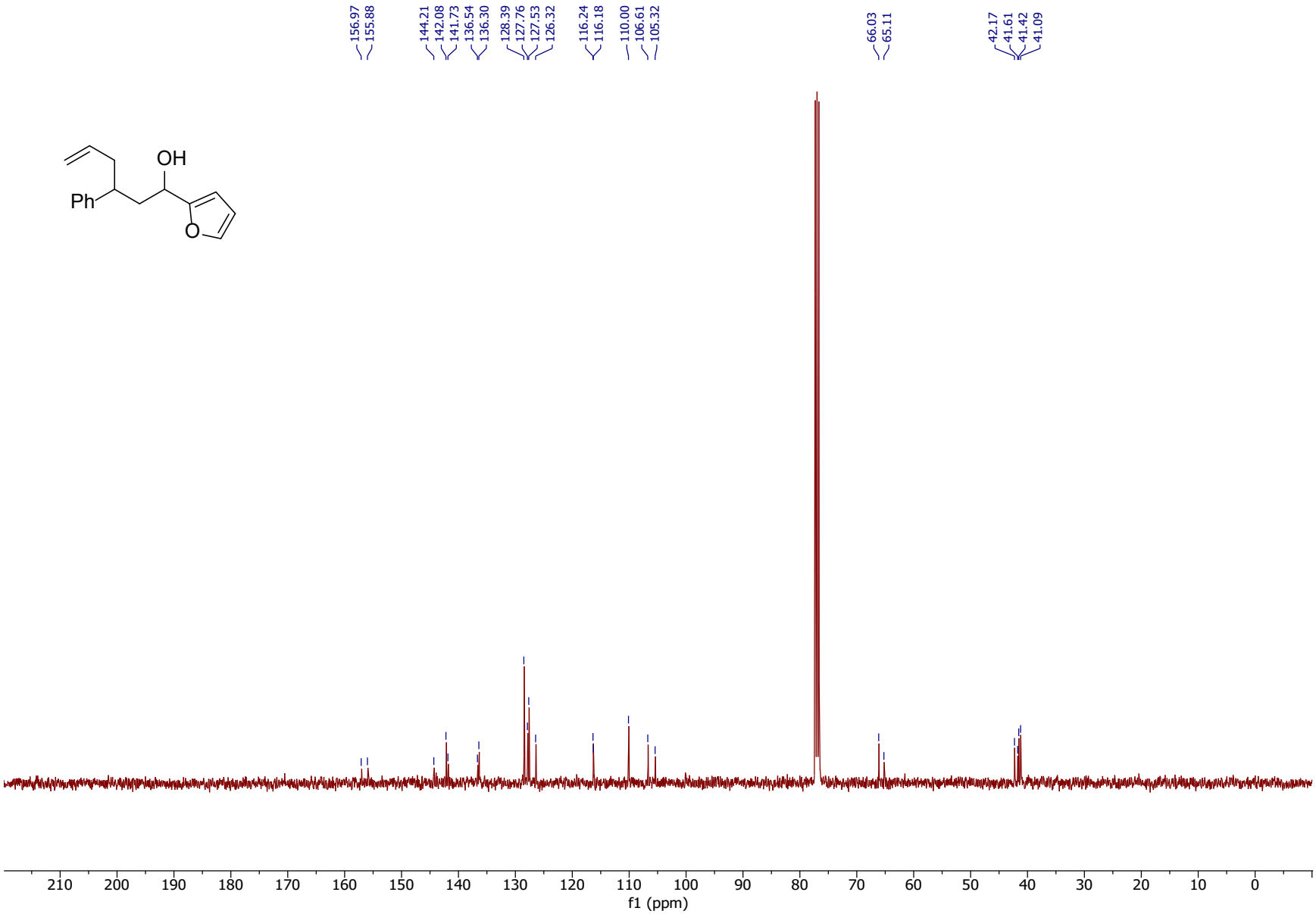

Figure S12: $^{13}C\{^{1}H\}$ (100 MHz, $CDCl_3$) of furanol 15b

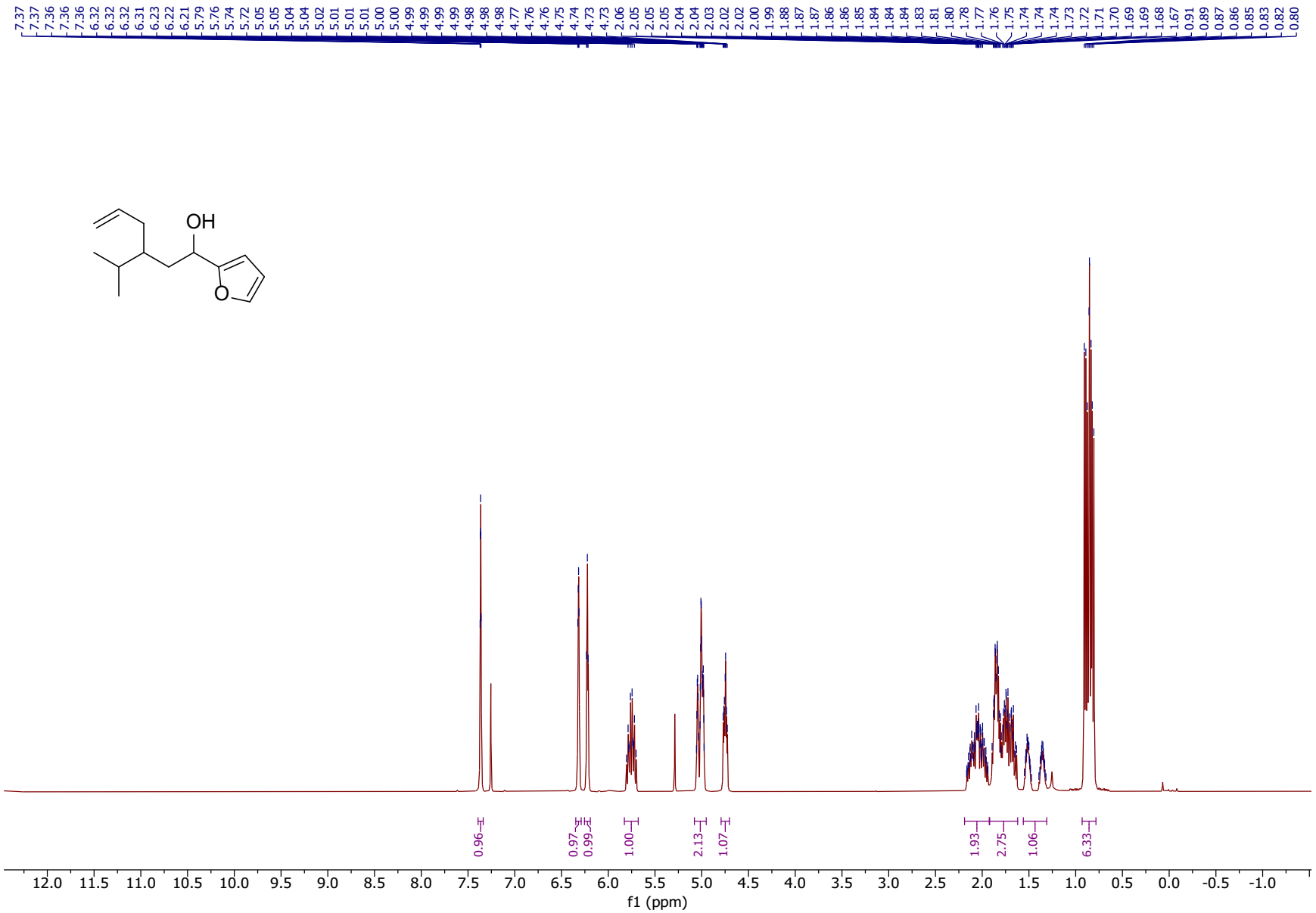

Figure S13: ^{1}H NMR (400 MHz, $CDCl_3$) of furanol 15c

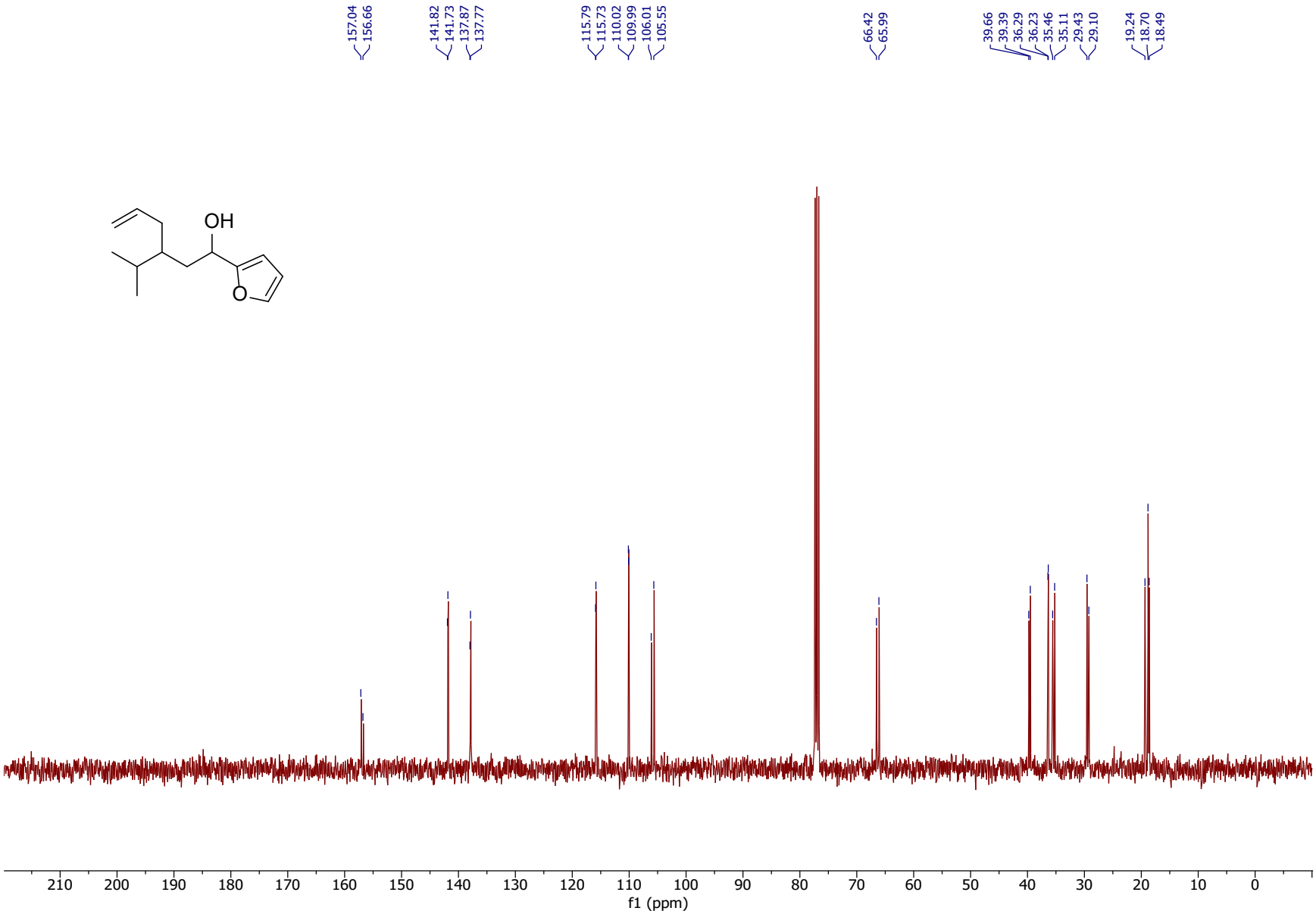

Figure S14: $^{13}C\{^{1}H\}$ (100 MHz, $CDCl_3$) of furanol 15c

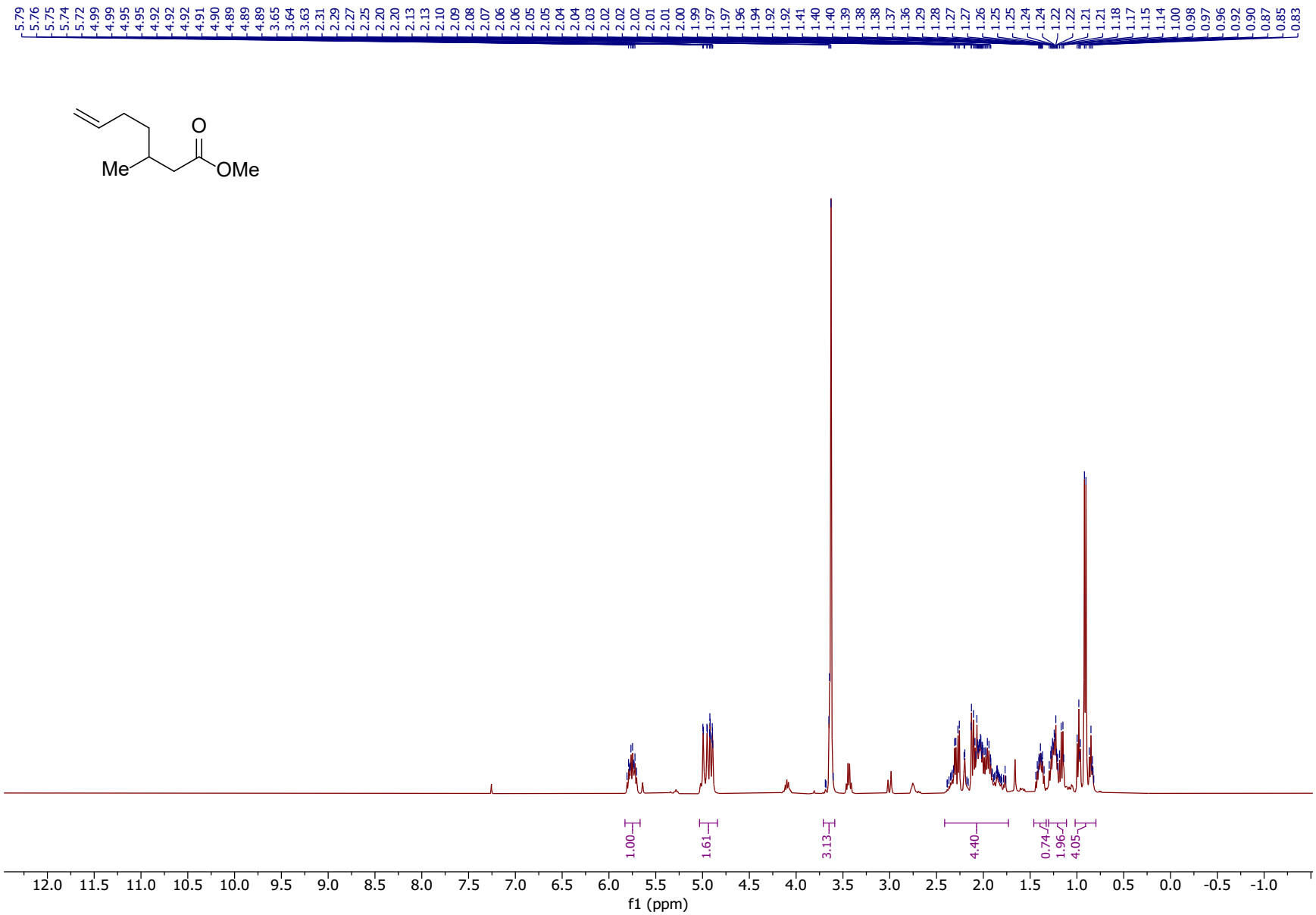

Figure S15: ^{1}H NMR (400 MHz, $CDCl_3$) of saturated ester 17

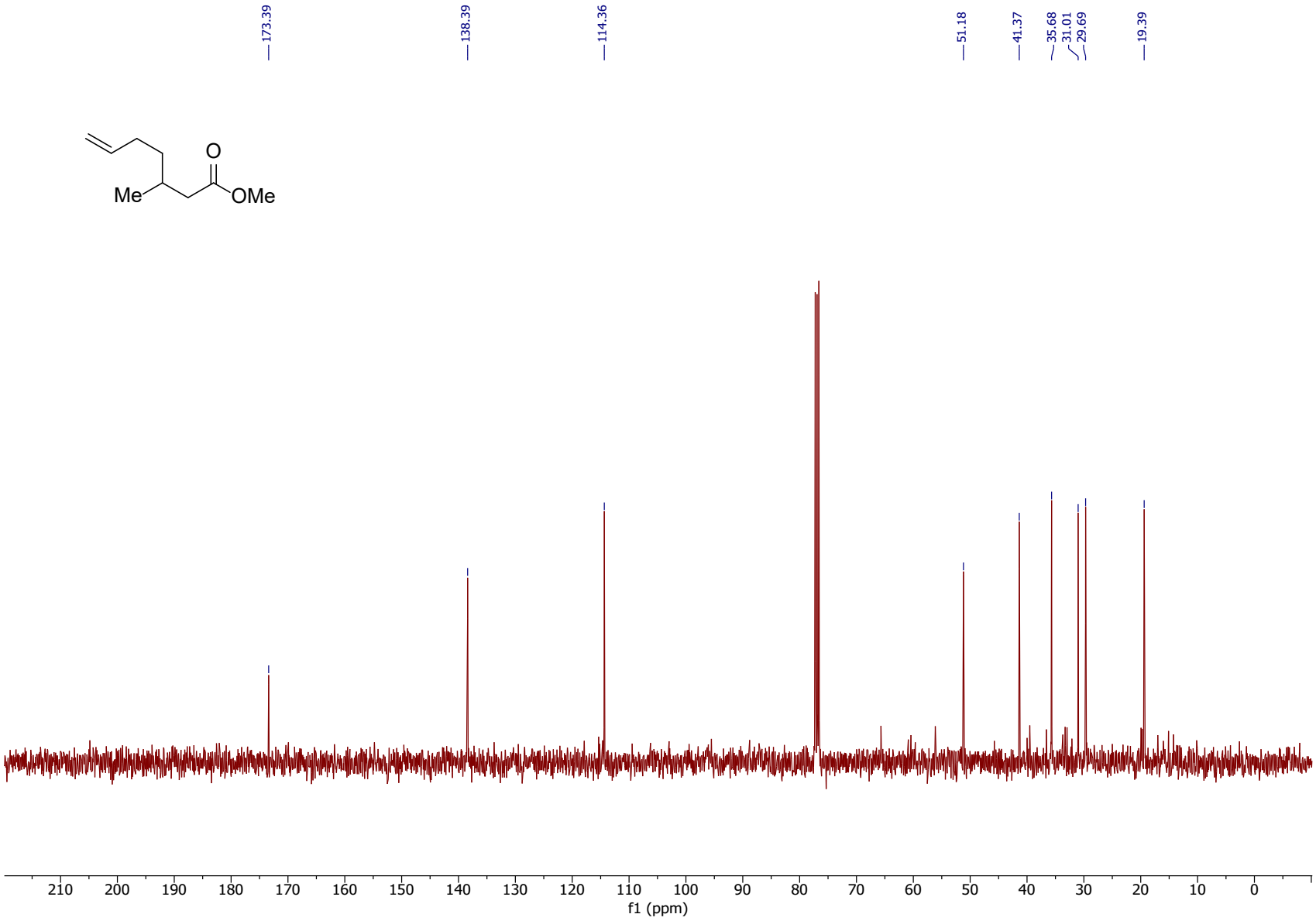

Figure S16: $^{13}C\{^{1}H\}$ (100 MHz, $CDCl_3$) of saturated ester 17

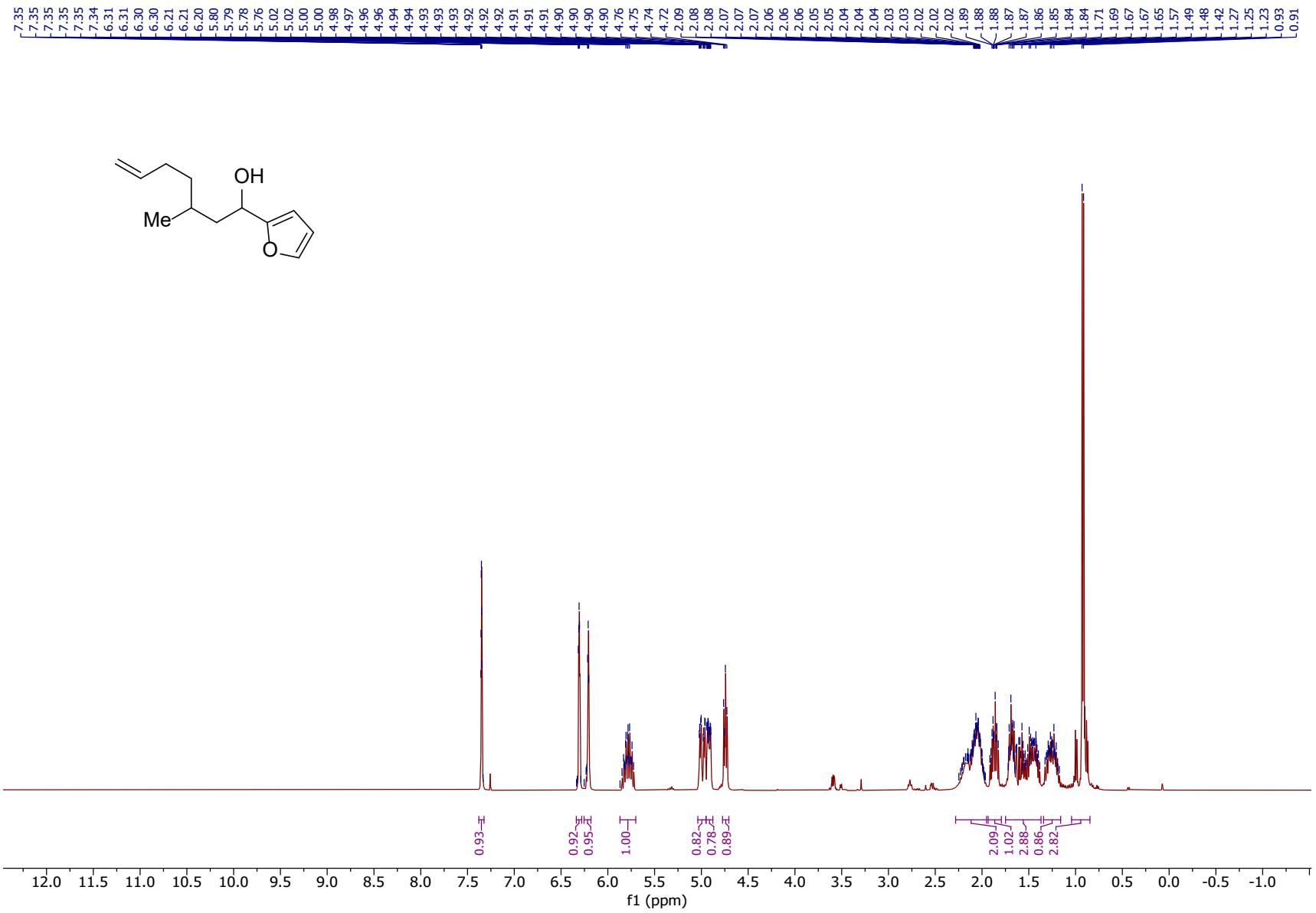

Figure S17: ^{1}H NMR (400 MHz, $CDCl_3$) of furanol 18

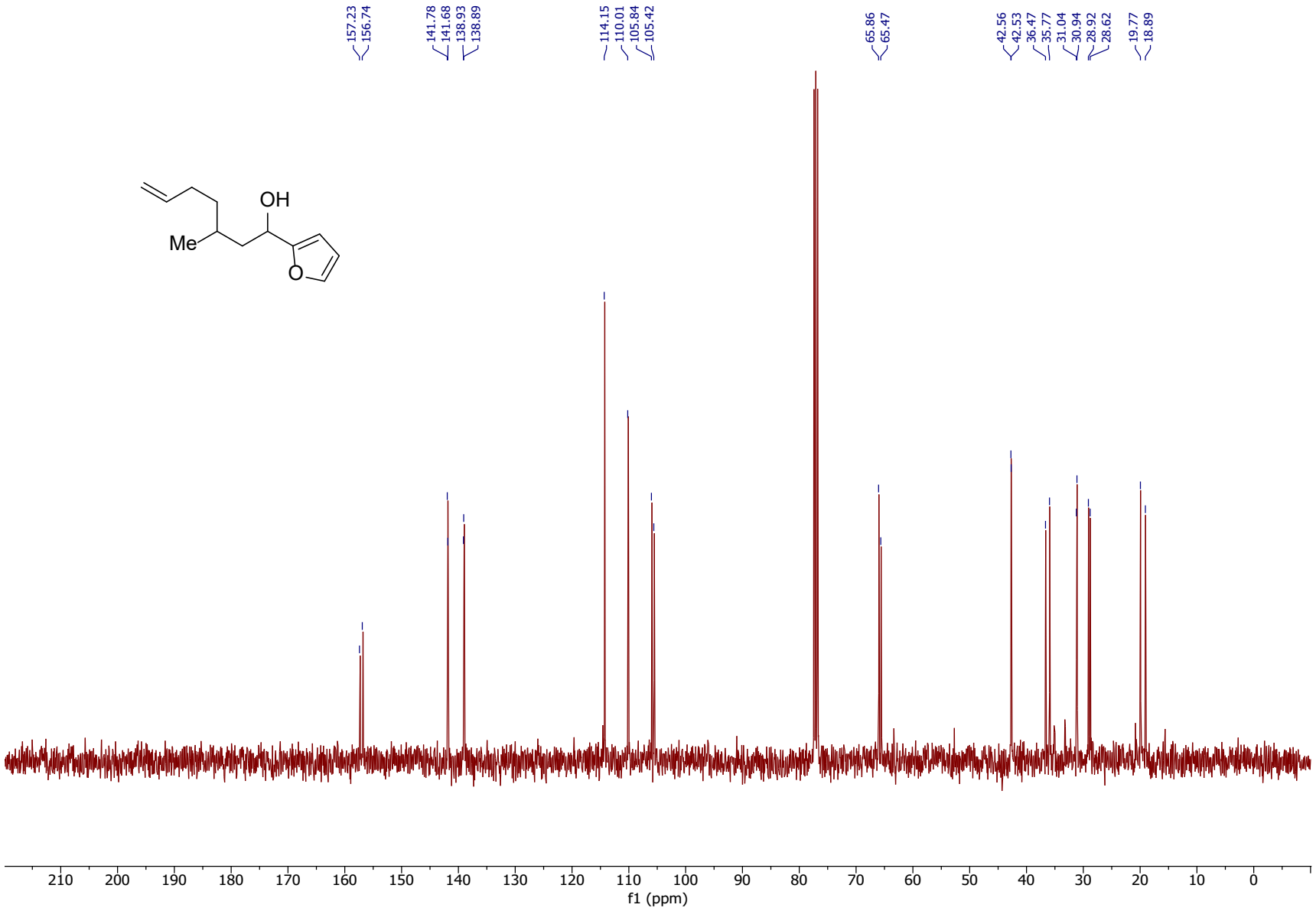

Figure S18: $^{13}C\{^{1}H\}$ (100 MHz, $CDCl_3$) of furanol 18

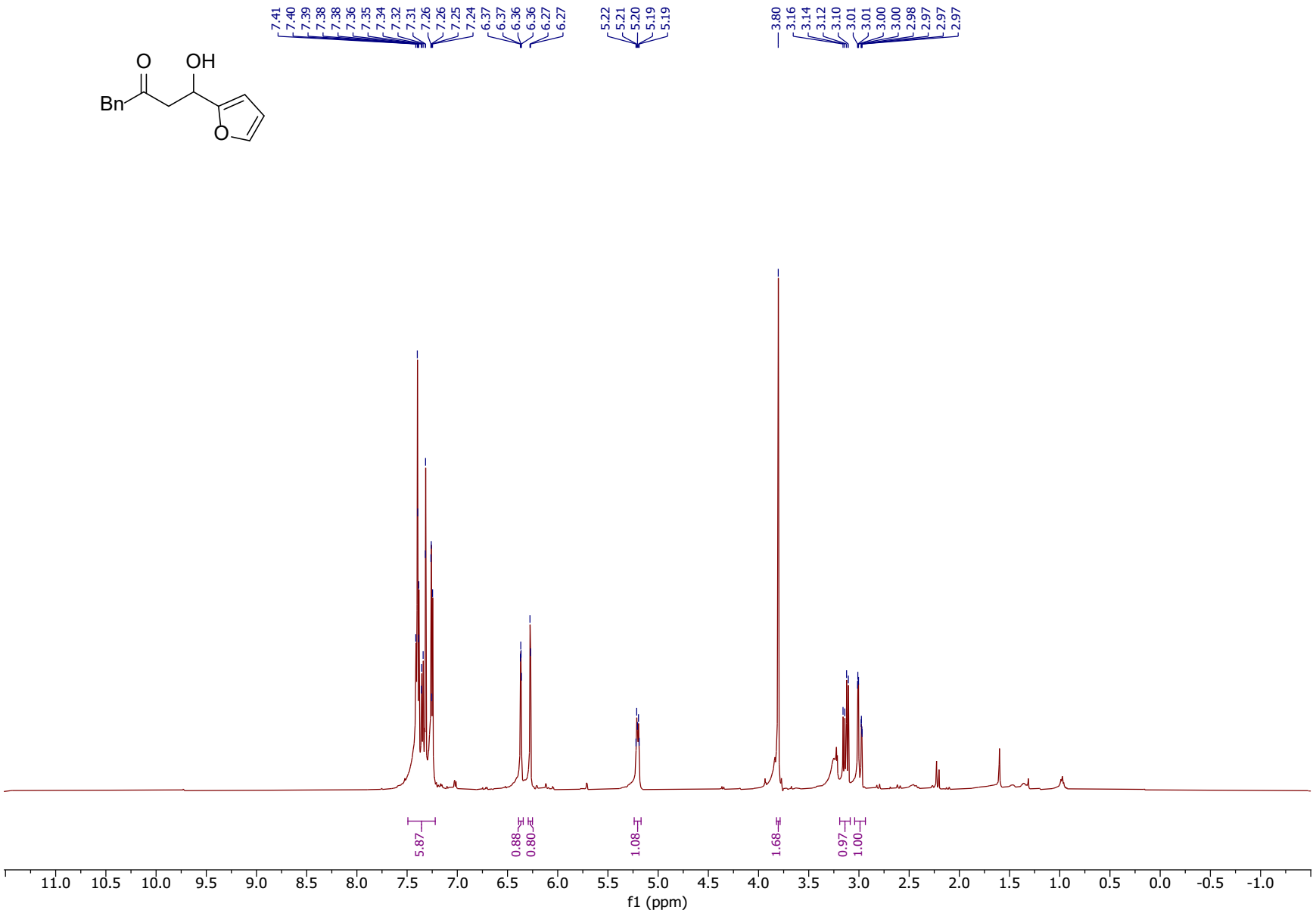

Figure S19: ^{1}H NMR (500 MHz, $CDCl_3$) of β-keto alcohol 19e

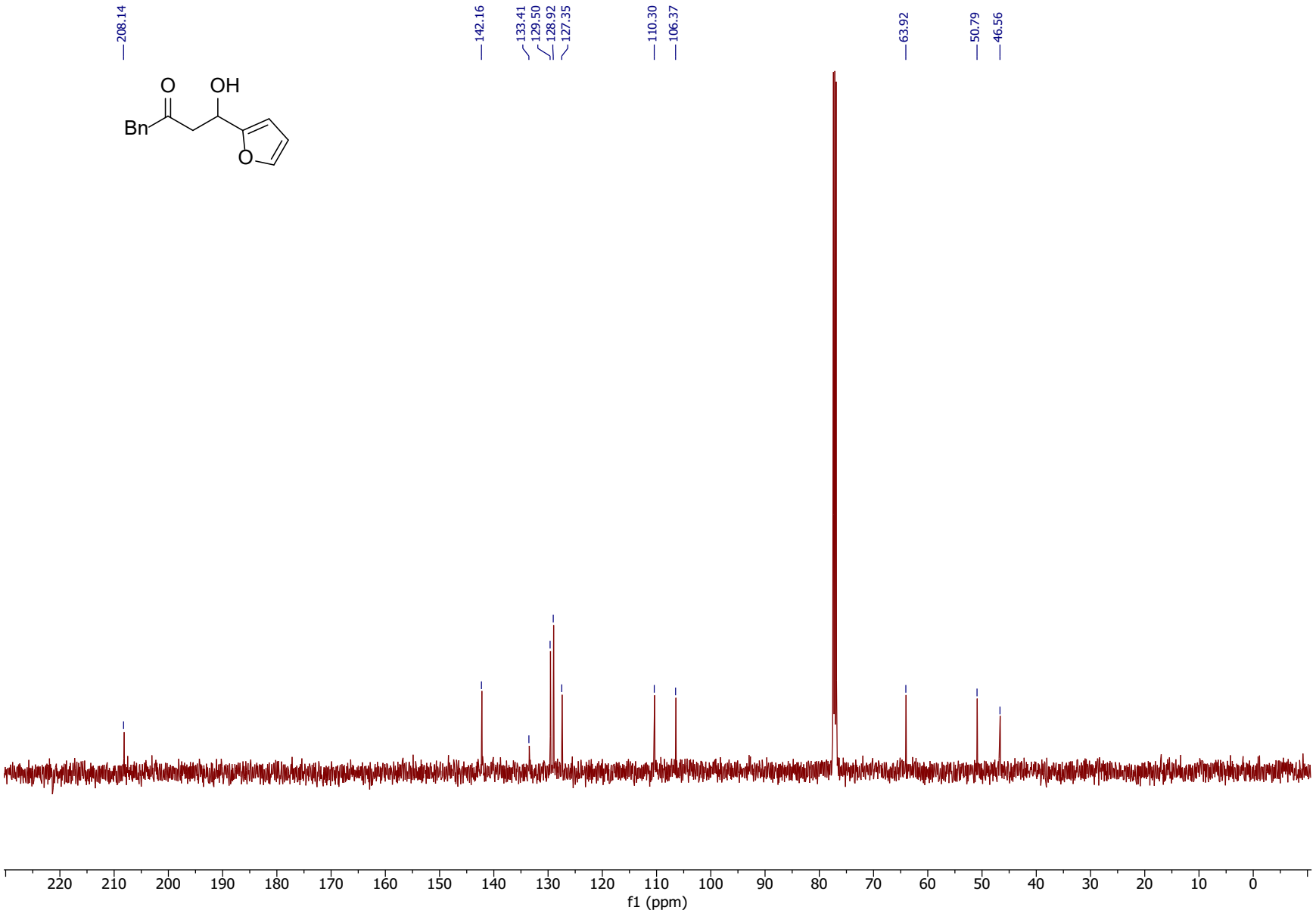

Figure S20: $^{13}C\{^{1}H\}$ (125 MHz, $CDCl_3$) of β-keto alcohol 19e

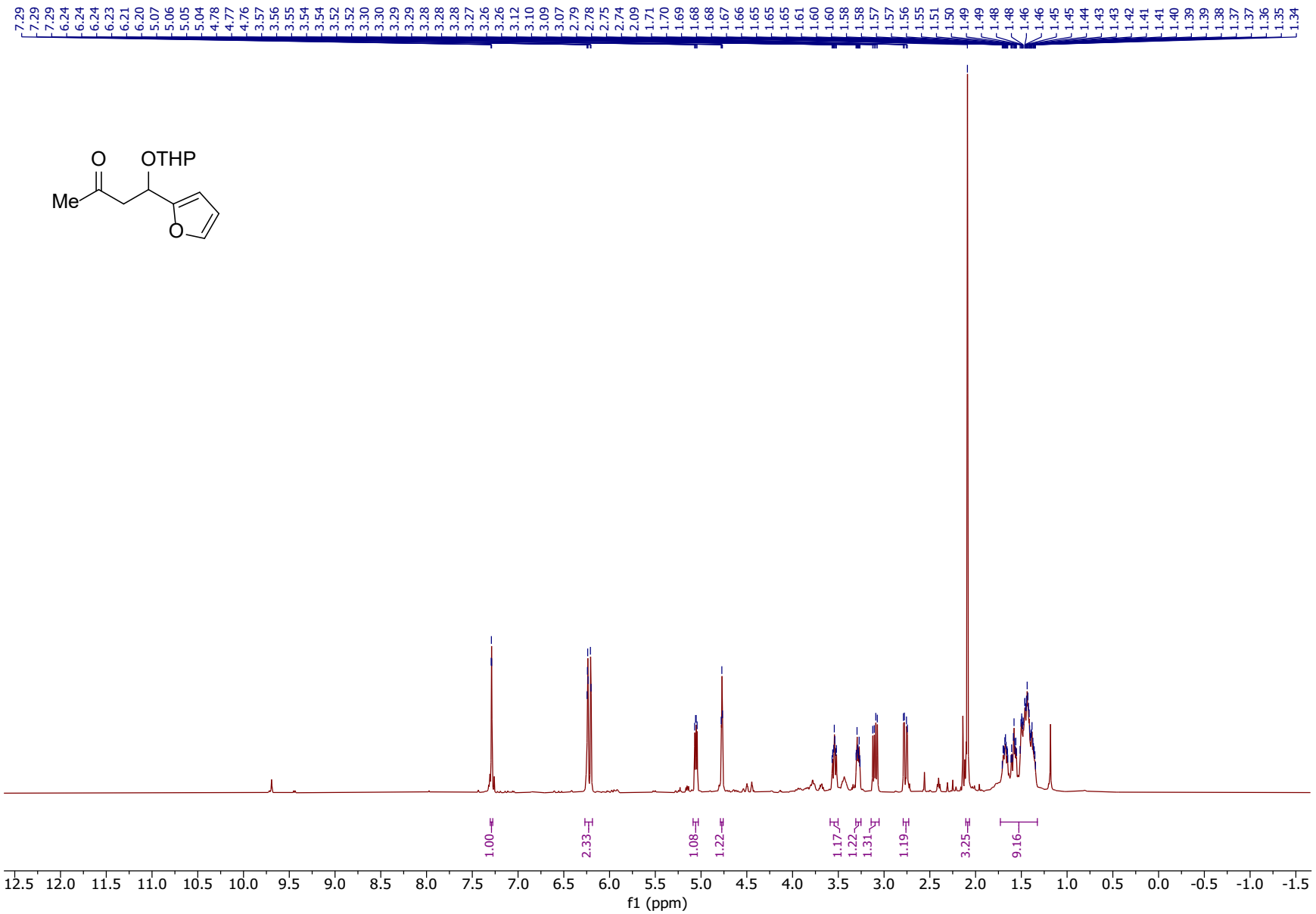

Figure S21: ^{1}H NMR (500 MHz, $CDCl_3$) of keto 20a

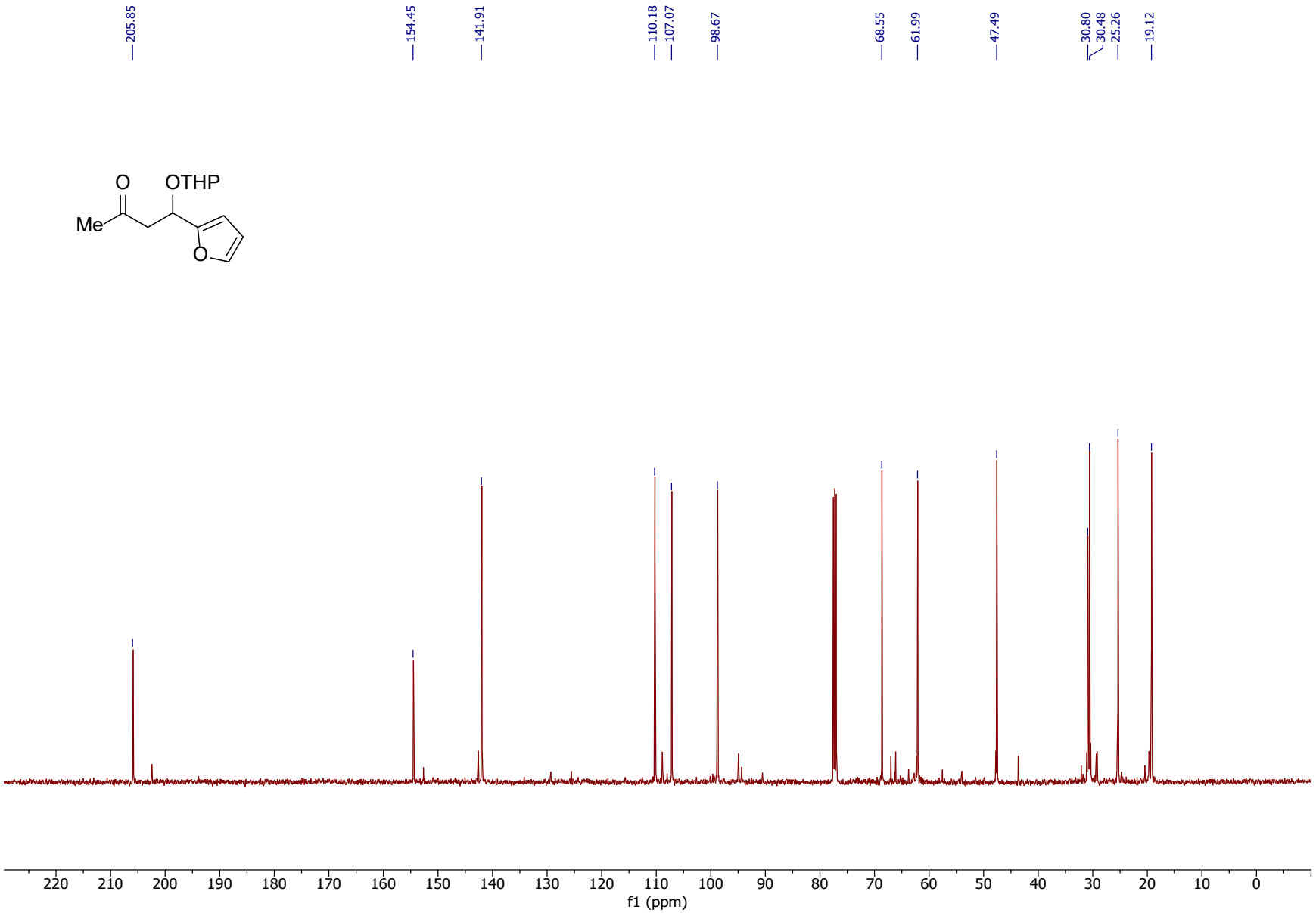

Figure S22: $^{13}C\{^{1}H\}$ (125 MHz, $CDCl_3$) of keto 20a

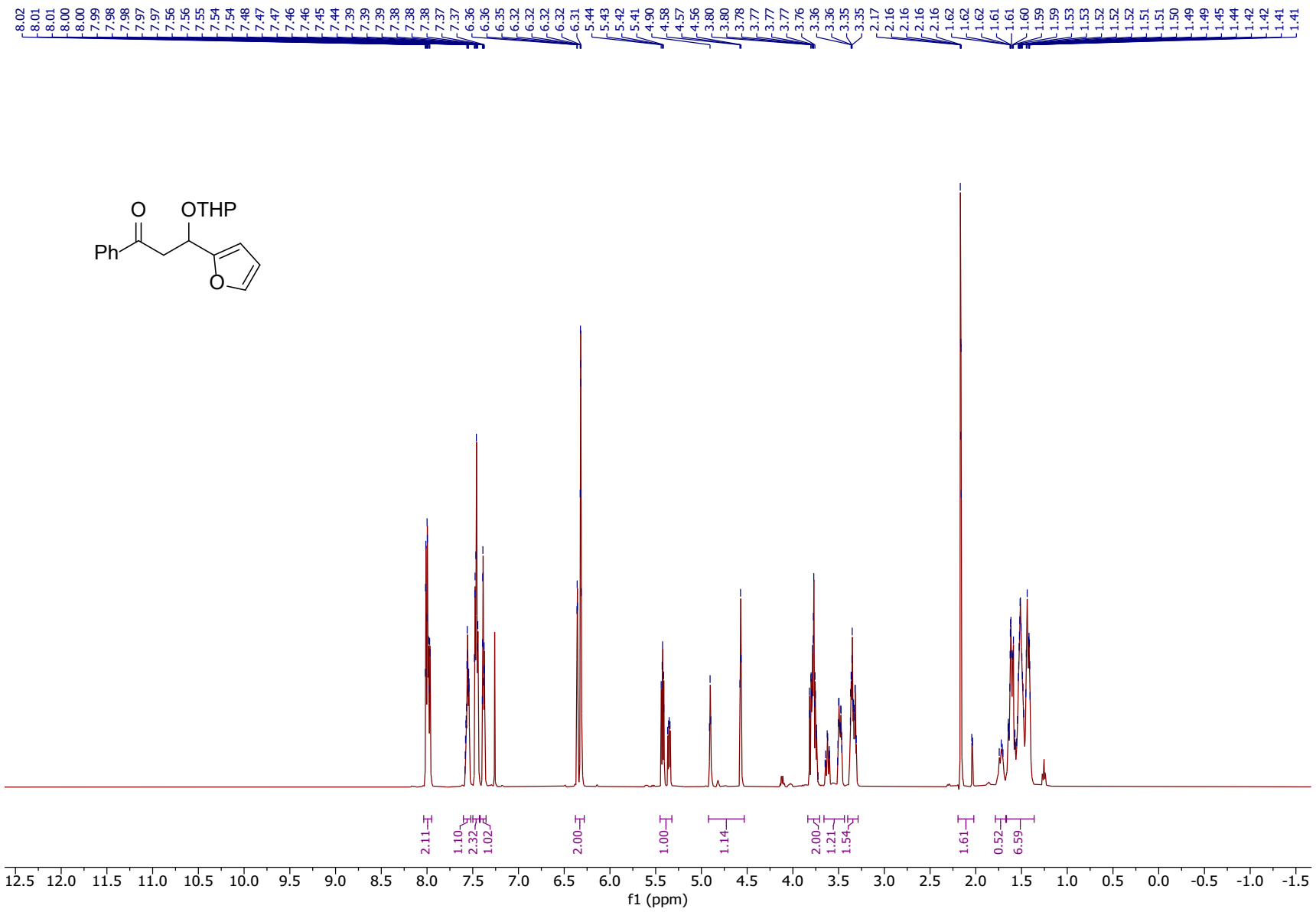

Figure S23: ^{1}H NMR (500 MHz, $CDCl_3$) of keto 20b

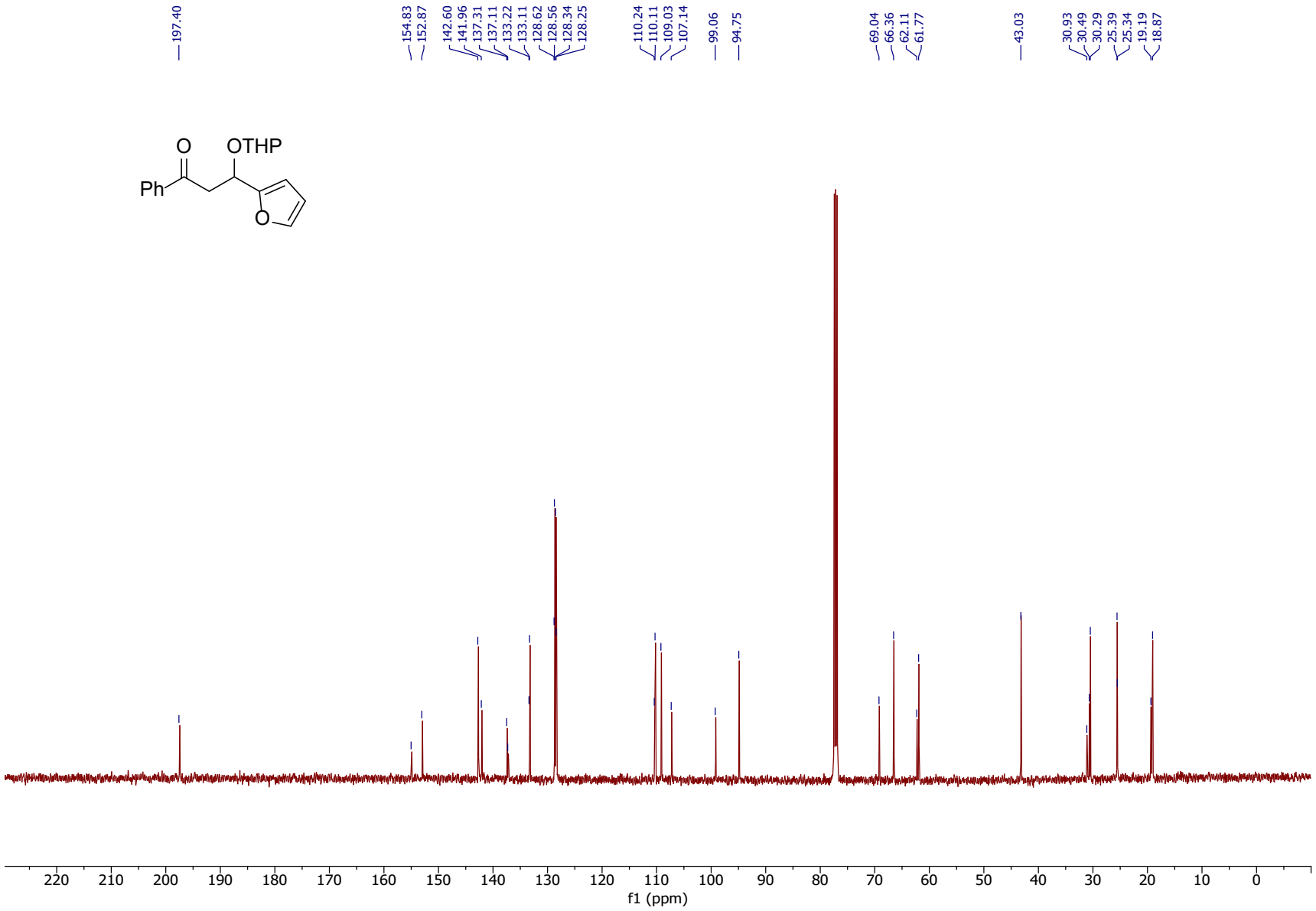

Figure S24: $^{13}C\{^{1}H\}$ (125 MHz, $CDCl_3$) of keto 20b

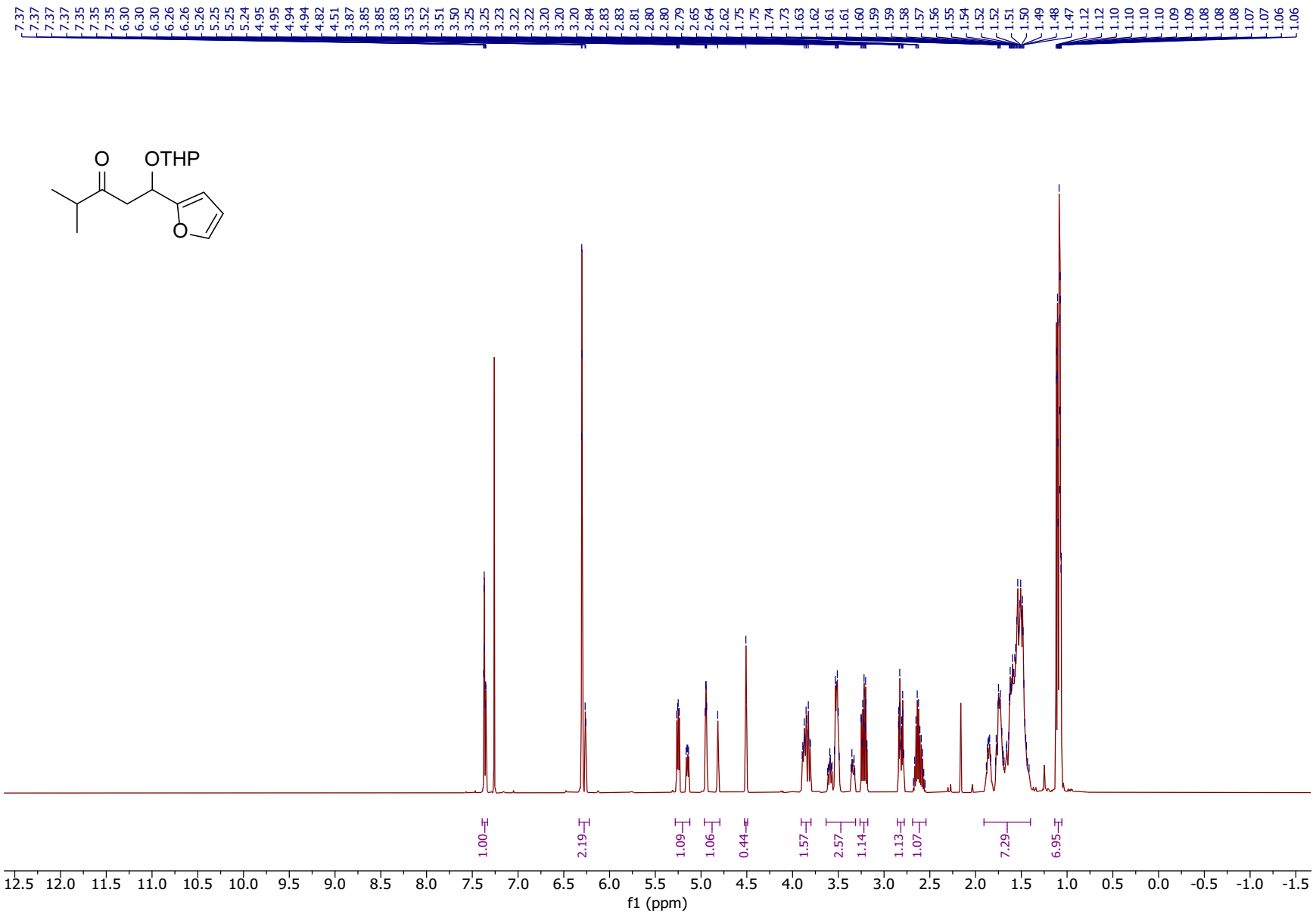

Figure S25: ^{1}H NMR (500 MHz, $CDCl_3$) of keto 20c

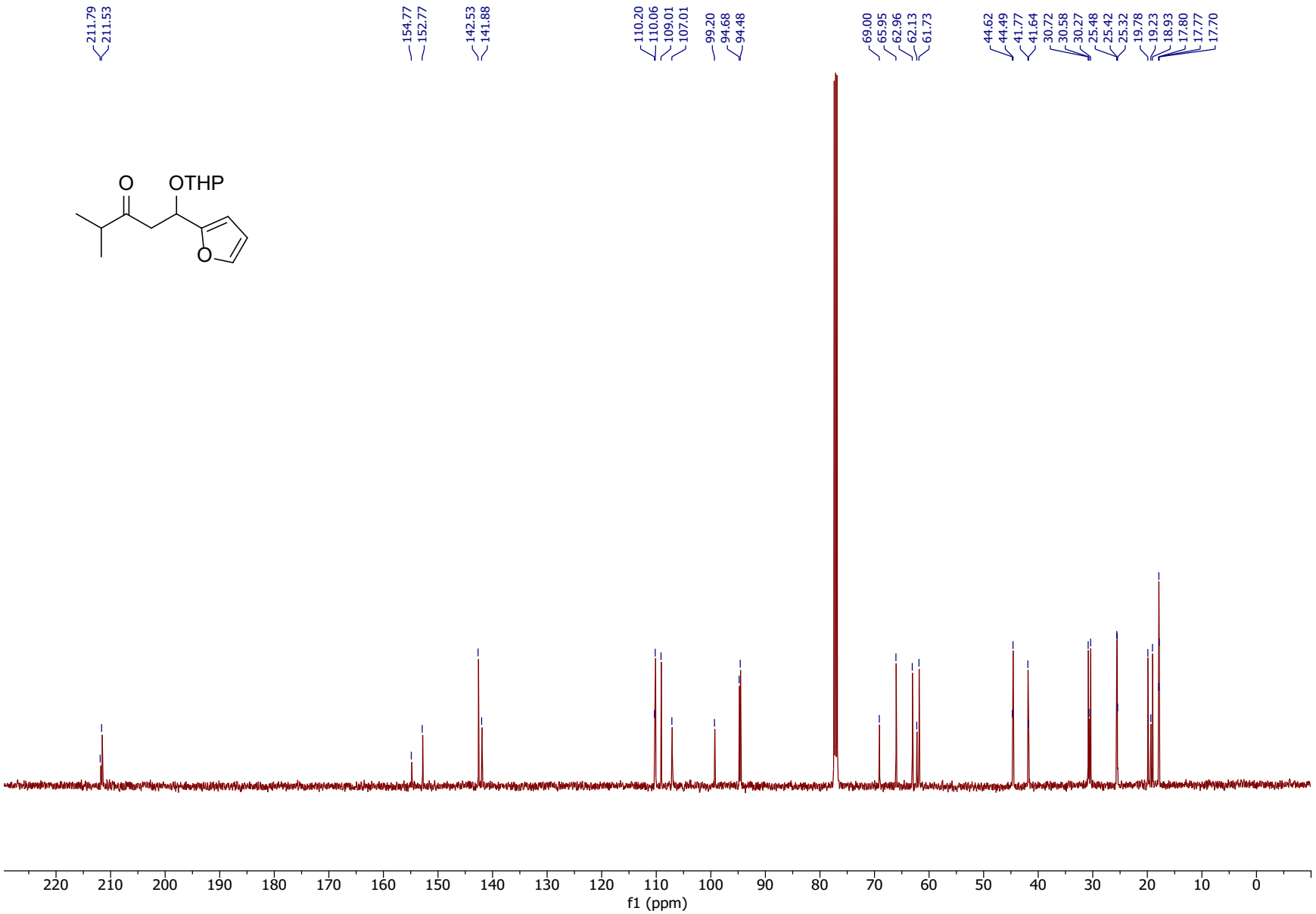

Figure S26: $^{13}C\{^{1}H\}$ (125 MHz, $CDCl_3$) of keto 20c

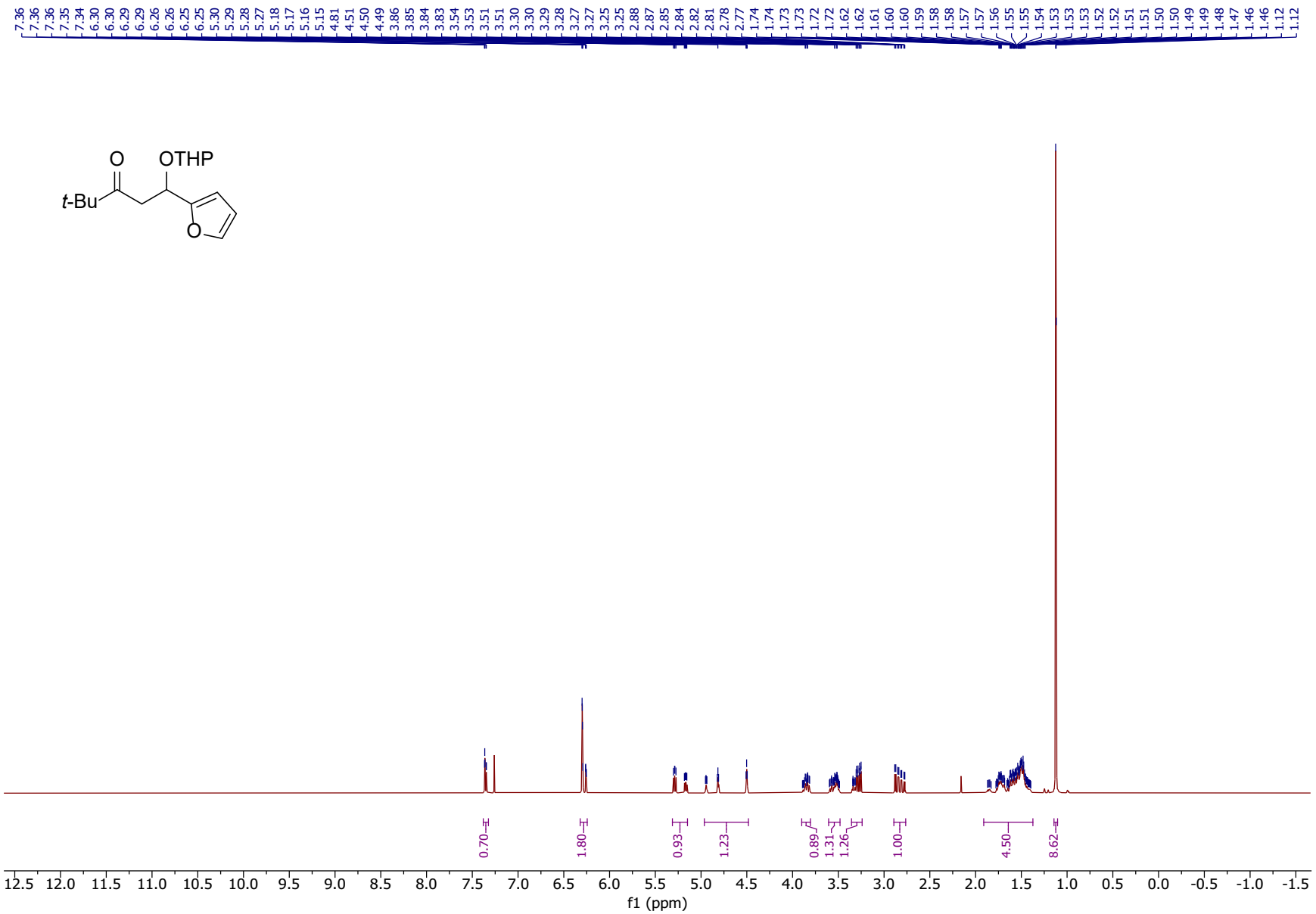

Figure S27: ^{1}H NMR (500 MHz, $CDCl_3$) of keto 20d

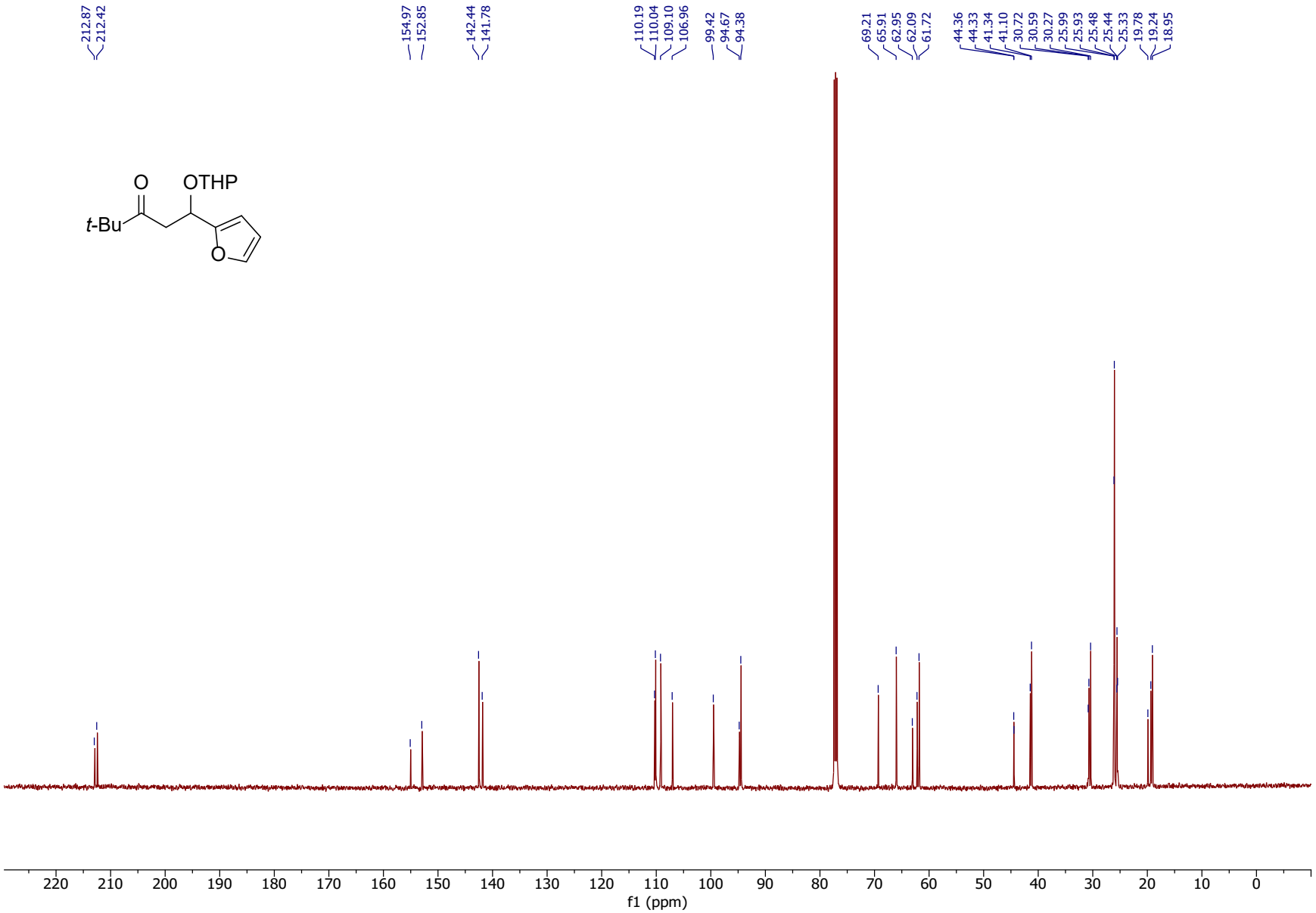

Figure S28: $^{13}C\{^{1}H\}$ (125 MHz, $CDCl_3$) of keto 20d

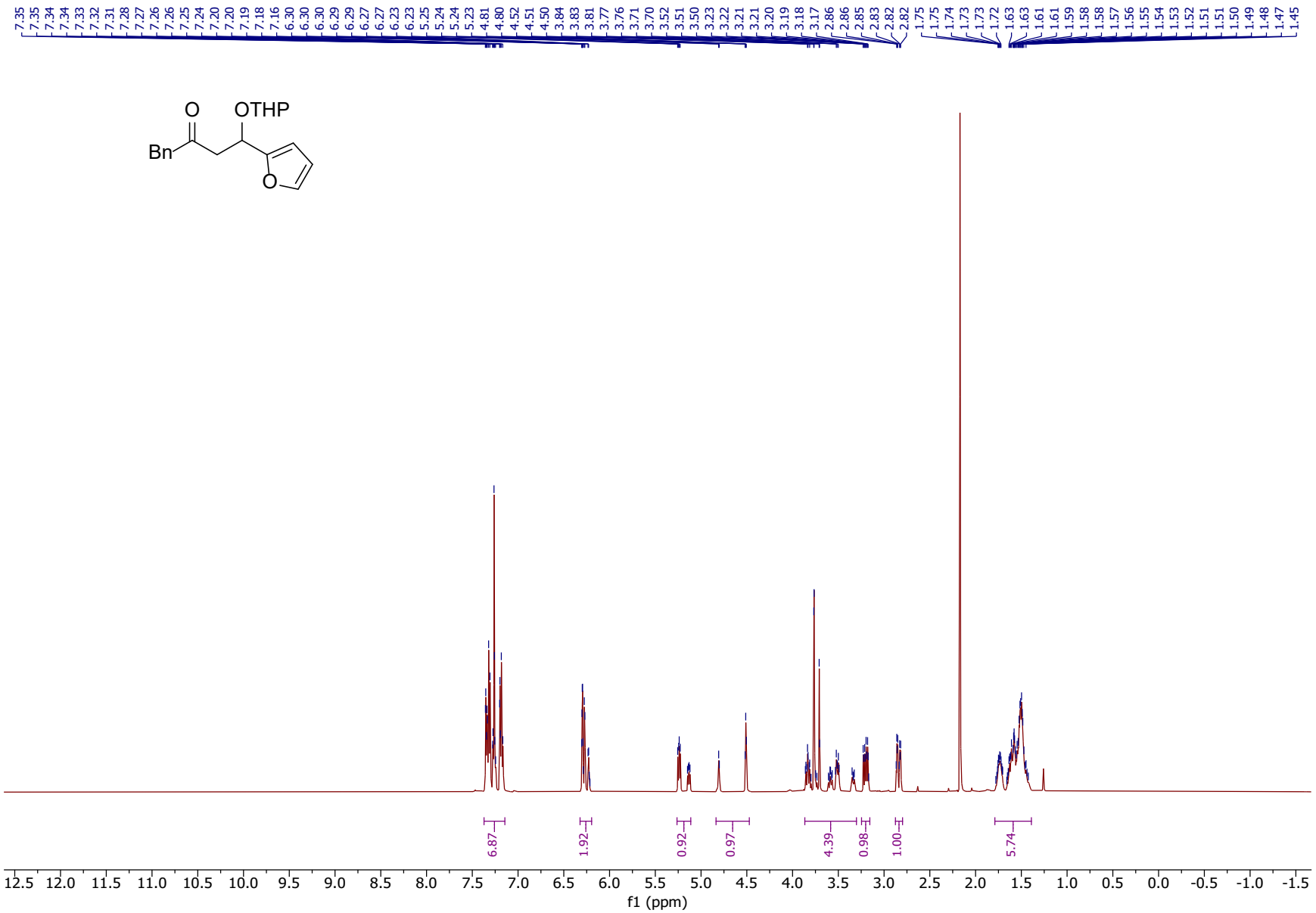

Figure S29: ^{1}H NMR (500 MHz, $CDCl_3$) of keto 20e

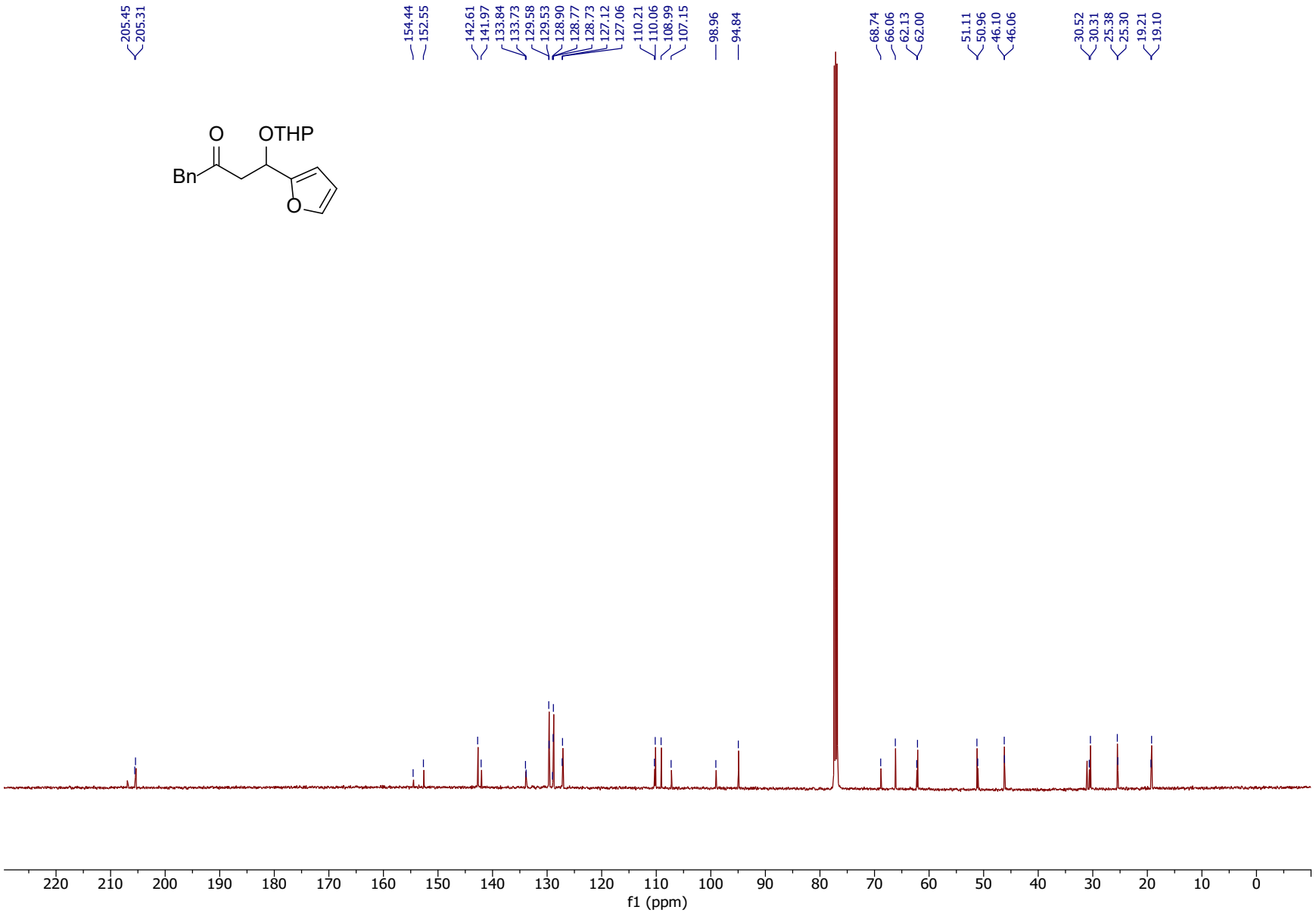

Figure S30: $^{13}C\{^{1}H\}$ (125 MHz, $CDCl_3$) of keto 20e

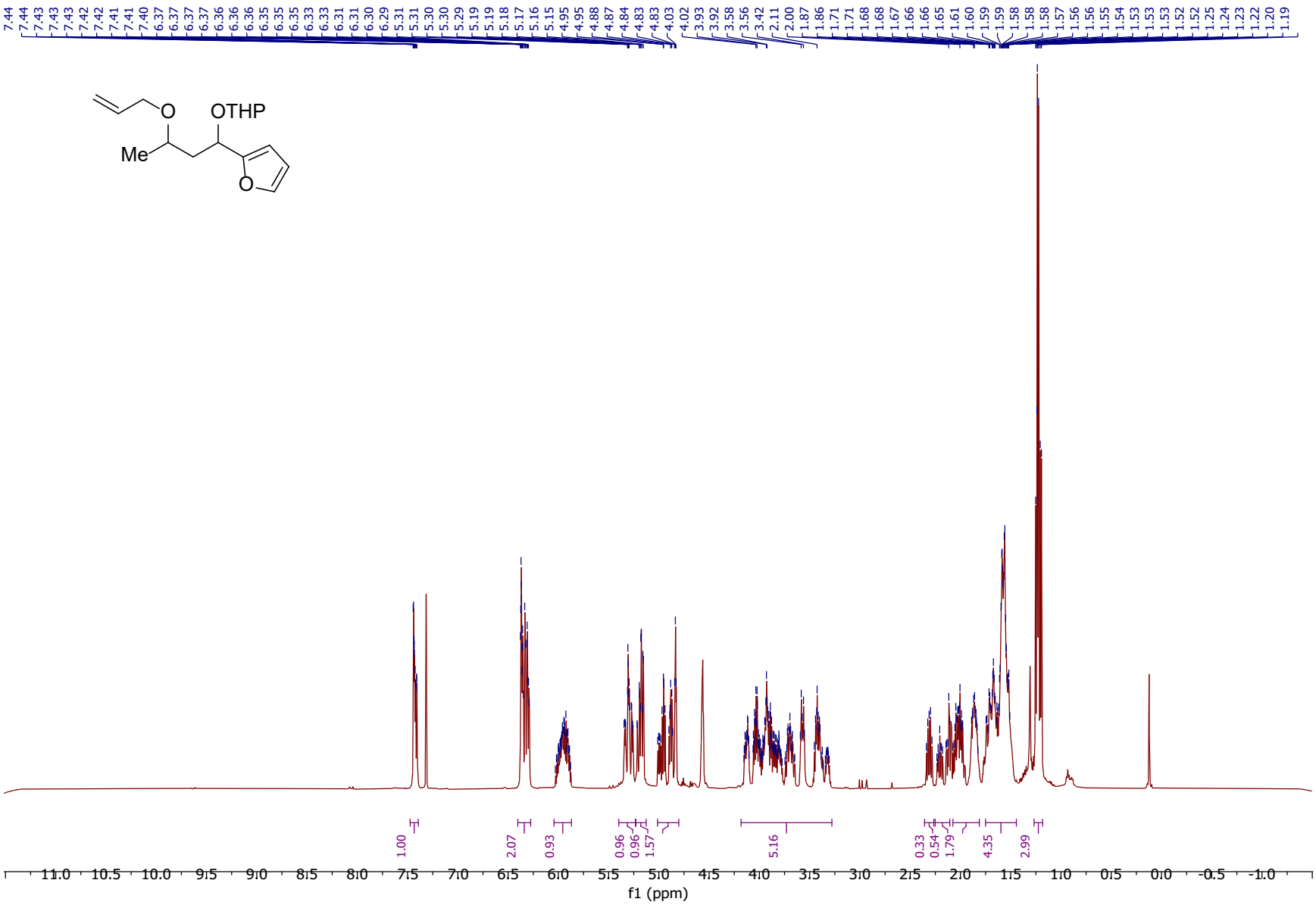

Figure S31: ^{1}H NMR (500 MHz, $CDCl_3$) of allyloxy 21a

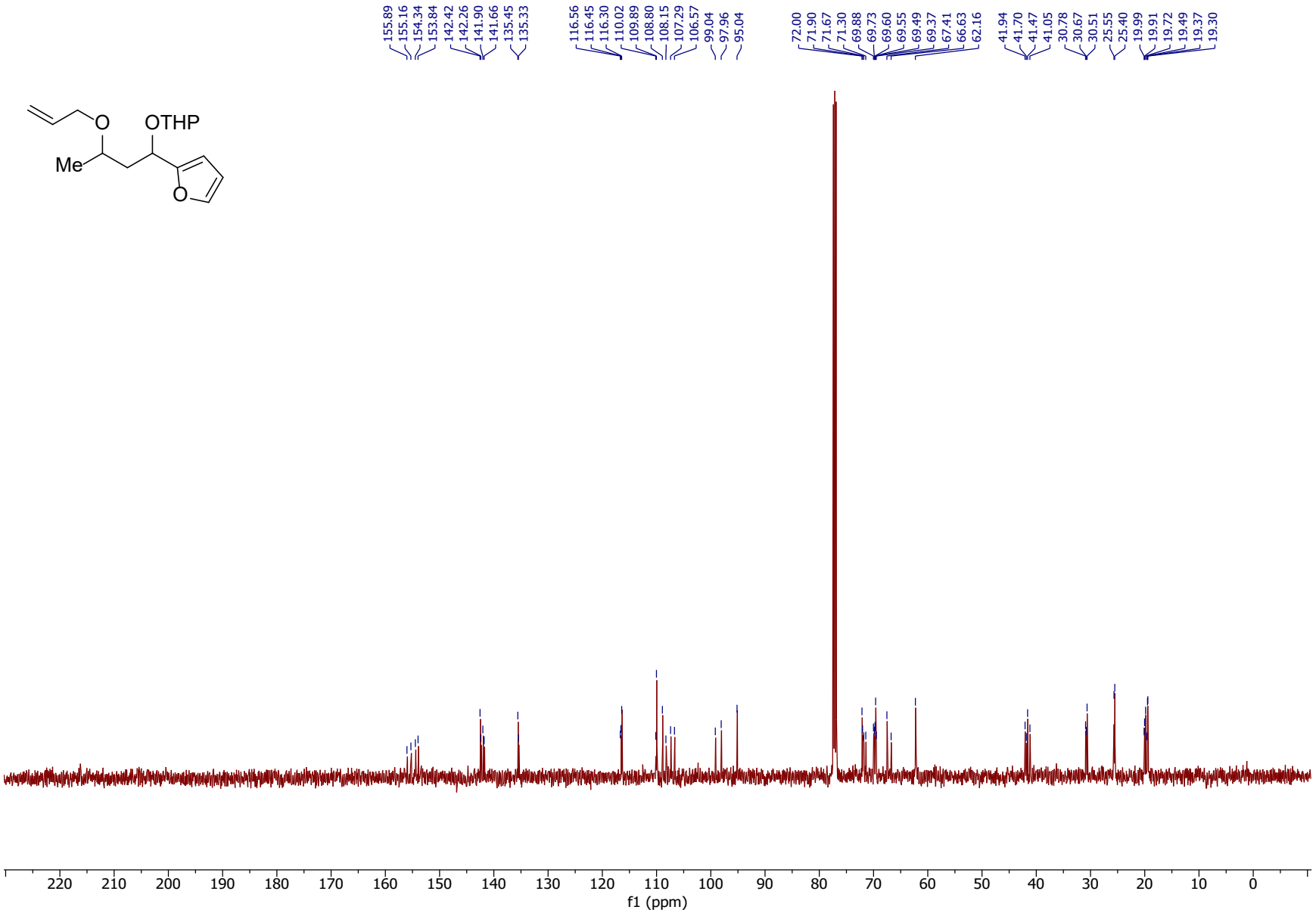

Figure S32: $^{13}C\{^{1}H\}$ (125 MHz, $CDCl_3$) of allyloxy 21a

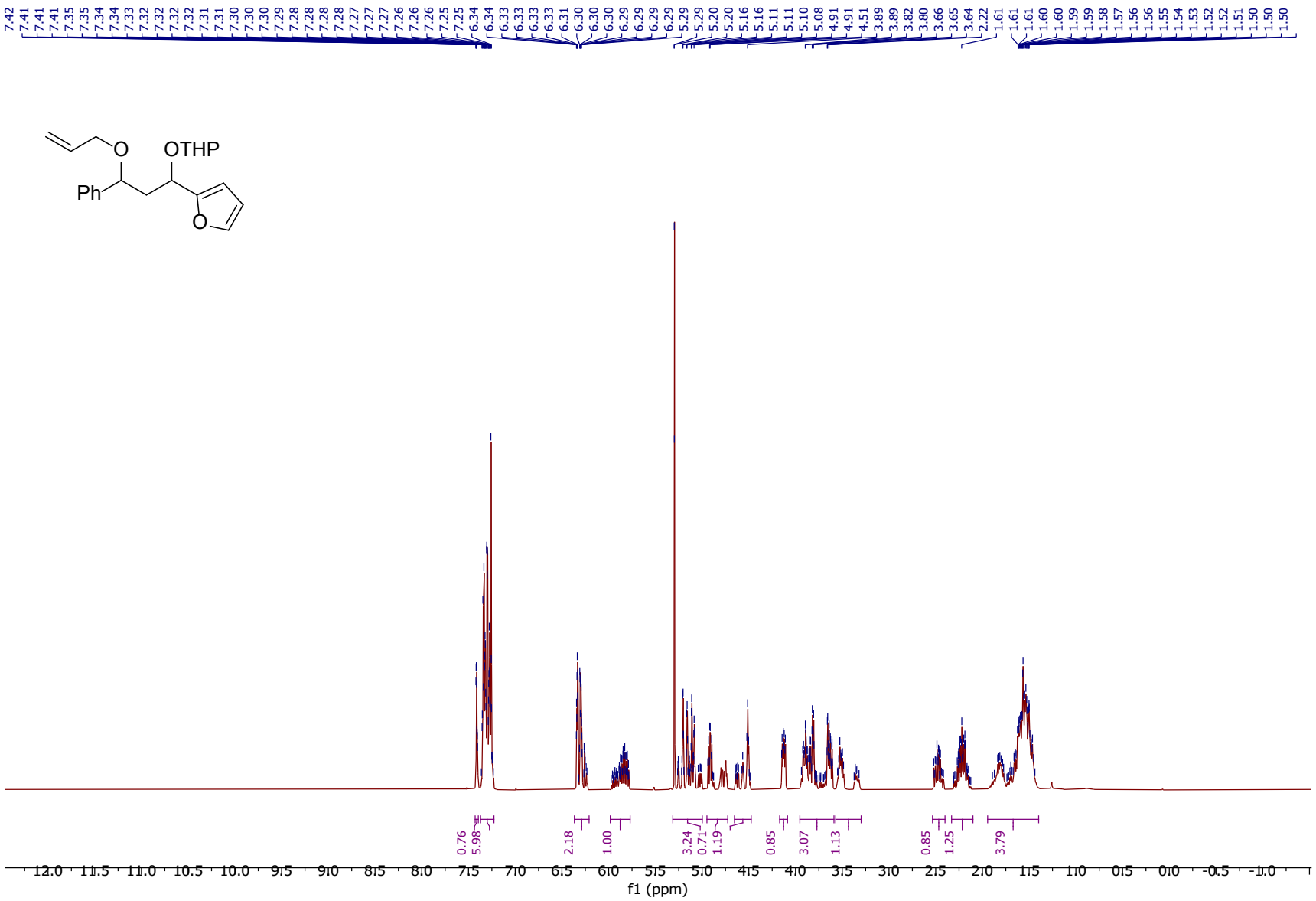

Figure S33: ^{1}H NMR (400 MHz, $CDCl_3$) of allyloxy 21b

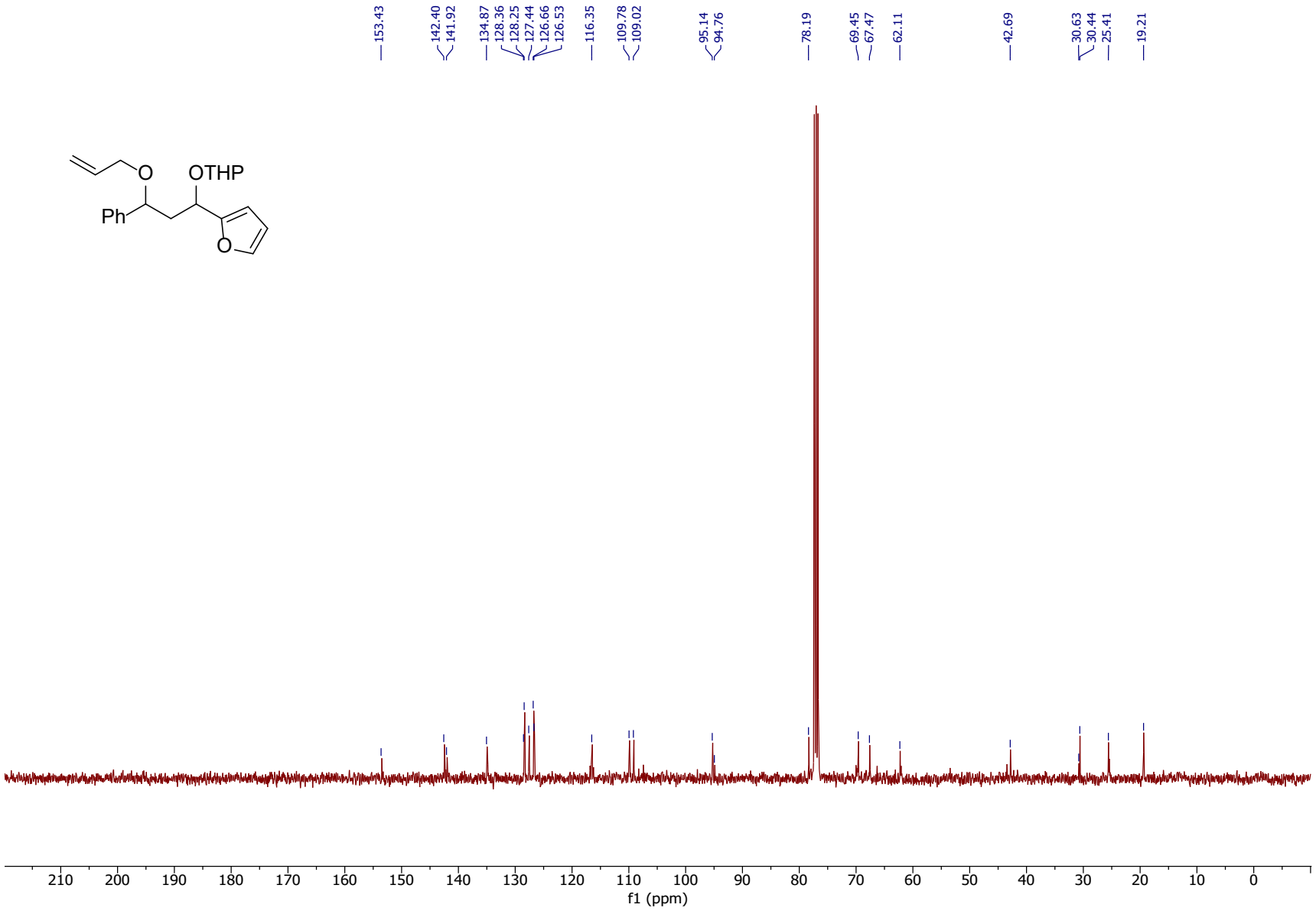

Figure S34: $^{13}C\{^{1}H\}$ (100 MHz, $CDCl_3$) of allyloxy 21b

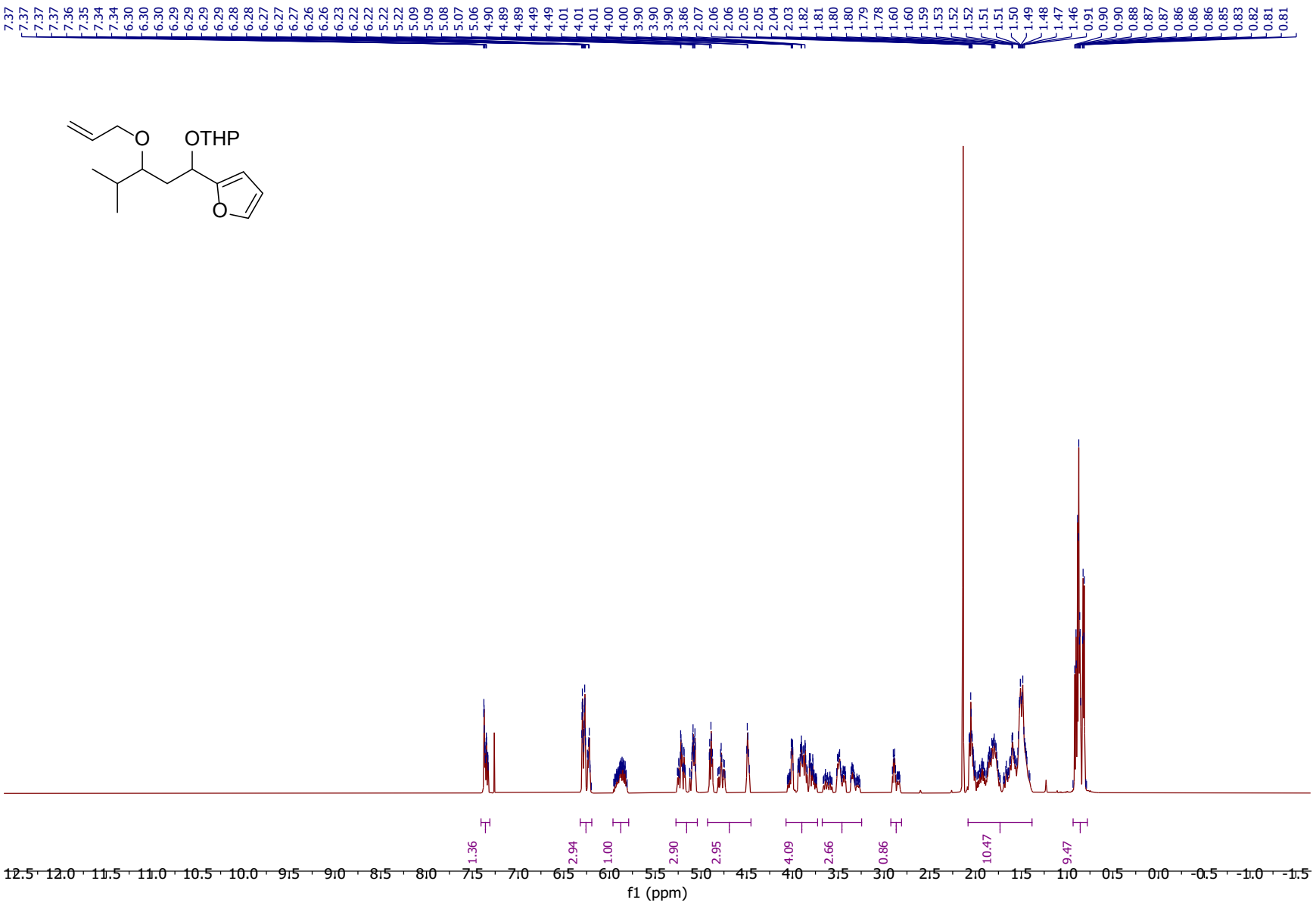

Figure S35: ^{1}H NMR (500 MHz, $CDCl_3$) of allyloxy 21c

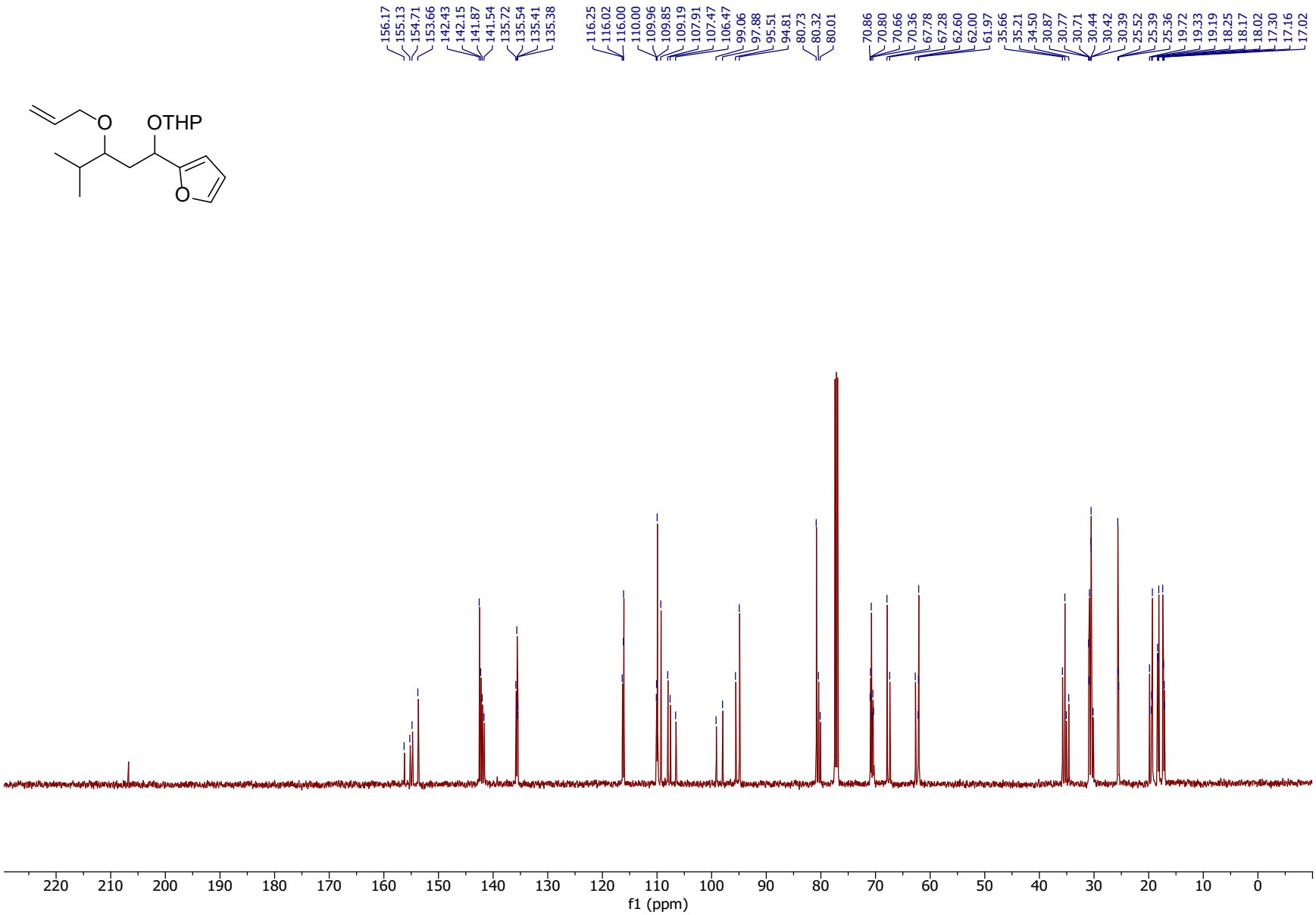

Figure S36: $^{13}C\{^{1}H\}$ (125 MHz, $CDCl_3$) of allyloxy 21c

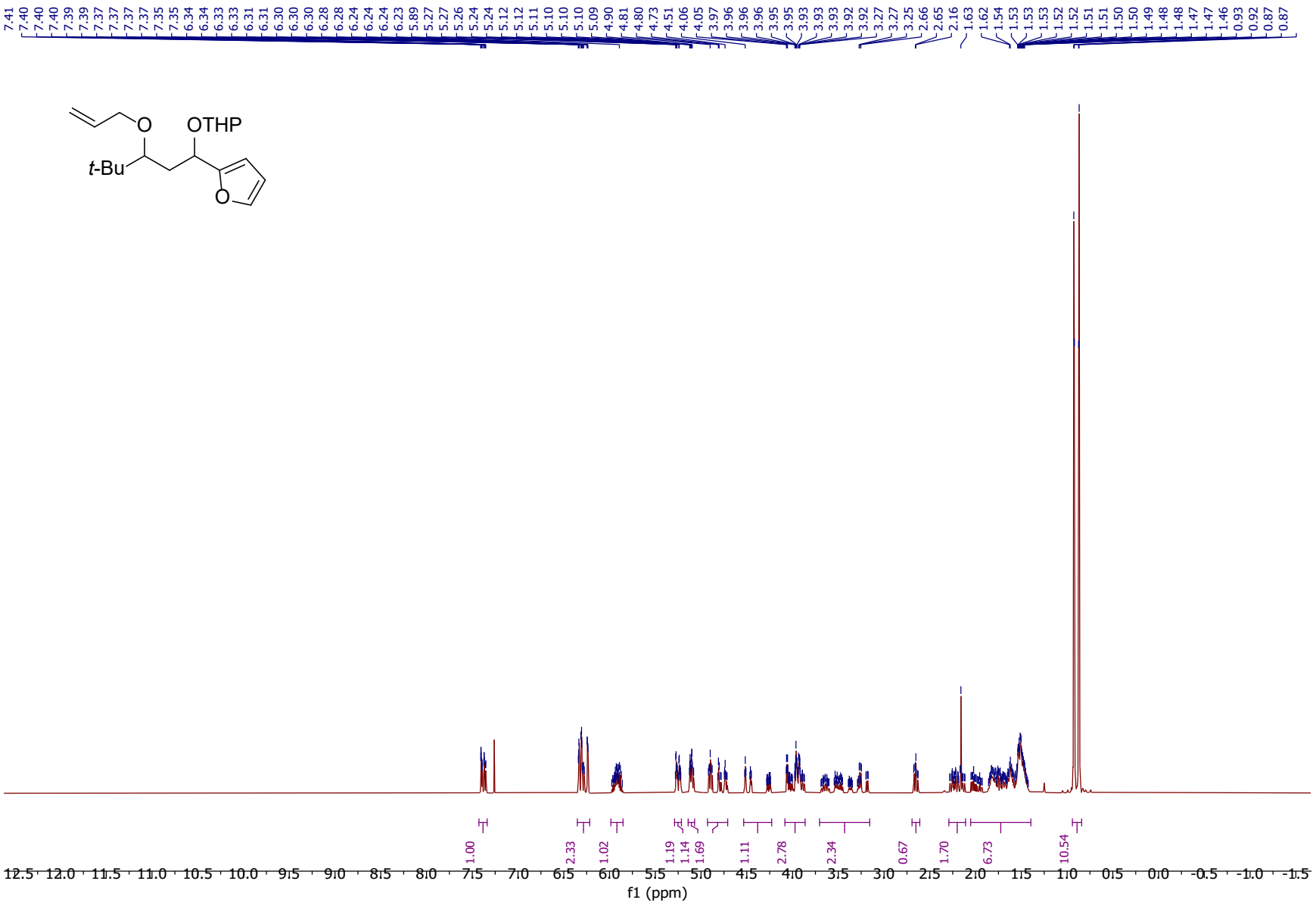

Figure S37: ^{1}H NMR (500 MHz, $CDCl_3$) of allyloxy 21d

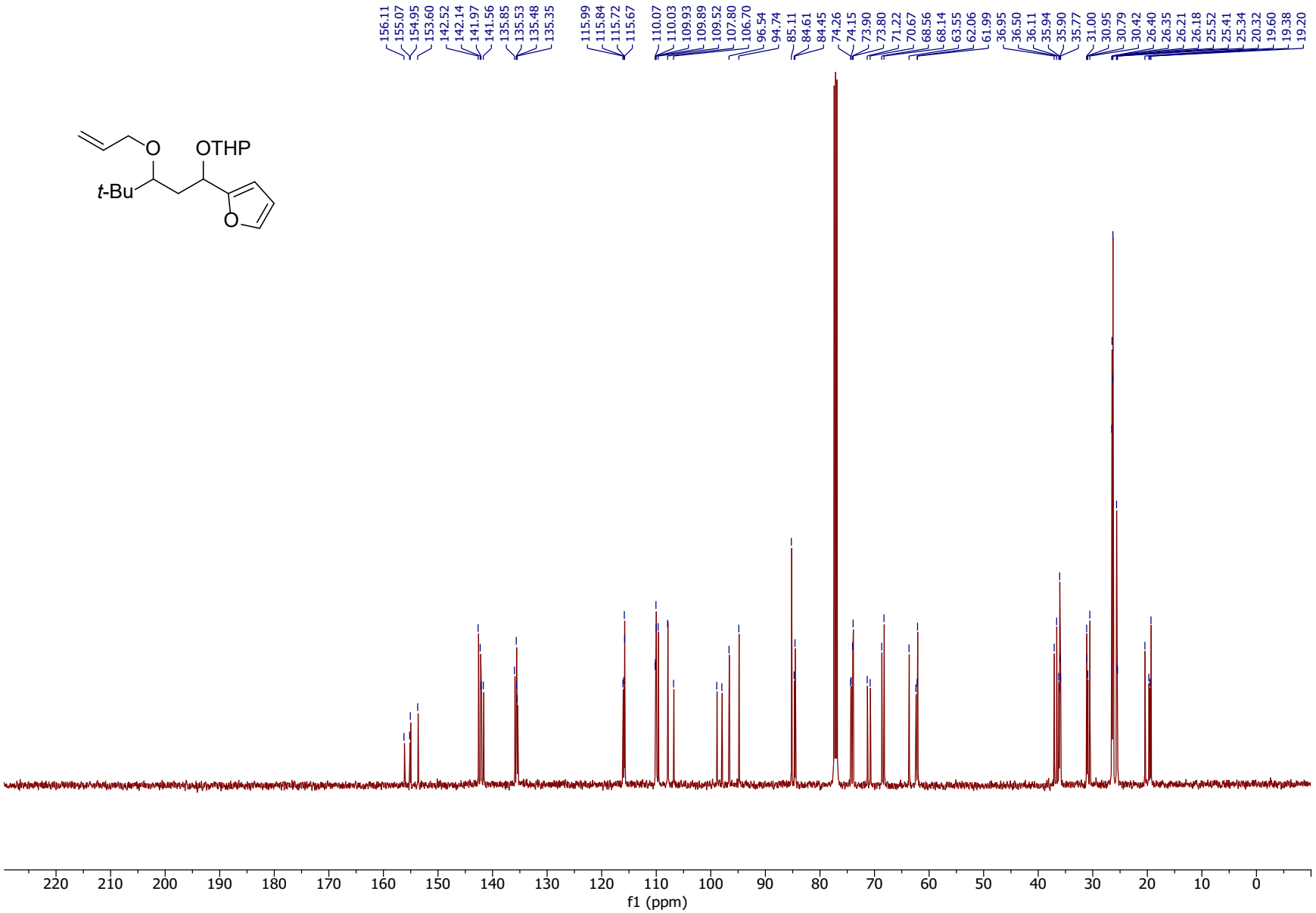

Figure S38: $^{13}C\{^{1}H\}$ (125 MHz, $CDCl_3$) of allyloxy 21d

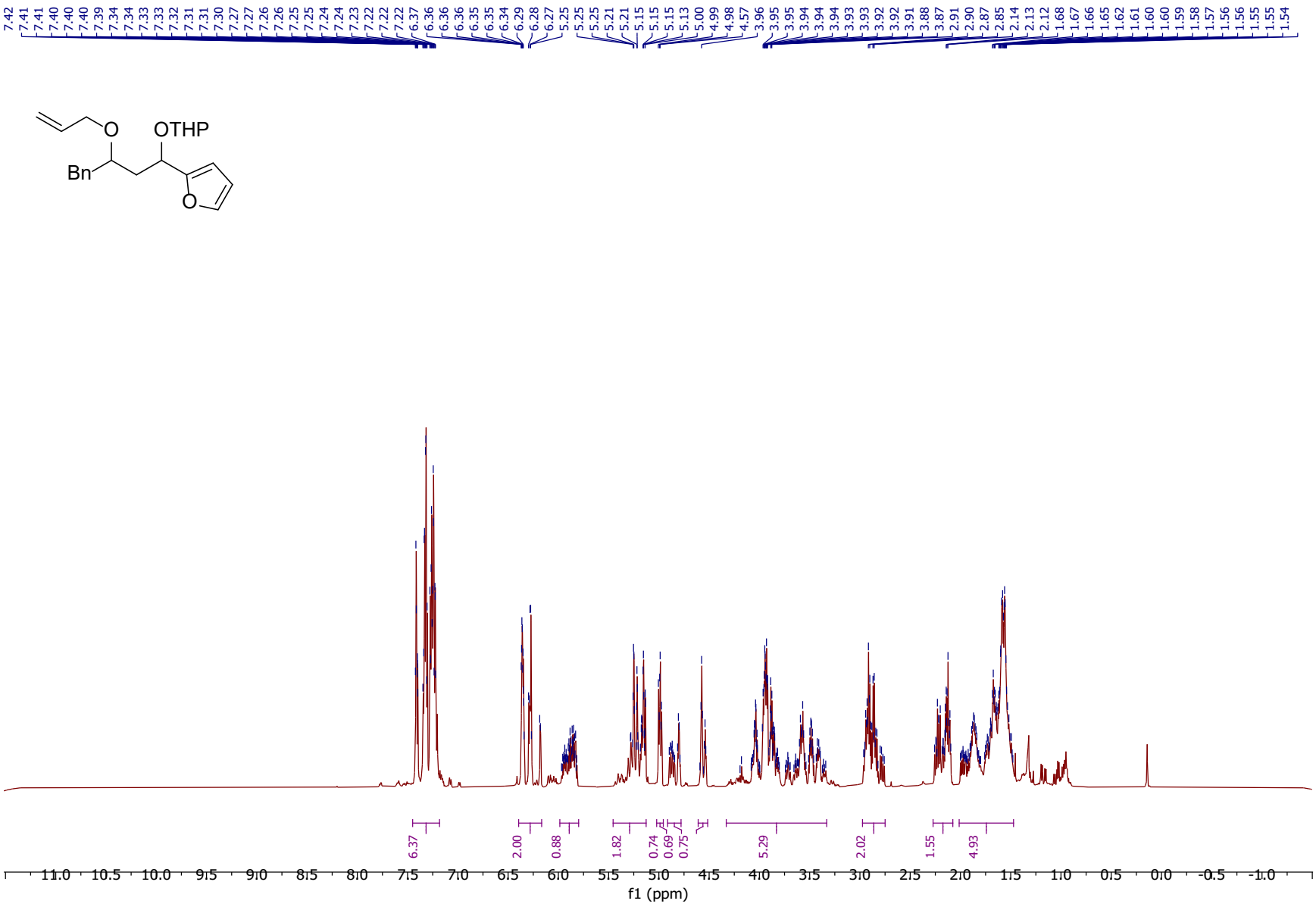

Figure S39: ^{1}H NMR (500 MHz, $CDCl_3$) of allyloxy 21e

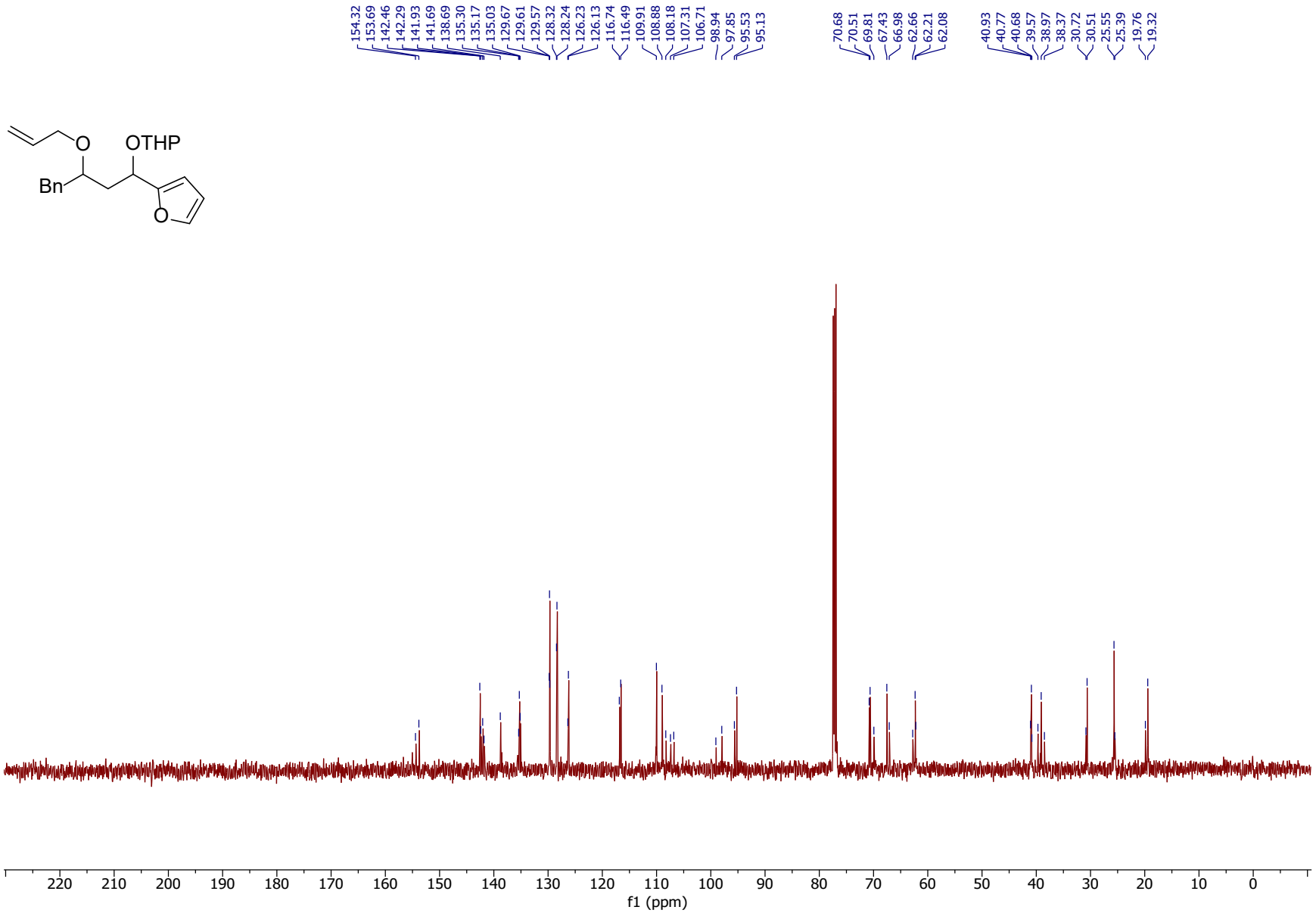

Figure S40: $^{13}C\{^{1}H\}$ (125 MHz, $CDCl_3$) of allyloxy 21e

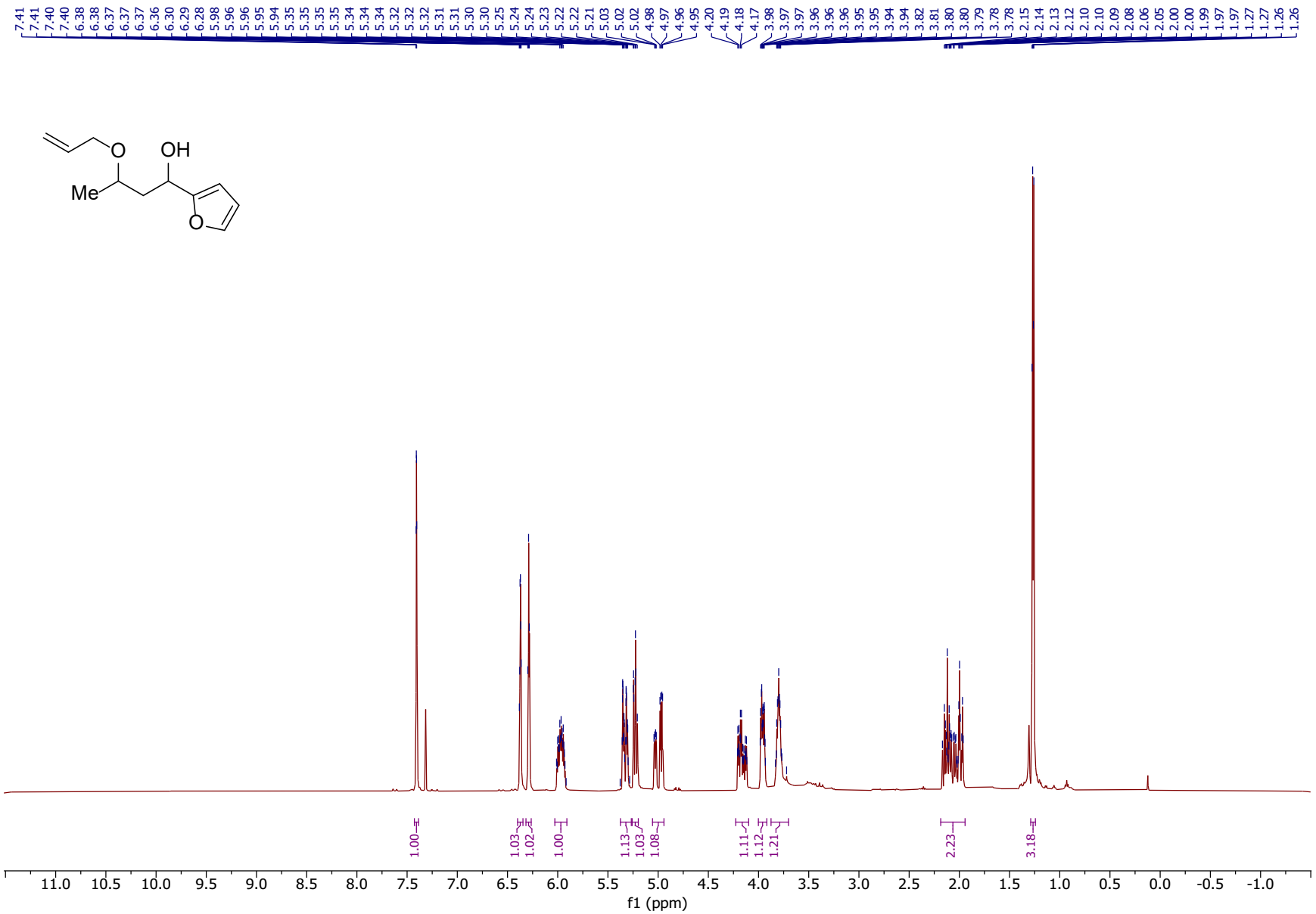

Figure S41: ^{1}H NMR (500 MHz, $CDCl_3$) of furanol 22a

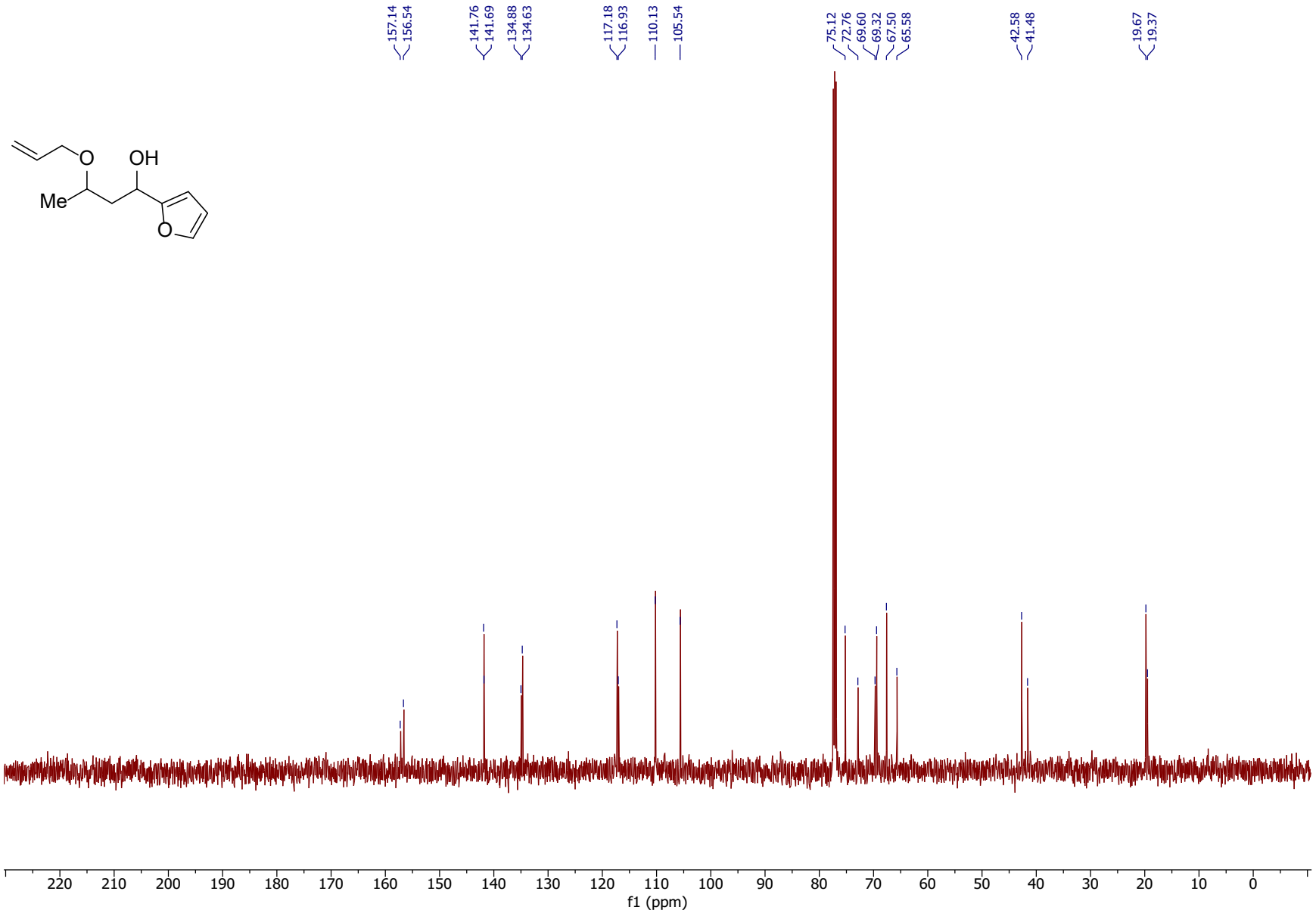

Figure S42: $^{13}C\{^{1}H\}$ (125 MHz, $CDCl_3$) of furanol 22a

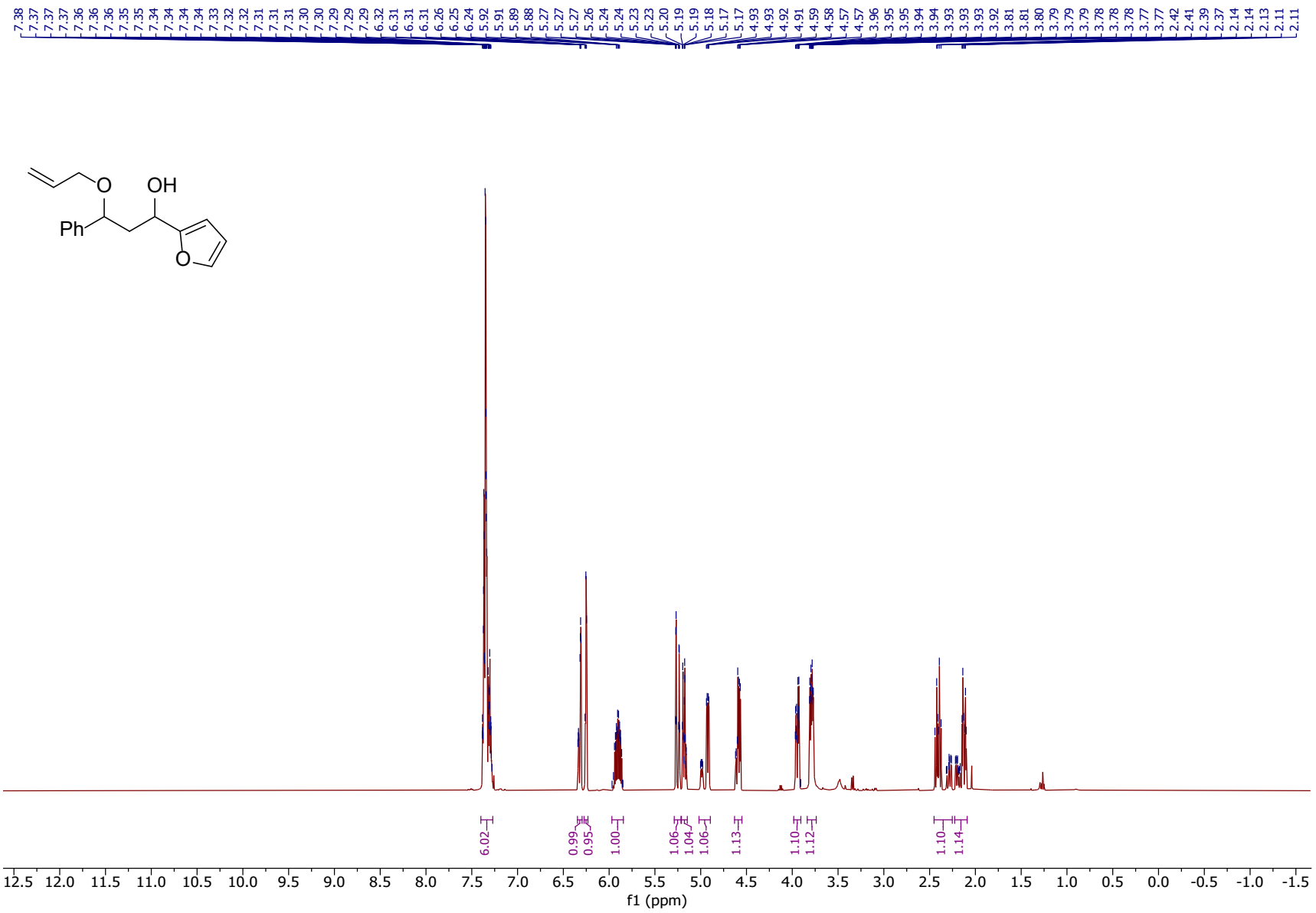

Figure S43: ^{1}H NMR (500 MHz, $CDCl_3$) of furanol 22b

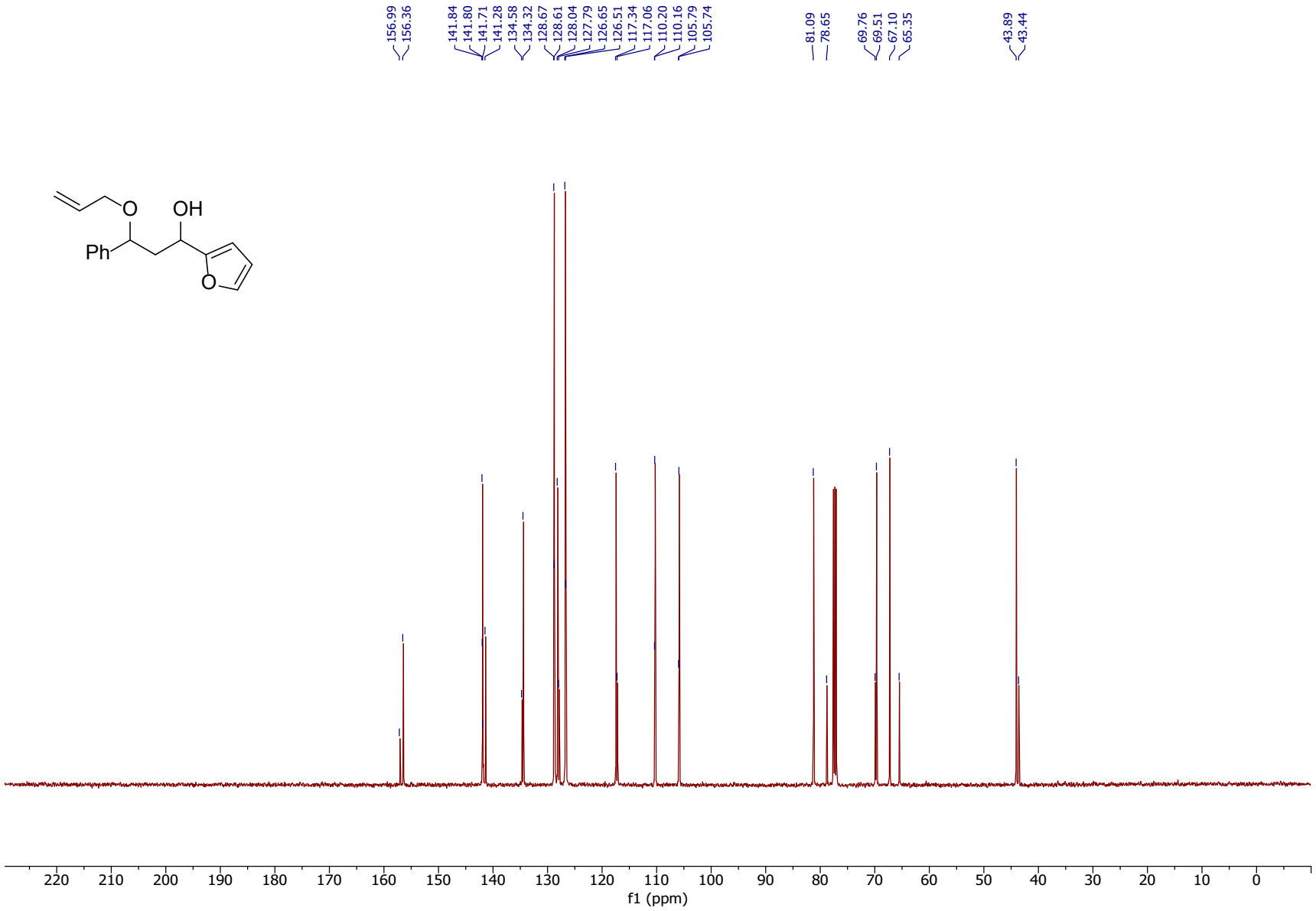

Figure S44: $^{13}C\{^{1}H\}$ (125 MHz, $CDCl_3$) of furanol 22b

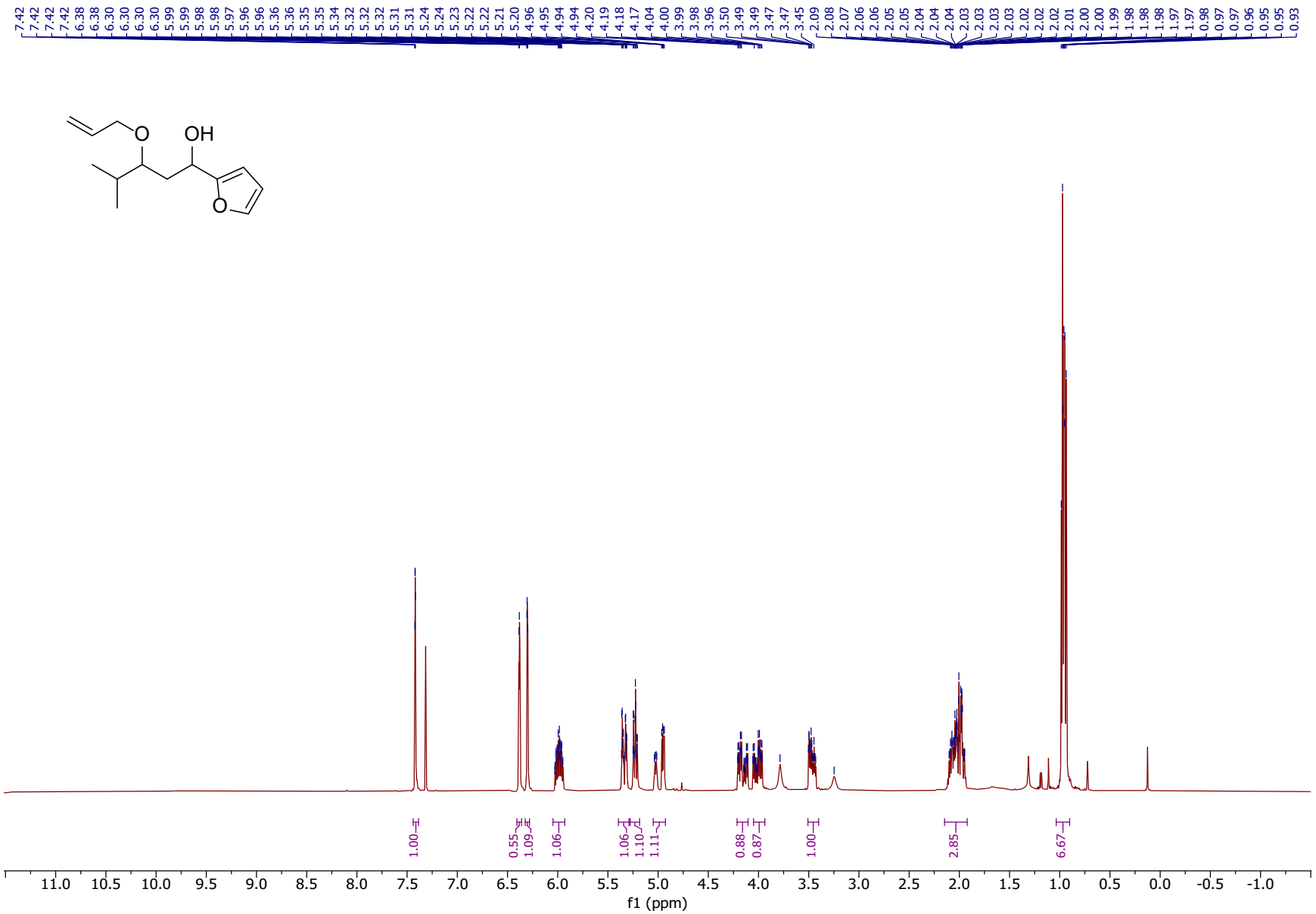

Figure S45: ^{1}H NMR (500 MHz, $CDCl_3$) of furanol 22c

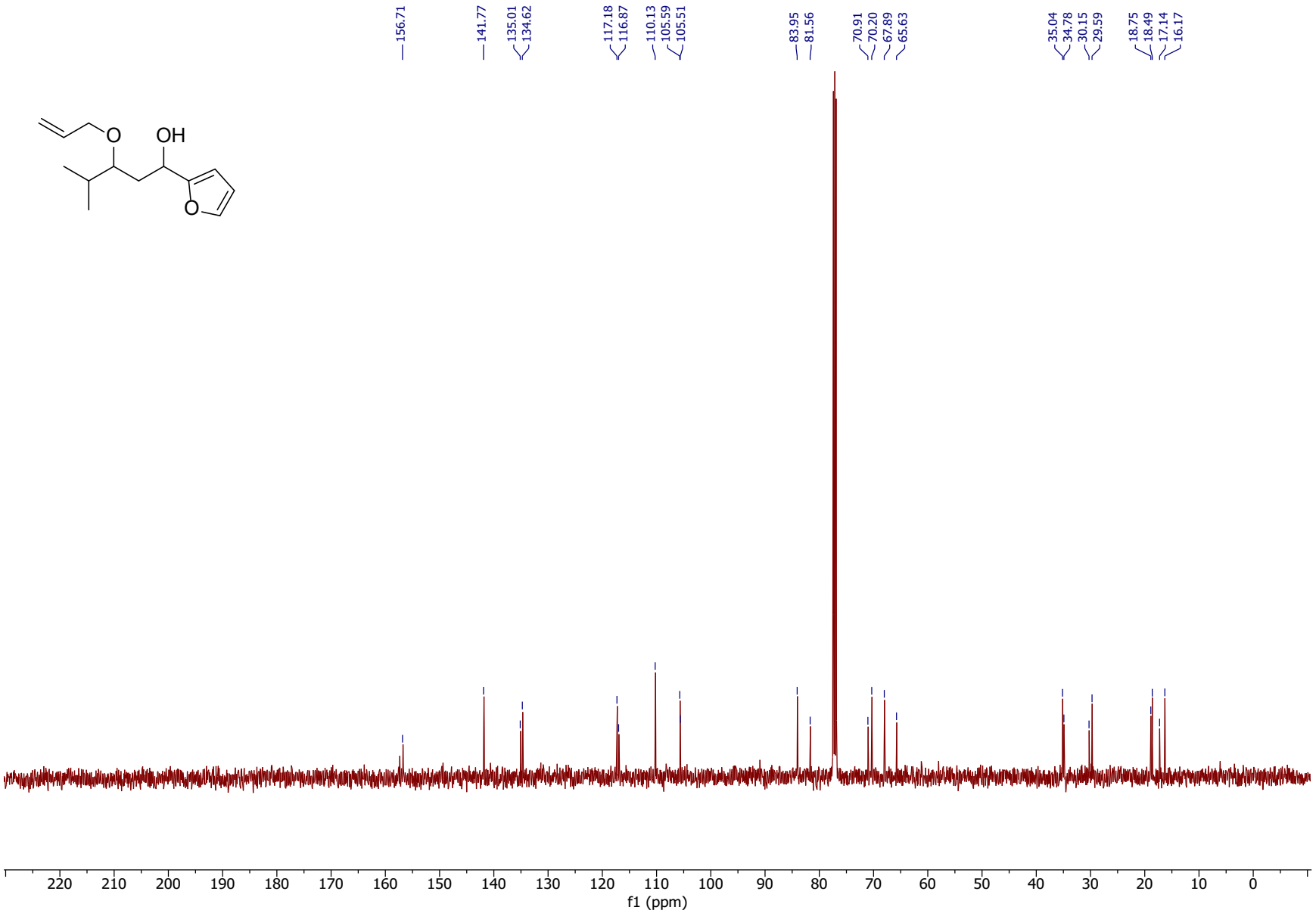

Figure S46: $^{13}C\{^{1}H\}$ (125 MHz, $CDCl_3$) of furanol 22c

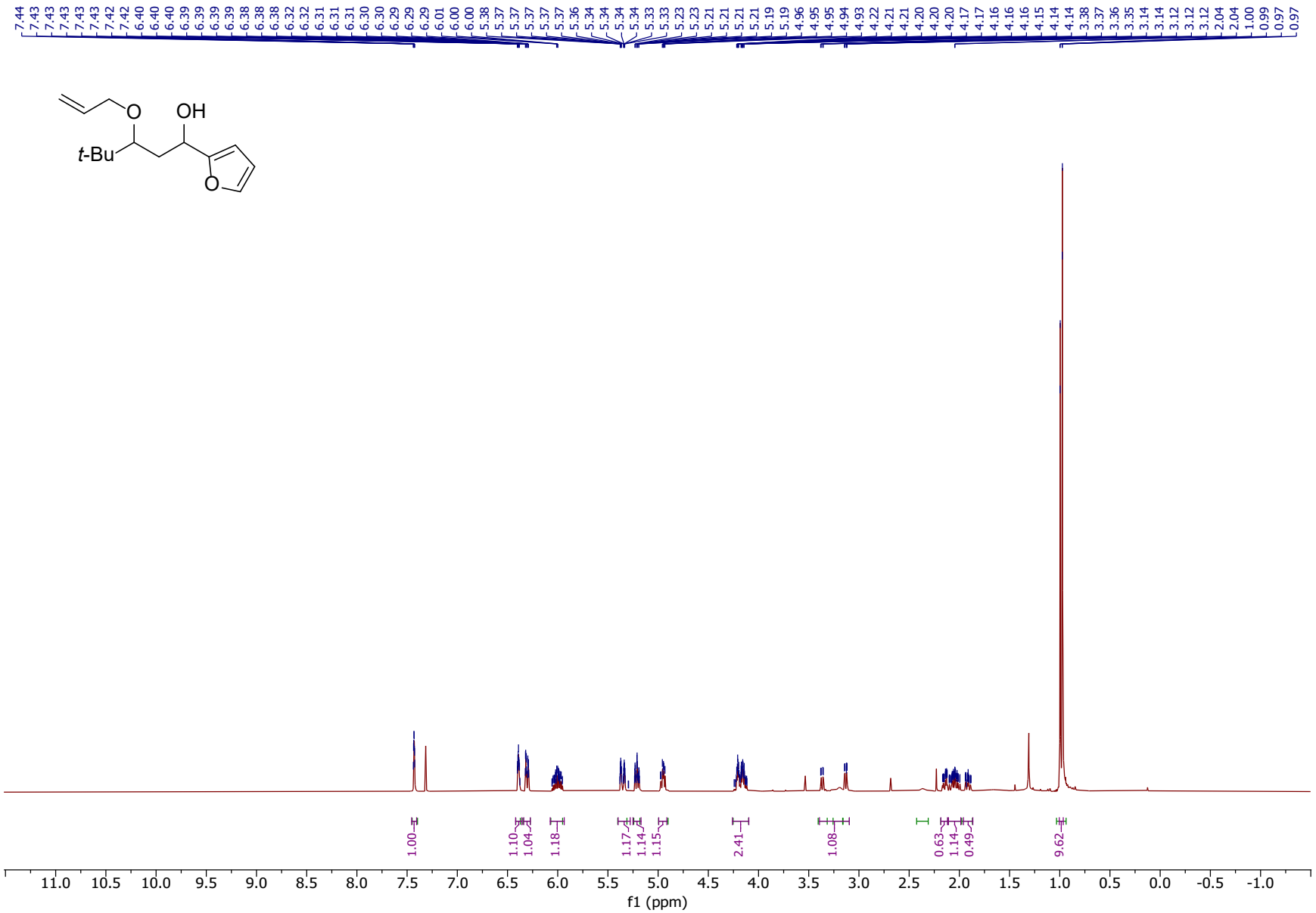

Figure S47: ^{1}H NMR (500 MHz, $CDCl_3$) of furanol 22d

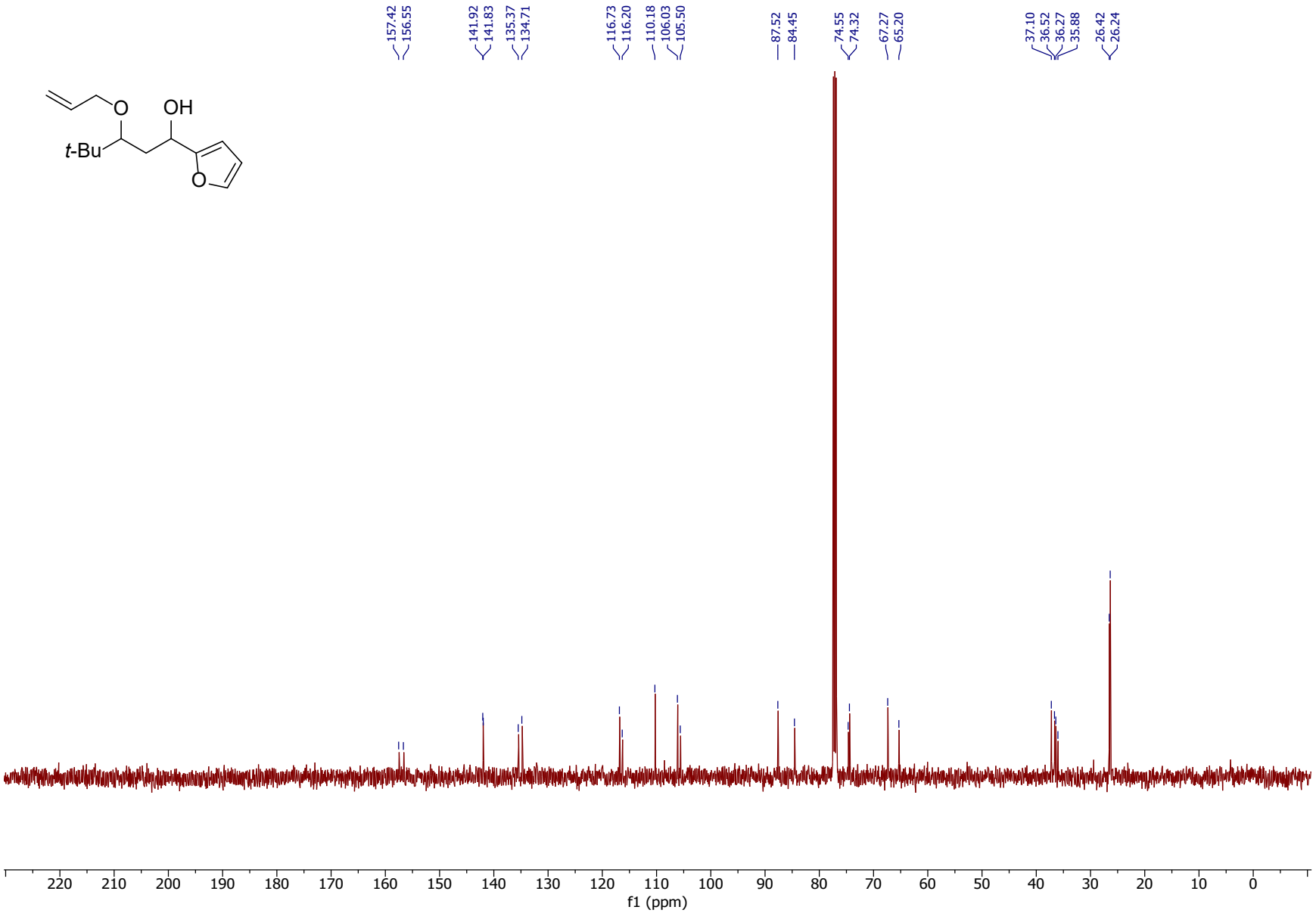

Figure S48: $^{13}C\{^{1}H\}$ (125 MHz, $CDCl_3$) of furanol 22d

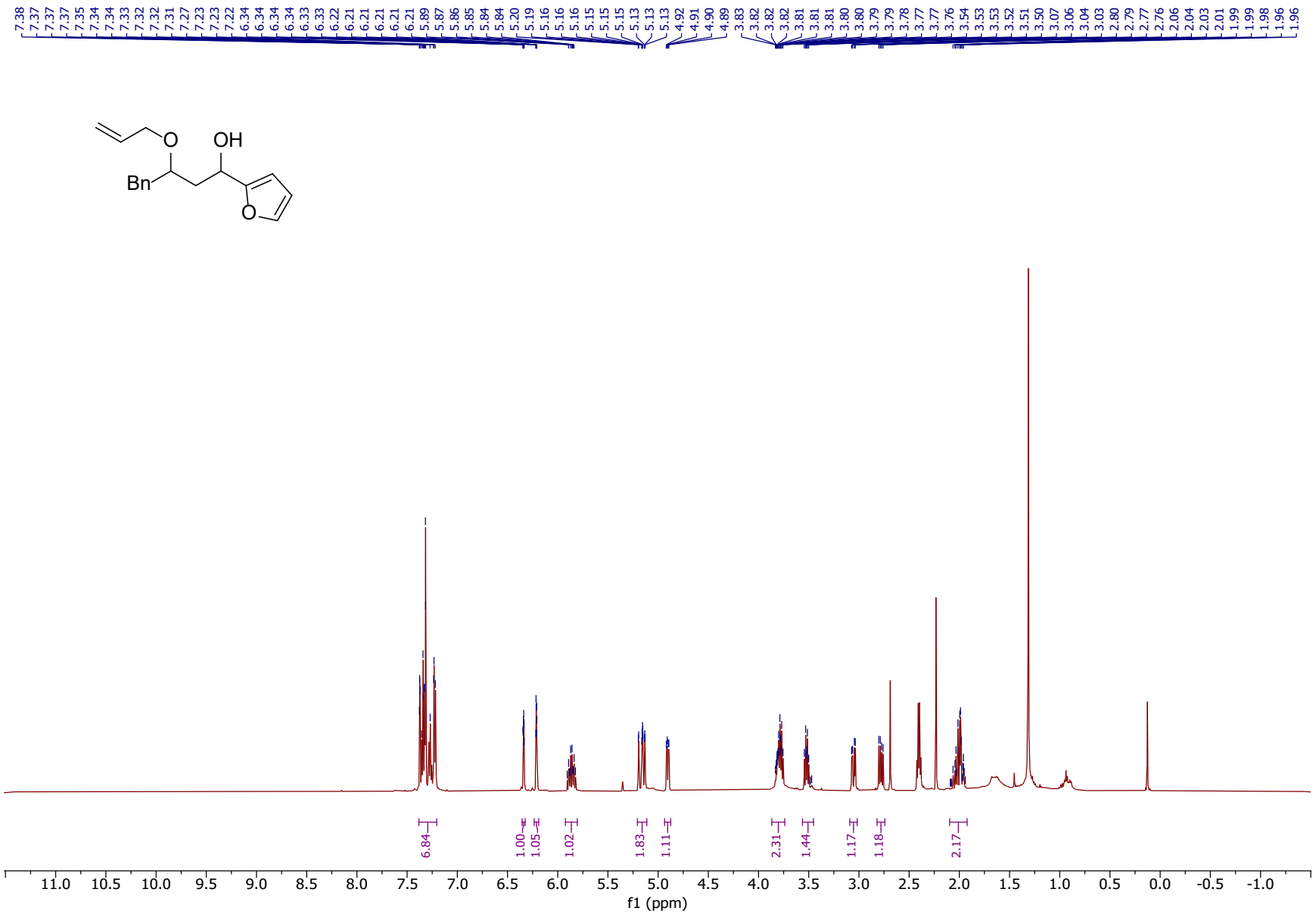

Figure S49: ^{1}H NMR (500 MHz, $CDCl_3$) of furanol 22e

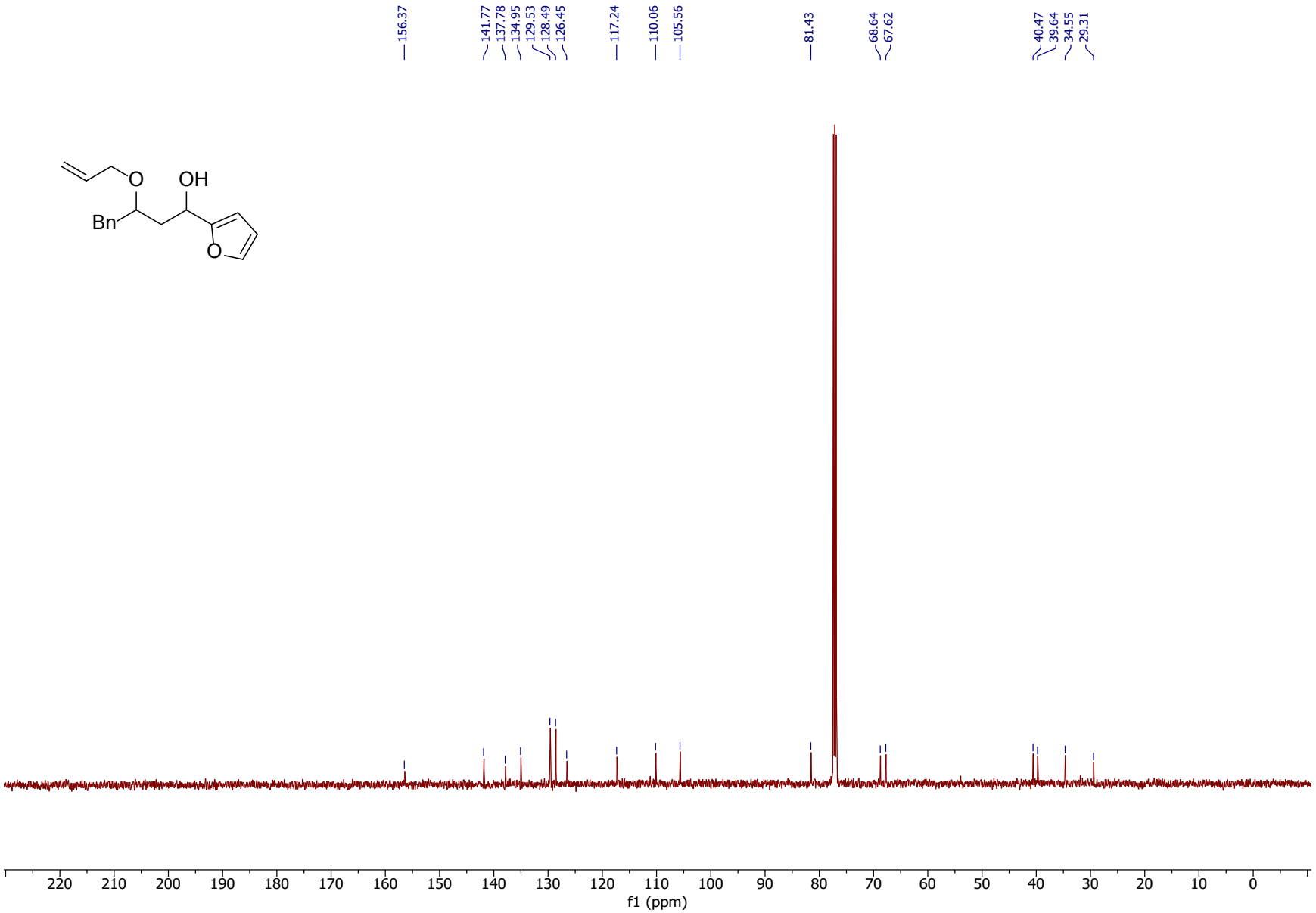

Figure S50: $^{13}C\{^{1}H\}$ (125 MHz, $CDCl_3$) of furanol 22e

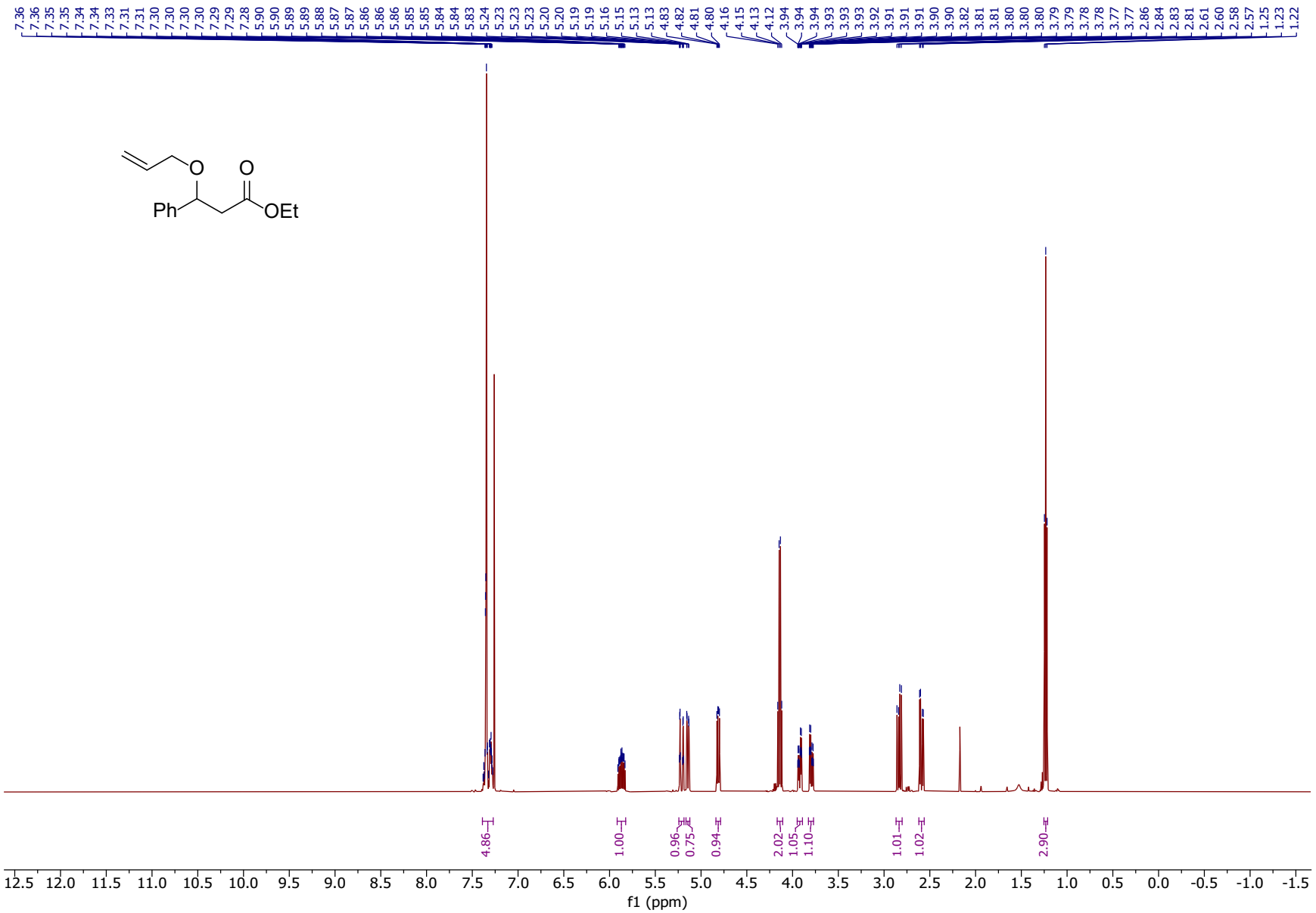

Figure S51: ^{1}H NMR (500 MHz, $CDCl_3$) of β-allyloxy ester 24b

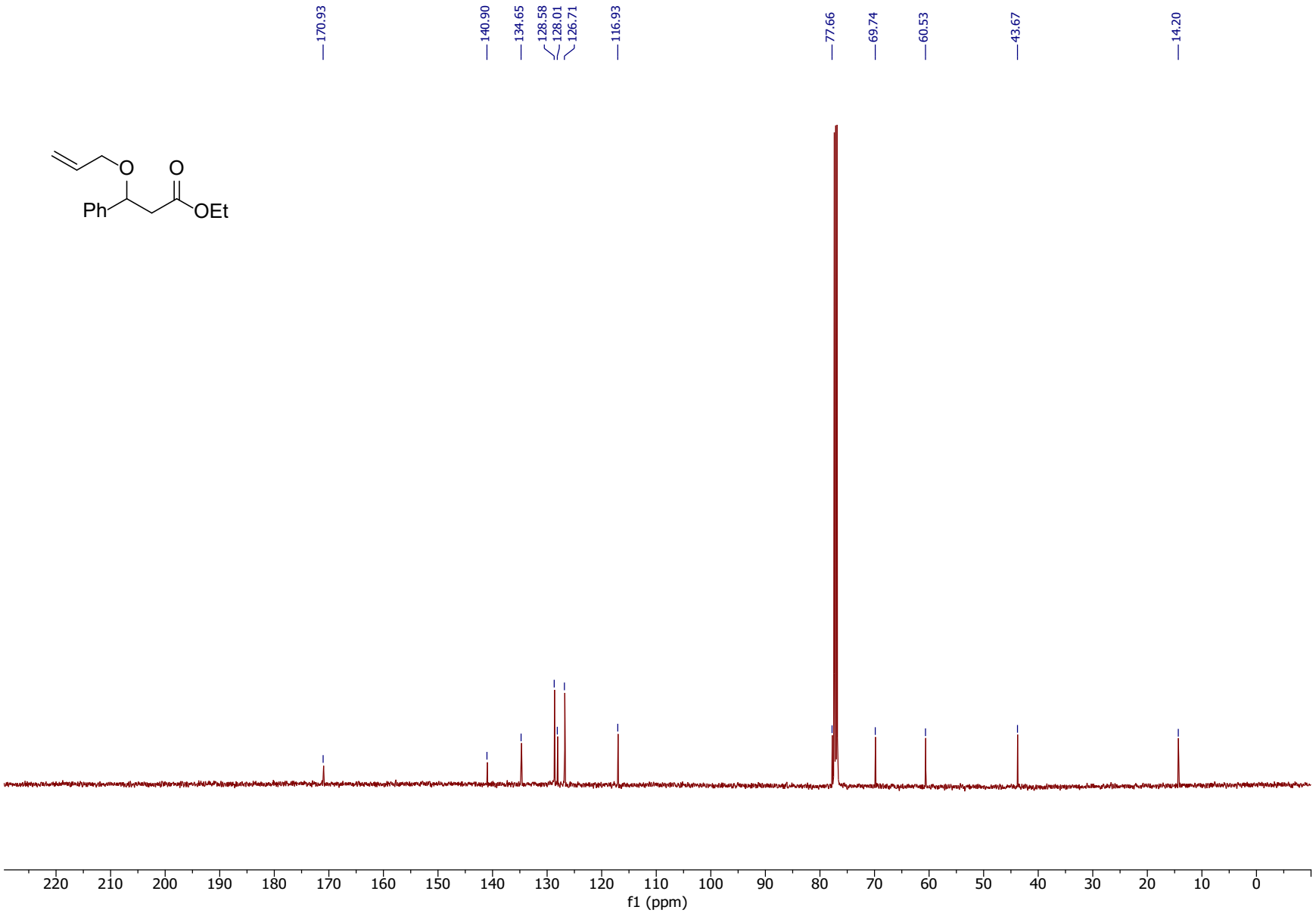

Figure S52: $^{13}C\{^{1}H\}$ (125 MHz, $CDCl_3$) of β-allyloxy ester 24b

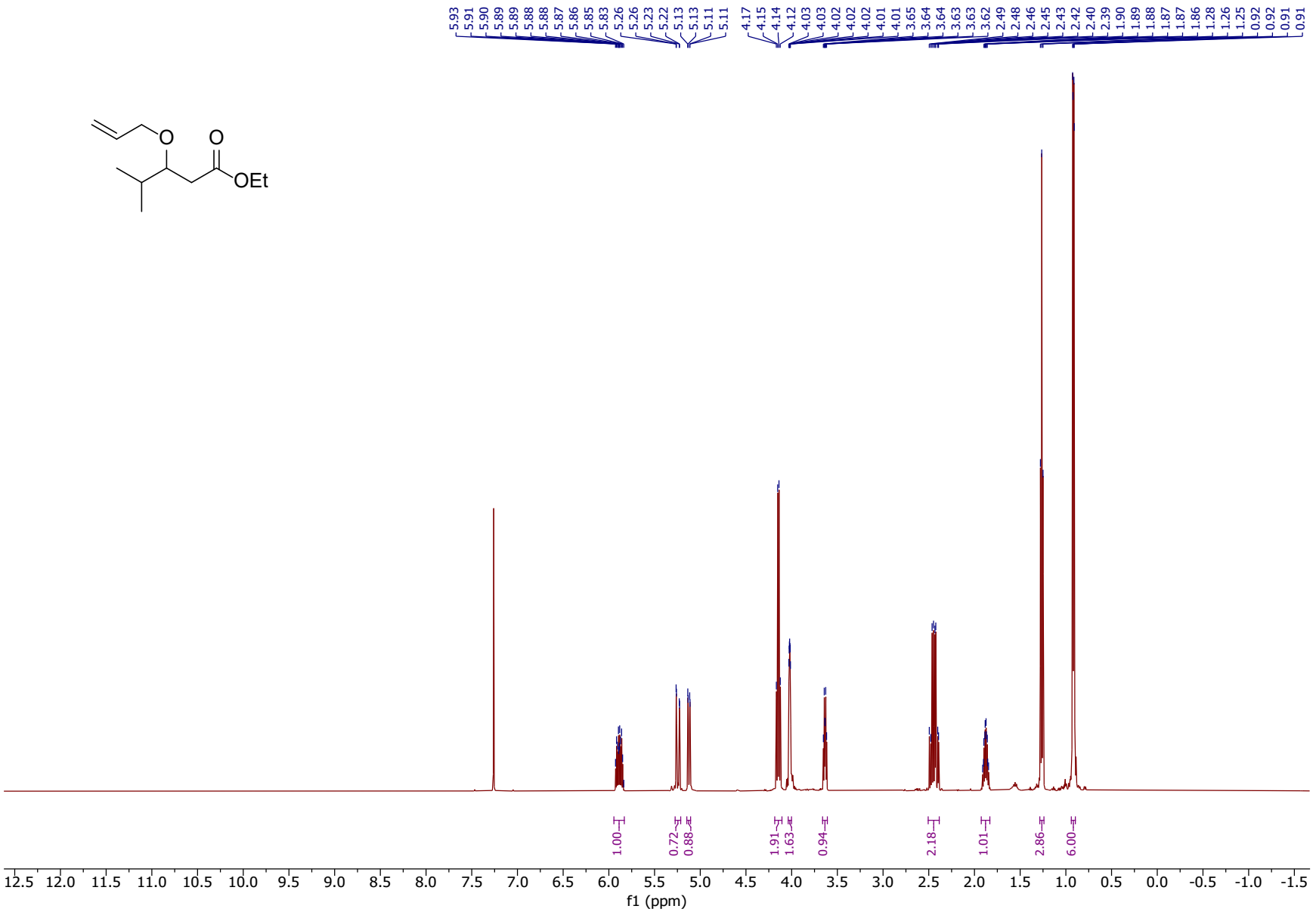

Figure S53: ^{1}H NMR (500 MHz, $CDCl_3$) of β-allyloxy ester 24c

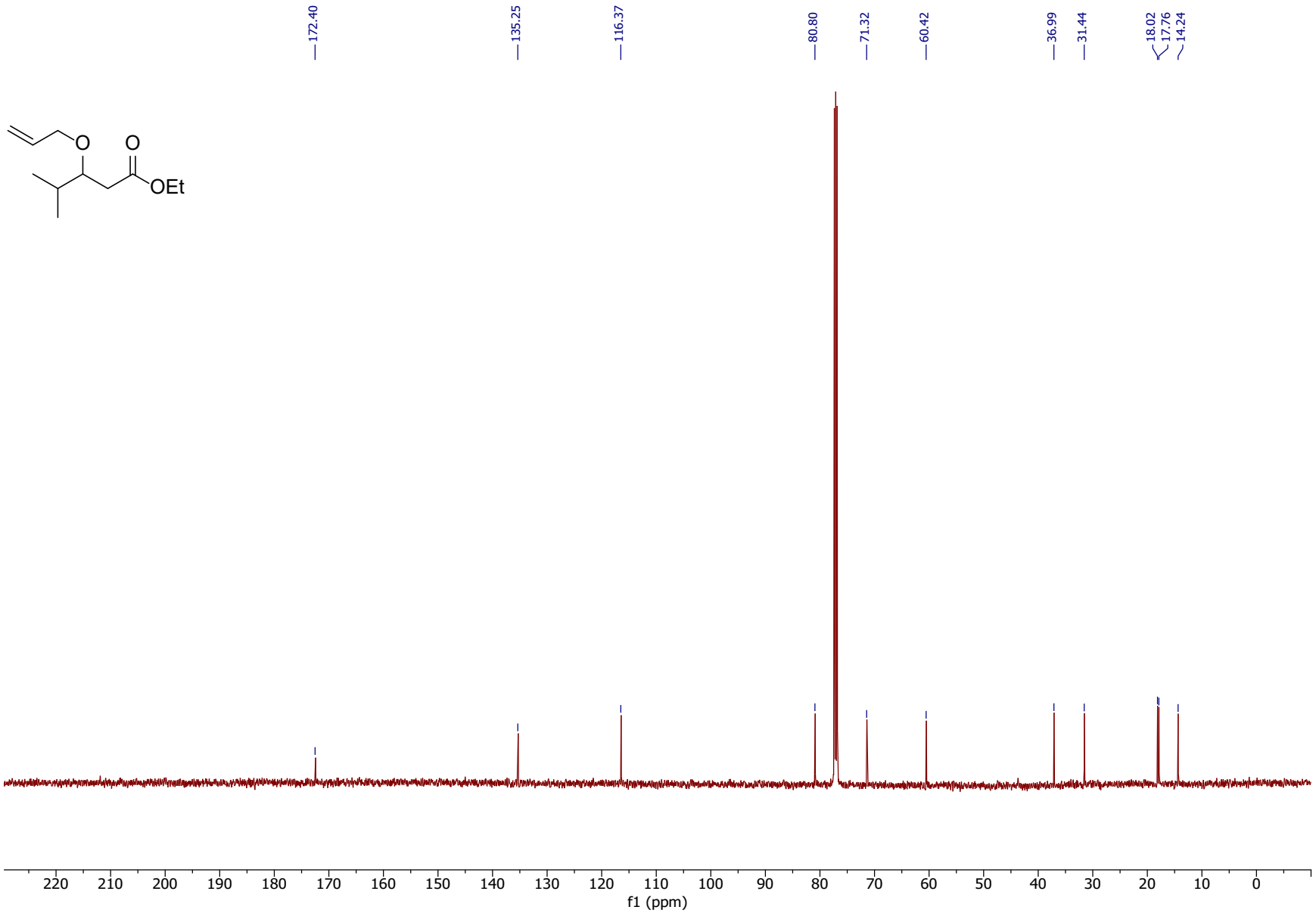

Figure S54: $^{13}C\{^{1}H\}$ (125 MHz, $CDCl_3$) of β-allyloxy ester 24c

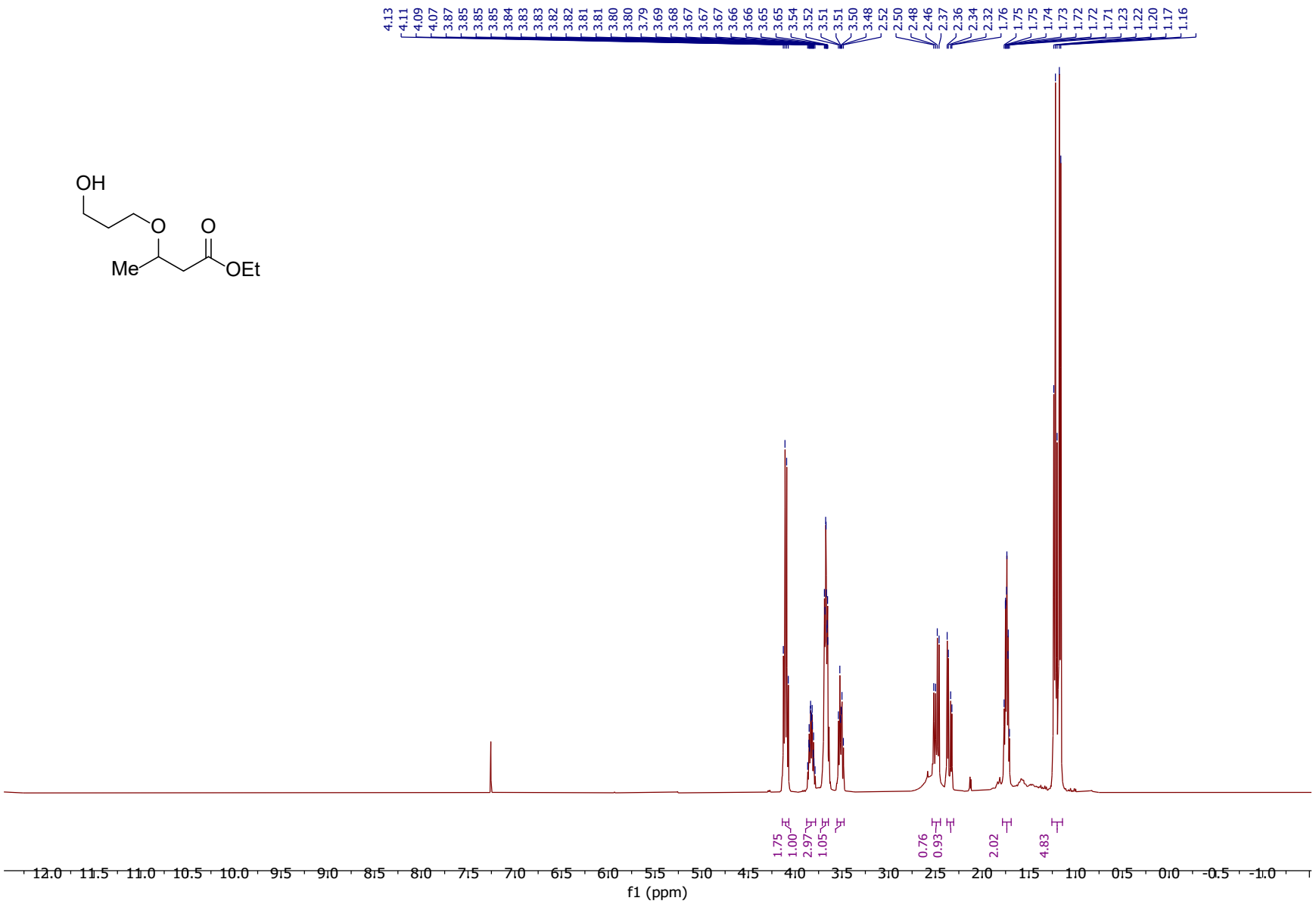

Figure S55: ^{1}H NMR (400 MHz, $CDCl_3$) of alcohol 25a

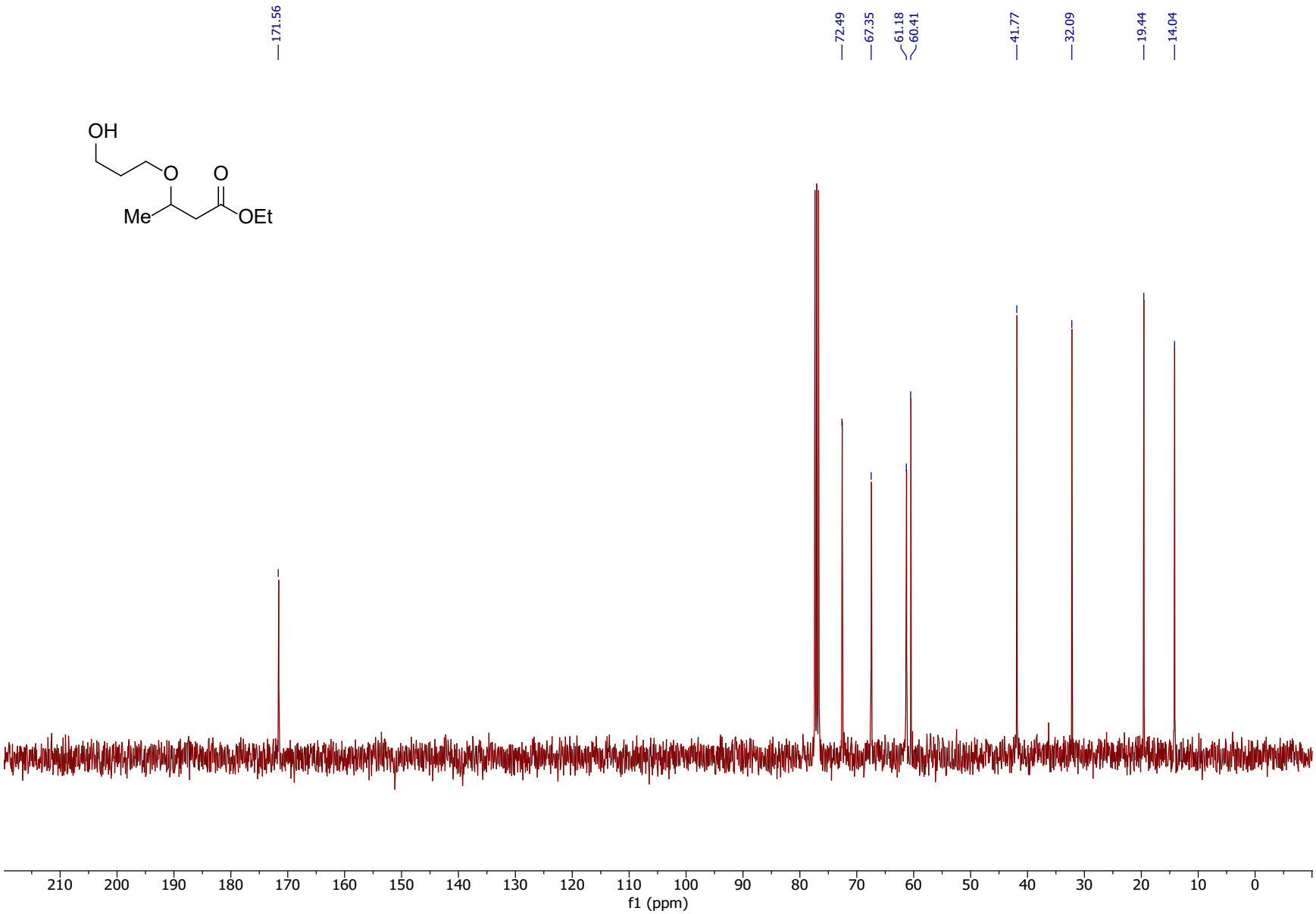

Figure S56: $^{13}C\{^{1}H\}$ (100 MHz, $CDCl_3$) of alcohol 25a

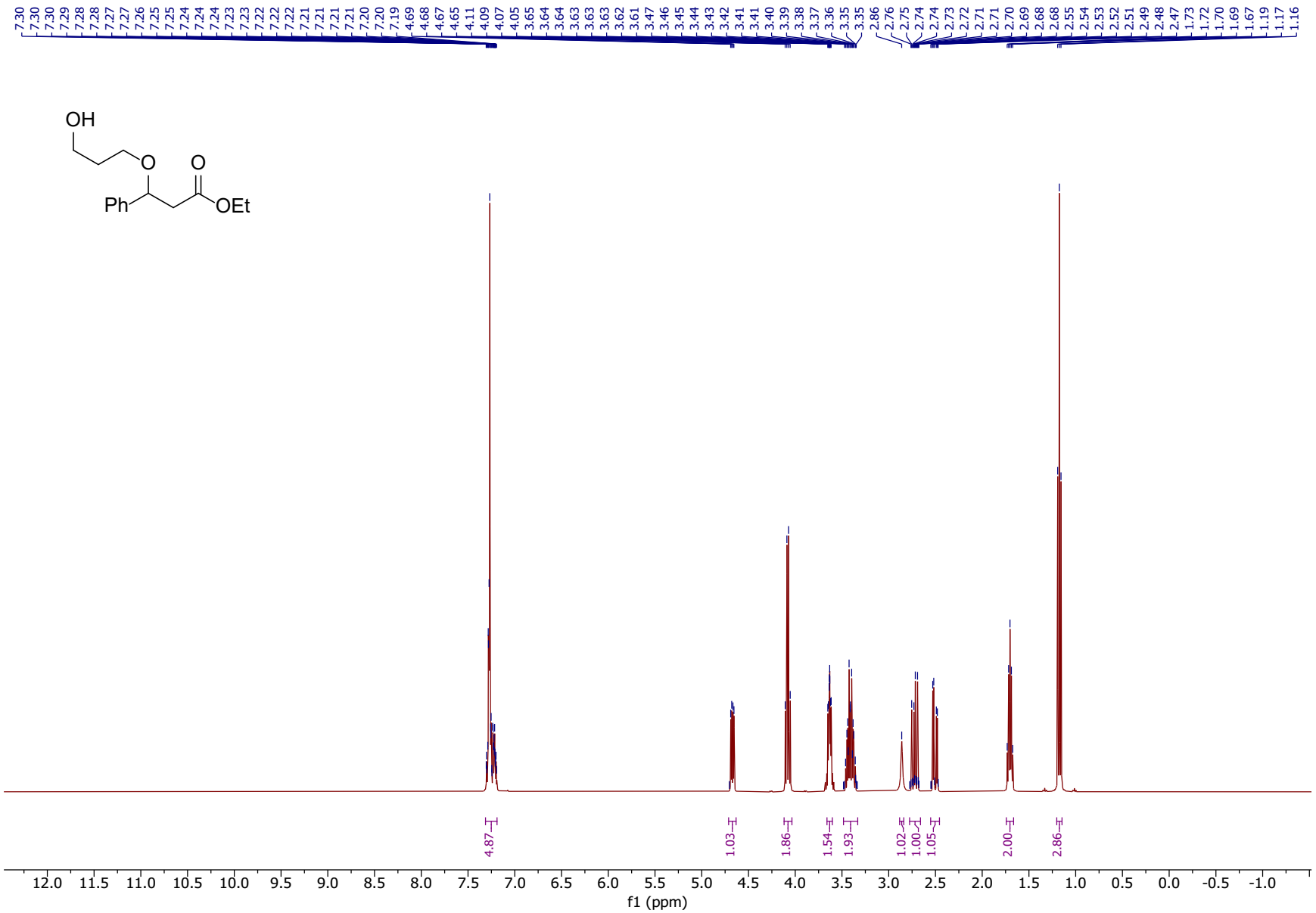

Figure S57: ^{1}H NMR (400 MHz, $CDCl_3$) of alcohol 25b

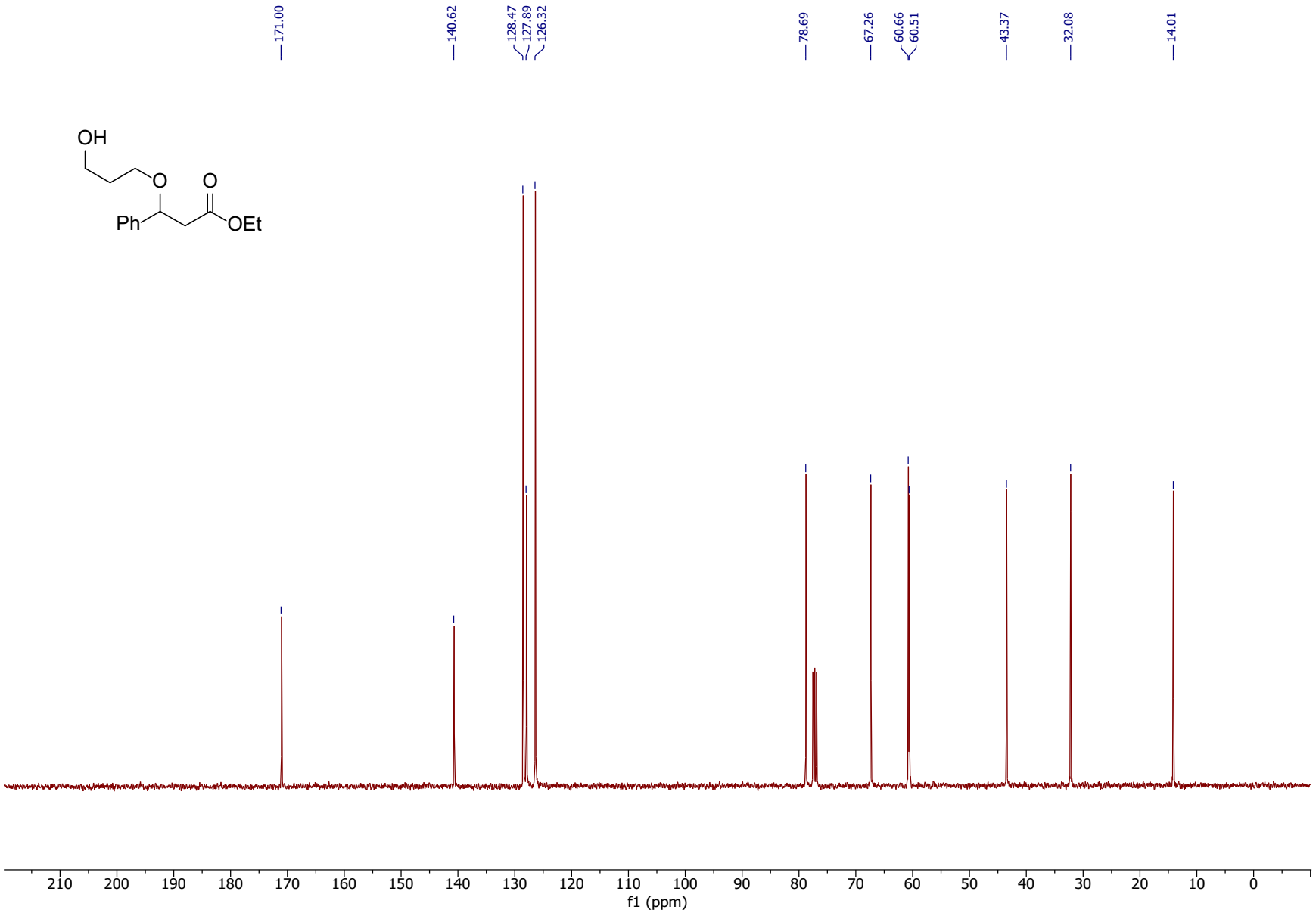

Figure S58: $^{13}C\{^{1}H\}$ (100 MHz, $CDCl_3$) of alcohol 25b

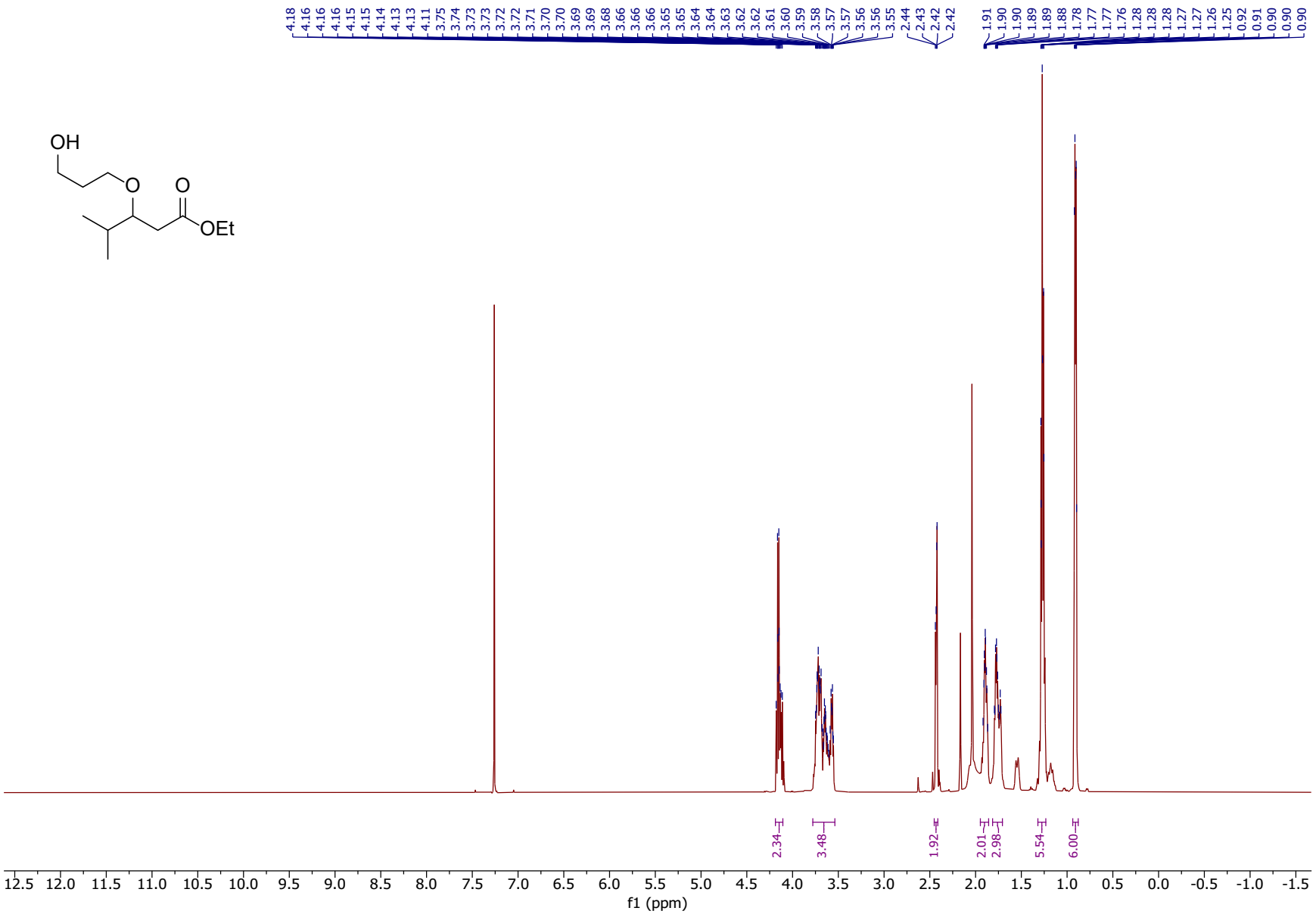

Figure S59: ^{1}H NMR (500 MHz, $CDCl_3$) of alcohol 25c

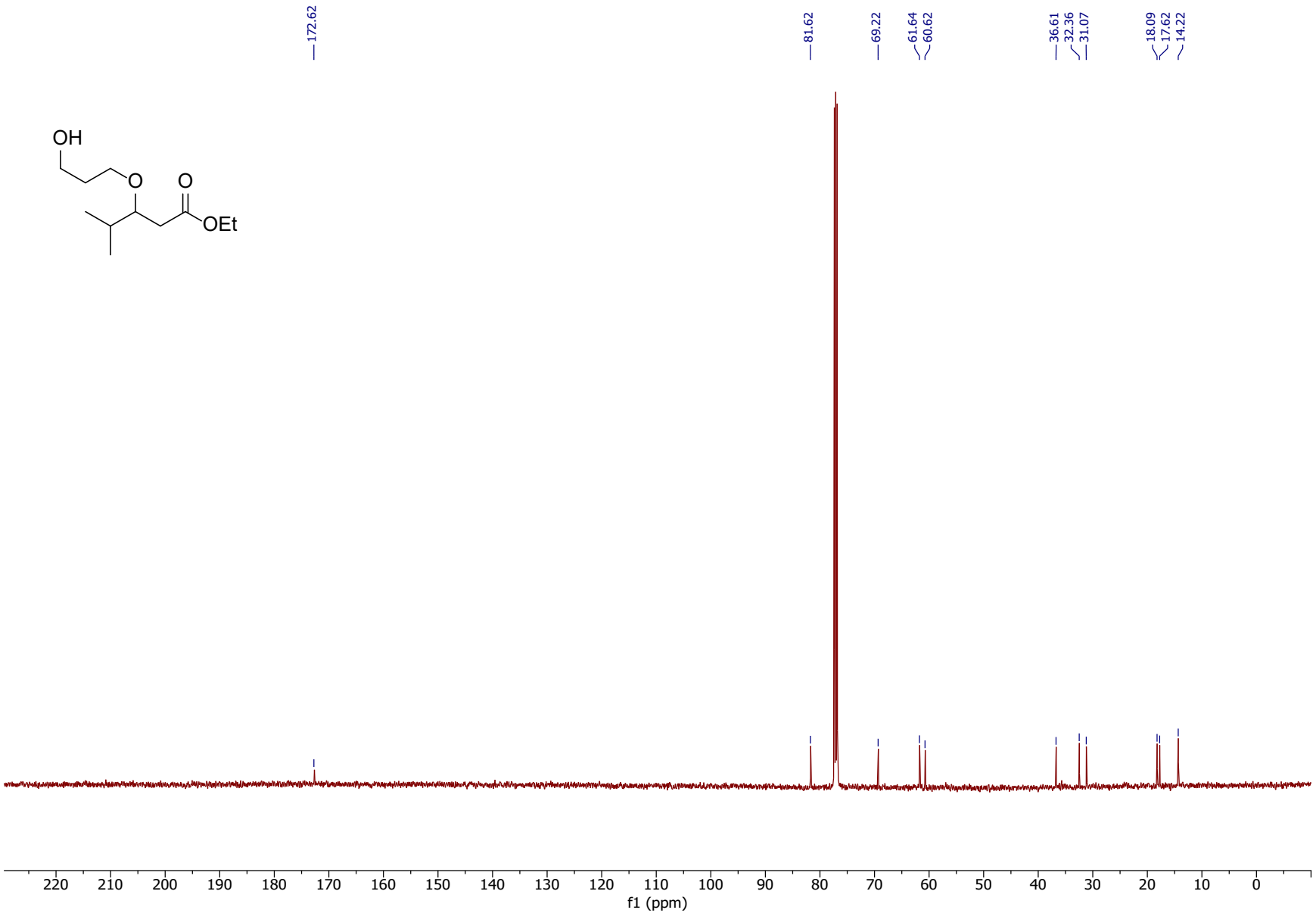

Figure S60: $^{13}C\{^{1}H\}$ (125 MHz, $CDCl_3$) of alcohol 25c

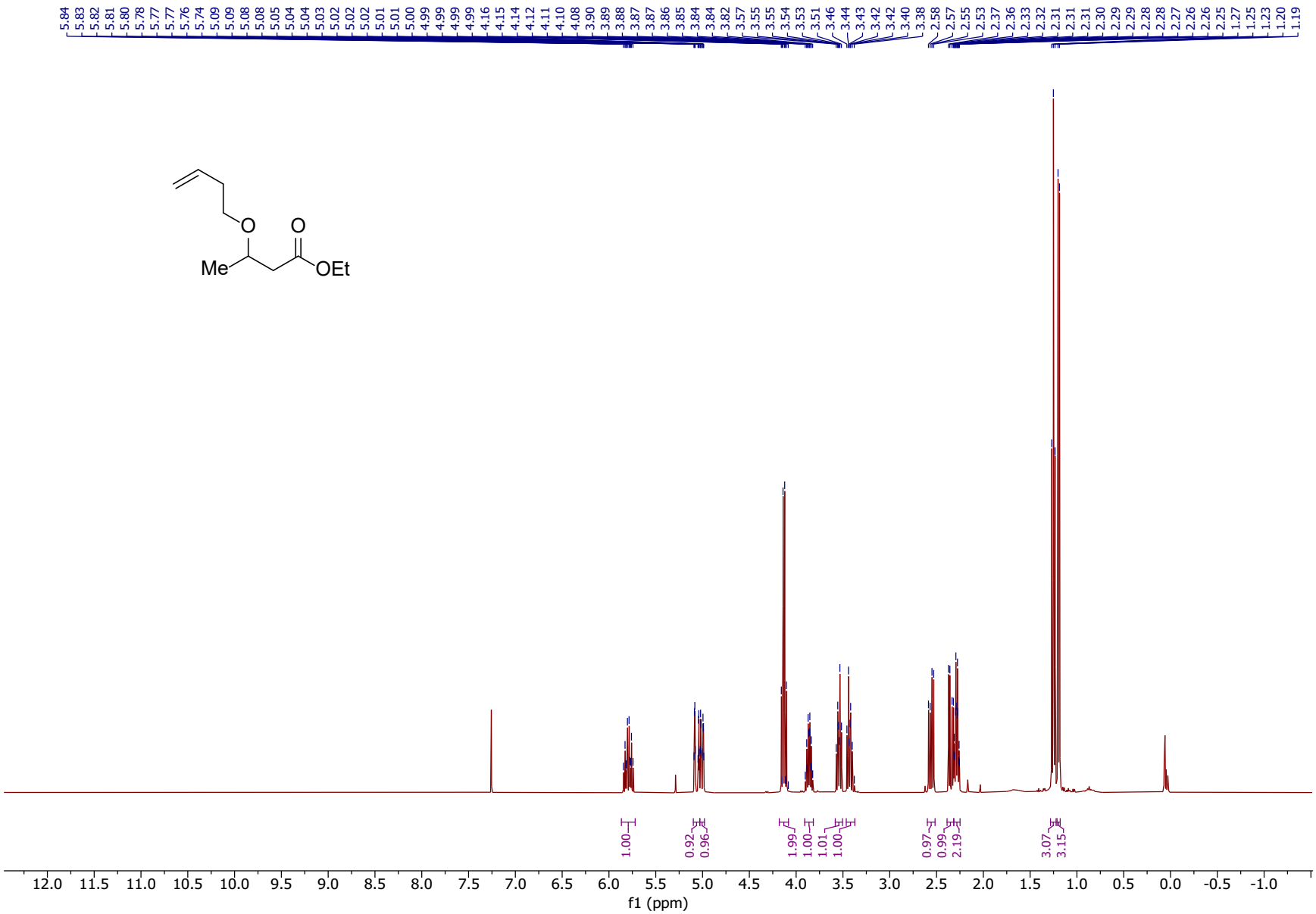

Figure S61: ^{1}H NMR (400 MHz, $CDCl_3$) of homoallyloxy 26a

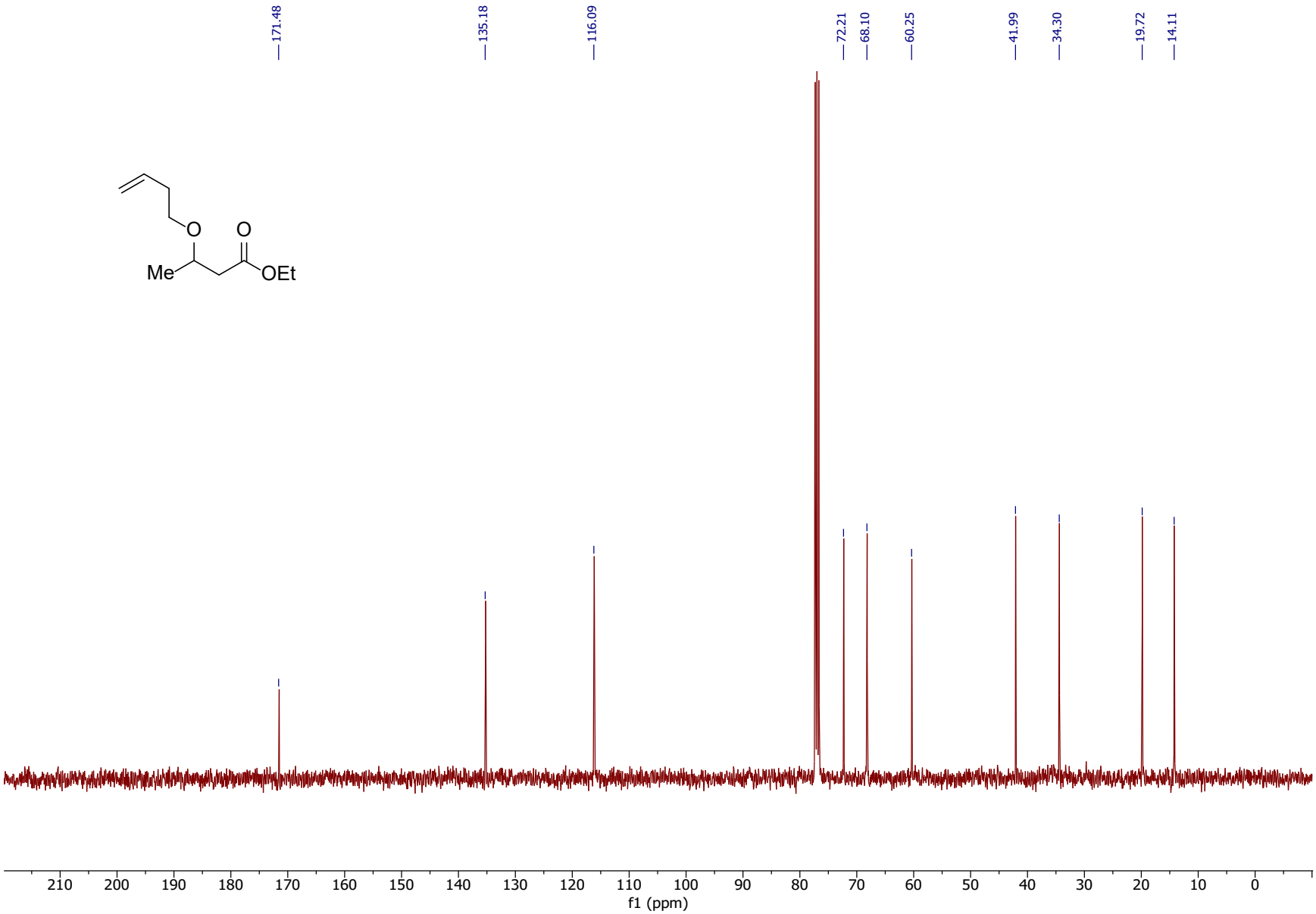

Figure S62: $^{13}C\{^{1}H\}$ (100 MHz, $CDCl_3$) of homoallyloxy 26a

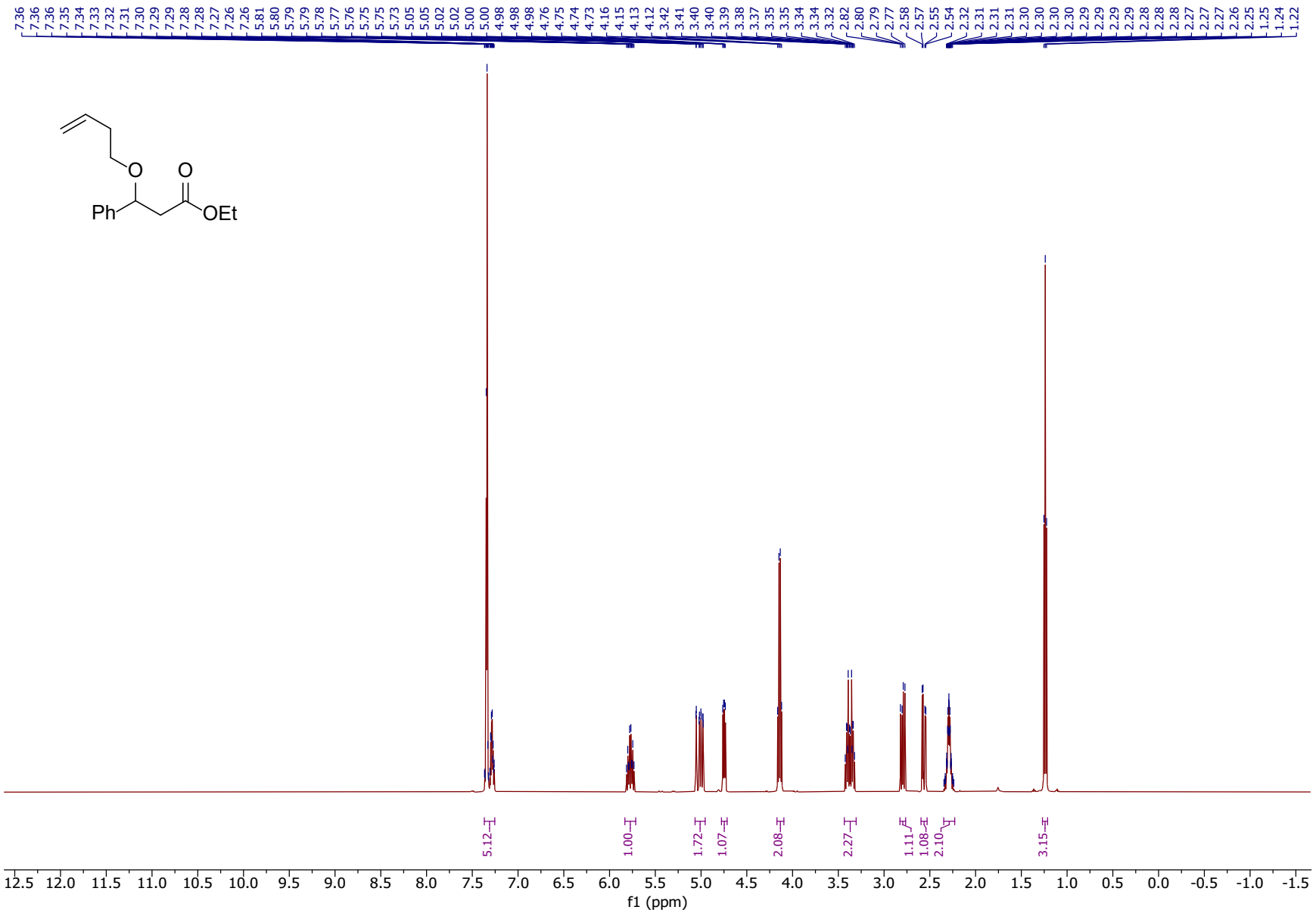

Figure S63: ^{1}H NMR (500 MHz, $CDCl_3$) of homoallyloxy 26b

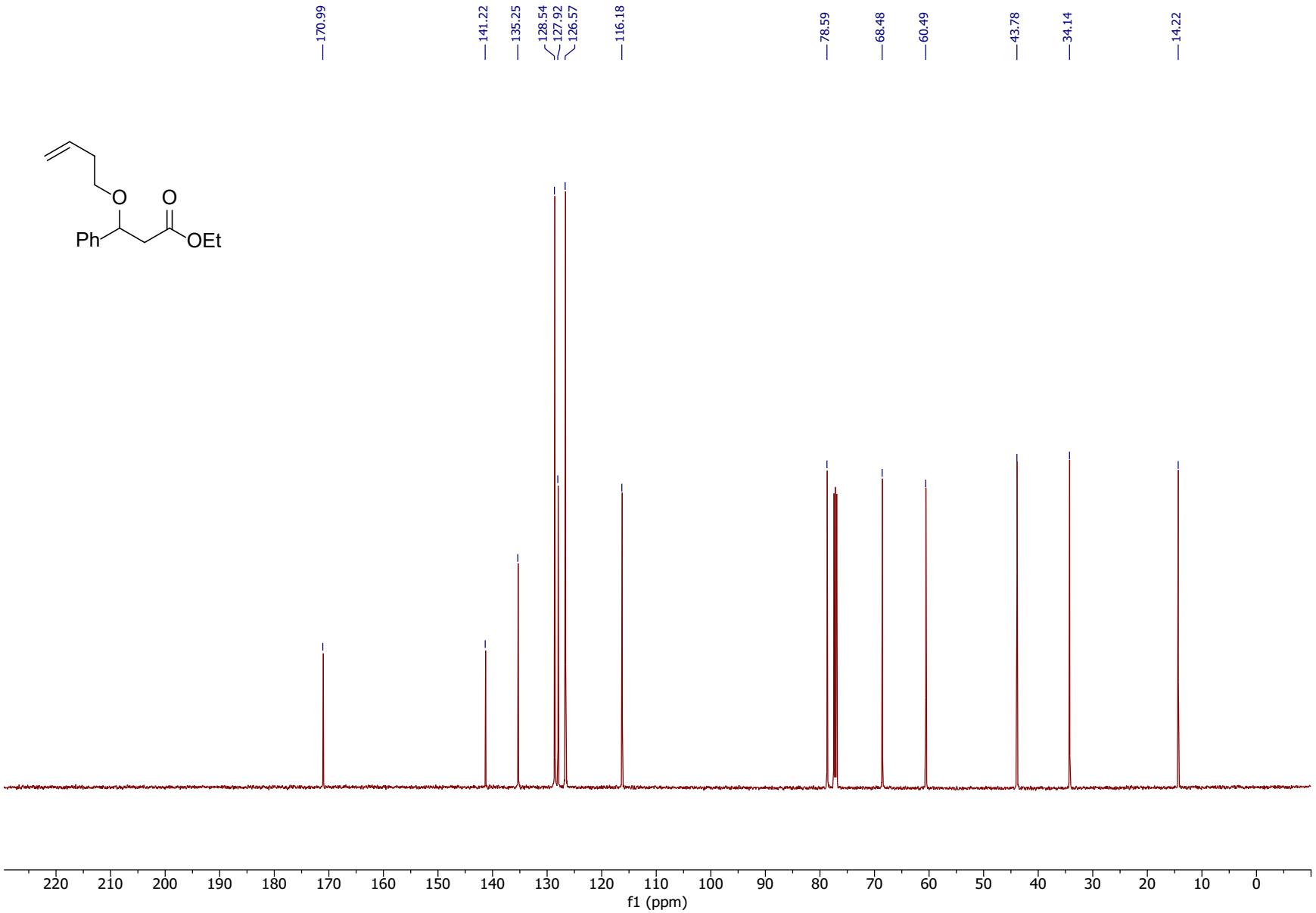

Figure S64: $^{13}C\{^{1}H\}$ (125 MHz, $CDCl_3$) of homoallyloxy 26b

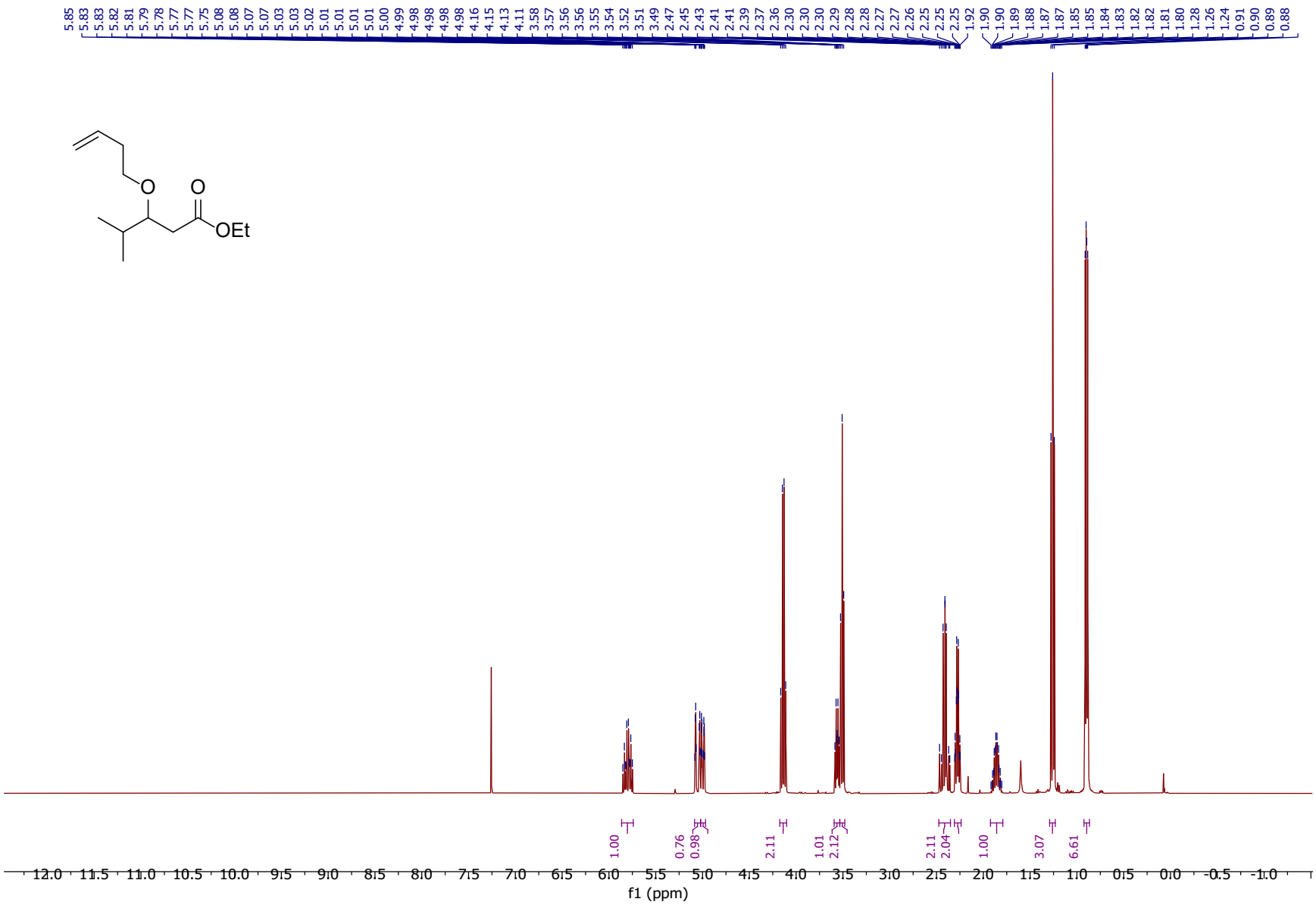

Figure S65: ^{1}H NMR (400 MHz, $CDCl_3$) of homoallyloxy 26c

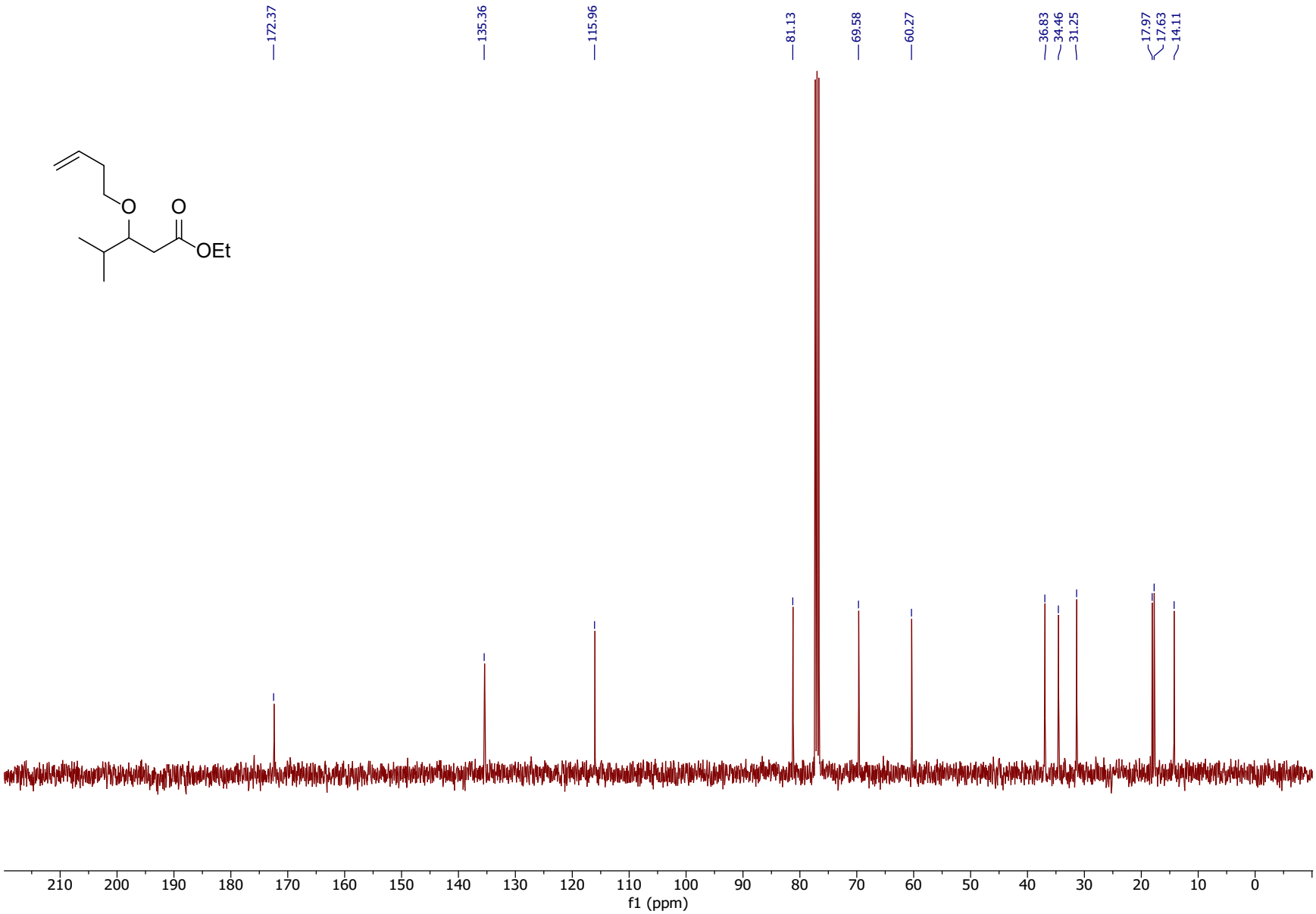

Figure S66: $^{13}C\{^{1}H\}$ (100 MHz, $CDCl_3$) of homoallyloxy 26c

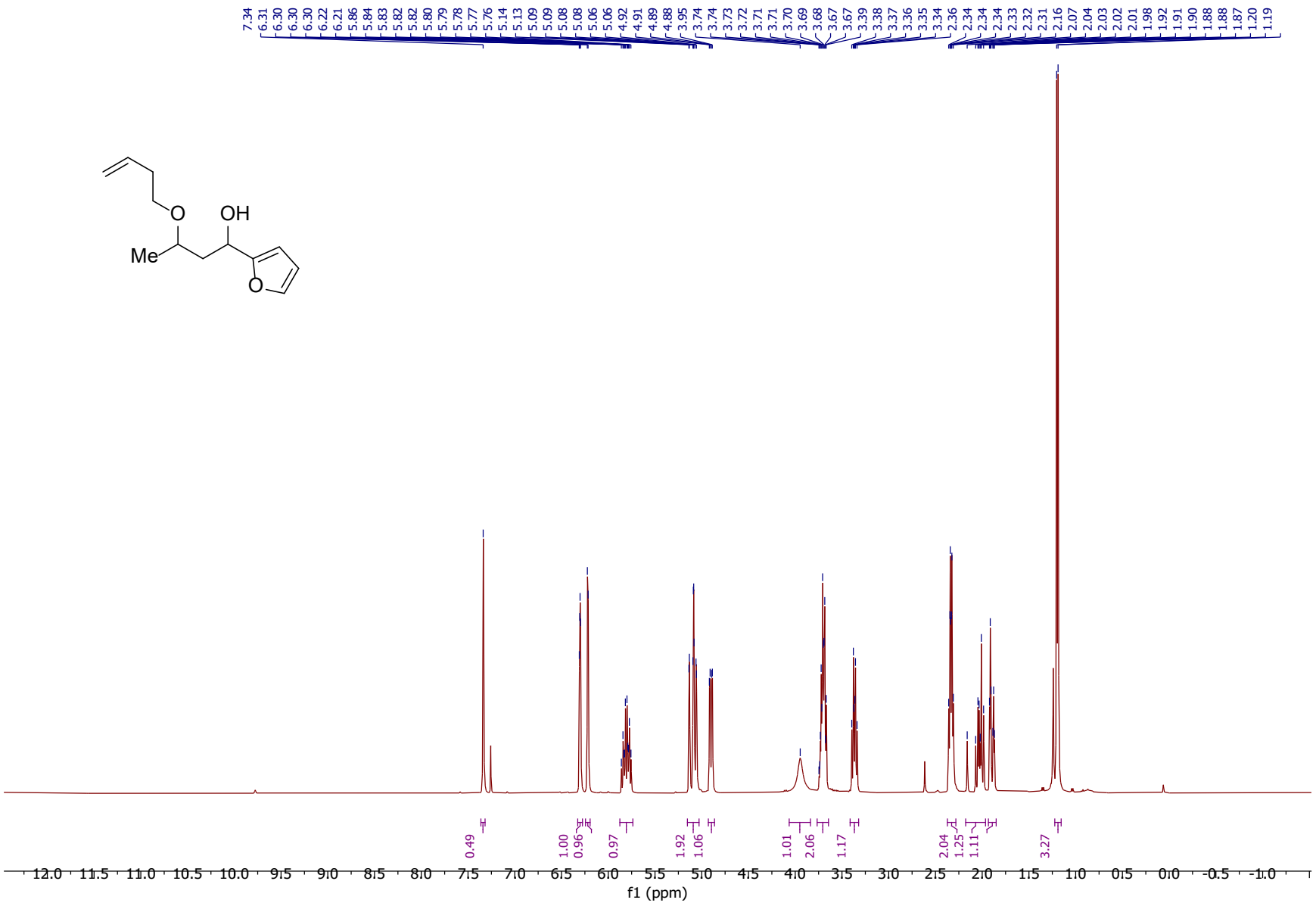

Figure S67: ^{1}H NMR (400 MHz, $CDCl_3$) of furanol 27a

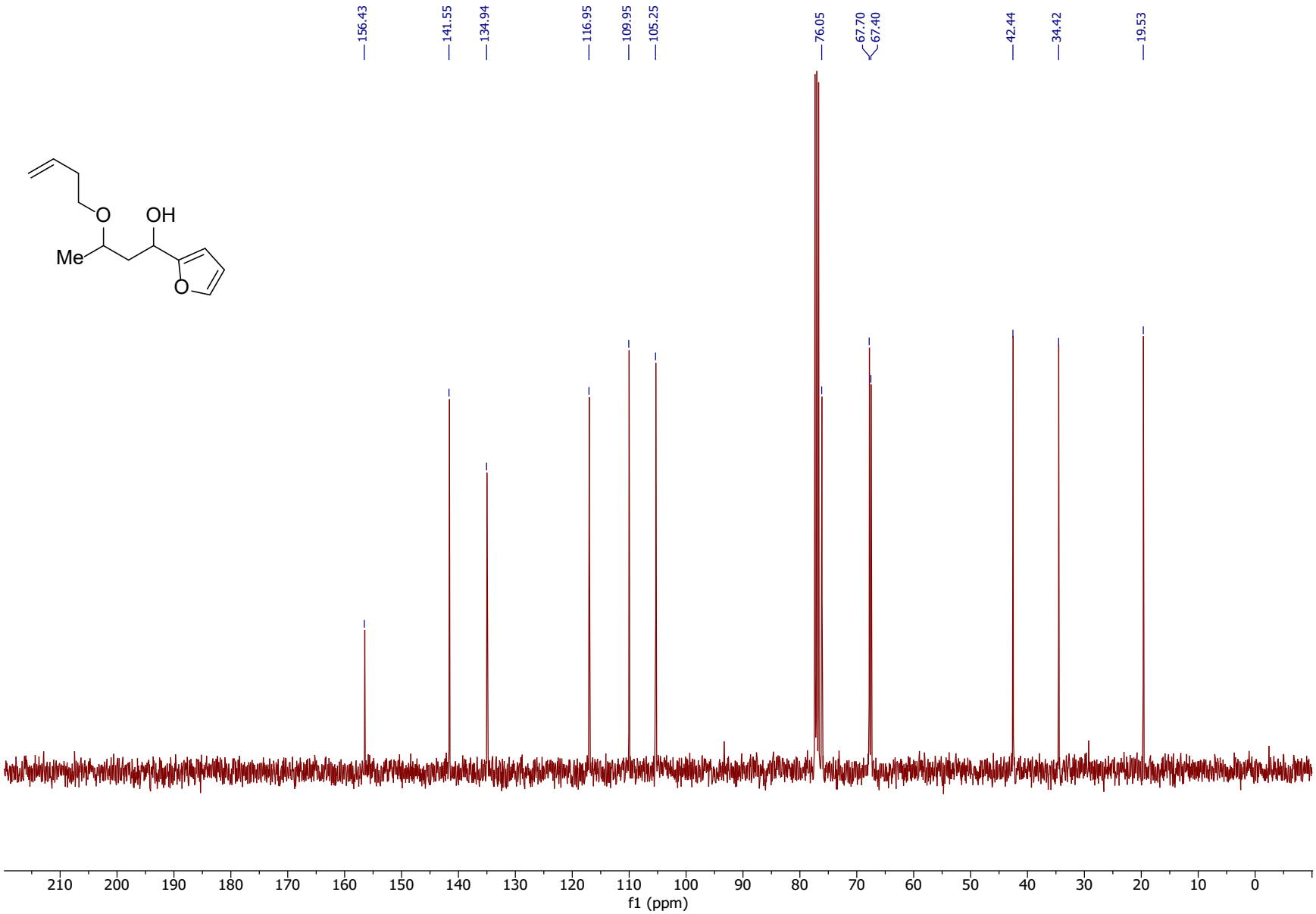

Figure S68: $^{13}C\{^{1}H\}$ (100 MHz, $CDCl_3$) of furanol 27a

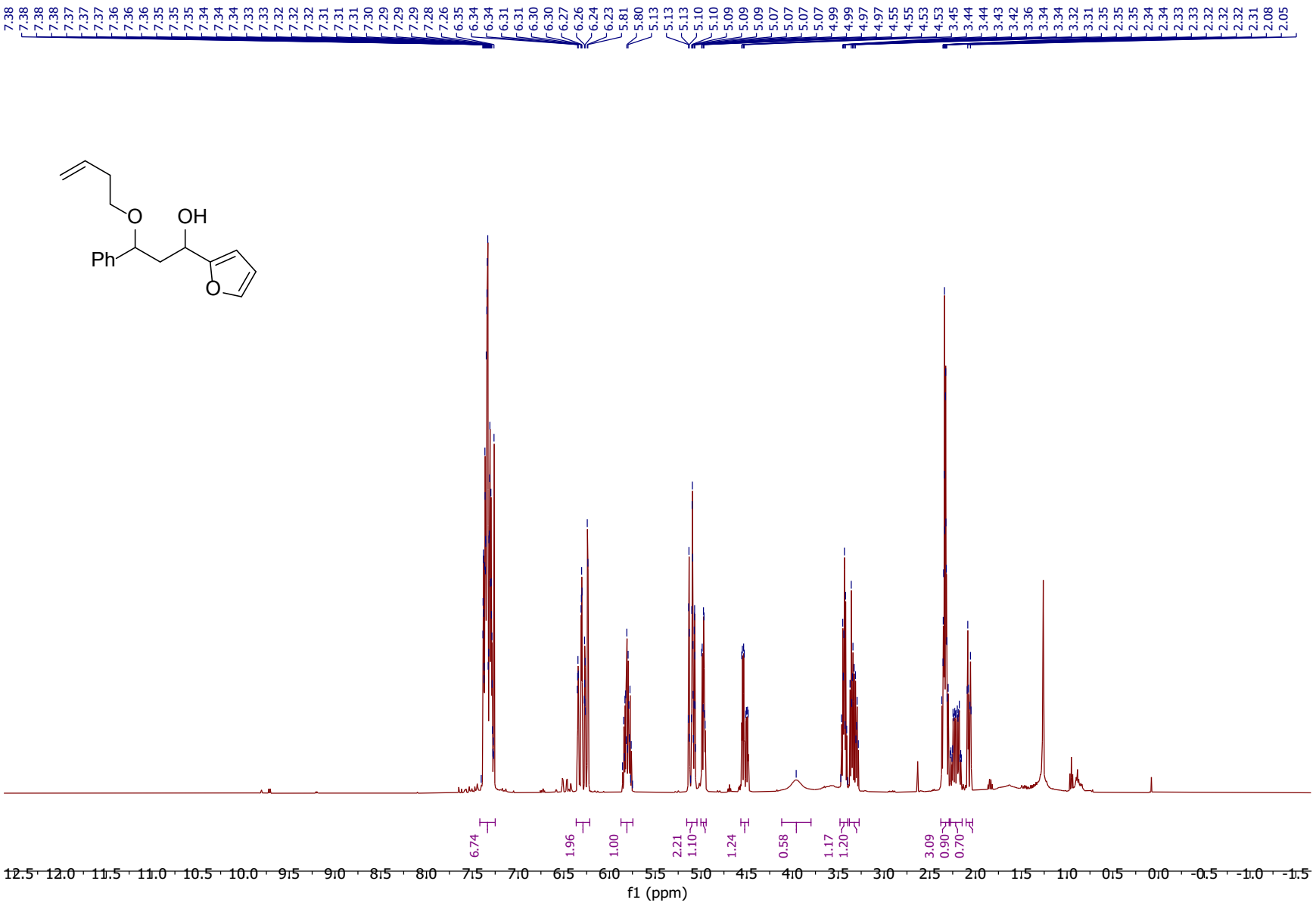

Figure S69: ^{1}H NMR (500 MHz, $CDCl_3$) of furanol 27b

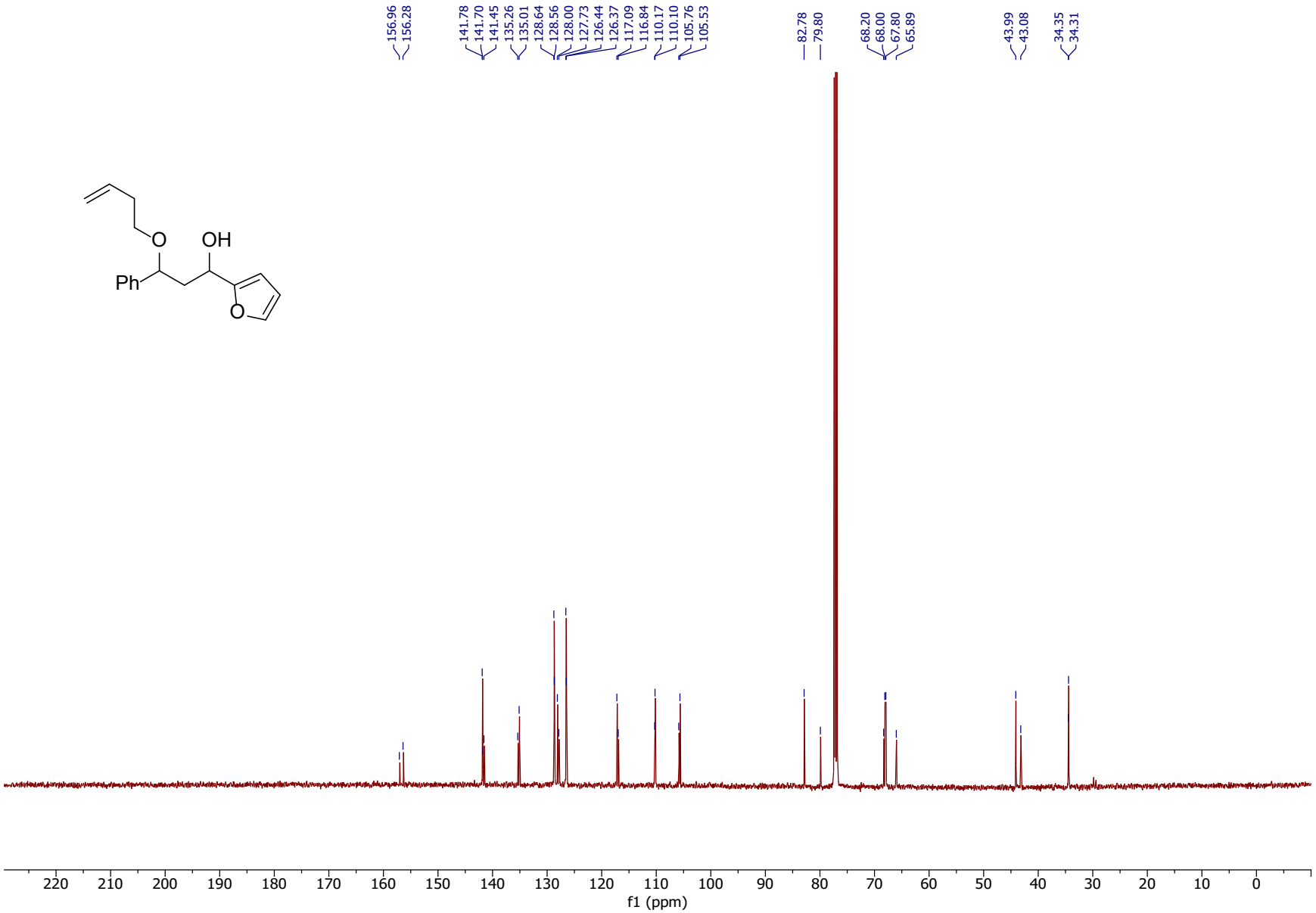

Figure S70: $^{13}C\{^{1}H\}$ (125 MHz, $CDCl_3$) of furanol 27b

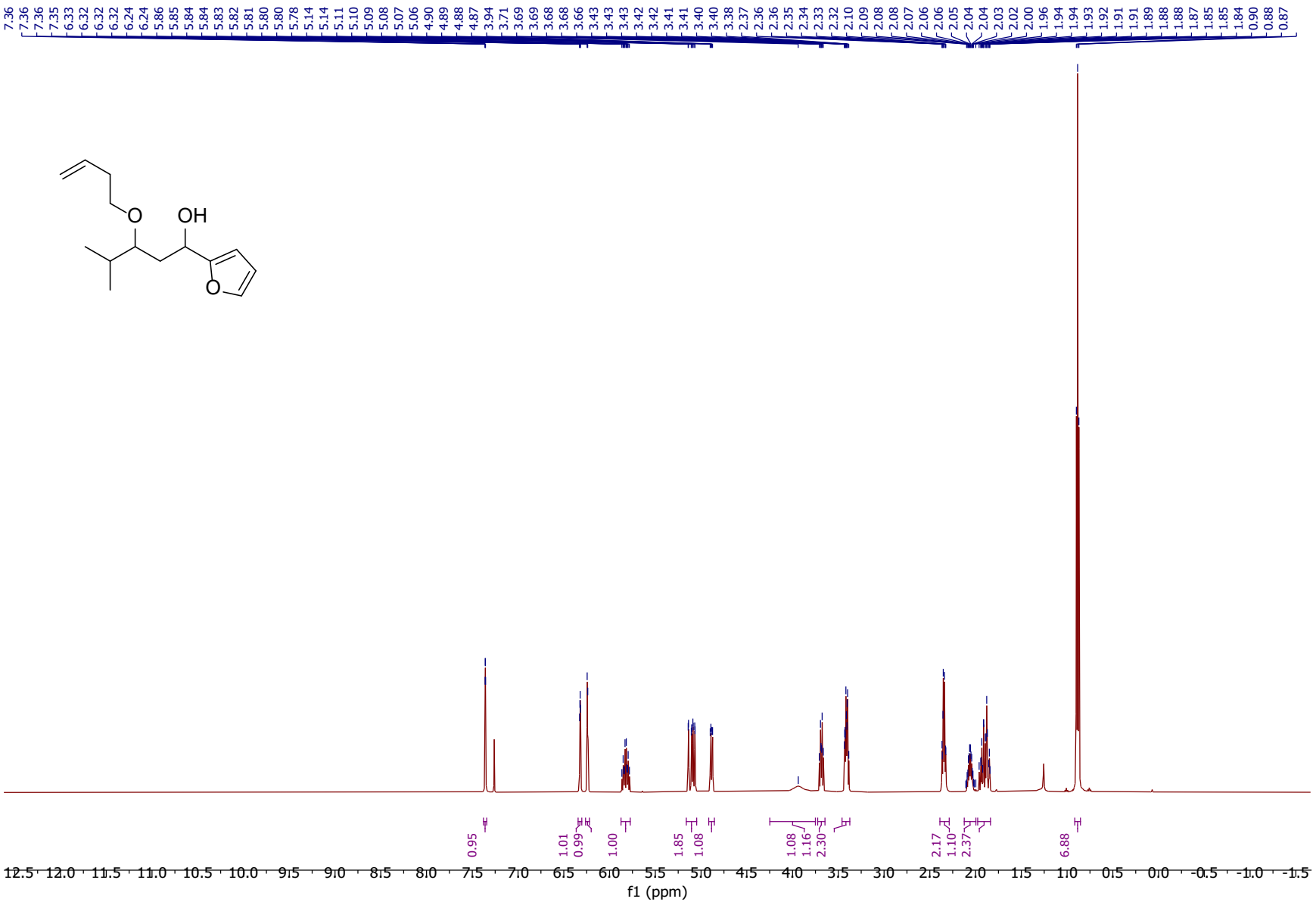

Figure S71: ^{1}H NMR (500 MHz, $CDCl_3$) of furanol 27c

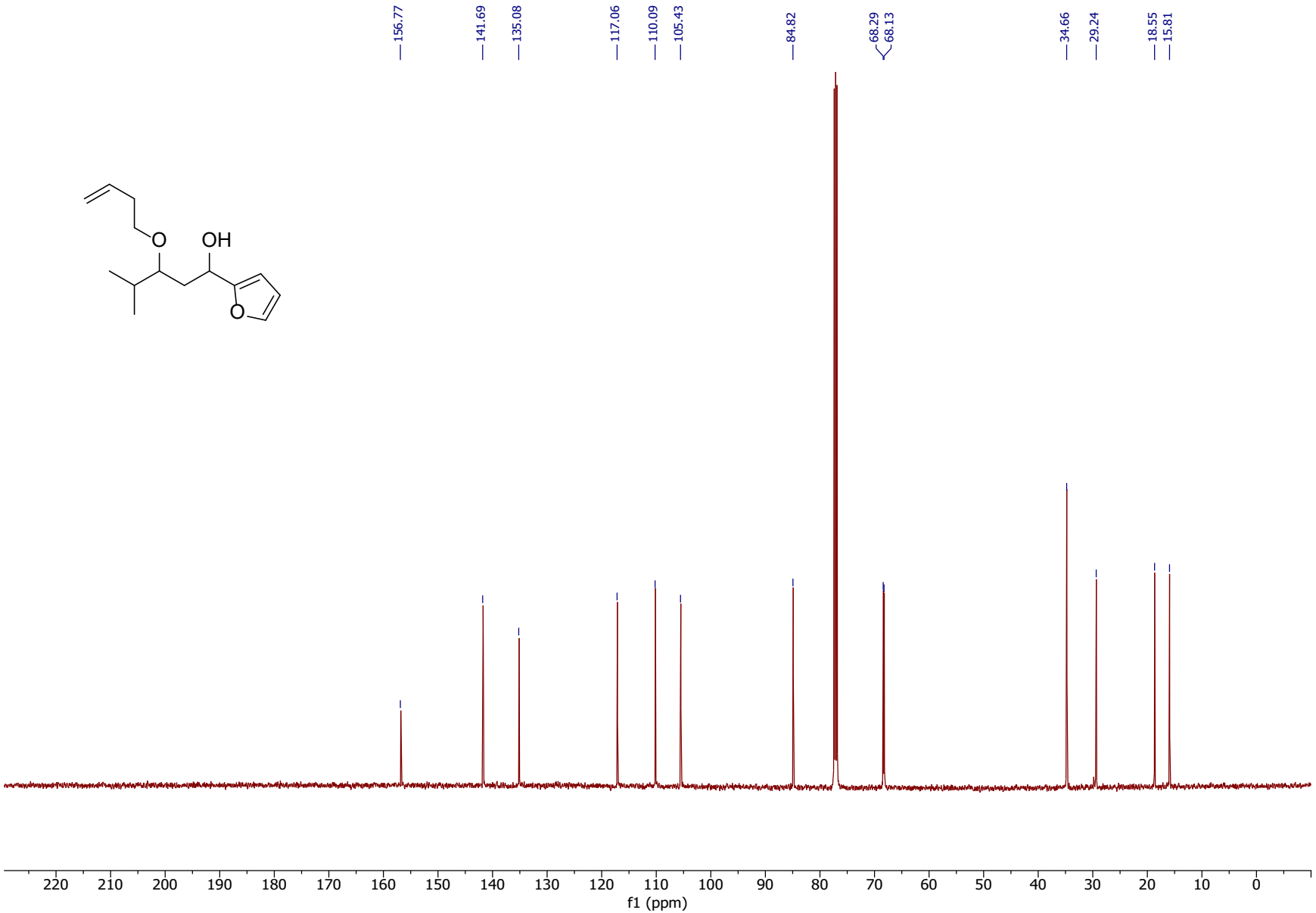

Figure S72: $^{13}C\{^{1}H\}$ (125 MHz, $CDCl_3$) of furanol 27c

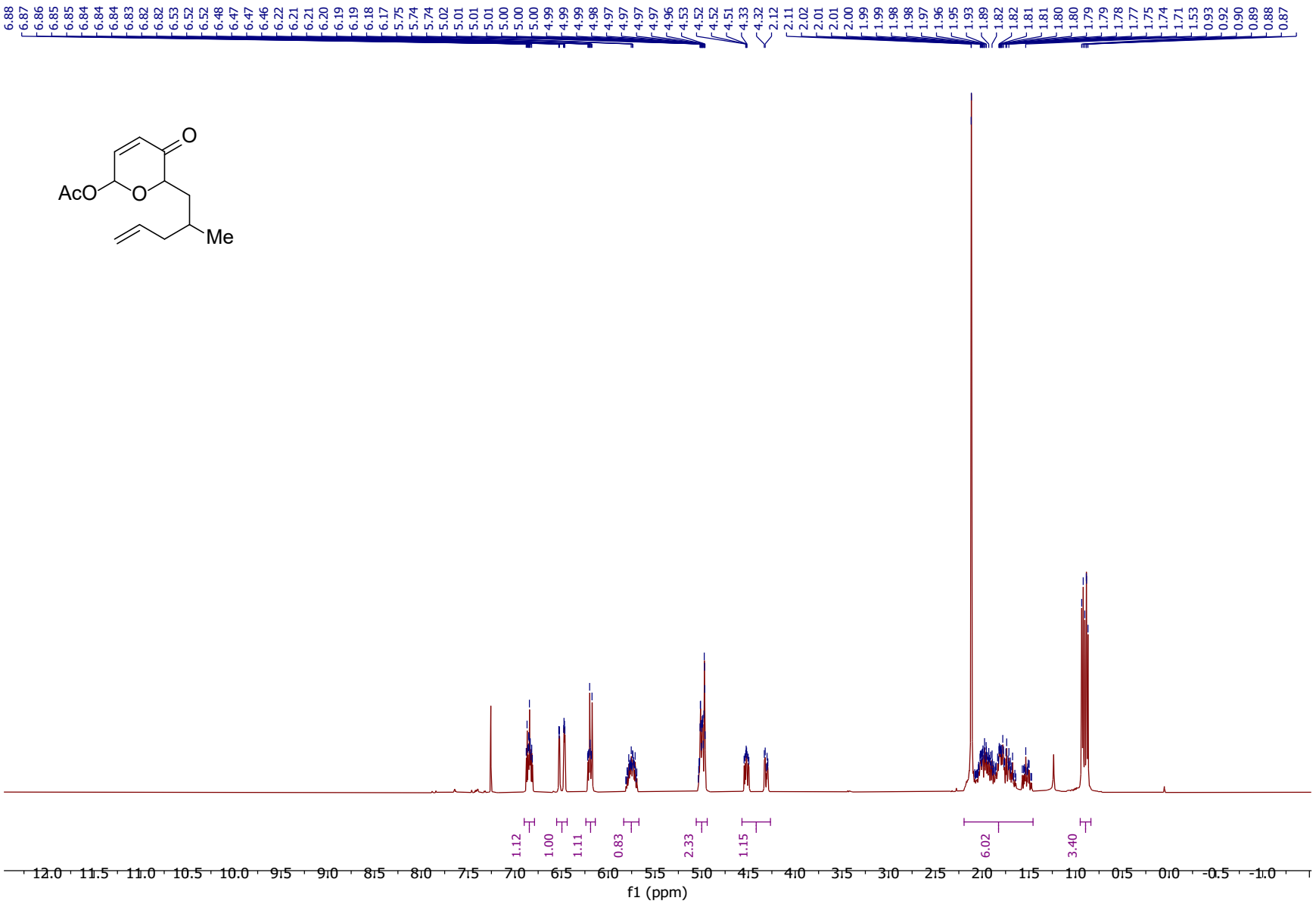

Figure S73: ^{1}H NMR (400 MHz, $CDCl_3$) of Achmatowicz product 9a

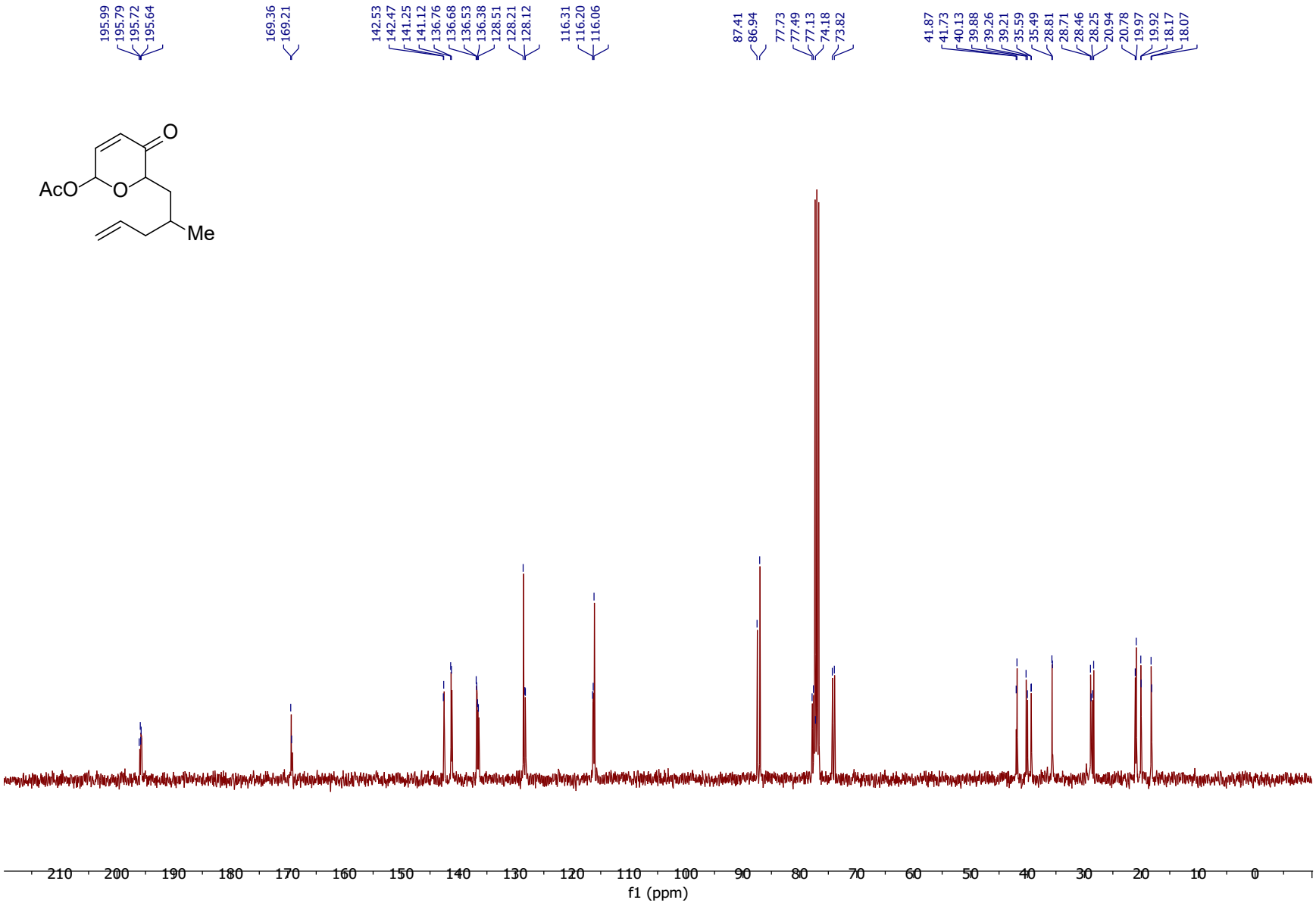

Figure S74: $^{13}C\{^{1}H\}$ (100 MHz, $CDCl_3$) of Achmatowicz product 9a

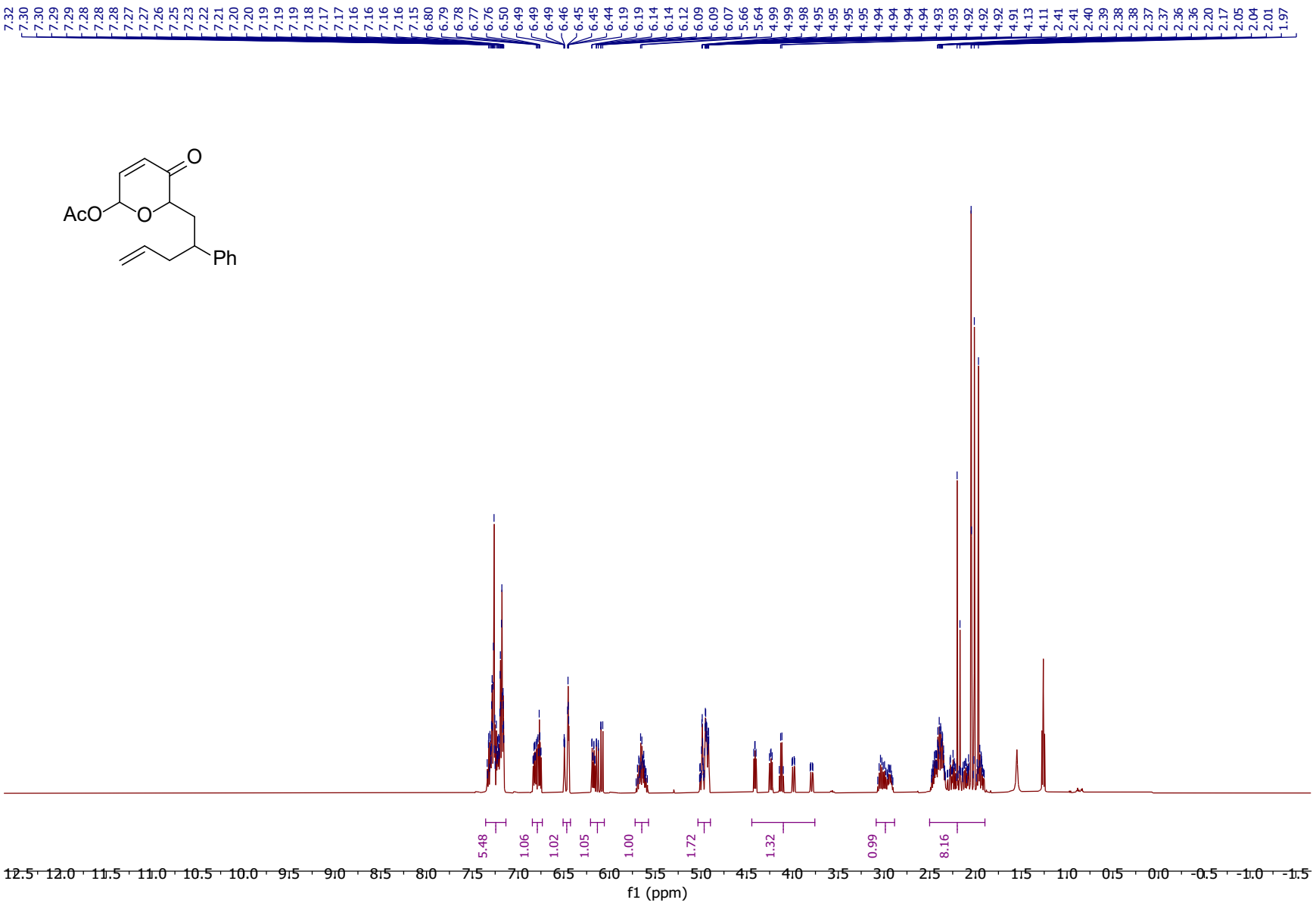

Figure S75: ^{1}H NMR (500 MHz, $CDCl_3$) of Achmatowicz product 9b

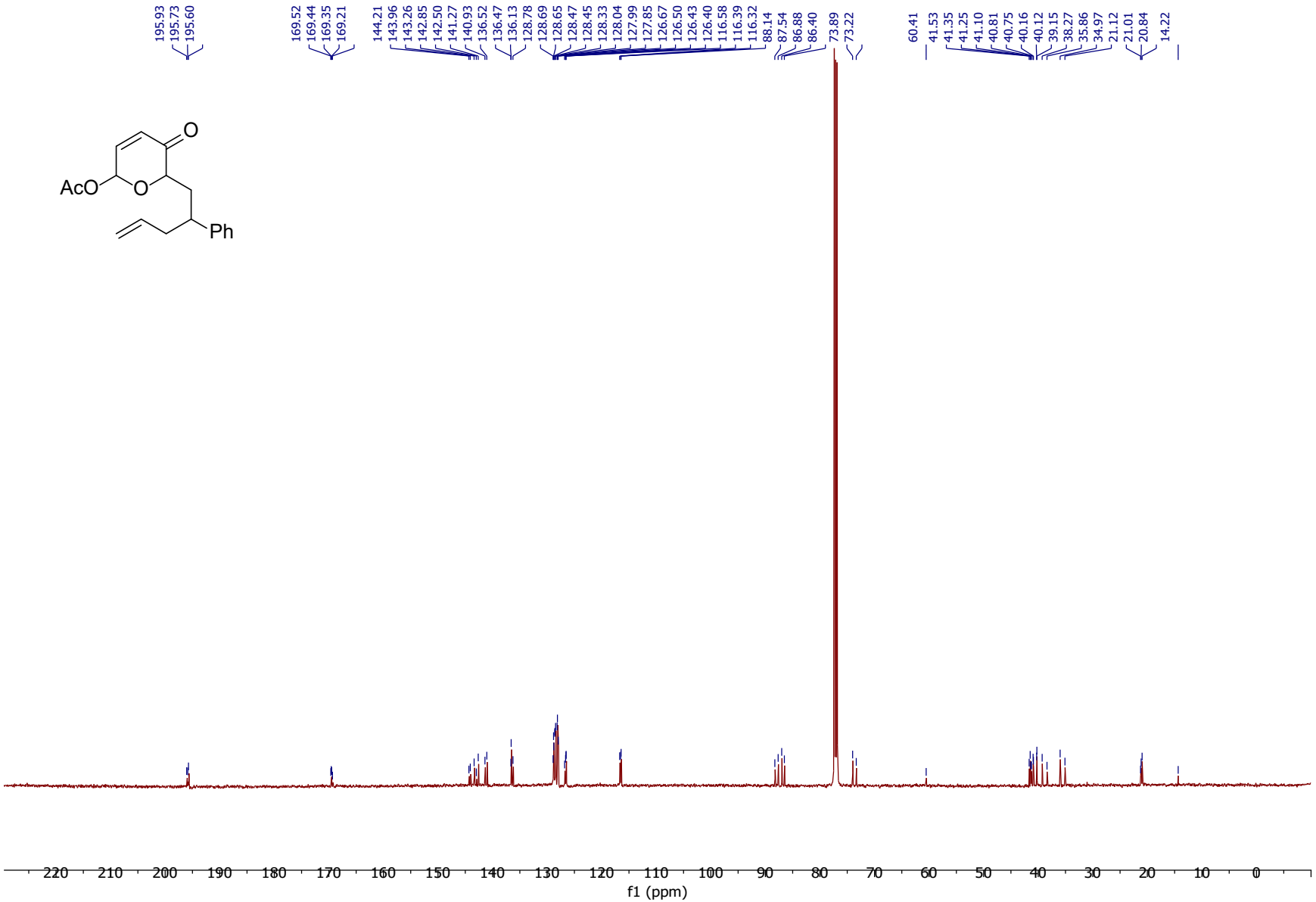

Figure S76: $^{13}C\{^{1}H\}$ (125 MHz, $CDCl_3$) of Achmatowicz product 9b

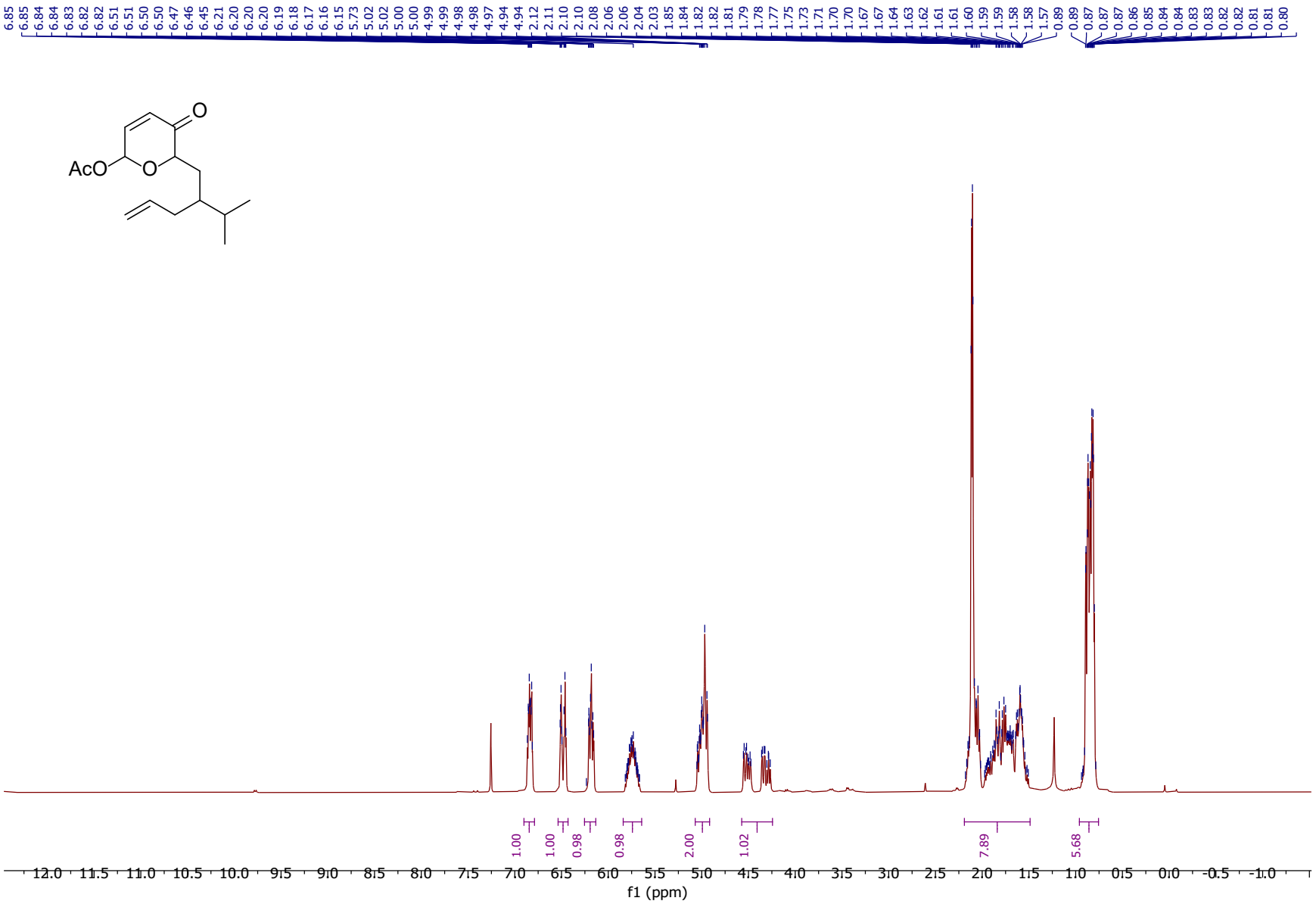

Figure S77: ^{1}H NMR (400 MHz, $CDCl_3$) of Achmatowicz product 9c

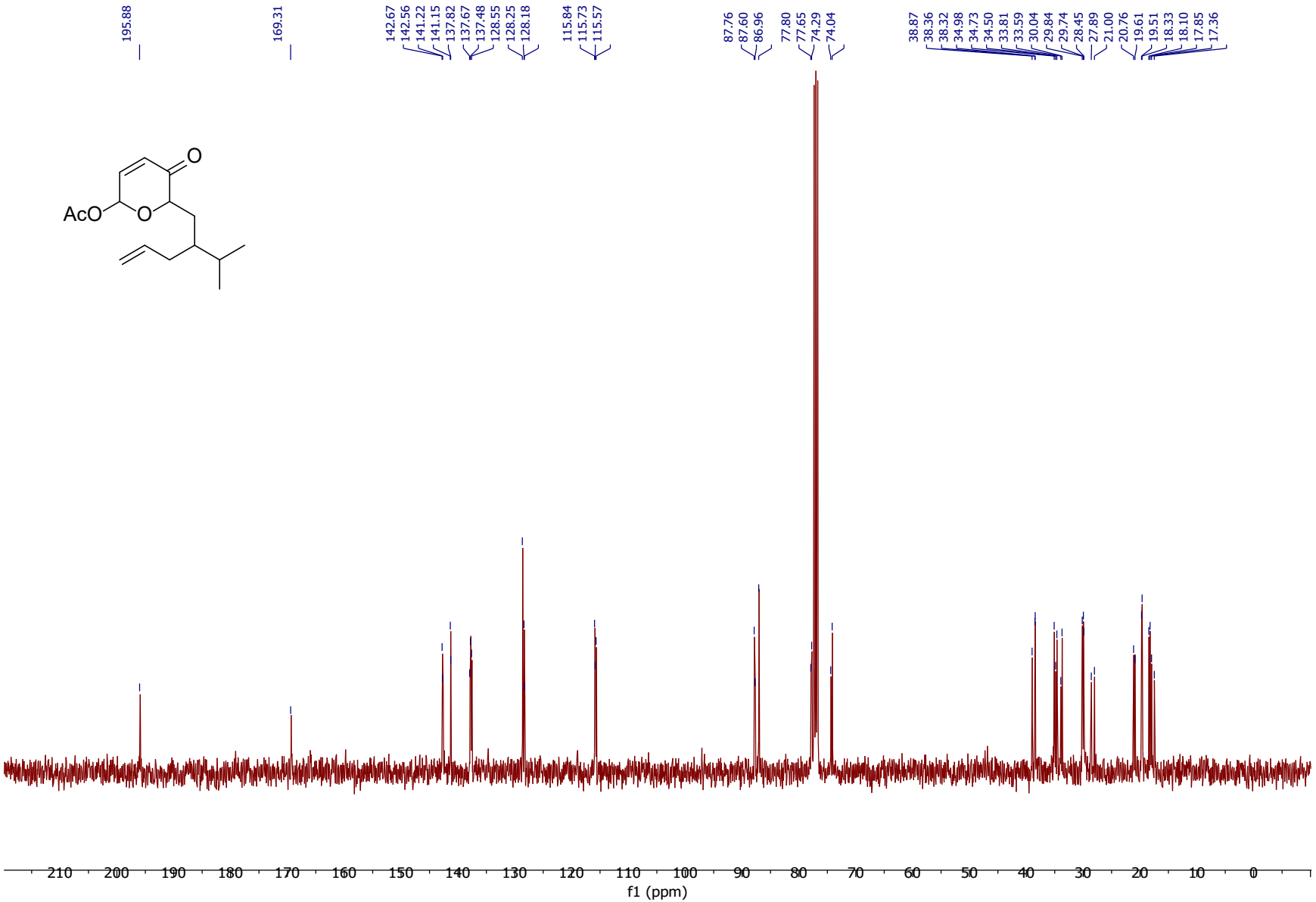

Figure S78: $^{13}C\{^{1}H\}$ (100 MHz, $CDCl_3$) of Achmatowicz product 9c

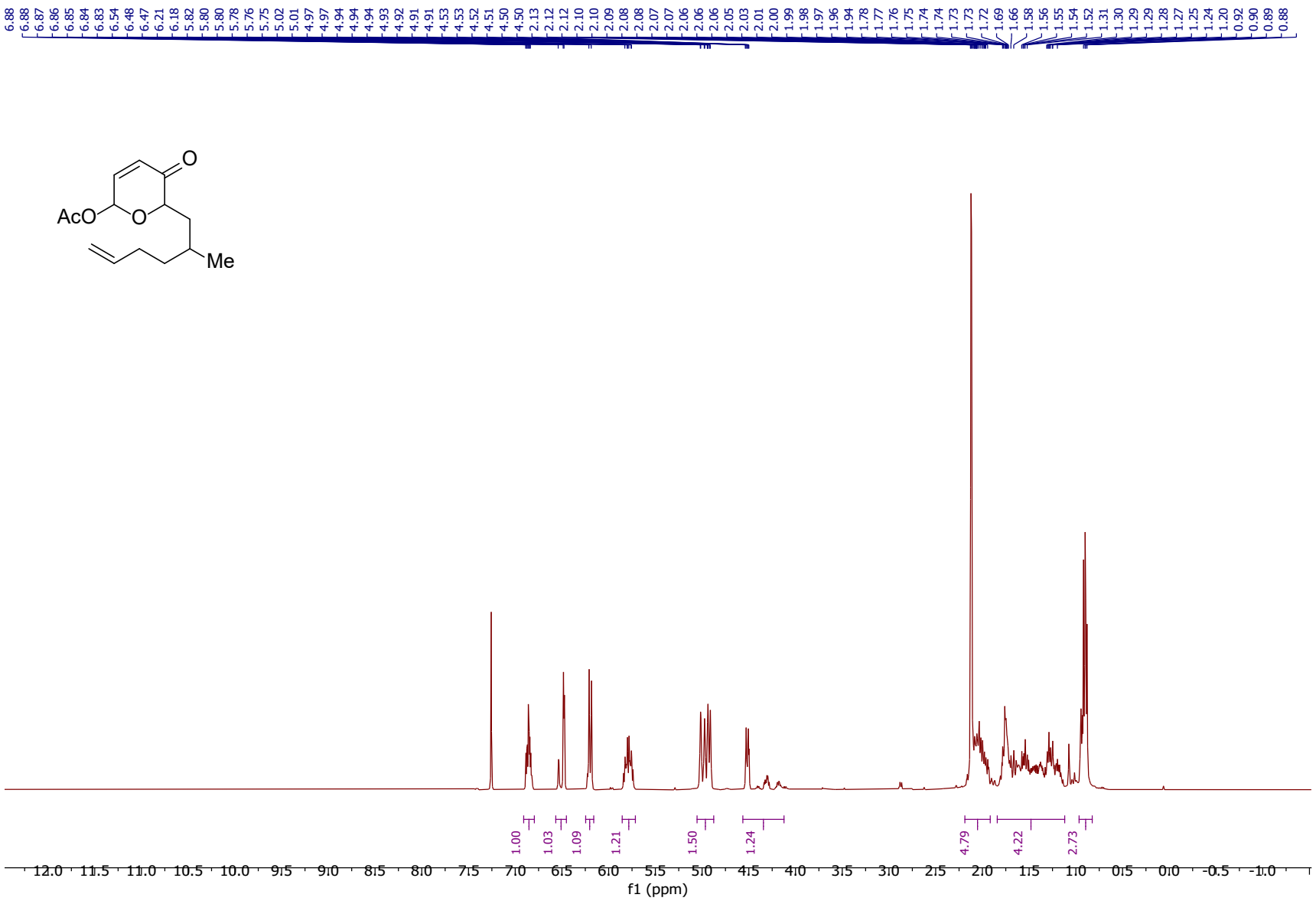

Figure S79: ^{1}H NMR (400 MHz, $CDCl_3$) of Achmatowicz product 9d

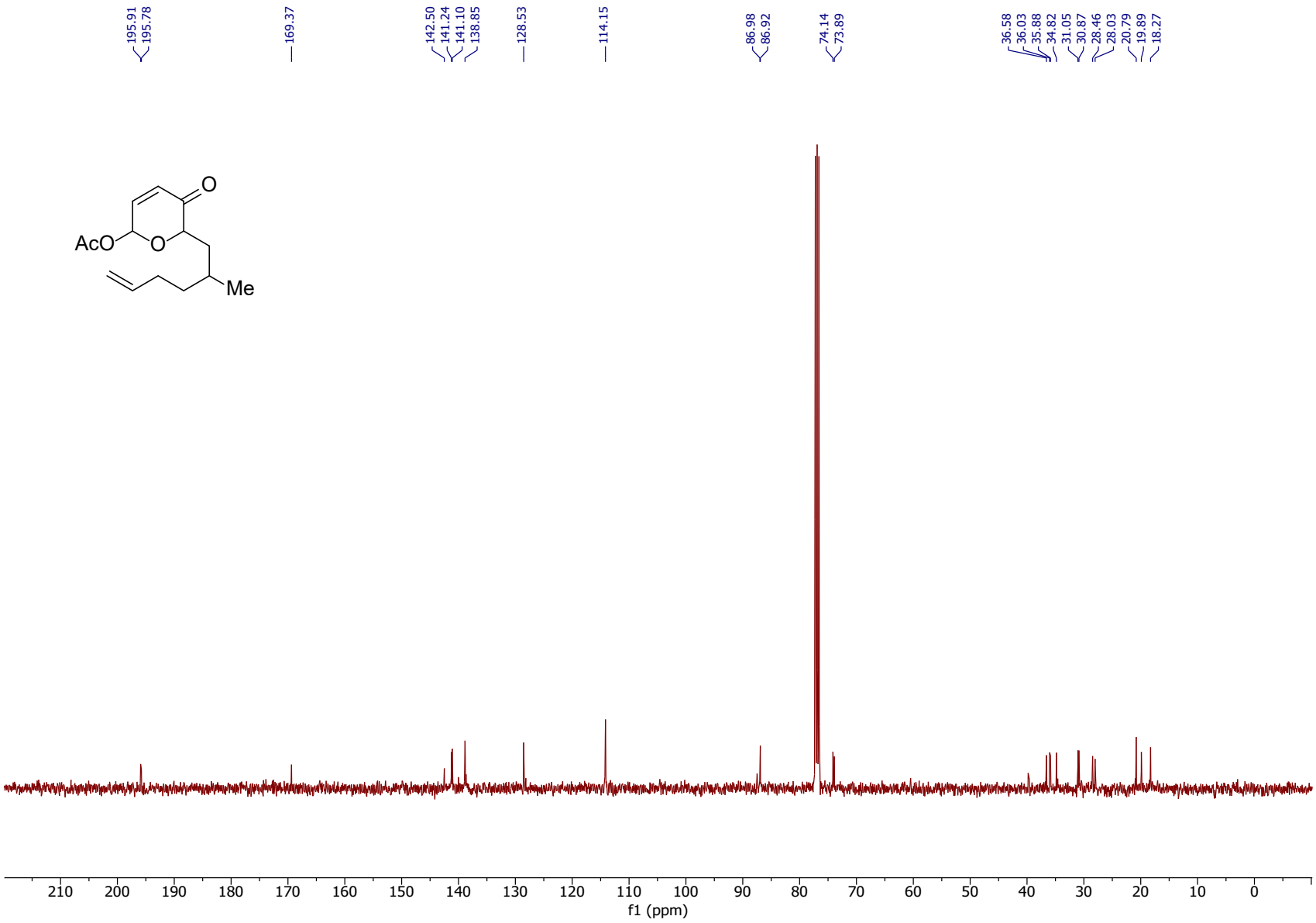

Figure S80: $^{13}C\{^{1}H\}$ (100 MHz, $CDCl_3$) of Achmatowicz product 9d

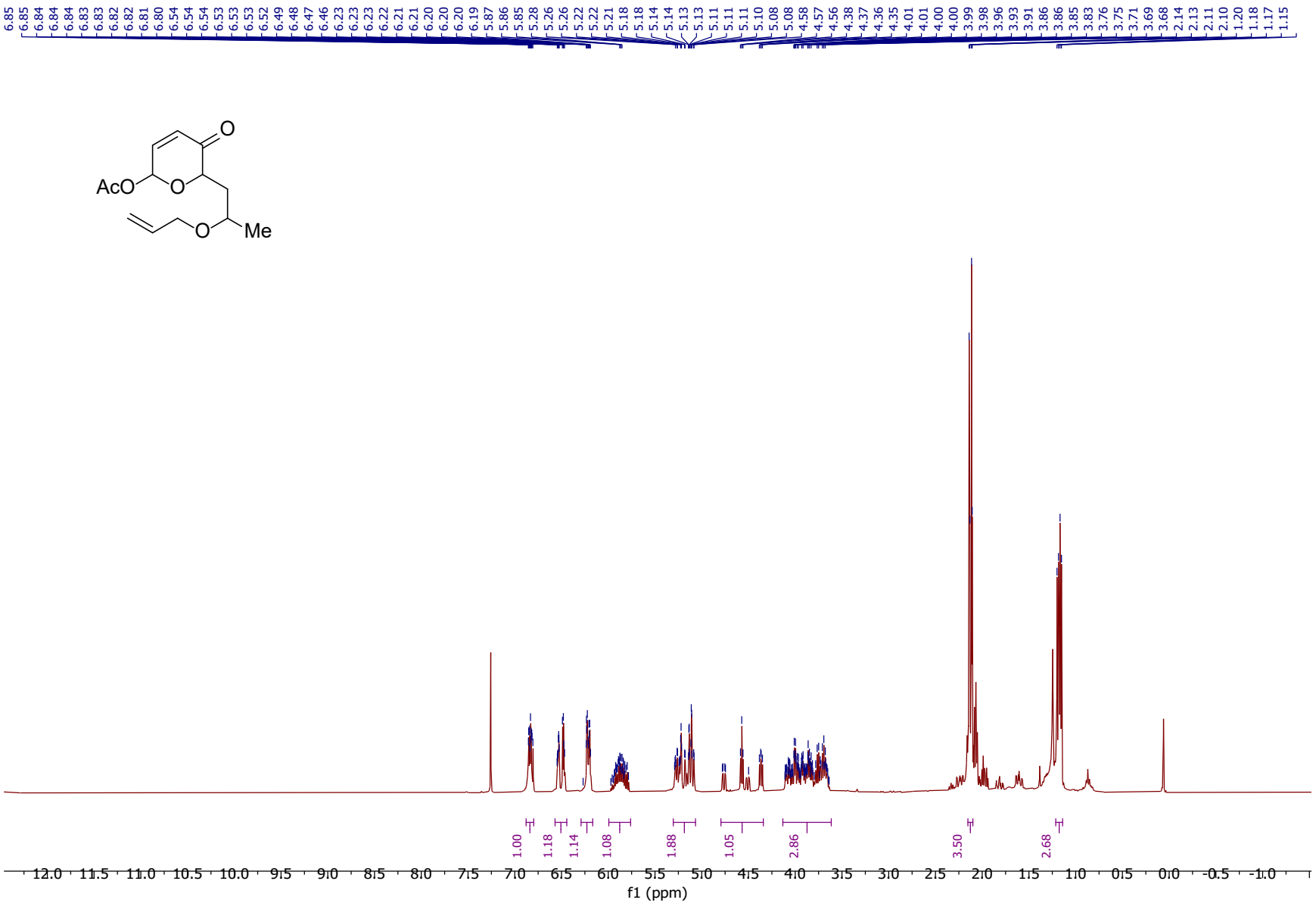

Figure S81: ^{1}H NMR (500 MHz, $CDCl_3$) of Achmatowicz product 9e

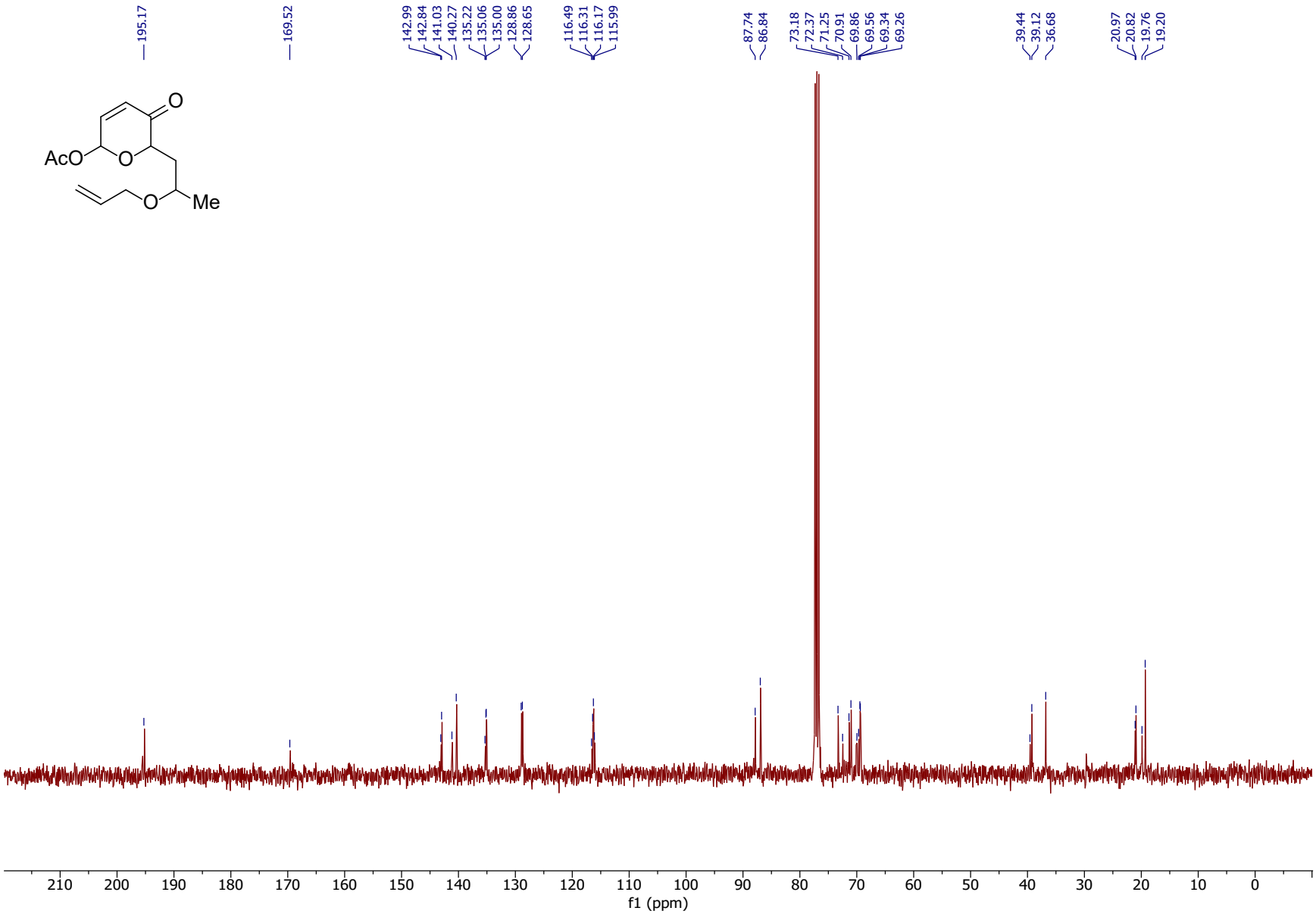

Figure S82: $^{13}C\{^{1}H\}$ (125 MHz, $CDCl_3$) of Achmatowicz 9e

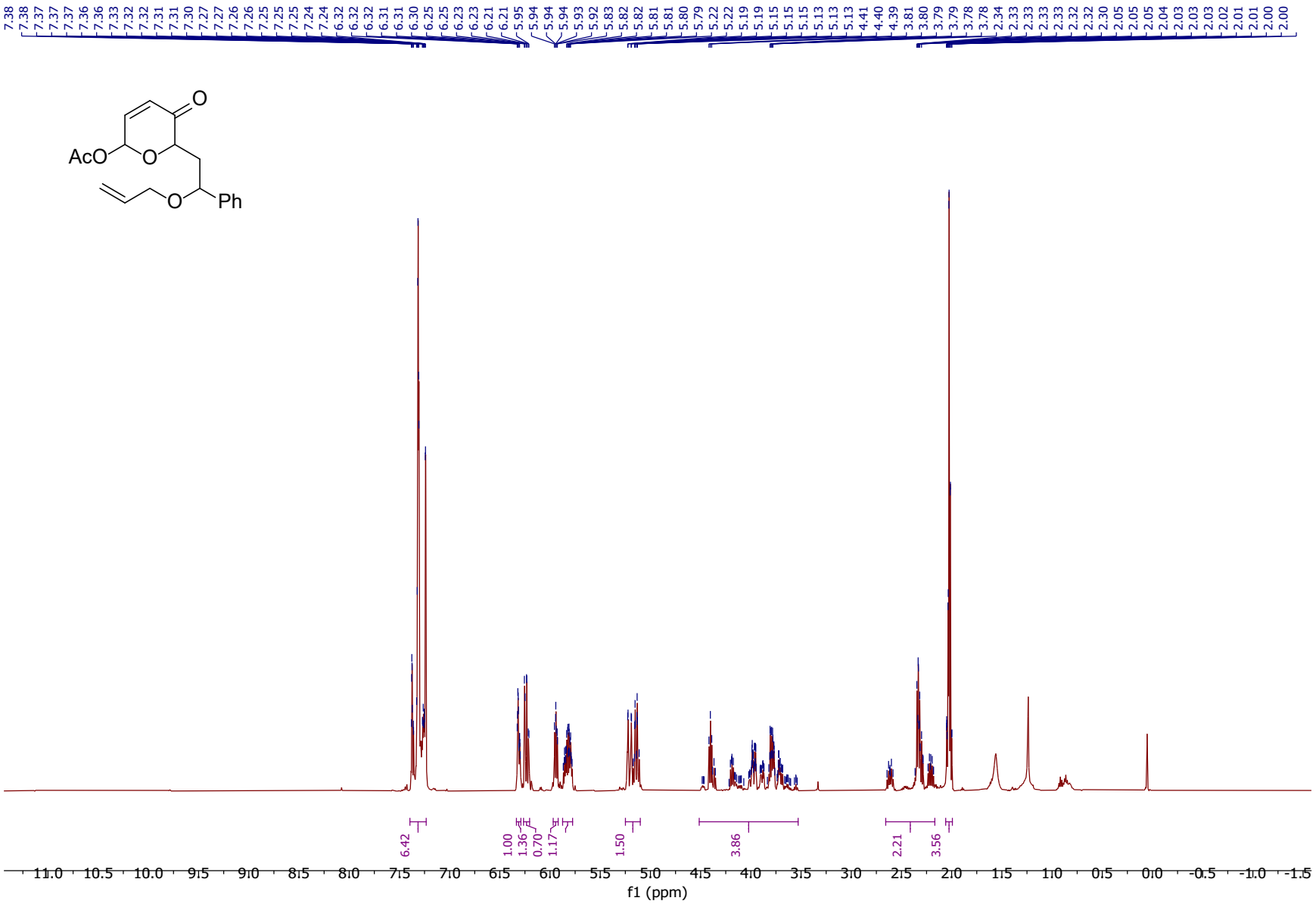

Figure S83: ^{1}H NMR (500 MHz, $CDCl_3$) of Achmatowicz product 9f

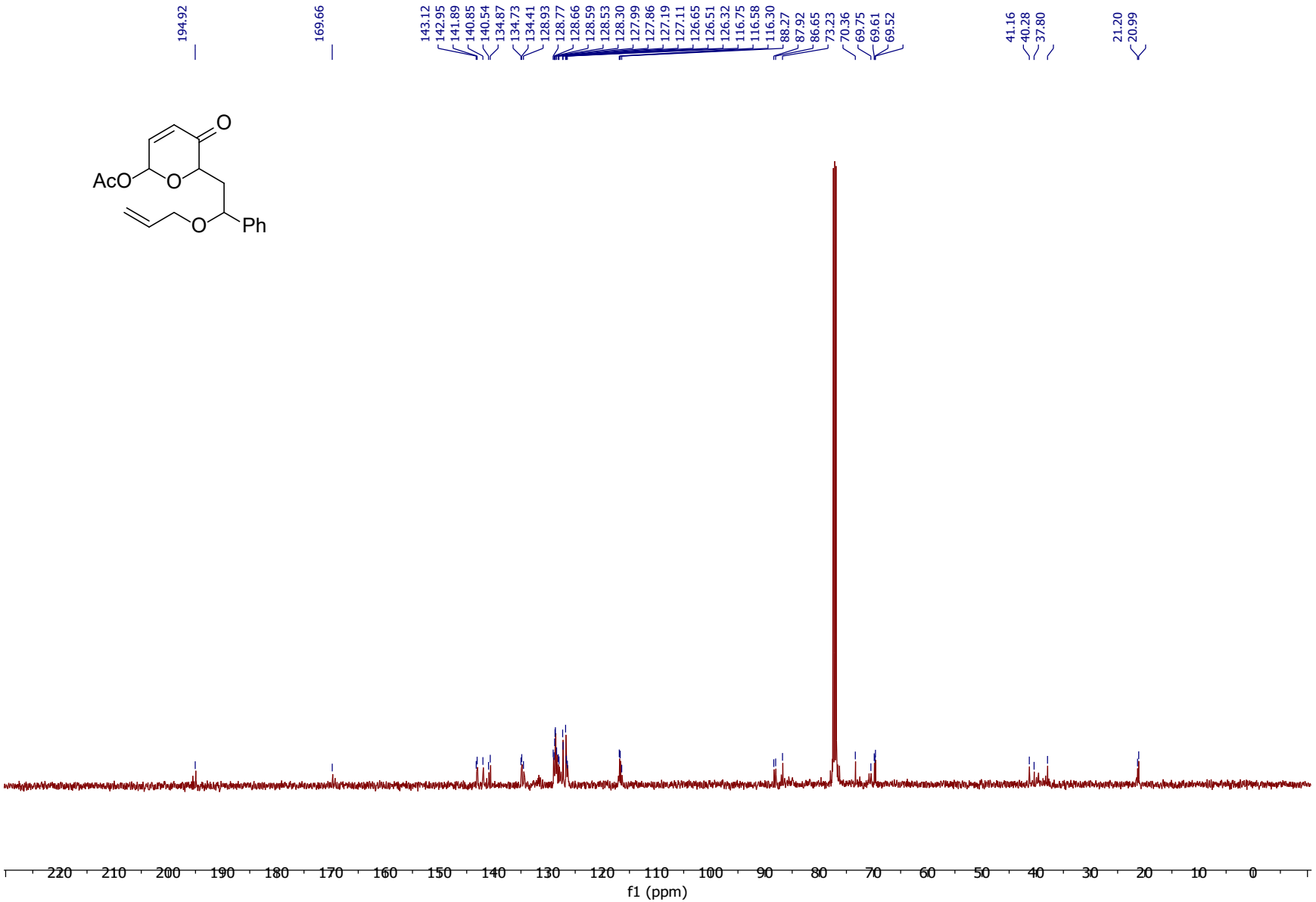

Figure S84: $^{13}C\{^{1}H\}$ (125 MHz, $CDCl_3$) of Achmatowiczz product 9f

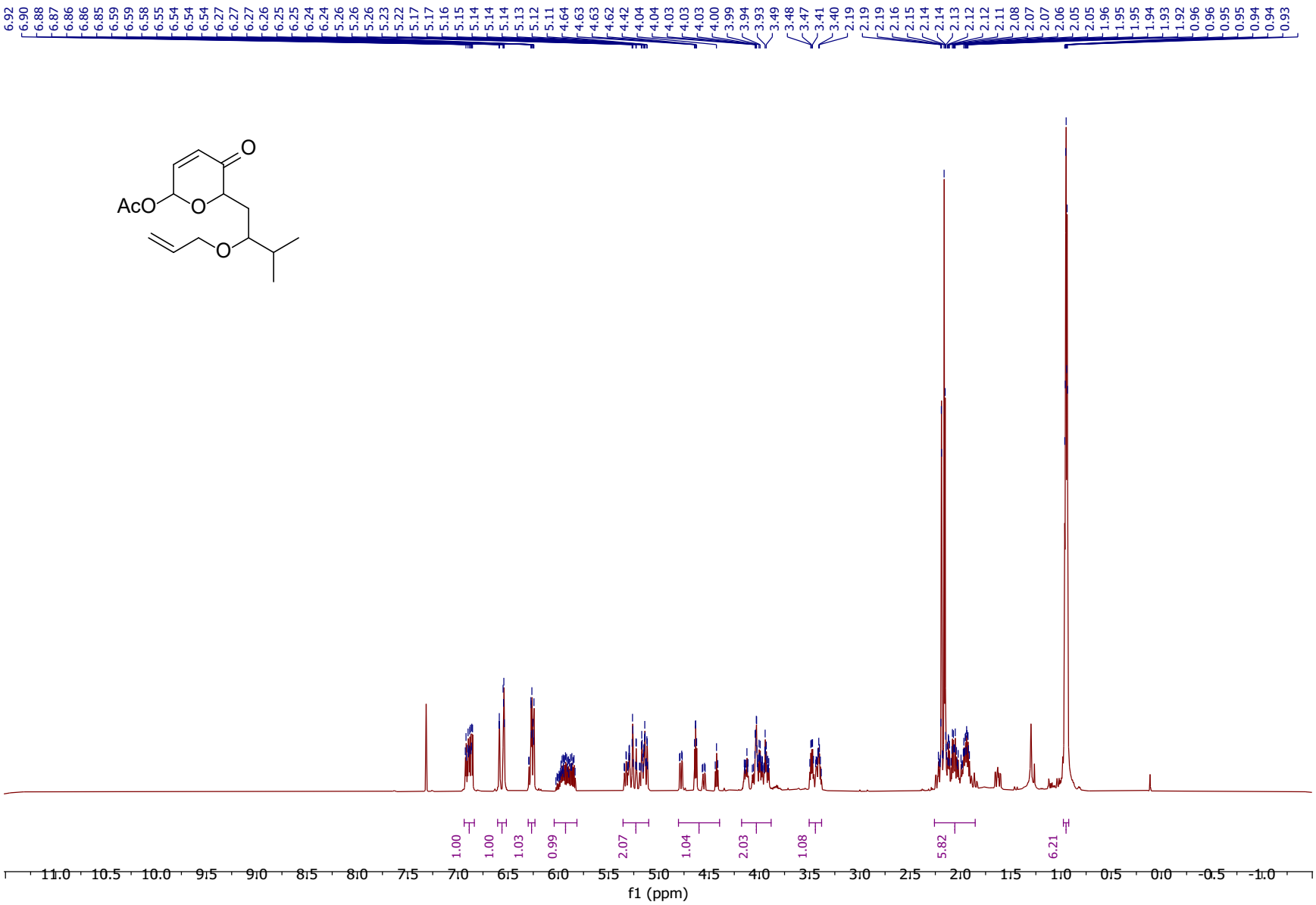

Figure S85: ^{1}H NMR (500 MHz, $CDCl_3$) of Achmatowicz product 9g

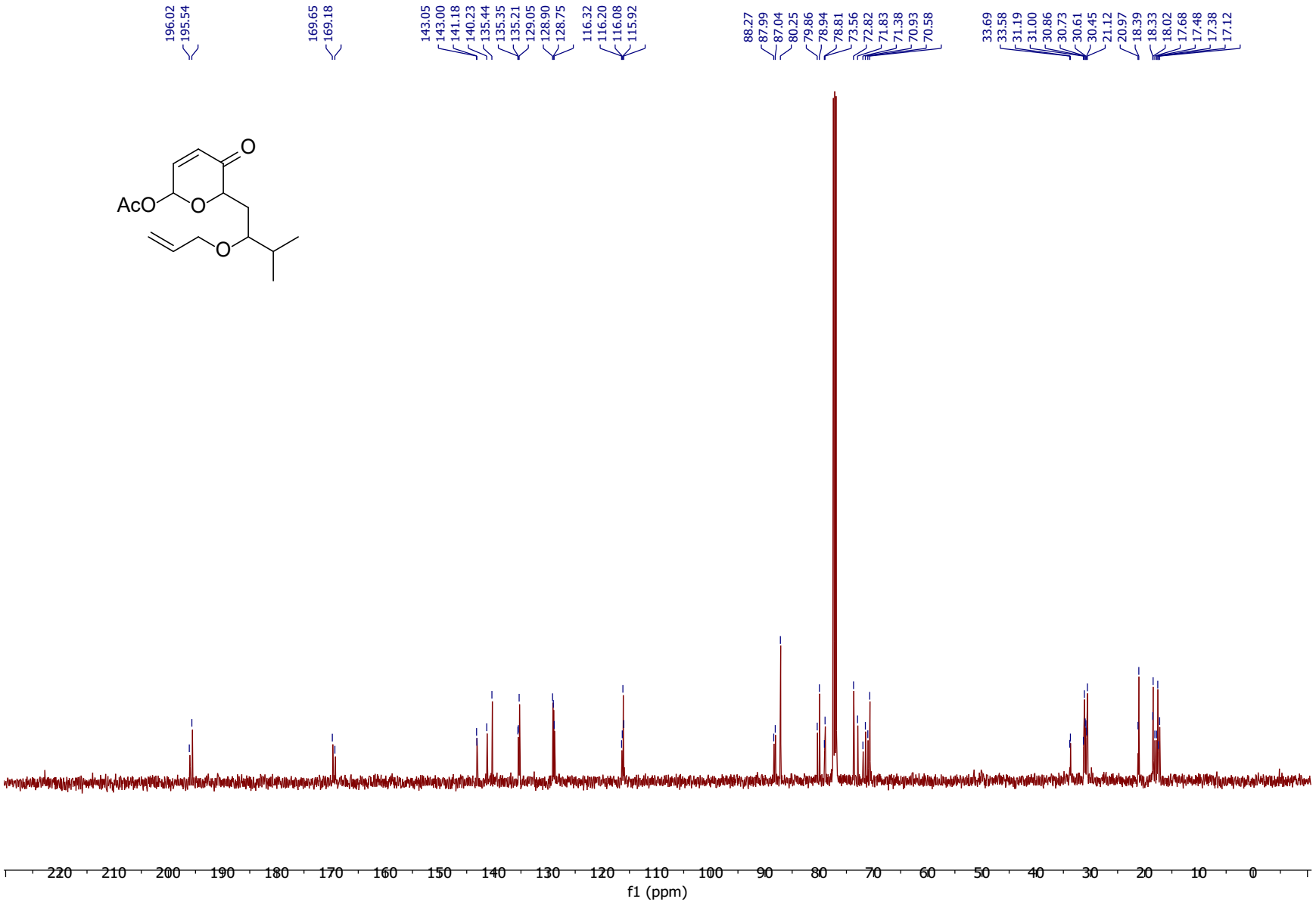

Figure S86: $^{13}C\{^{1}H\}$ (125 MHz, $CDCl_3$) of Achmatowicz 9g

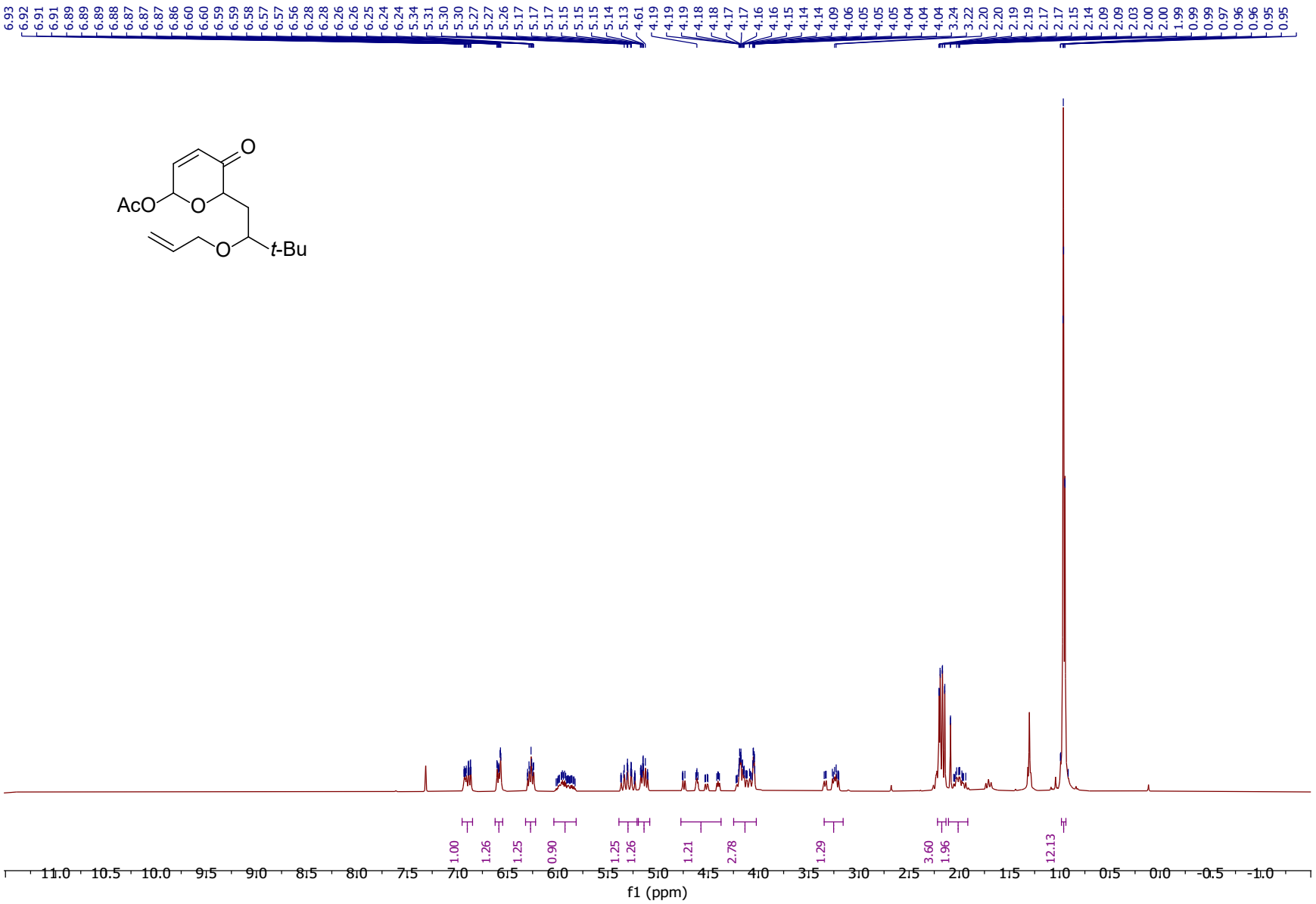

Figure S87: ^{1}H NMR (500 MHz, $CDCl_3$) of Achmatowicz product 9h

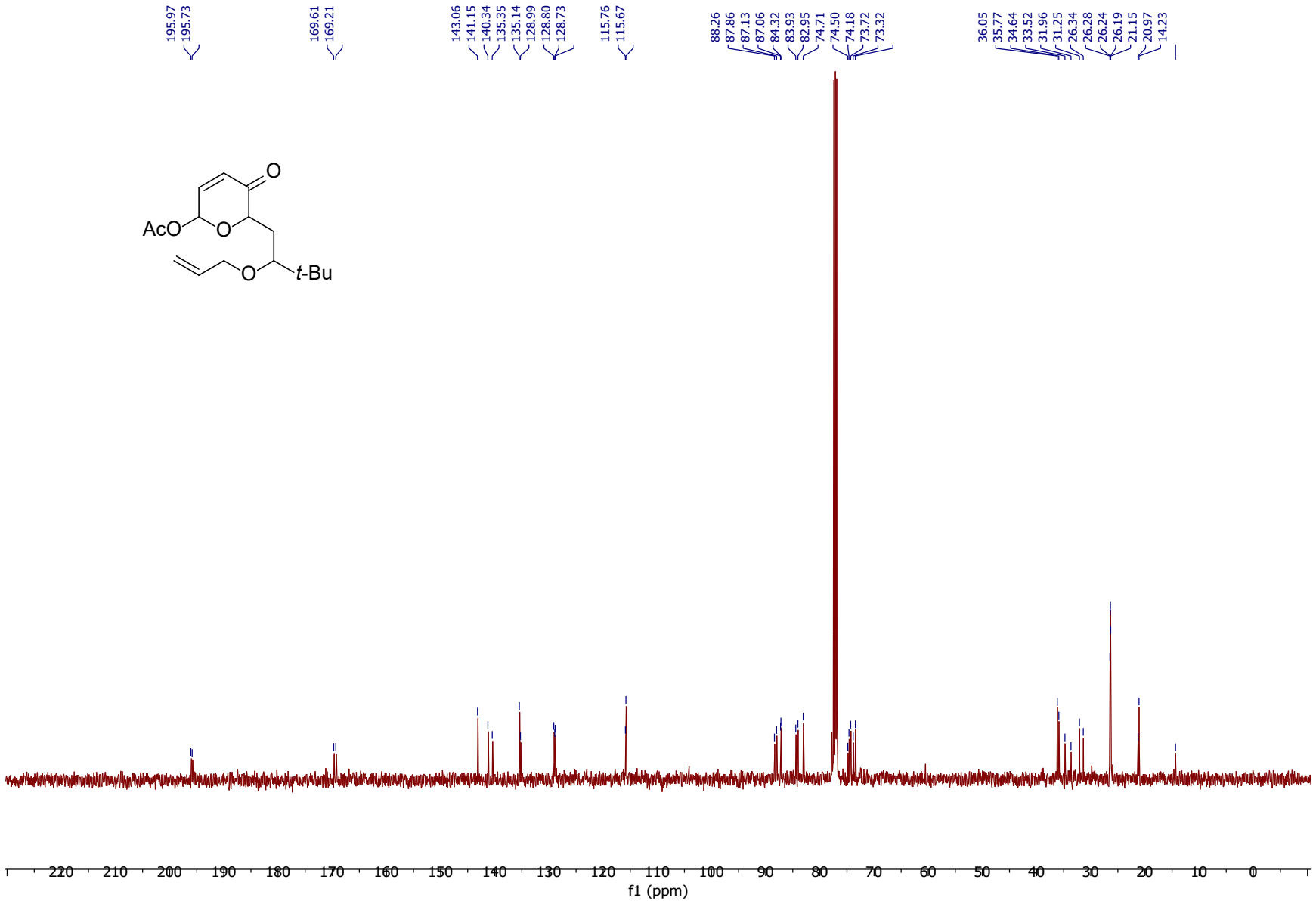

Figure S88: $^{13}C\{^{1}H\}$ (125 MHz, $CDCl_3$) of Achmatowicz product 9h

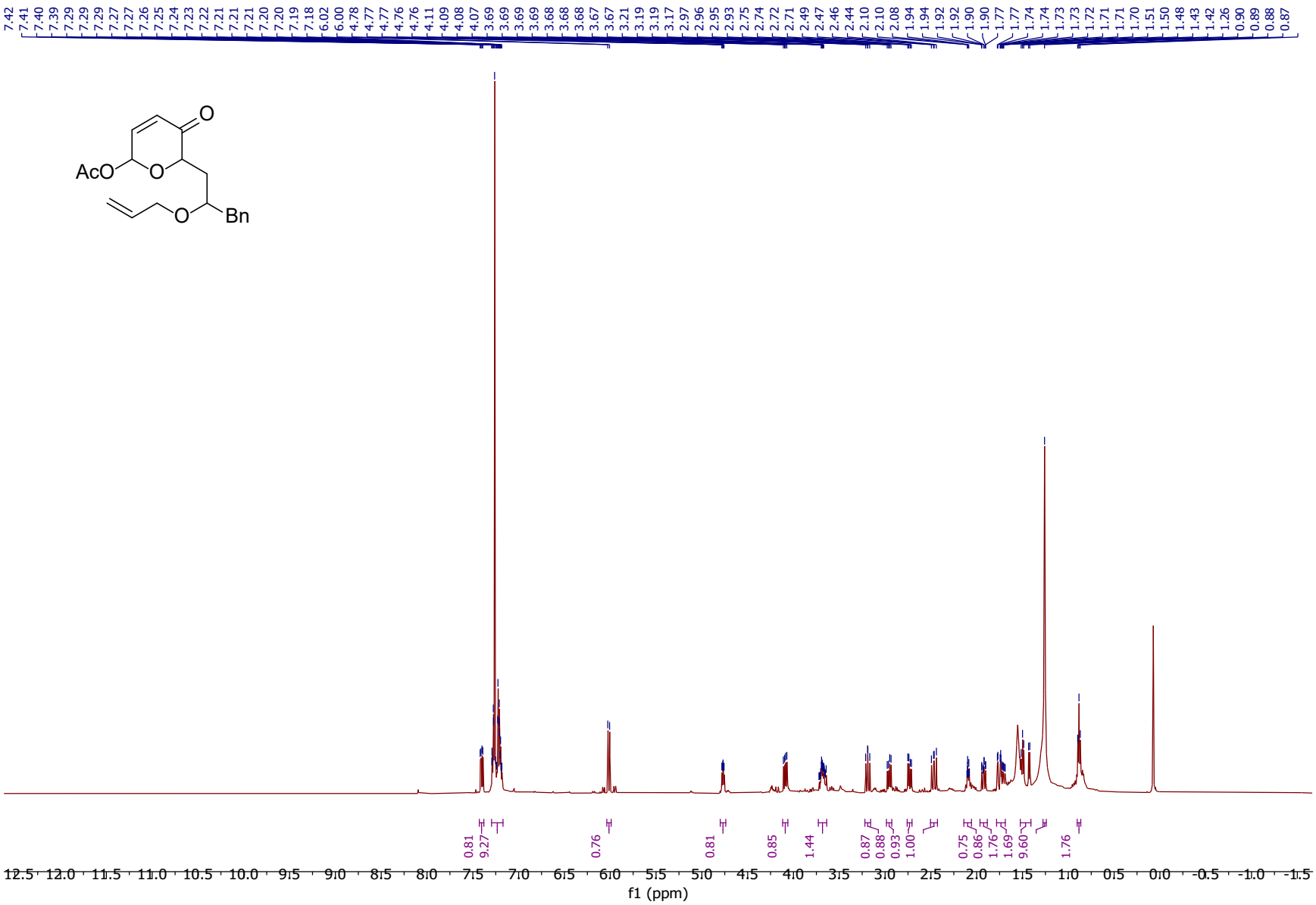

Figure S89: ^{1}H NMR (500 MHz, $CDCl_3$) of Achmatowicz product 9i

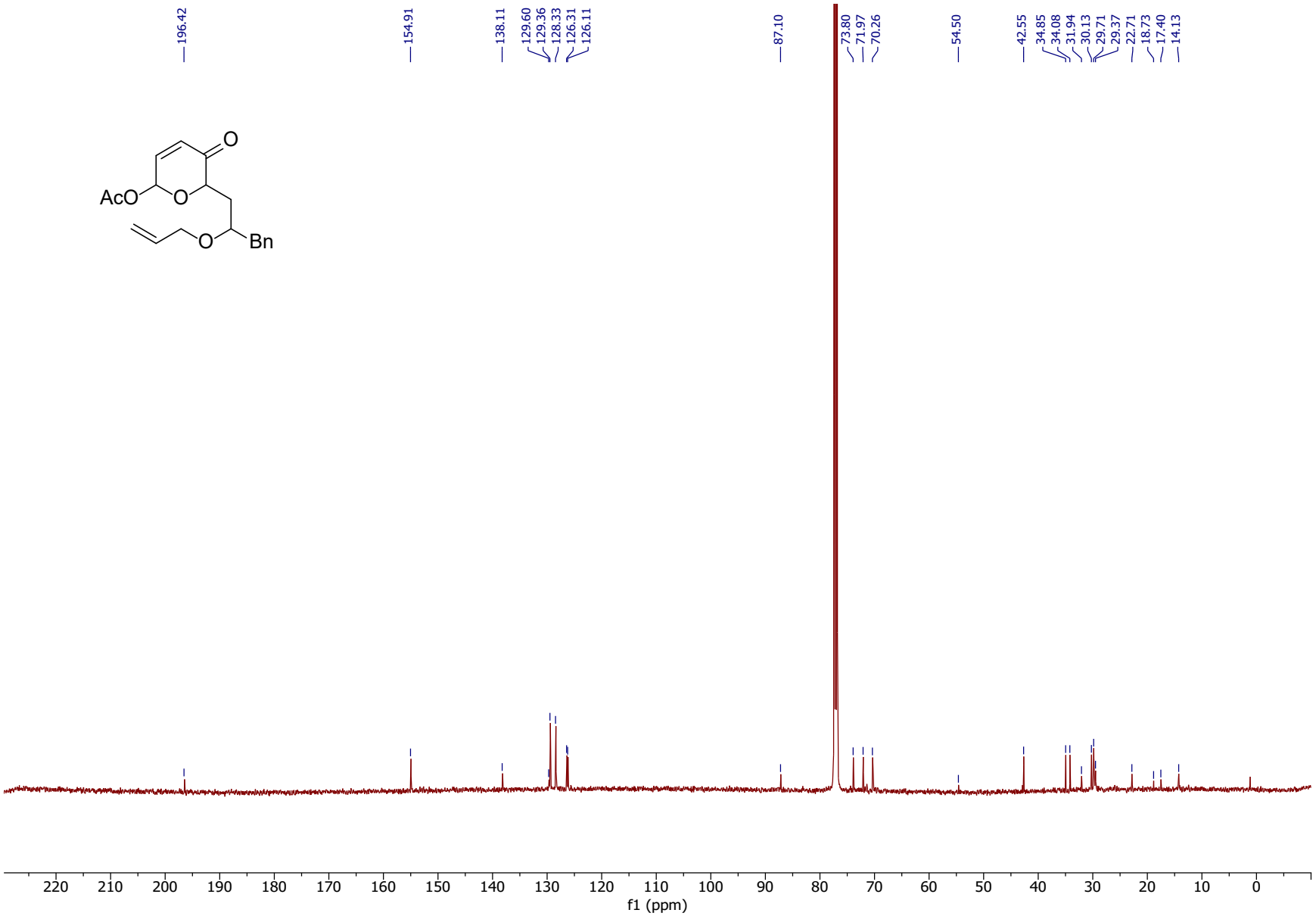

Figure S90: $^{13}C\{^{1}H\}$ (125 MHz, $CDCl_3$) of Achmatowicz product 9i

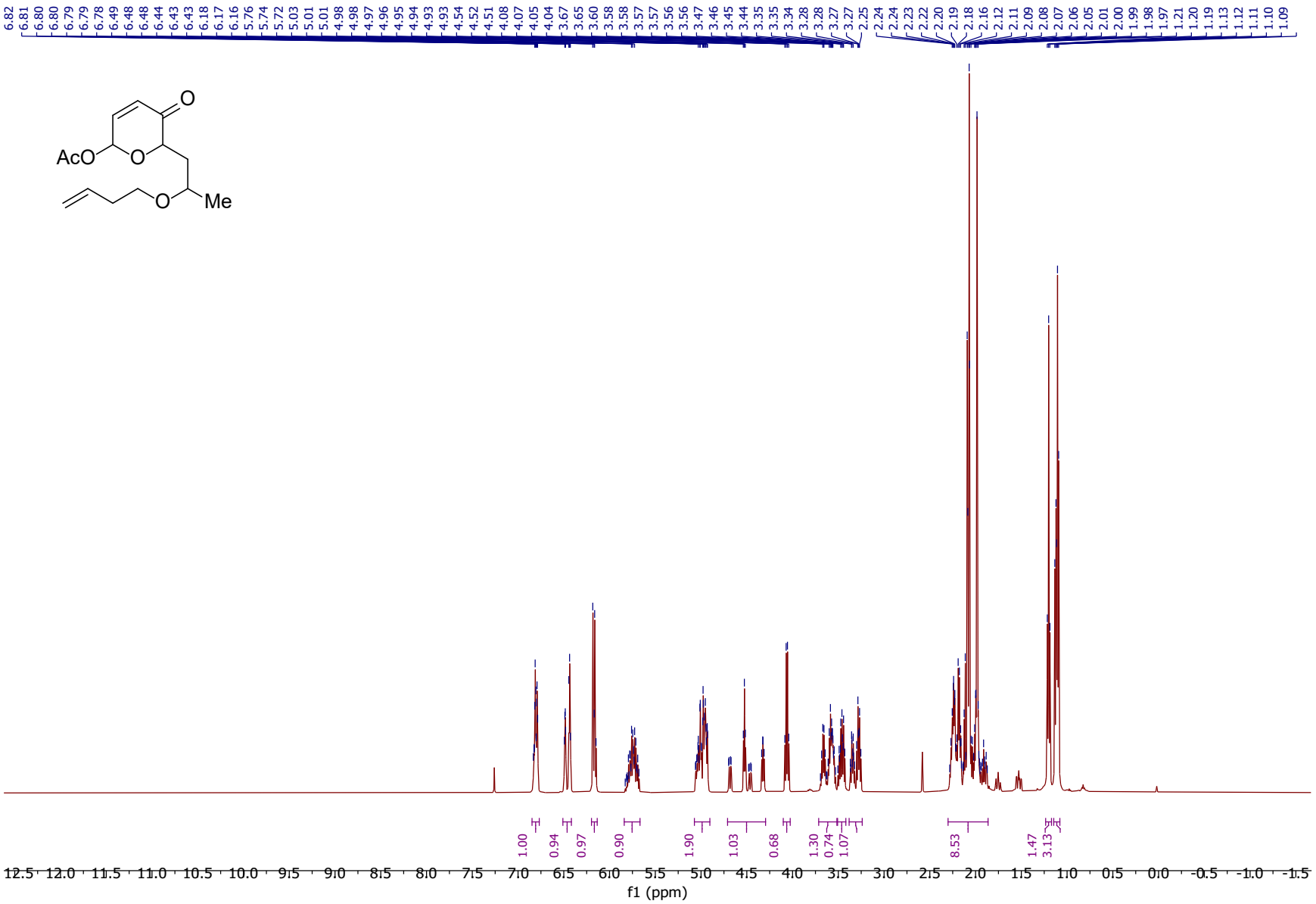

Figure S91: ^{1}H NMR (500 MHz, $CDCl_3$) of Achmatowicz product 9j

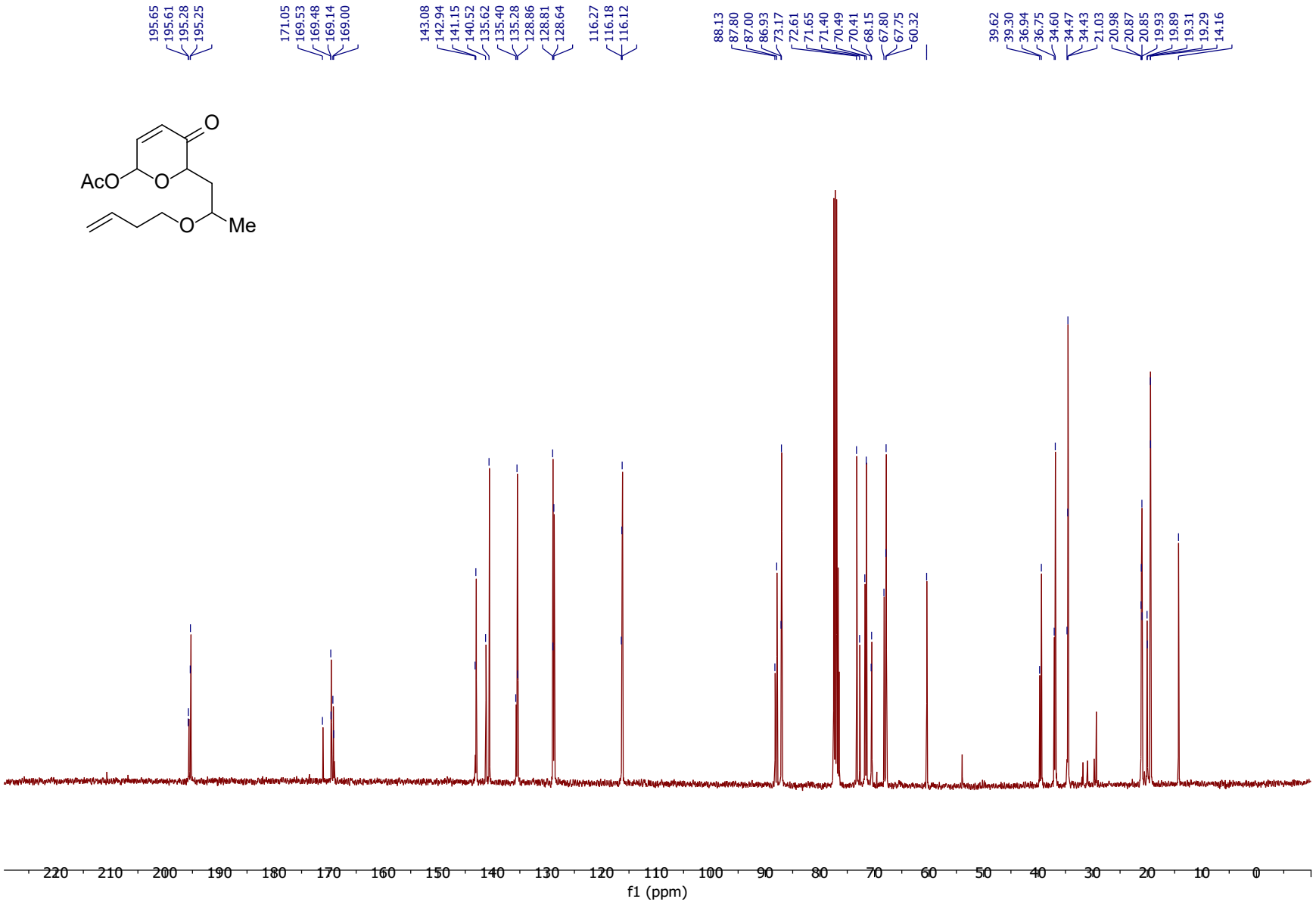

Figure S92: $^{13}C\{^{1}H\}$ (125 MHz, $CDCl_3$) of Achmatowicz product 9j

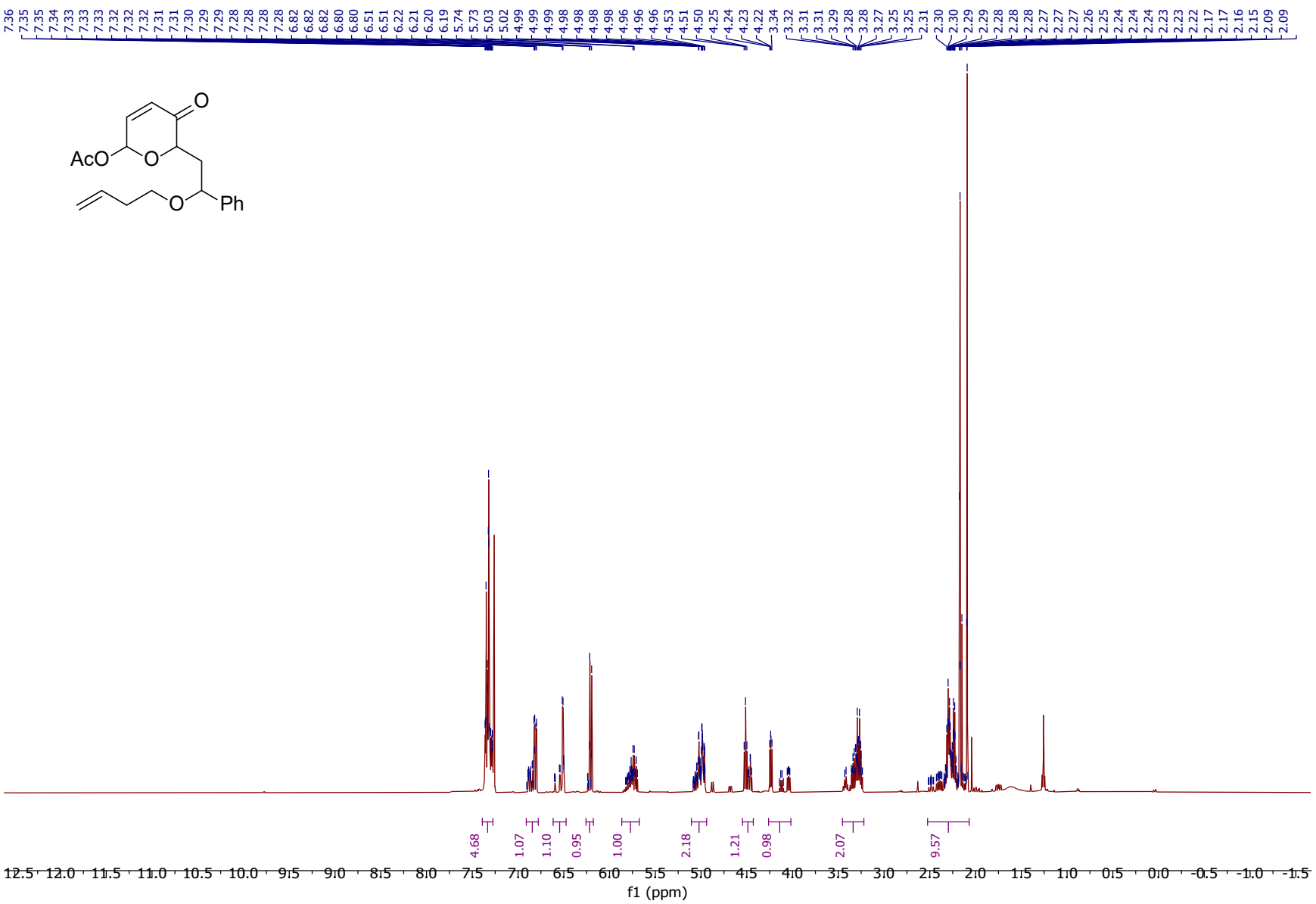

Figure S93: ^{1}H NMR (500 MHz, $CDCl_3$) of Achmatowicz product 9k

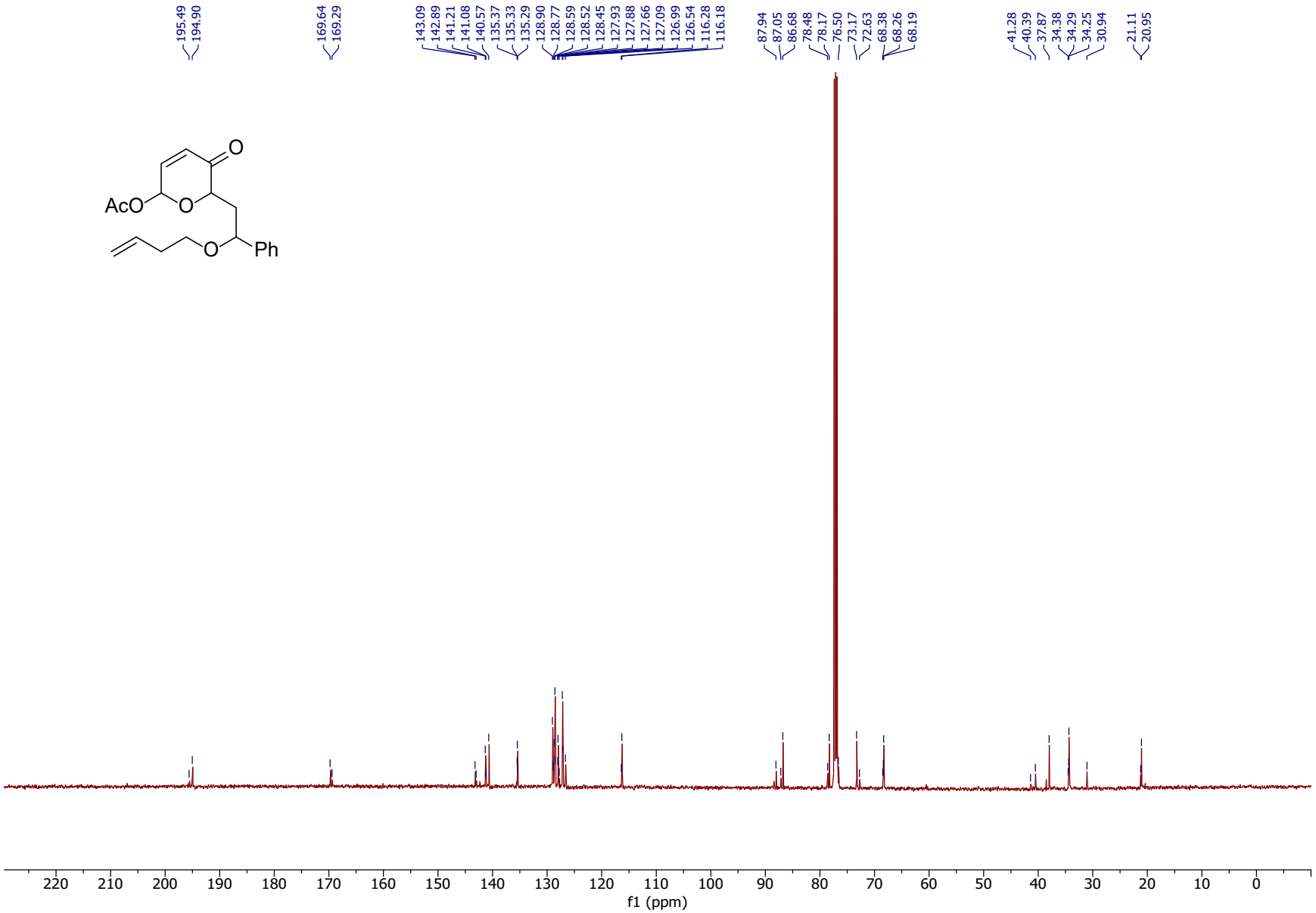

Figure S94: $^{13}C\{^{1}H\}$ (125 MHz, $CDCl_3$) of Achmatowicz product 9k

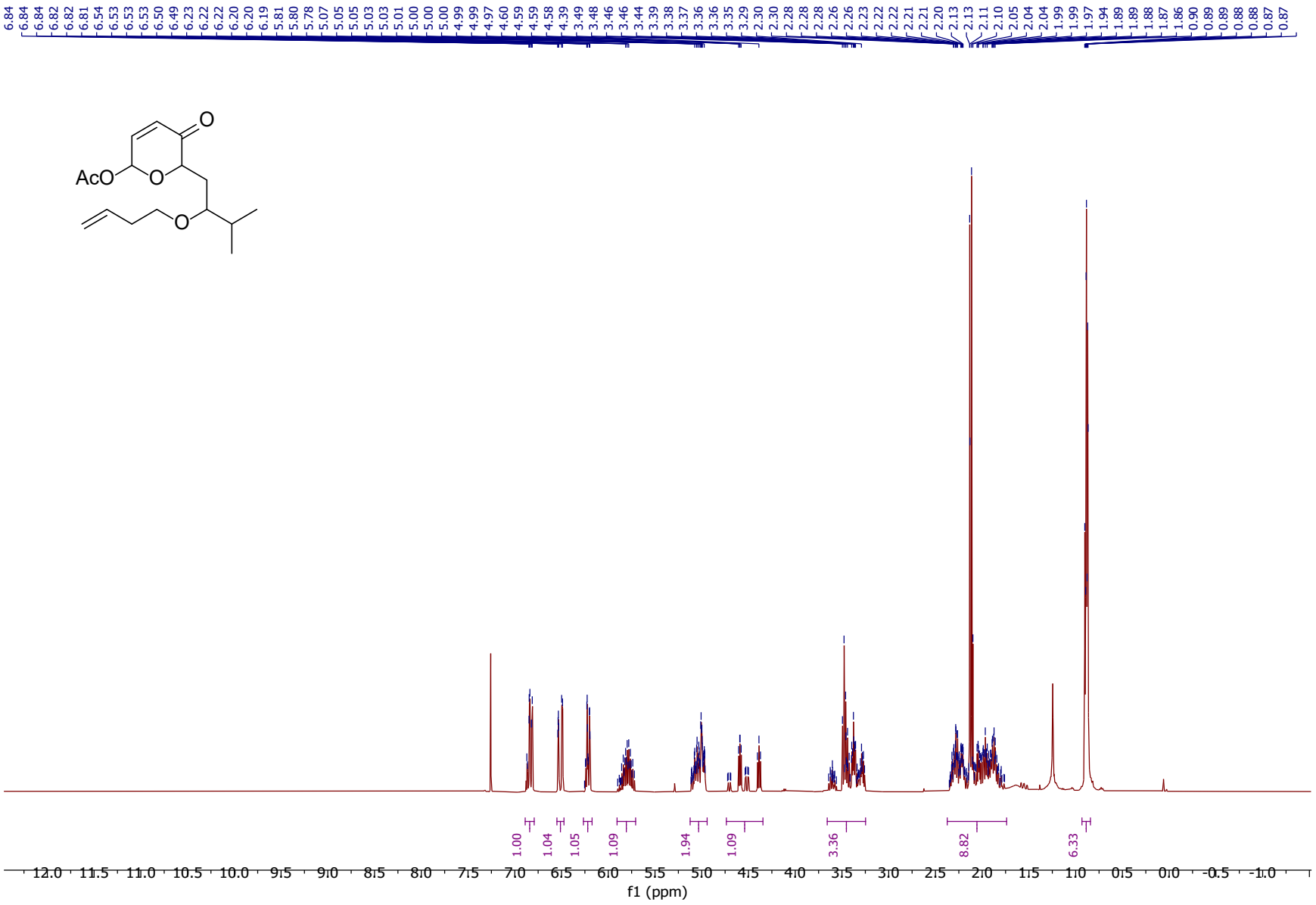

Figure S95: ^{1}H NMR (400 MHz, $CDCl_3$) of Achmatowicz product 9l

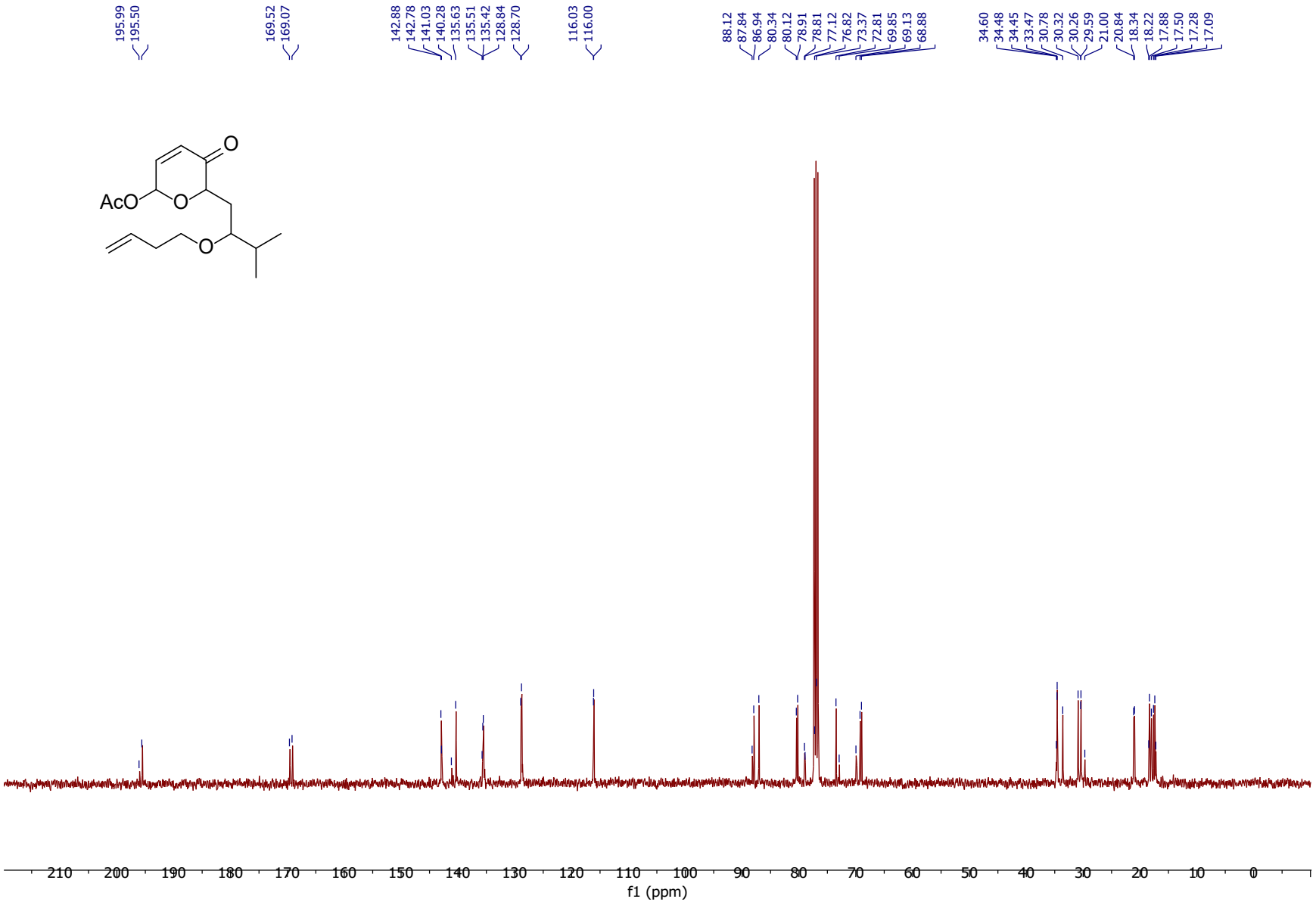

Figure S96: $^{13}C\{^{1}H\}$ (100 MHz, $CDCl_3$) of Achmatowicz 9l

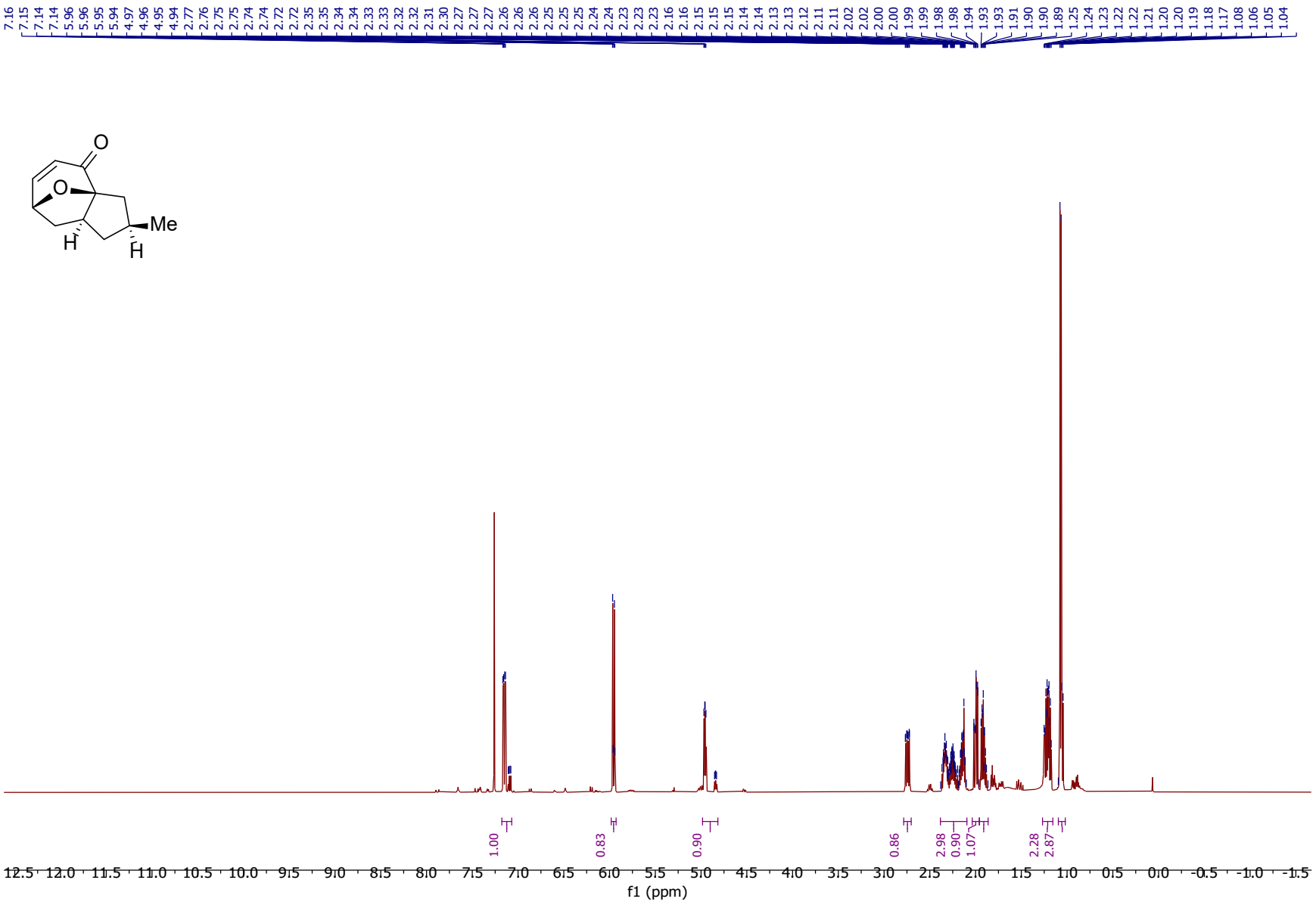

Figure S97: ^{1}H NMR (500 MHz, $CDCl_3$) of cycloadduct 10a

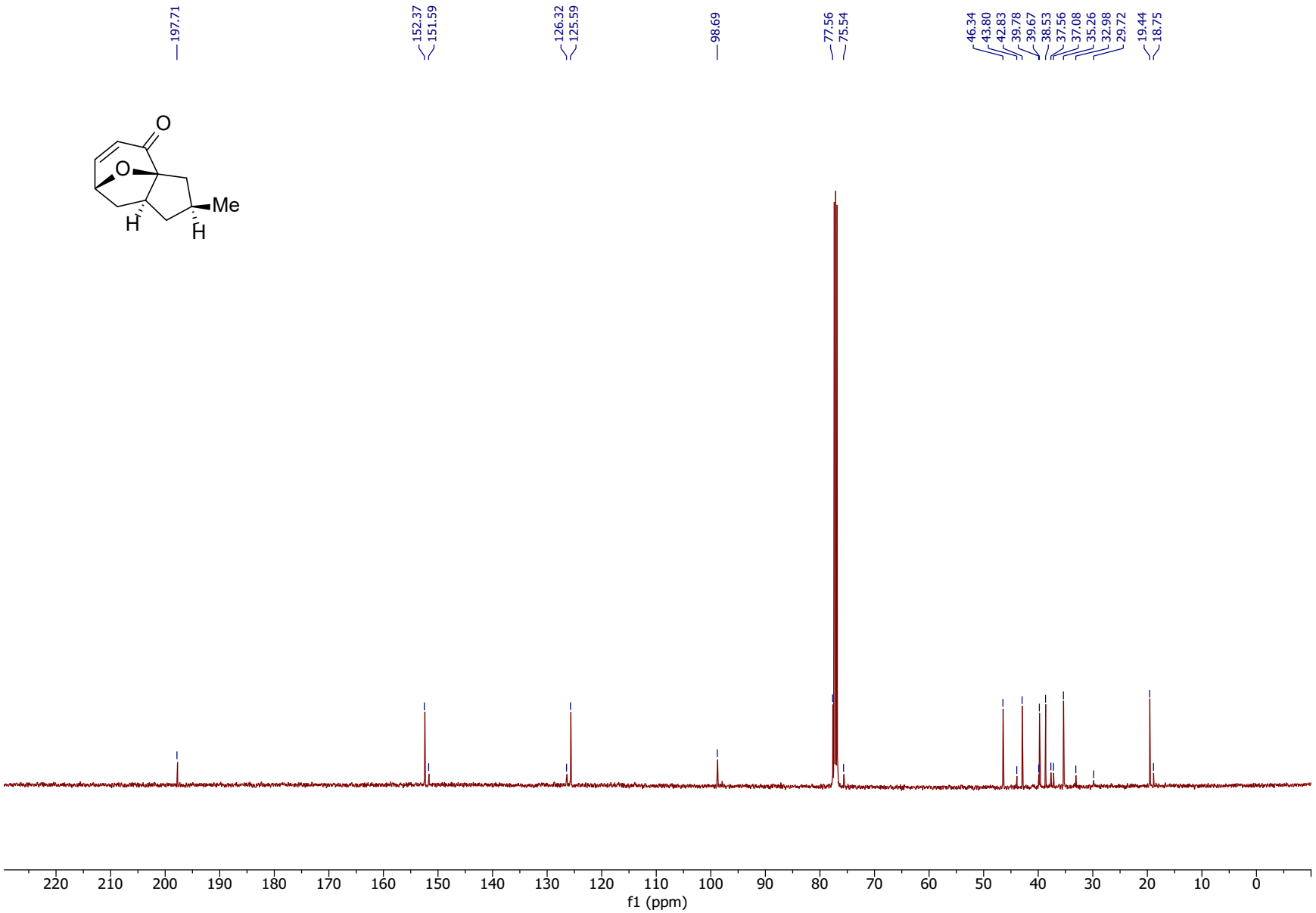

Figure S98: $^{13}C\{^{1}H\}$ (125 MHz, $CDCl_3$) of cycloadduct 10a

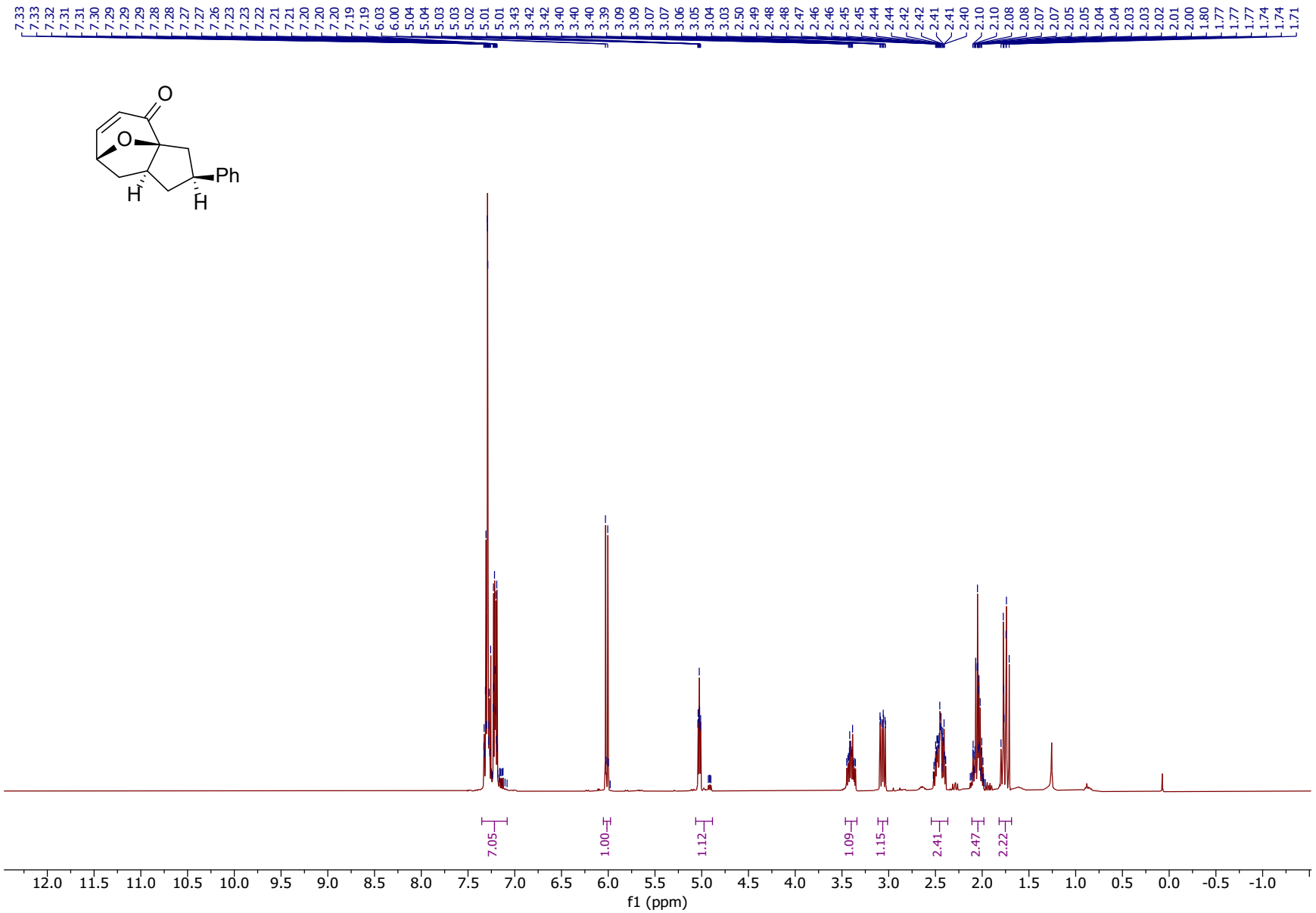

Figure S99: ^{1}H NMR (500 MHz, $CDCl_3$) of cycloadduct 10b

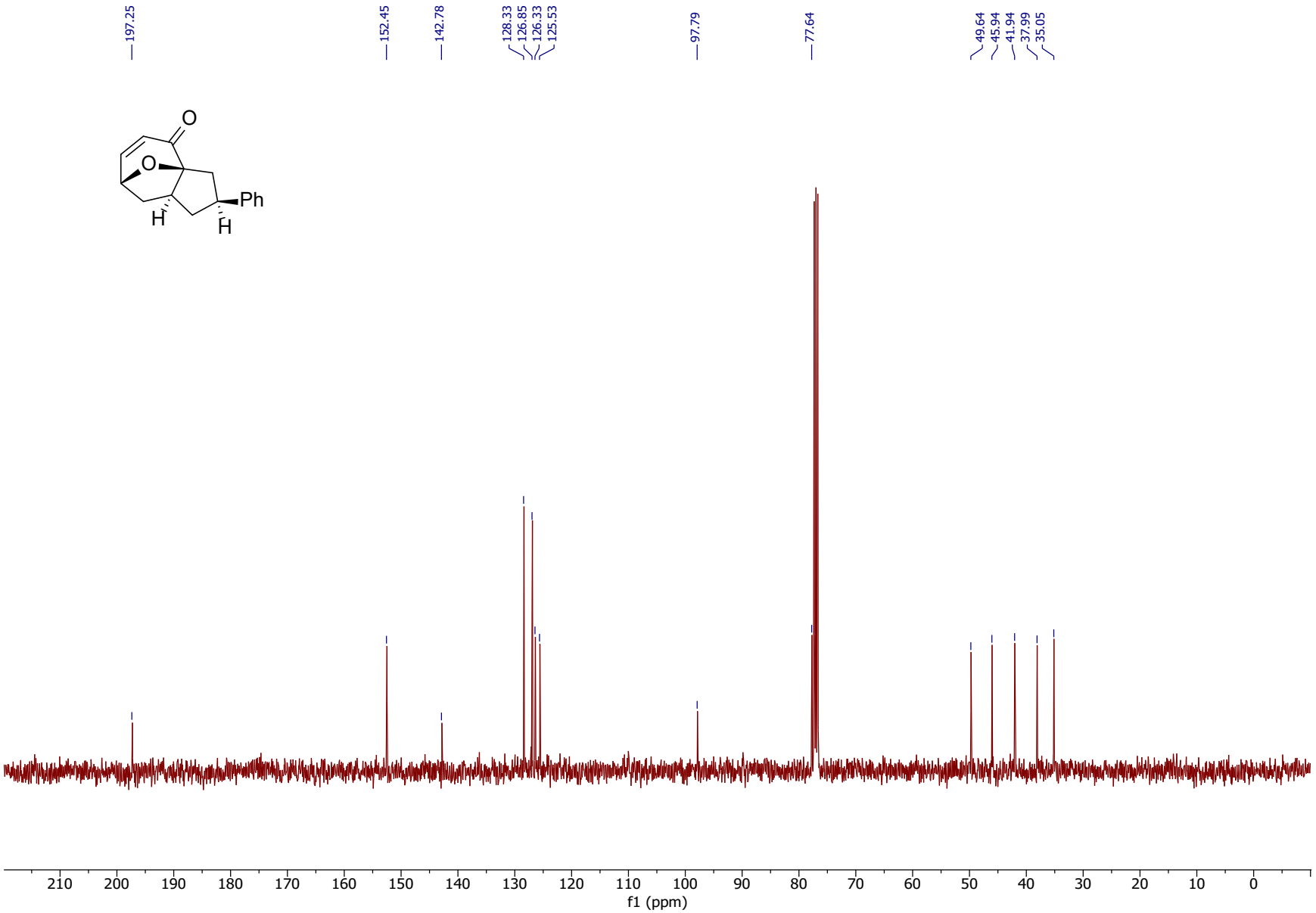

Figure S100: $^{13}C\{^{1}H\}$ (125 MHz, $CDCl_3$) of cycloadduct 10b

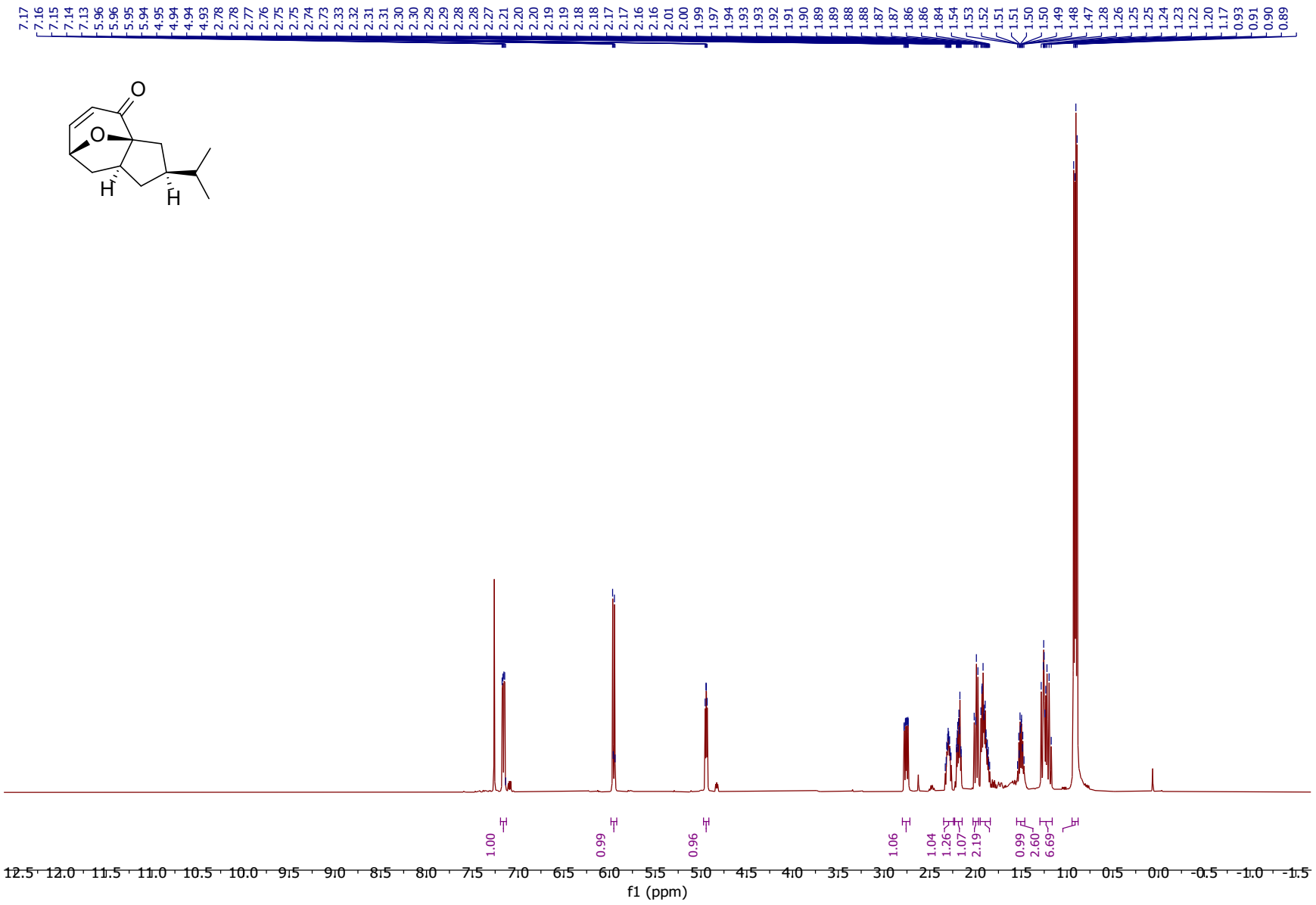

Figure S101: ^{1}H NMR (500 MHz, $CDCl_3$) of cycloadduct 10c

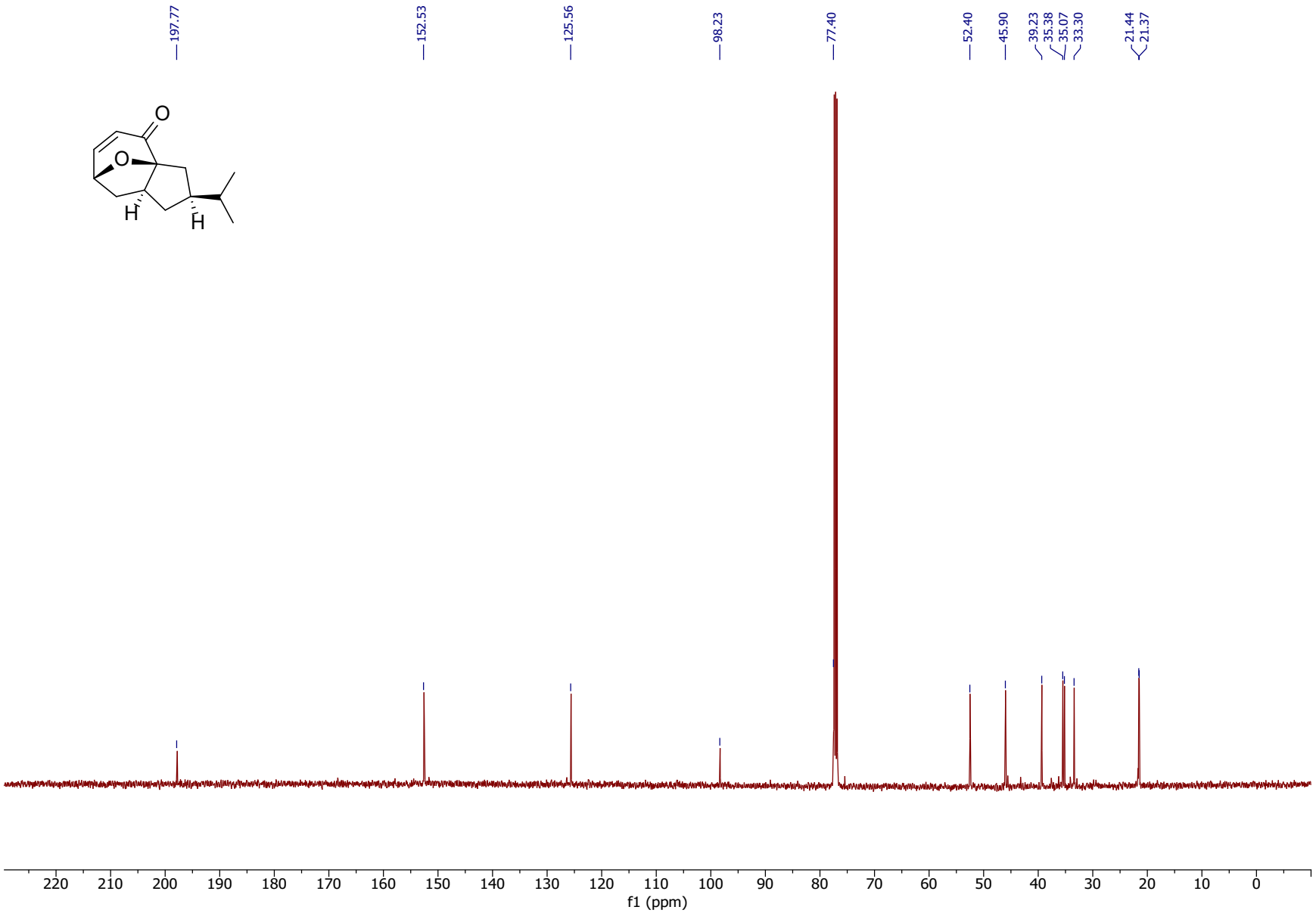

Figure S102: $^{13}C\{^{1}H\}$ (125 MHz, $CDCl_3$) of cycloadduct 10c

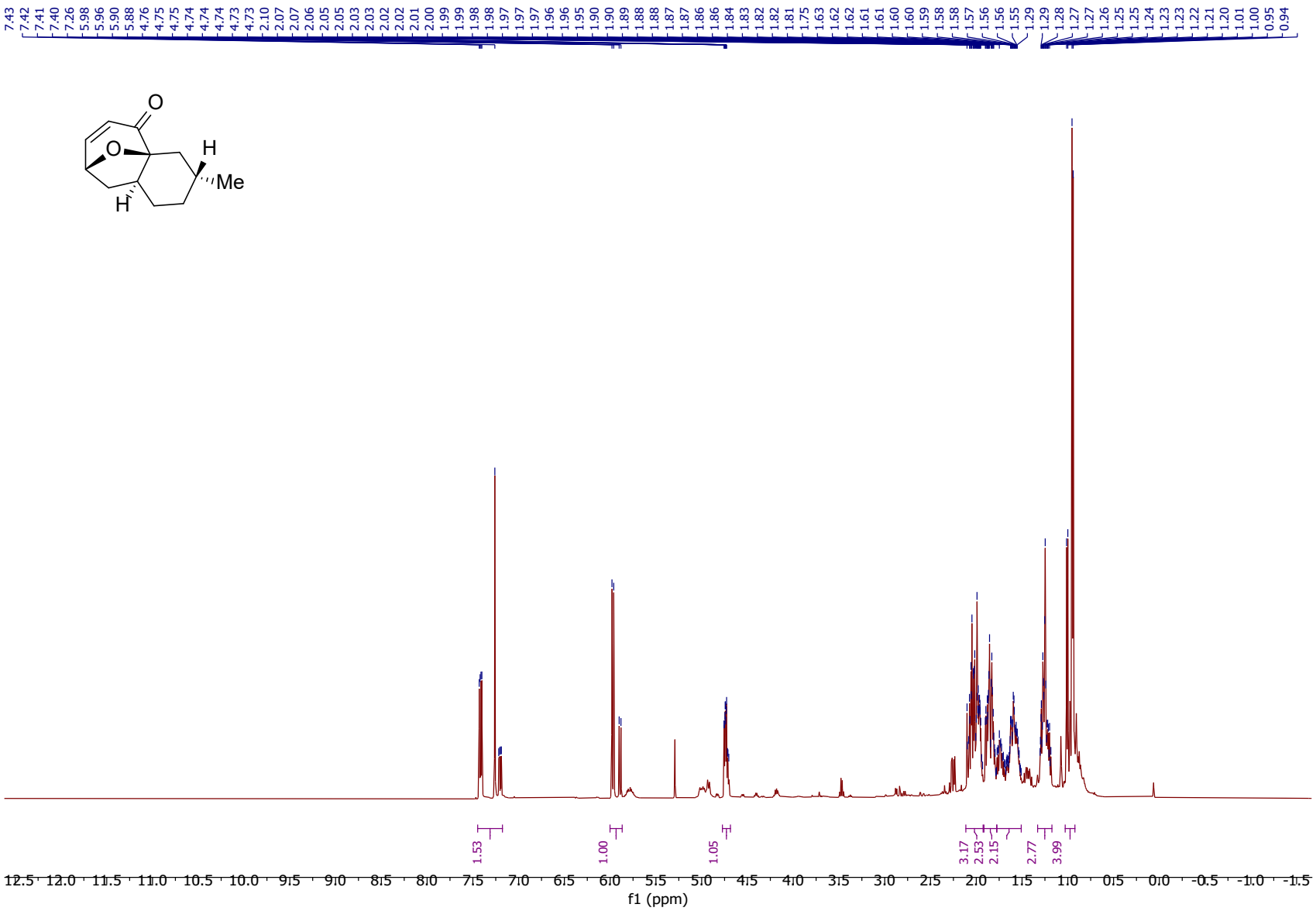

Figure S103: ^{1}H NMR (500 MHz, $CDCl_3$) of cycloadduct 10d

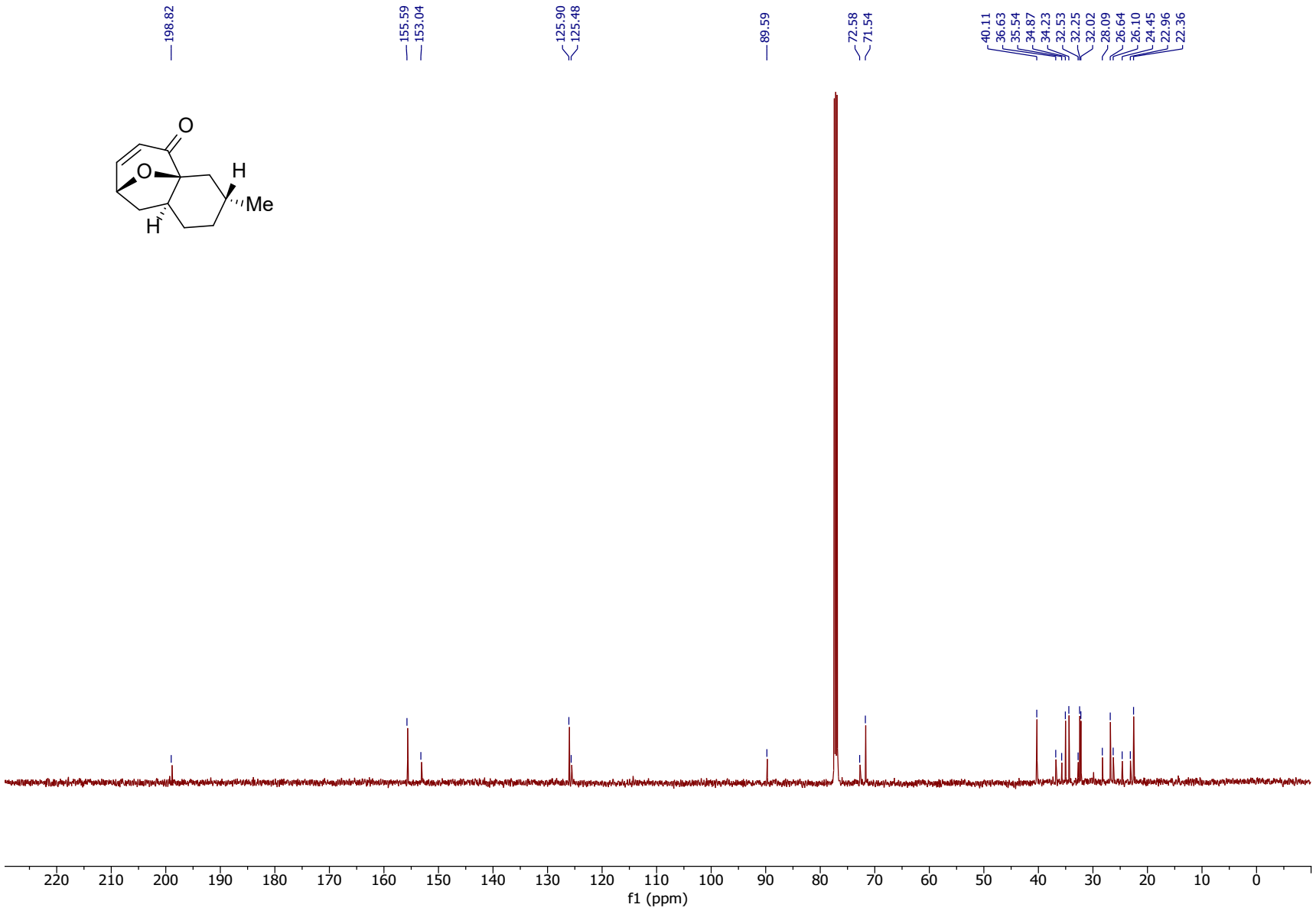

Figure S104: $^{13}C\{^{1}H\}$ (125 MHz, $CDCl_3$) of cycloadduct 10d

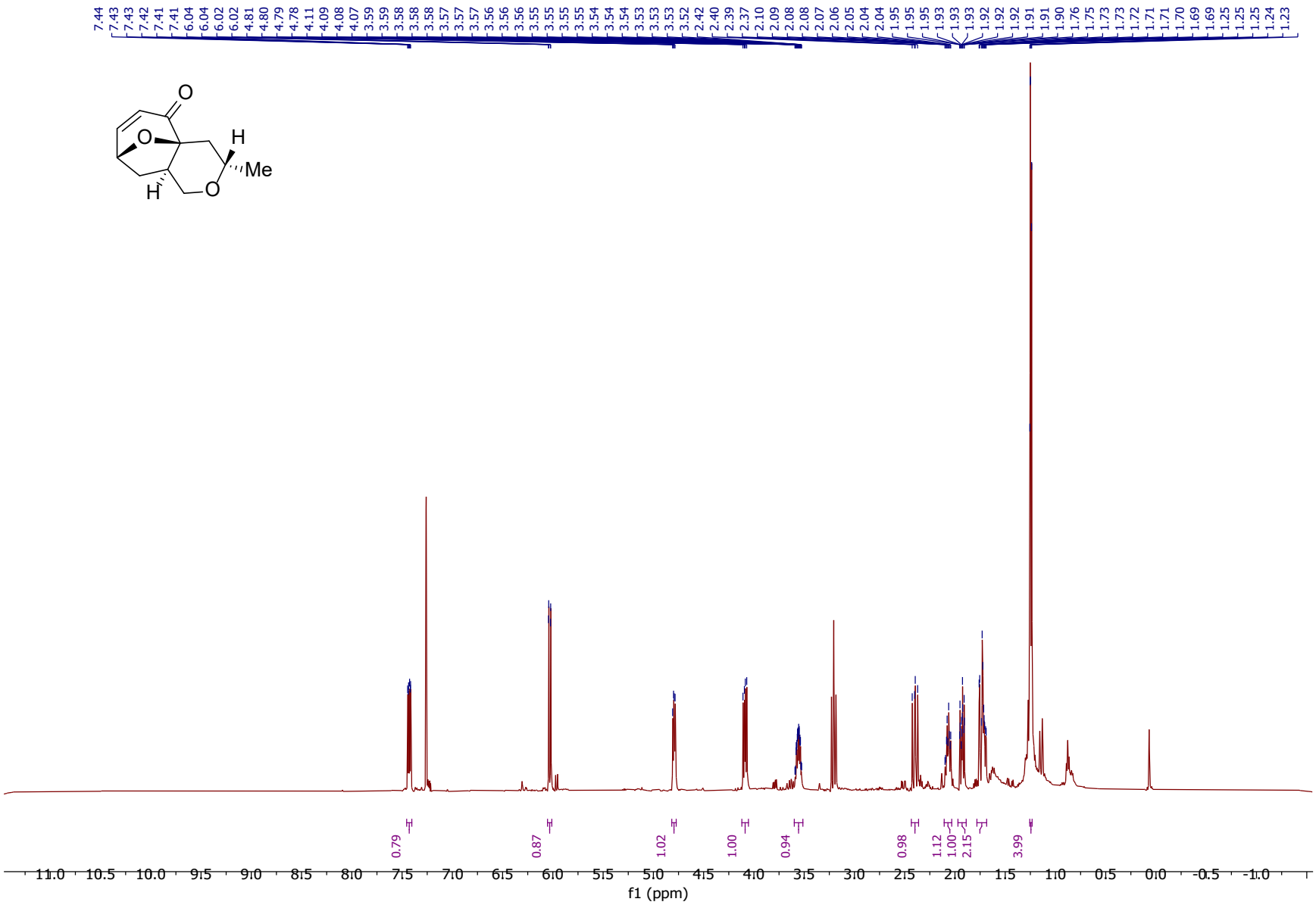

Figure S105: ^{1}H NMR (500 MHz, $CDCl_3$) of cycloadduct 10e

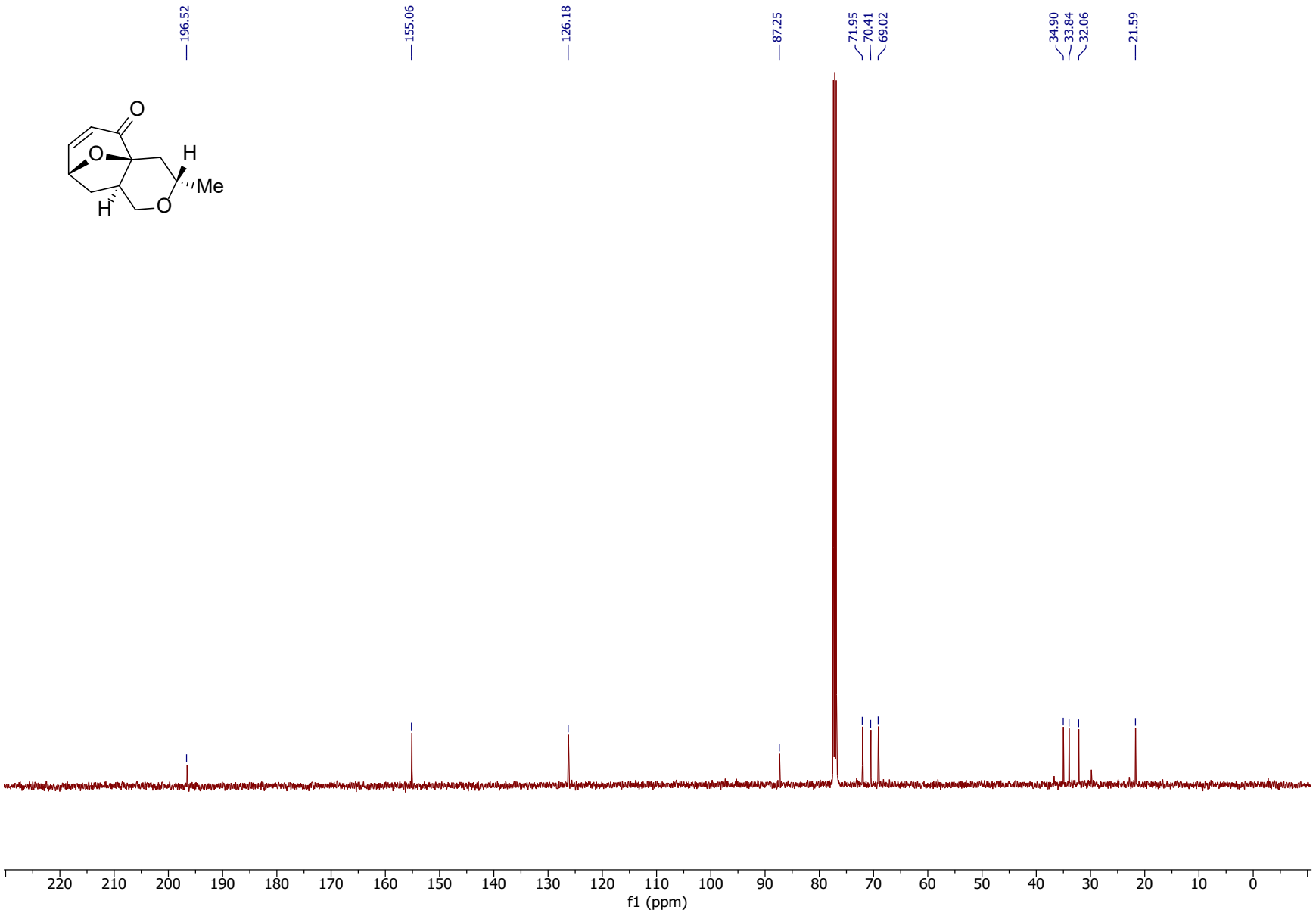

Figure S106: $^{13}C\{^{1}H\}$ (125 MHz, $CDCl_3$) of cycloadduct 10e

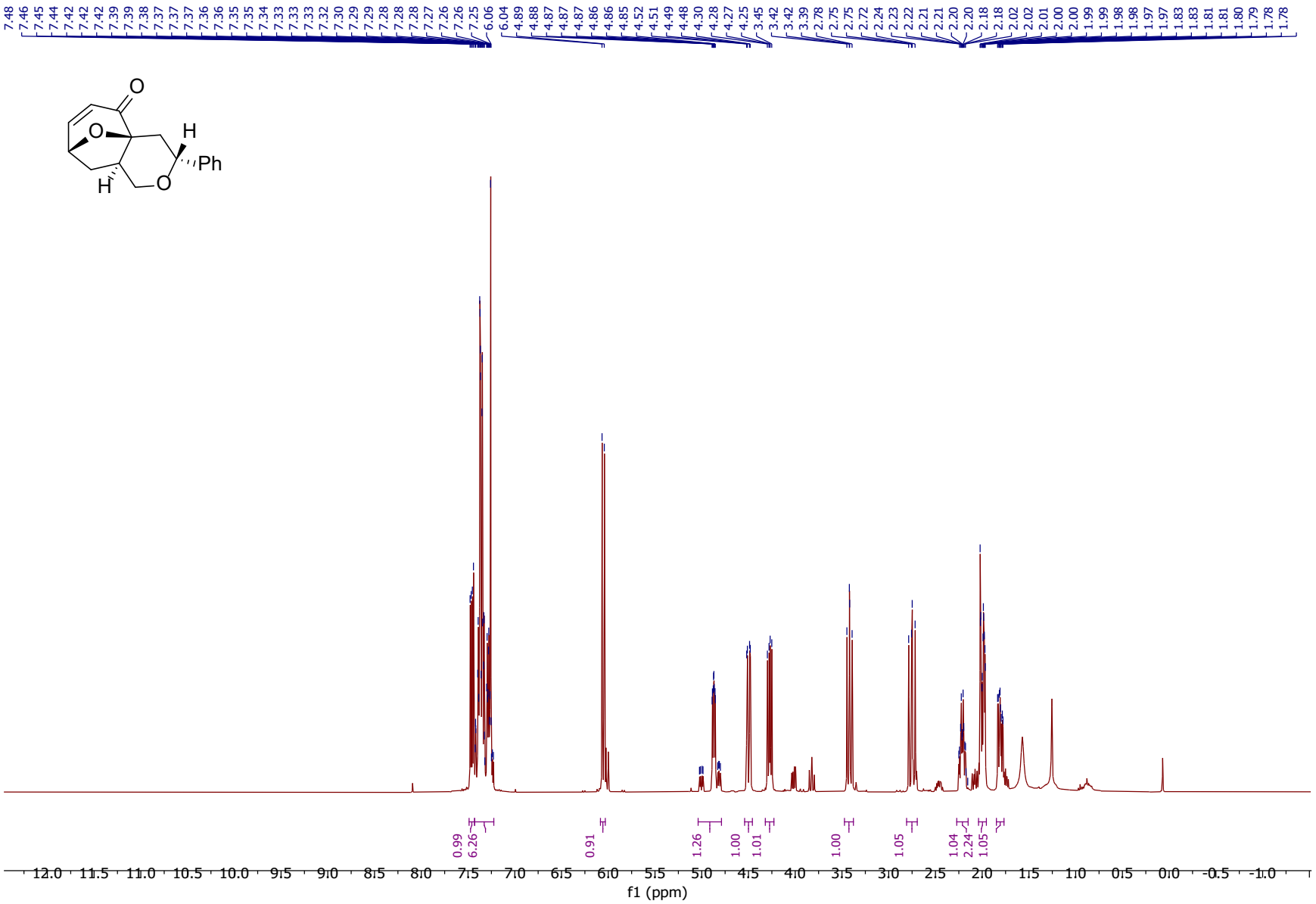

Figure S107: ^{1}H NMR (400 MHz, $CDCl_3$) of cycloadduct 10f

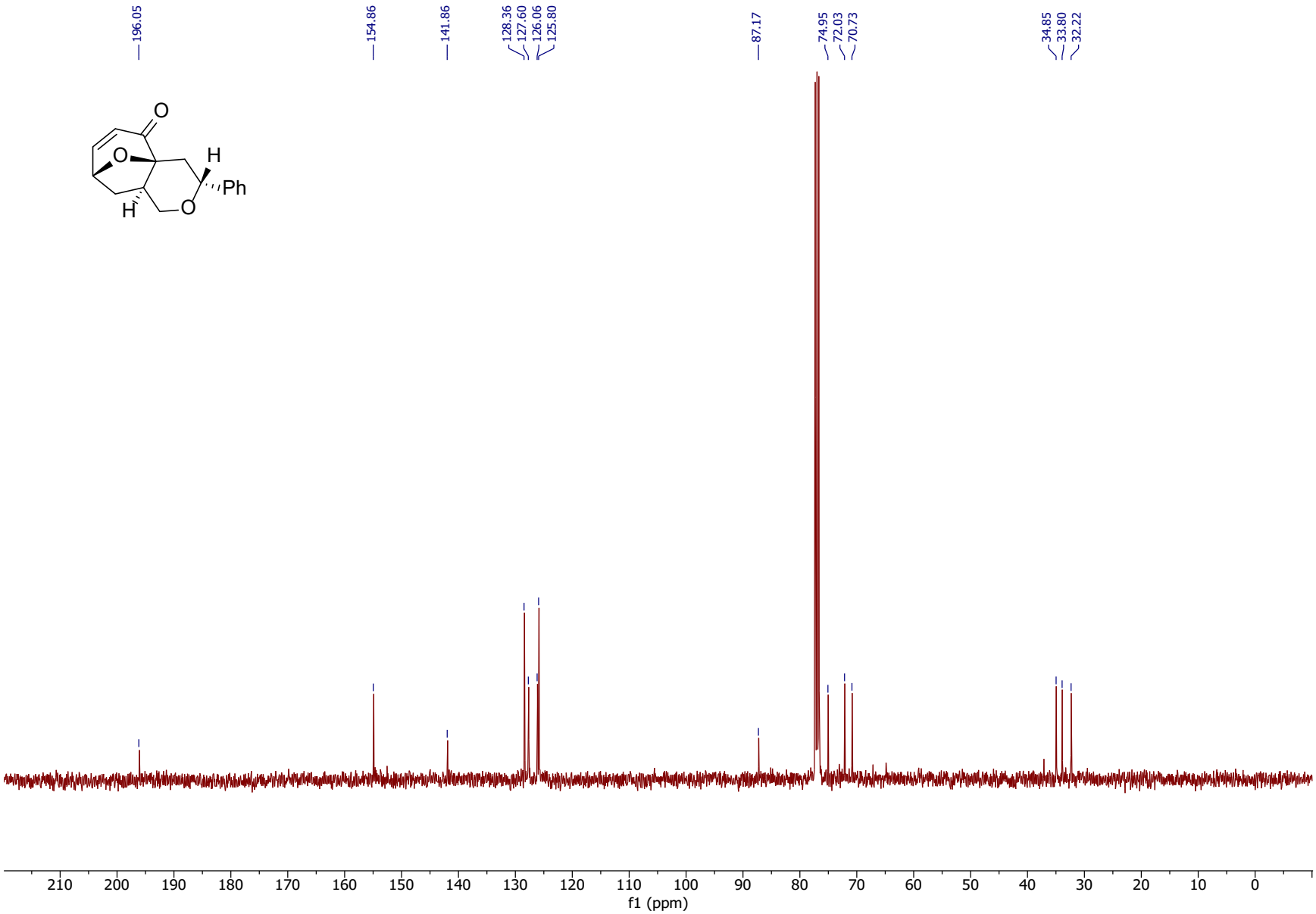

Figure S108: $^{13}C\{^{1}H\}$ (100 MHz, $CDCl_3$) of cycloadduct 10f

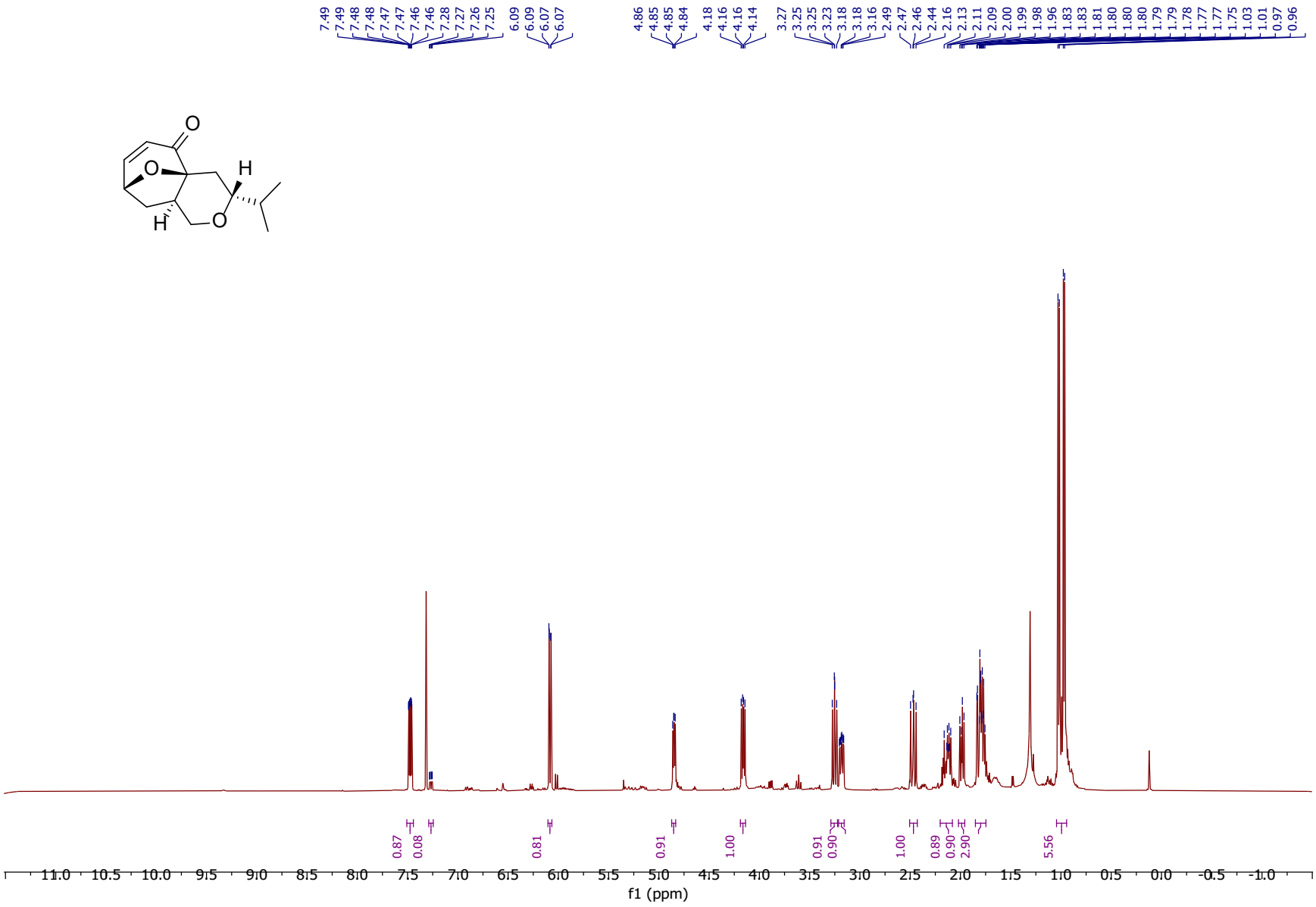

Figure S109: ^{1}H NMR (500 MHz, $CDCl_3$) of cycloadduct 10g

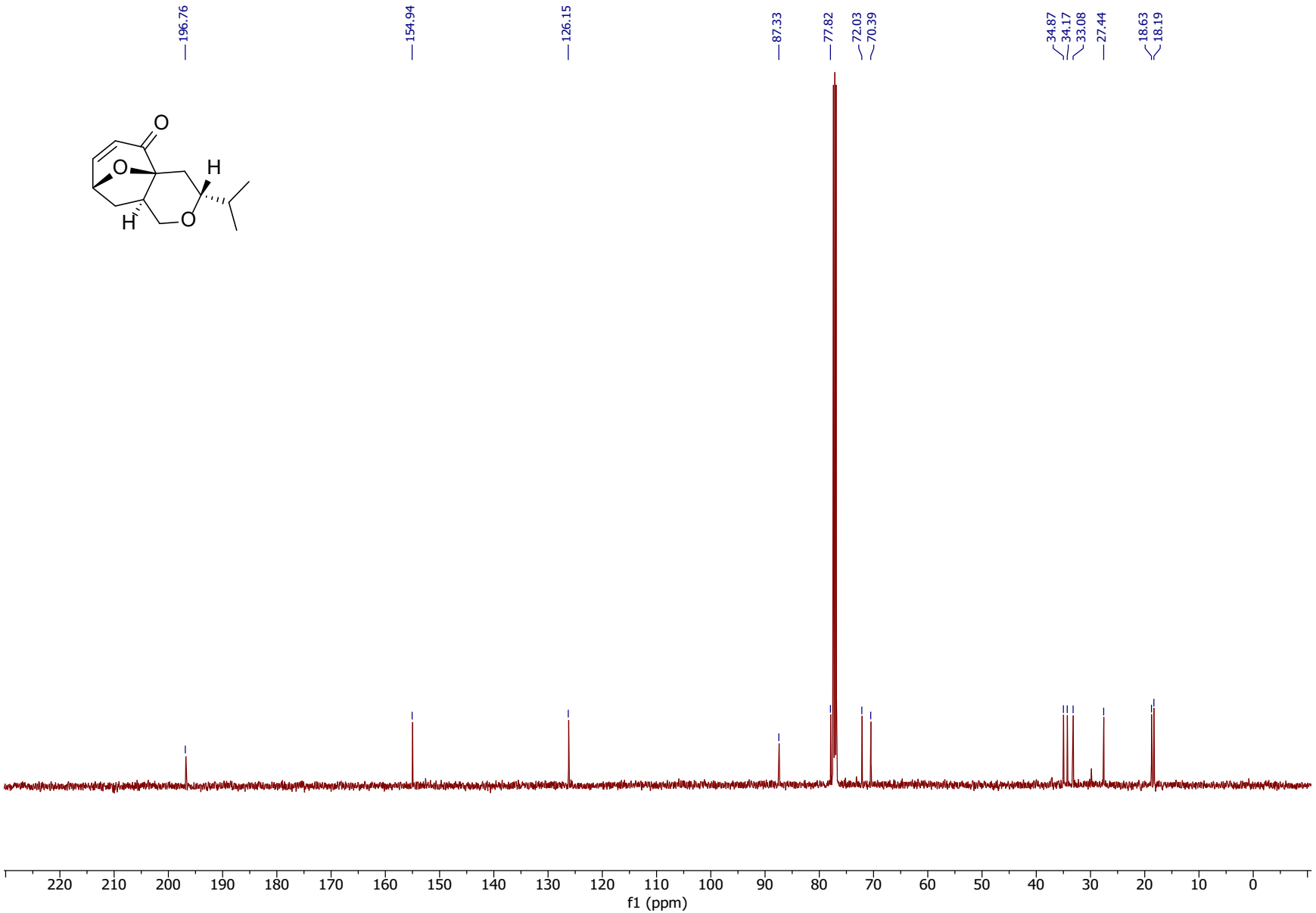

Figure S100: $^{13}C\{^{1}H\}$ (125 MHz, $CDCl_3$) of cycloadduct 10g

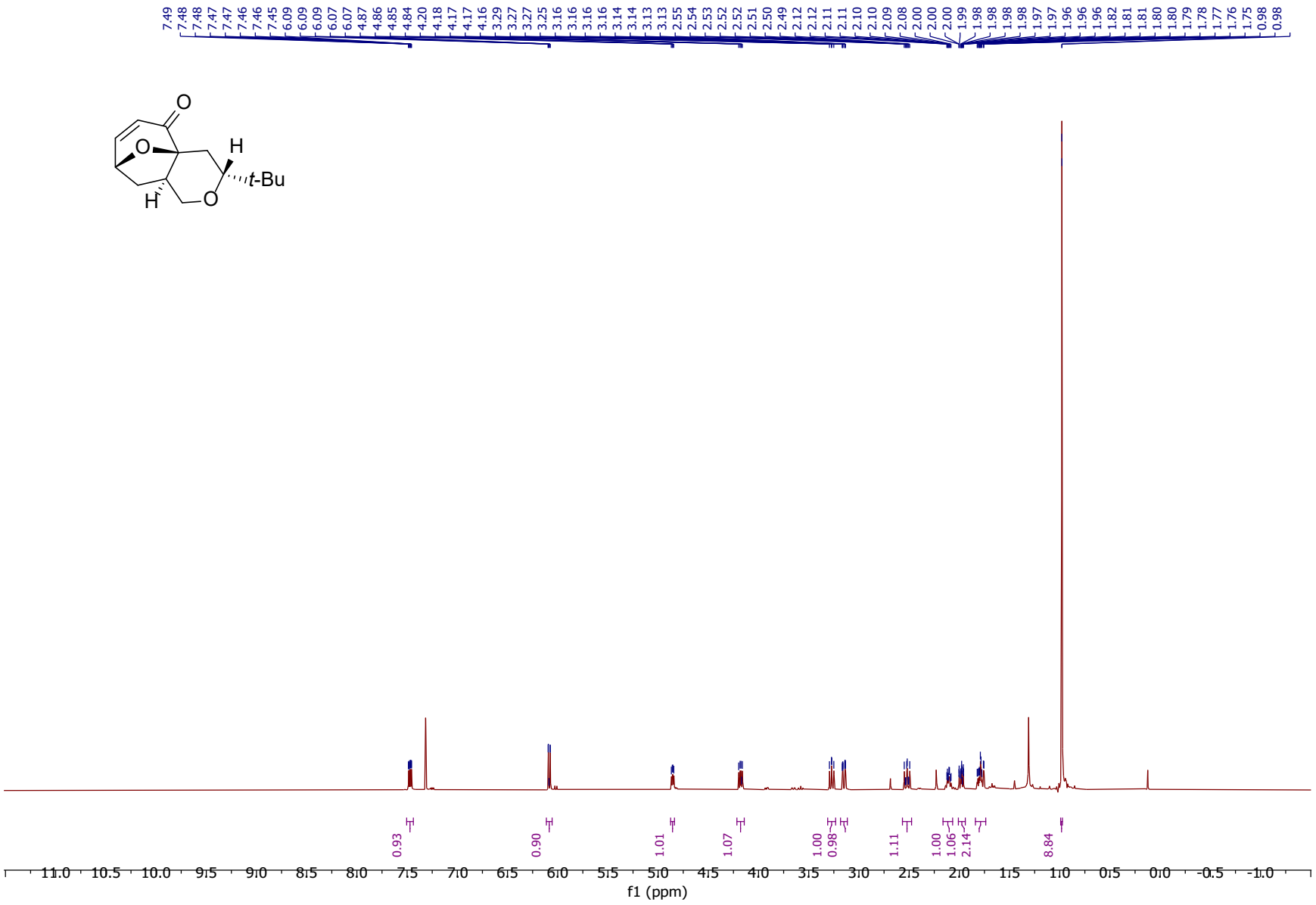

Figure S111: ^{1}H NMR (500 MHz, $CDCl_3$) of cycloadduct 10h

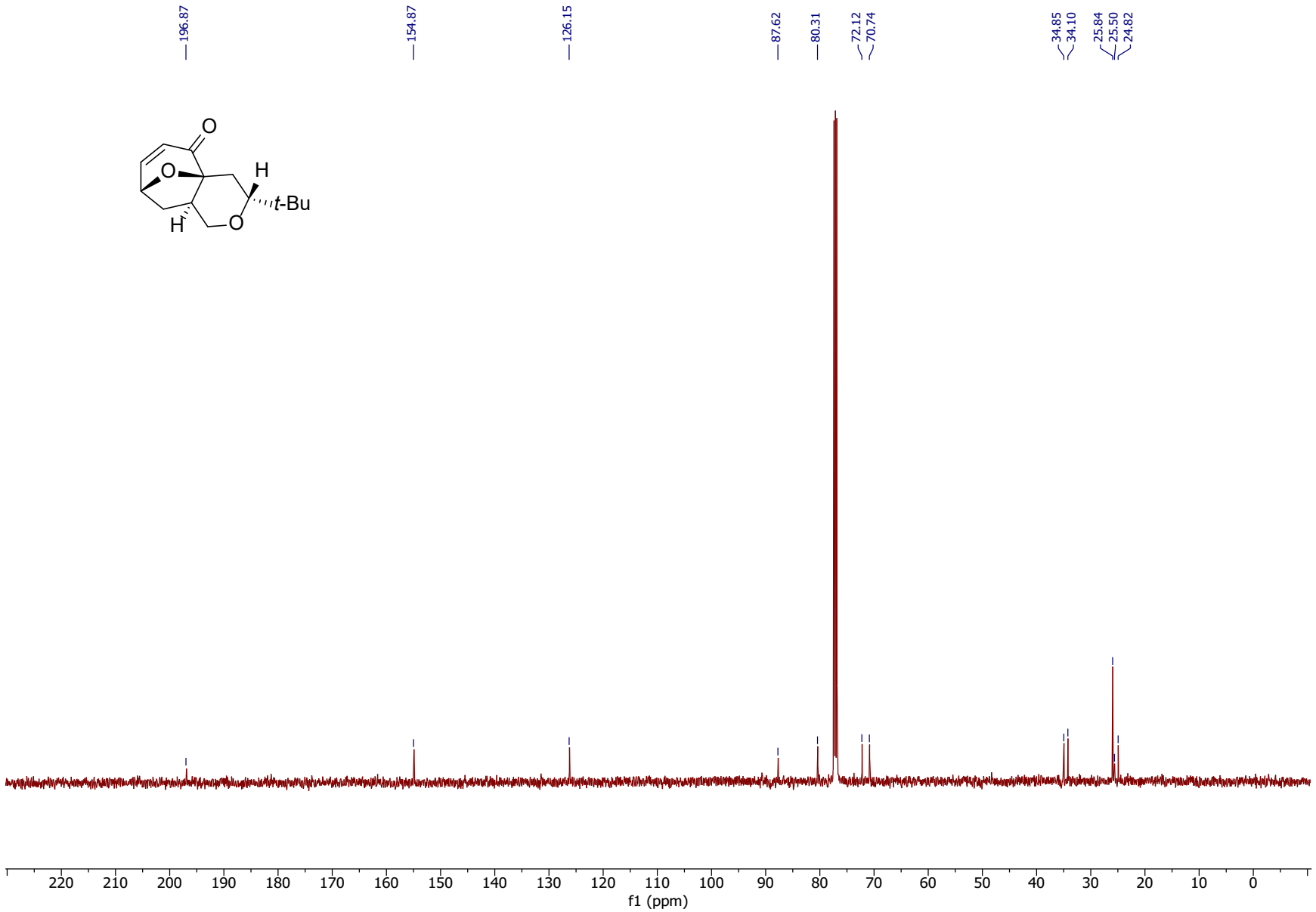

Figure S112: $^{13}C\{^{1}H\}$ (125 MHz, $CDCl_3$) of cycloadduct 10h

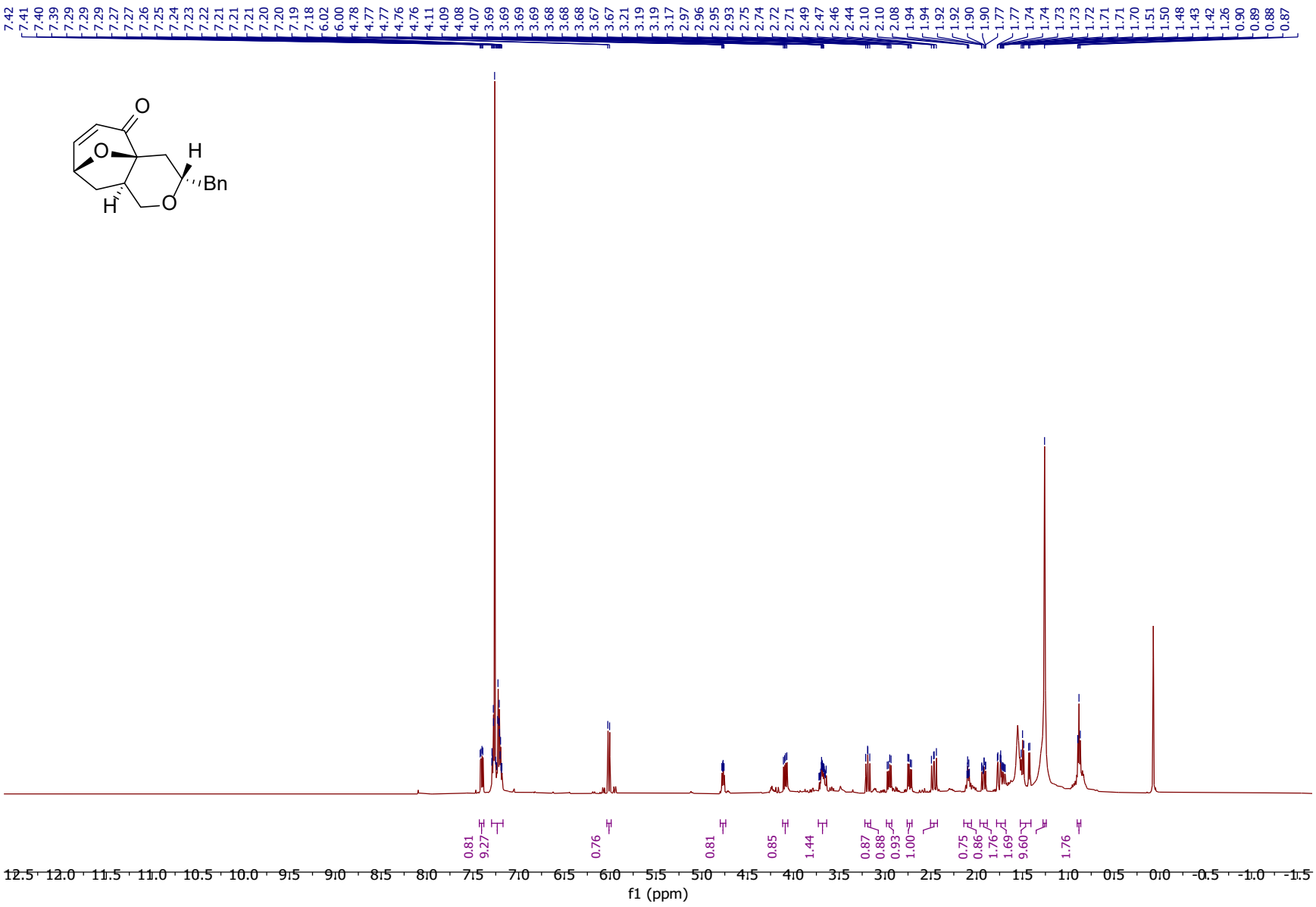

Figure S113: ^{1}H NMR (500 MHz, $CDCl_3$) of cycloadduct 10i

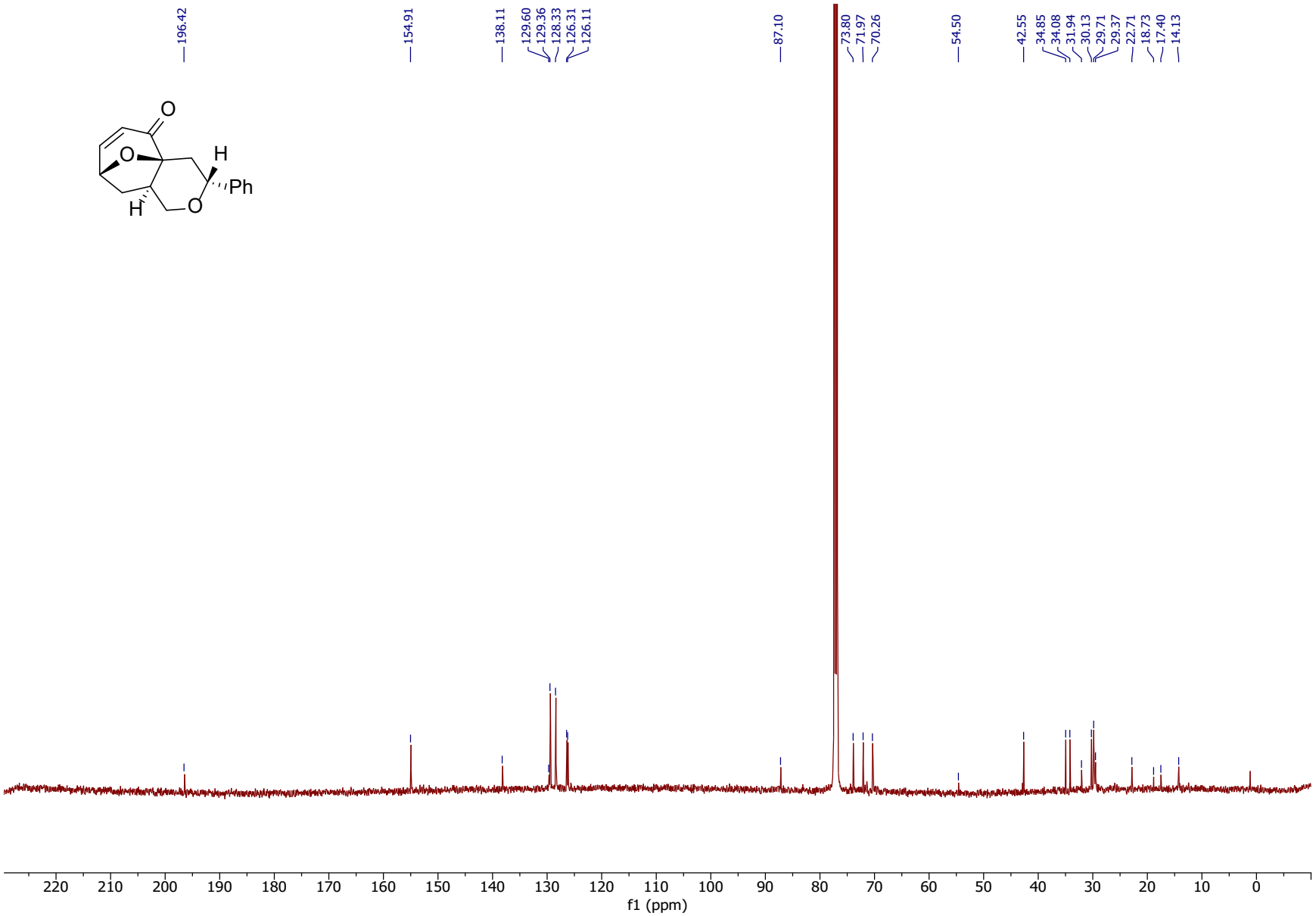

Figure S114: $^{13}C\{^{1}H\}$ (125 MHz, $CDCl_3$) of cycloadduct 10i

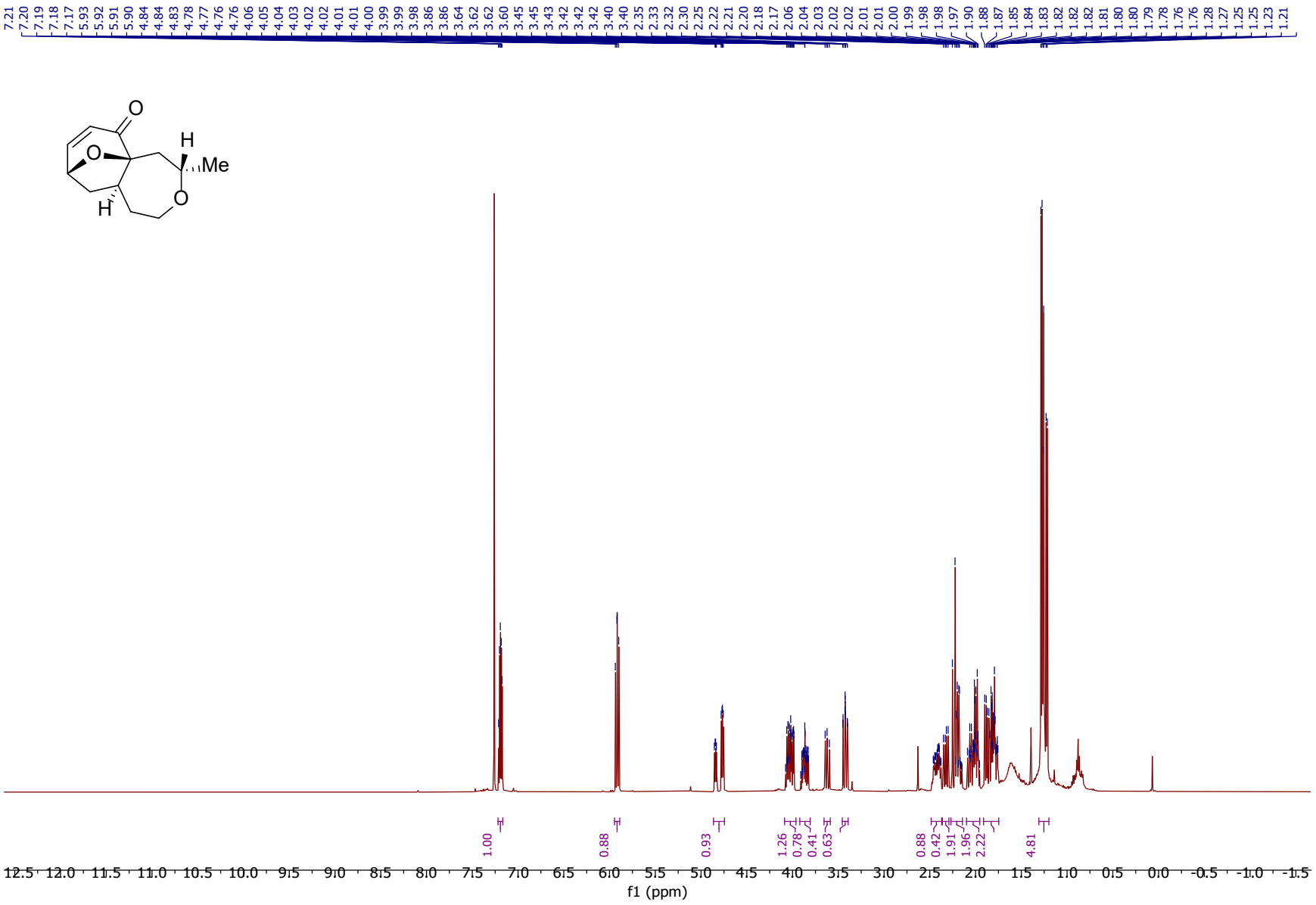

Figure S115: ^{1}H NMR (500 MHz, $CDCl_3$) of cycloadduct 10j

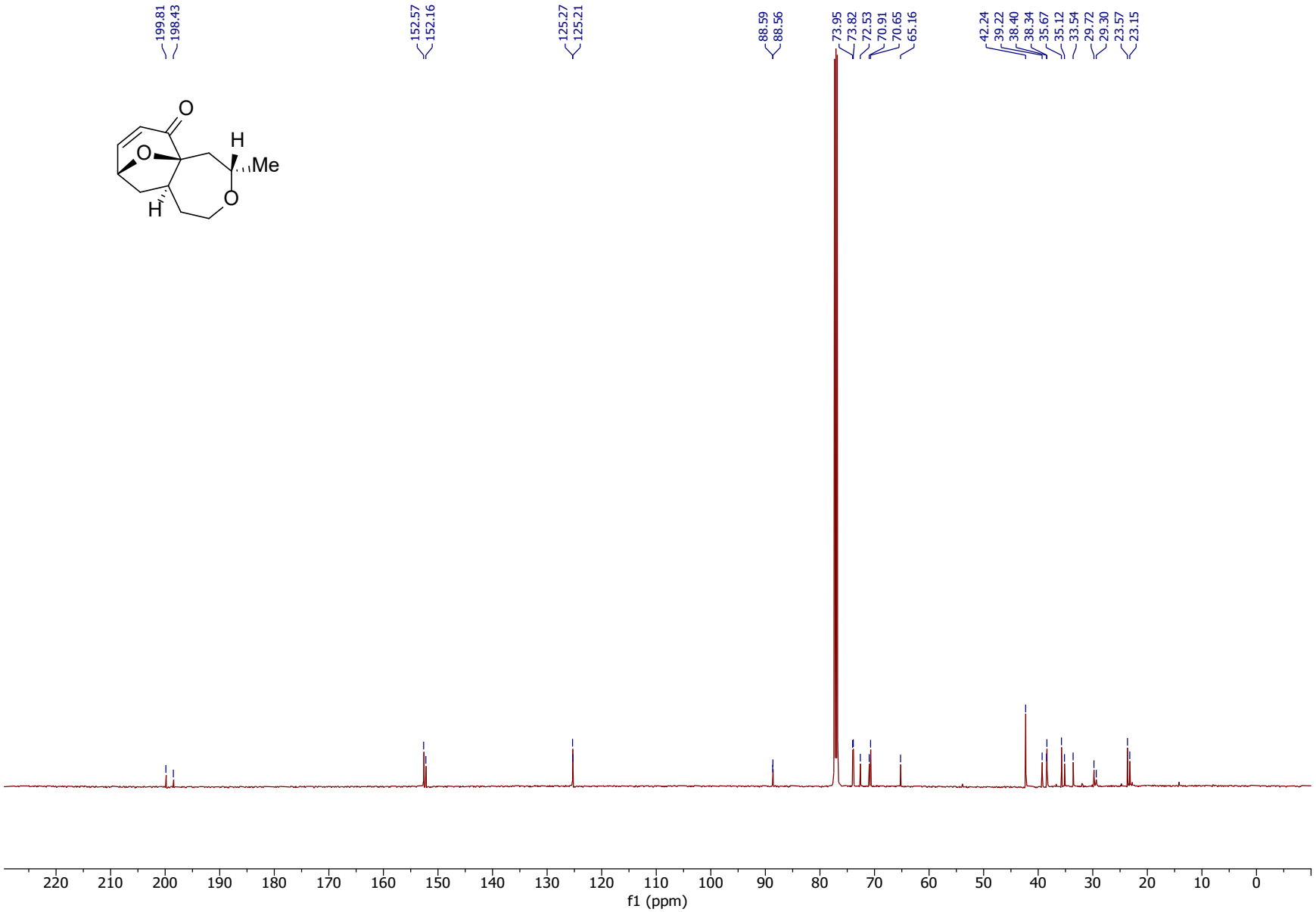

Figure S116: $^{13}C\{^{1}H\}$ (125 MHz, $CDCl_3$) of cycloadduct 1i

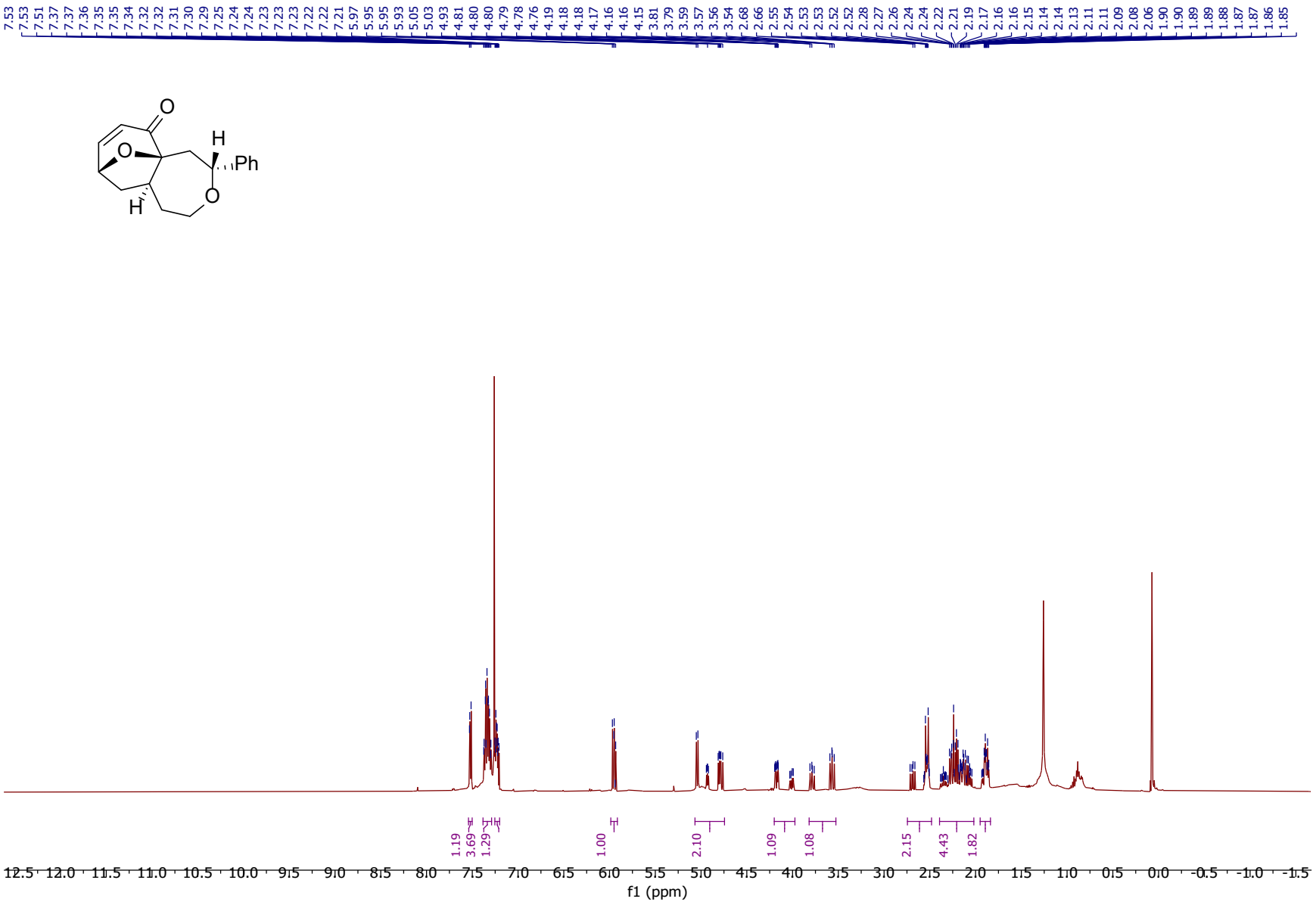

Figure S117: ^{1}H NMR (500 MHz, $CDCl_3$) of cycloadduct 1k

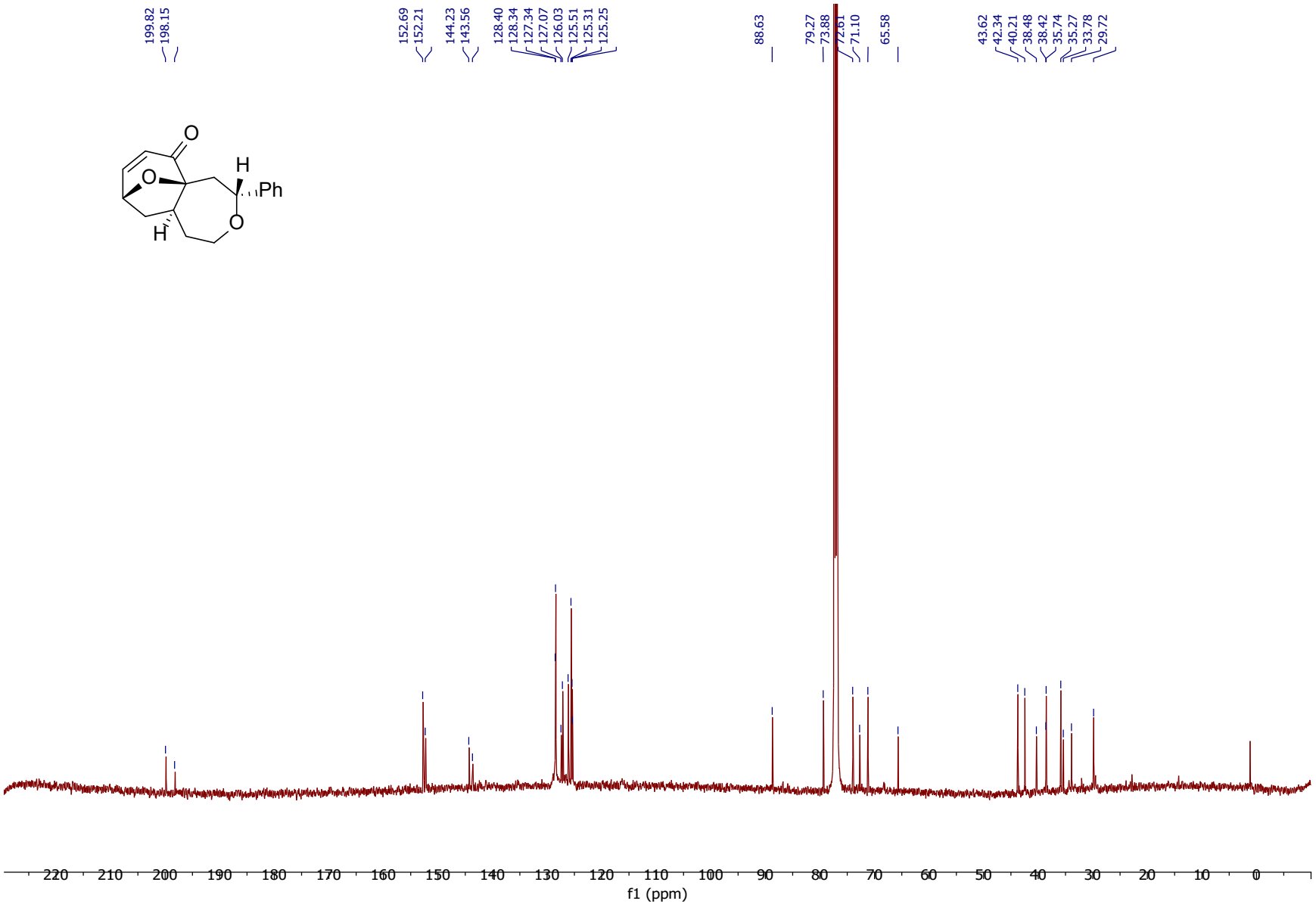

Figure S118: $^{13}C\{^{1}H\}$ (125 MHz, $CDCl_3$) of cycloadduct 1k

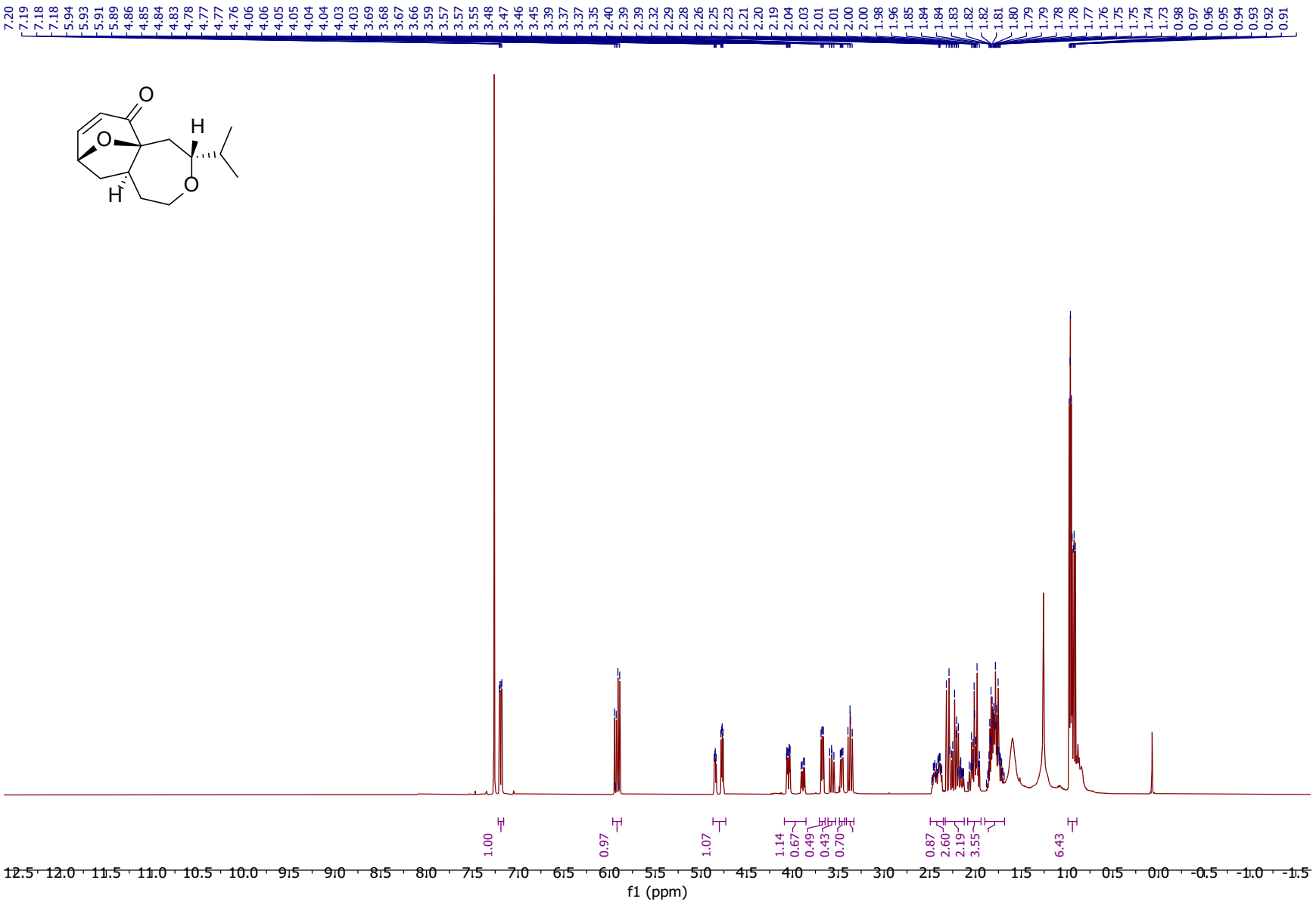

Figure S119: ^{1}H NMR (500 MHz, $CDCl_3$) of cycloadduct 1j

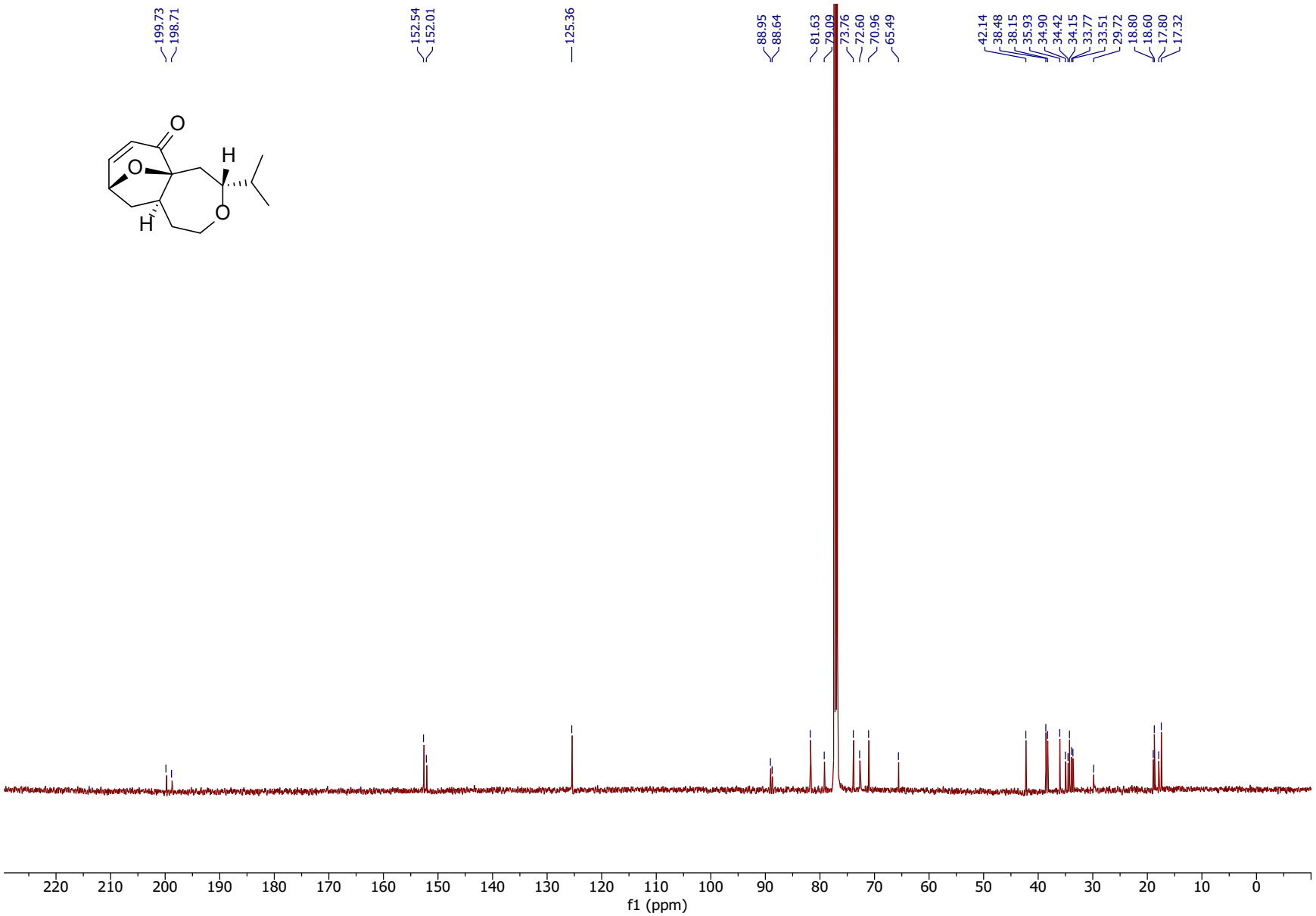

Figure S120: $^{13}C\{^{1}H\}$ (125 MHz, $CDCl_3$) of cycloadduct 1j

HPLC analysis of compounds 10a and 10d:

The HPLC of **10a** was performed with a YMC-ODS-AQ 55 reverse phase column, a flow rate of 1.0 mL/min, a stock concentration of 5 mg/mL, an injection volume of 10 µL, and a solvent ratio of 80:20 of H_2O:CH_3CN. The Purity by HPLC was determined to be > 99%.

```
Acq. Instrument : GHOSH LC 1                      Location :   P1-A-01
Injection Date  : 7/11/2025 12:51:54 PM               Inj :   1
                                                 Inj Volume : 25.000 µl
Different Inj Volume from Sample Entry!  Actual Inj Volume : 10.000 µl
Acq. Method     : C:\Chem32\1\Methods\DENVER C18.M
Last changed    : 7/11/2025 12:48:58 PM by SYSTEM
                  (modified after loading)
Analysis Method : C:\Chem32\1\Methods\UgiDiastereomersAmlanDONOTUSE.M
Last changed    : 9/30/2025 1:15:42 PM by SYSTEM
Method Info     : Amlan's Method

Sample Info     : YMC-ODS-AQ 55
                  80:20 H2O:CH3CN
                  1 mL/min
                  254 nm
                  5 uL inj
                  5 mg/mL
```

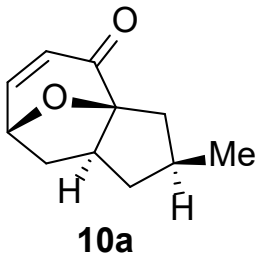

10a

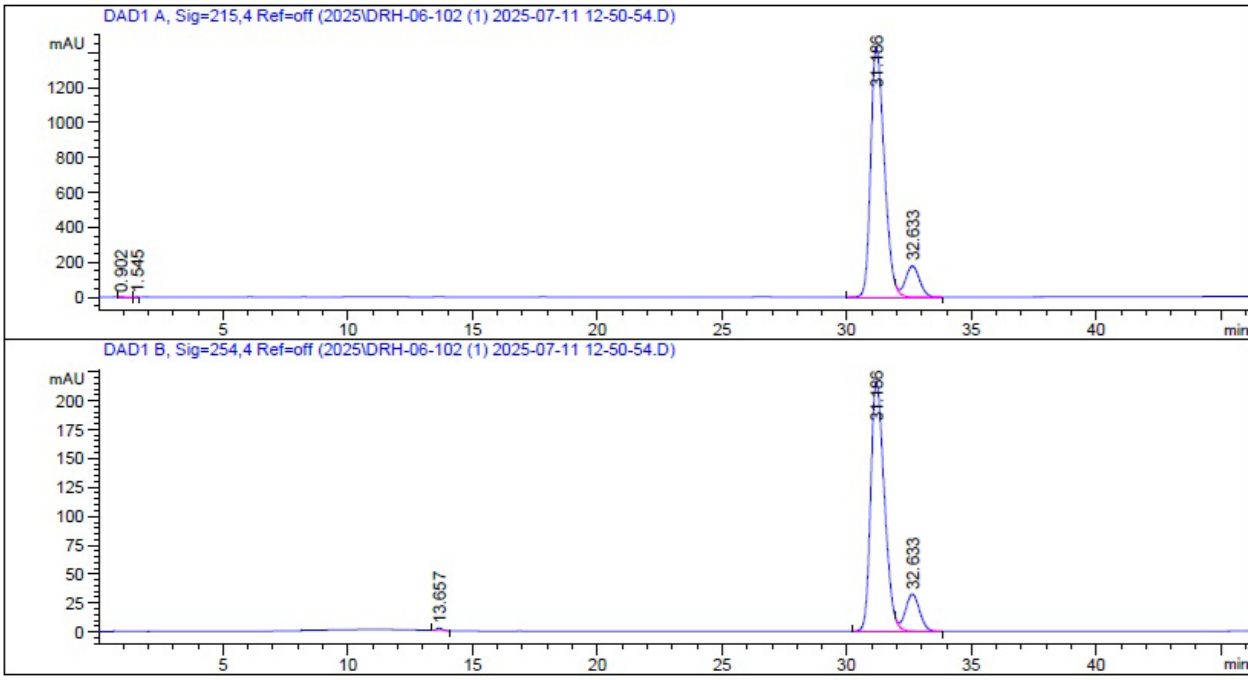

Signal 1: DAD1 A, Sig=215,4 Ref=off

Peak #	RetTime [min]	Type	Width [min]	Area [mAU*s]	Height [mAU]	Area %
1	0.902	BB	0.0692	14.19115	2.89385	0.0233
2	1.545	BB	0.0566	7.94182	2.17740	0.0130
3	31.186	BV R	0.5897	5.40867e4	1428.45215	88.8128
4	32.633	VB E	0.6049	6790.81104	176.49683	11.1508
Totals :				6.08997e4	1610.02022	

Signal 2: DAD1 B, Sig=254,4 Ref=off

Peak #	RetTime [min]	Type	Width [min]	Area [mAU*s]	Height [mAU]	Area %
1	13.657	BB	0.2296	27.90012	1.83287	0.2936
2	31.186	BV R	0.5932	8240.27930	215.92734	86.7133
3	32.633	VB E	0.5963	1234.72095	31.99082	12.9931
Totals :				9502.90037	249.75103	

HPLC of 10d

The HPLC of **10d** was performed with a YMC PACK ODS-A reverse phase column, a flow rate of 1.0 mL/min, a stock concentration of 5 mg/mL, an injection volume of 10 µL, and a solvent ratio of 80:20 of H_2O:CH_3CN. The Purity by HPLC was determined to be 98.18 %.

```
Acq. Instrument : GHOSH LC 1                    Location :   P2-D-01
Injection Date  : 5/22/2025 2:30:13 PM               Inj :   1
                                              Inj Volume : 5.000 µl
Acq. Method     : C:\CHEM32\1\METHODS\GHOSH GROUP MAIN.M
Last changed    : 5/22/2025 1:53:43 PM by SYSTEM
                  (modified after loading)
Analysis Method : C:\CHEM32\1\METHODS\GHOSH GROUP MAIN.M
Last changed    : 6/11/2025 1:15:14 PM by SYSTEM
                  (modified after loading)
Sample Info     : YMC PACK ODS-A
                  70:30 H2O:CH3CN
                  1.0 mL/min
                  215 nm
                  254 nm
                  5 uL inj
                  2 mg/mL
```

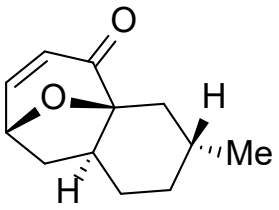

10d

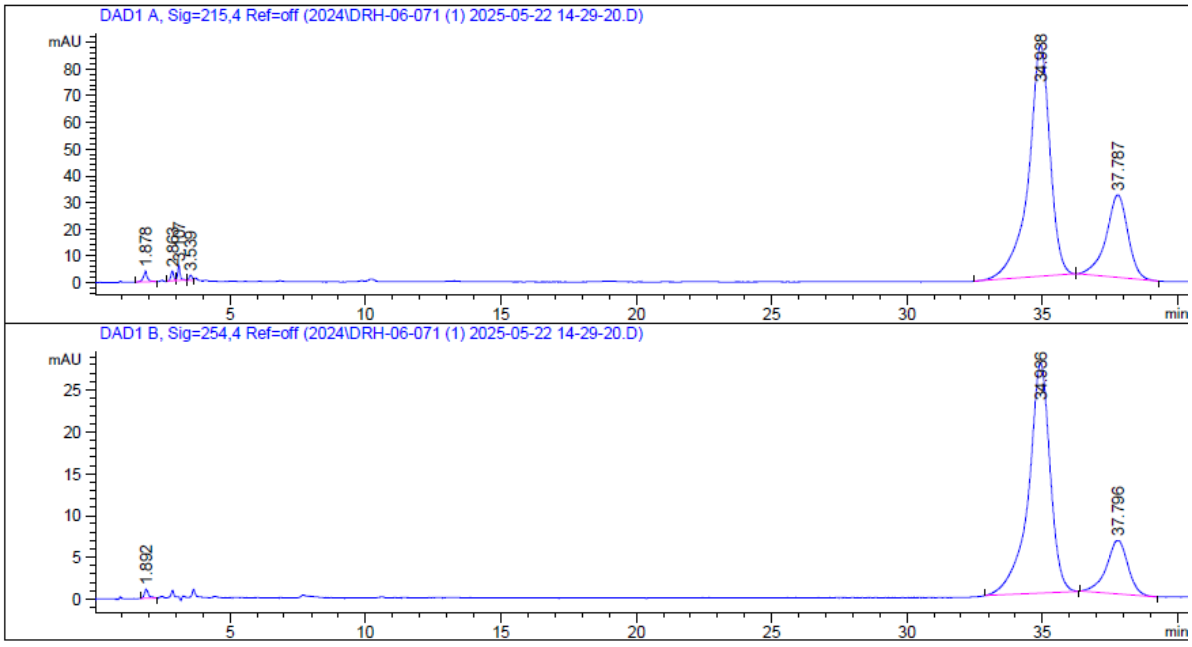

Signal 1: DAD1 A, Sig=215,4 Ref=off

Peak #	RetTime [min]	Type	Width [min]	Area [mAU*s]	Height [mAU]	Area %
1	1.878	BB	0.1390	41.16866	3.96995	0.6177
2	2.863	BV	0.1156	28.35458	3.77753	0.4255
3	3.107	VB	0.0996	37.04682	5.57244	0.5559
4	3.539	BV	0.1147	14.70393	1.93297	0.2206
5	34.938	BB	0.8145	4805.94141	86.73250	72.1132
6	37.787	BB	0.8317	1737.22461	30.91215	26.0671
Totals :				6664.44000	132.89755	

Signal 2: DAD1 B, Sig=254,4 Ref=off

Peak #	RetTime [min]	Type	Width [min]	Area [mAU*s]	Height [mAU]	Area %
1	1.892	BB	0.1356	11.72485	1.14394	0.6186
2	34.936	BB	0.8127	1529.28345	27.50285	80.6843
3	37.796	BB	0.7198	354.38232	6.42203	18.6971
Totals :				1895.39063	35.06882	

X-Ray Diffraction Data

Single crystals of **10b** and **10e** were coated with Fomblin oil and quickly transferred to the goniometer head of a Bruker Quest diffractometer with kappa geometry, an I-μ-S microsource X-ray tube, laterally graded multilayer (Goebel) mirror single crystal for monochromatization, and a Photon-III C14 area detector. Examination and data collection were performed with Cu Kα radiation (λ = 1.54178 Å) at 150 K.

Single crystals of **10f** were coated with Fomblin oil and quickly transferred to the goniometer head of a Bruker Quest diffractometer with a fixed chi angle, a sealed tube fine focus X-ray tube, single crystal curved graphite incident beam monochromator, a Photon II area detector. Examination and data collection were performed with Mo Kα radiation (λ = 0.71073 Å) at 150 K. Both systems were cooled with an Oxford Crysosystems low temperature device.

Data were collected, reflections were indexed and processed, and the files scaled and corrected for absorption using APEX5[1] and TWINABS or SADABS[2] respectively. The space groups were assigned using XPREP within the SHELXTL suite of programs[3,4] and solved by dual methods using ShelXT[5] and refined by full matrix least squares against F^2 with all reflections using Shelxl2019[6] using the graphical interface Shelxle.[7] If not specified otherwise H atoms attached to carbon were positioned geometrically and constrained to ride on their parent atoms. C-H bond

distances were constrained to 0.95 Å for aromatic and alkene C-H and CH_2 and moieties, and to 1.00, 0.99 and 0.98 Å for aliphatic C-H, CH_2 and CH_3 moieties, respectively. U_{iso}(H) values were set to a multiple of U_{eq}(C) with 1.5 for CH_3 and 1.2 for C-H and CH_2 respectively.

Additional data collection and refinement details can be found in the Supporting Information. Complete crystallographic data, in CIF format, have been deposited with the Cambridge Crystallographic Data Centre. CCDC 2411050, 2408404, and 2470759 contain the supplementary crystallographic data for this paper. These data can be obtained free of charge from The Cambridge Crystallographic Data Centre via www.ccdc.cam.ac.uk/data_request/cif.

X-ray crystal structure of 10b (CCDC 2411050)

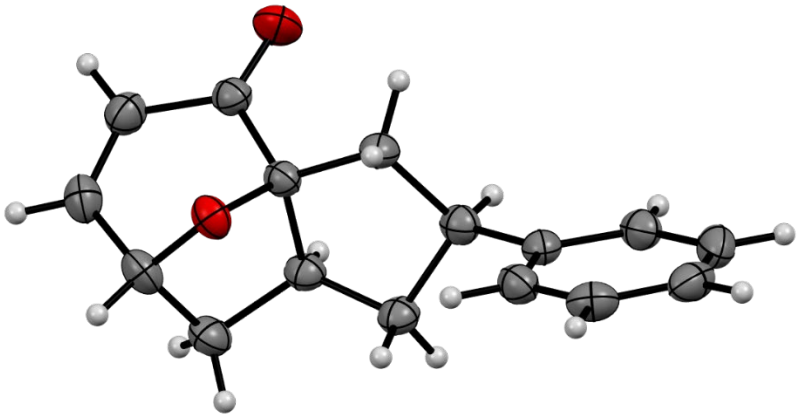

ORTEP plot of **10b** with thermal ellipsoids shown at the 50% probability level

Table S1. Crystal data and structure refinement for 10b

Crystal data	
Chemical formula	$C_{16}H_{16}O_2$
M_r	240.29
Crystal system, space group	Monoclinic, $P2_1/c$
Temperature (K)	150
a, b, c (Å)	10.2958 (11), 10.1721 (10), 12.0183 (16)
β (°)	97.742 (9)
V (Å^3)	1247.2 (2)
Z	4
Radiation type	Cu $K\alpha$
μ (mm^{-1})	0.66
Crystal size (mm)	0.23 × 0.06 × 0.01
Data collection	
Diffractometer	Bruker AXS D8 Quest
Absorption correction	Multi-scan TWINABS 2012/1: Krause, L., Herbst-Irmer, R., Sheldrick G.M. & Stalke D. (2015). J. Appl. Cryst. 48 3-10.
T_{min}, T_{max}	0.694, 0.747
No. of measured, independent and	2672, 2672, 2081

observed [$I > 2\sigma(I)$] reflections	
R_{int}	0.082
$(\sin \theta/\lambda)_{max}$ (Å^{-1})	0.639
Refinement	
$R[F^2 > 2\sigma(F^2)]$, $wR(F^2)$, S	0.057, 0.166, 1.11
No. of reflections	2672
No. of parameters	163
H-atom treatment	H-atom parameters constrained
$\Delta\rho_{max}$, $\Delta\rho_{min}$ (e Å^{-3})	0.28, −0.27

X-ray crystal structure of 10f (CCDC 2408404)

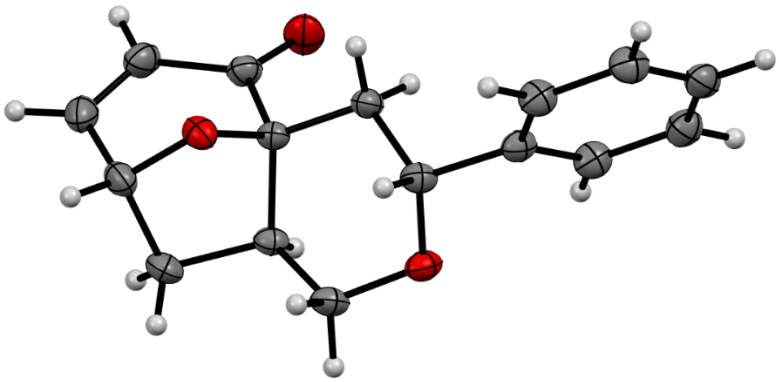

ORTEP plot of **10f** with thermal ellipsoids shown at the 50% probability level

Table S2. Crystal data and structure refinement for 10f

Crystal data	
Chemical formula	$C_{16}H_{16}O_3$
M_r	256.29
Crystal system, space group	Orthorhombic, *Pna*2$_1$
Temperature (K)	150
a, *b*, *c* (Å)	13.5957 (4), 5.5652 (2), 17.3345 (5)
V (Å^3)	1311.58 (7)
Z	4
Radiation type	Mo *K*α
μ (mm^{-1})	0.09
Crystal size (mm)	0.40 × 0.23 × 0.17
Data collection	
Diffractometer	Bruker AXS D8 Quest
Absorption correction	Multi-scan *SADABS* 2016/2: Krause, L., Herbst-Irmer, R., Sheldrick G.M. & Stalke D., J. Appl. Cryst. 48 (2015) 3-10
T_{min}, T_{max}	0.694, 0.747
No. of measured, independent and	28105, 4751, 4206

observed [$I > 2\sigma(I)$] reflections	
R_{int}	0.034
$(\sin \theta/\lambda)_{max}$ (Å^{-1})	0.770
Refinement	
$R[F^2 > 2\sigma(F^2)]$, $wR(F^2)$, S	0.035, 0.093, 1.06
No. of reflections	4751
No. of parameters	172
No. of restraints	1
H-atom treatment	H-atom parameters constrained
$\Delta\rho_{max}$, $\Delta\rho_{min}$ (e Å^{-3})	0.25, −0.18
Absolute structure	Flack x determined using 1718 quotients [(I+)-(I-)]/[(I+)+(I-)] (Parsons, Flack and Wagner, Acta Cryst. B69 (2013) 249-259).
Absolute structure parameter	0.0 (2)

X-ray crystal structure of 10e (CCDC 2470759)

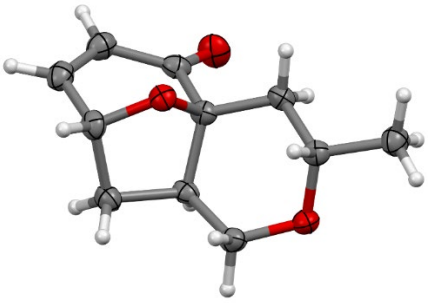

ORTEP plot of **10e** with thermal ellipsoids shown at the 50% probability level

Table S1. Crystal data and structure refinement for 10e

Crystal data	
Chemical formula	$C_1H_4O_3$
M_r	194.22
Crystal system, space group	Monoclinic, $P2_1/c$
Temperature (K)	150
a, b, c (Å)	8.8005 (10), 16.8892 (19), 6.6655 (8)
β (°)	108.072 (5)
V (Å^3)	941.84 (19)
Z	4
Radiation type	Cu $K\alpha$
μ (mm^{-1})	0.81
Crystal size (mm)	0.28 × 0.03 × 0.01
Data collection	
Diffractometer	Bruker AXS D8 Quest

Absorption correction	Multi-scan *SADABS* 2016/2: Krause, L., Herbst-Irmer, R., Sheldrick G.M. & Stalke D., J. Appl. Cryst. 48 (2015) 3-10
T_{min}, T_{max}	0.635, 0.754
No. of measured, independent and observed [$I > 2\sigma(I)$] reflections	25222, 2057, 1844
R_{int}	0.051
$(\sin \theta/\lambda)_{max}$ (Å^{-1})	0.640
Refinement	
$R[F^2 > 2\sigma(F^2)]$, $wR(F^2)$, S	0.038, 0.094, 1.07
No. of reflections	2057
No. of parameters	128
H-atom treatment	H-atom parameters constrained
$\Delta\rho_{max}$, $\Delta\rho_{min}$ (e Å^{-3})	0.22, −0.26

References

(1) Bruker (2023). Apex5 v2023.9-2, SAINT V8.40B, Bruker AXS Inc.: Madison (WI), USA, 2023.
(2) Krause, L., Herbst-Irmer, R., Sheldrick, G.M. & Stalke, D. (2015). J. Appl. Cryst. 48, 3-10.
(3) SHELXTL suite of programs, Version 6.14, 2000-2003, Bruker Advanced X-ray Solutions, Bruker AXS Inc., Madison, Wisconsin: USA
(4) Sheldrick, G.M. A short history of SHELX. *Acta Crystallogr A* **2008**, *64* (1), 112–122.
(5) Sheldrick, G. M., SHELXT--Integrated space-group and crystal-structure determination, *Acta Crystallogr A*. **2015**, *A71*, 3-8.
(6) a) Sheldrick, G.M. University of Göttingen, Germany, 2018. b) Sheldrick, G.M. Crystal structure refinement with SHELXL. *Acta Crystallogr Sect C Struct Chem*. **2015**, *71* (1), 3–8.
(7) Hübschle, C.B., Sheldrick, G.M. & Dittrich, B. ShelXle: a Qt graphical user interface for SHELXL. *J. Appl. Crystallogr*. **2011**, *44* (6), 1281–1284.